THE LOWER DARLING REGIONAL STEADY STATE GROUNDWATER FLOW MODEL

by

Ross S. Brodie

AGSO RECORD 1998/19

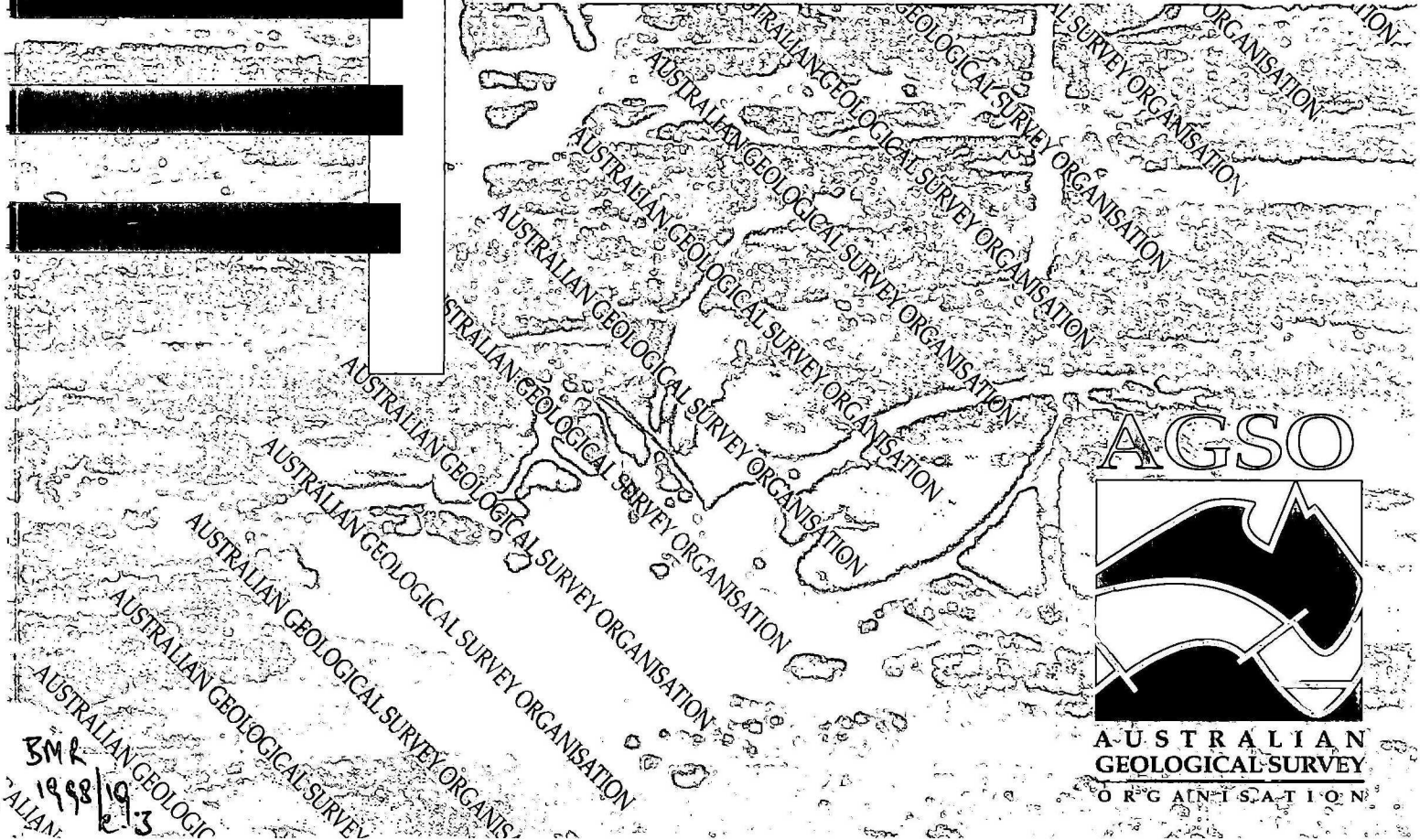

THE LOWER DARLING REGIONAL STEADY STATE GROUNDWATER FLOW MODEL

AGSO Record 1998/19

NRMS Project D5039
Murray Darling Basin Groundwater Modelling

Ross S. Brodie

Geohazards, Land & Water Resources Division
Australian Geological Survey Organisation
Canberra

DEPARTMENT OF PRIMARY INDUSTRIES AND ENERGY

Minister for Primary Industries and Energy: Hon. J. Anderson, M.P.
Minister for Resources and Energy: Senator the Hon. W.R. Parer
Secretary: Ken Matthews

AUSTRALIAN GEOLOGICAL SURVEY ORGANISATION

Executive Director: Neil Williams

ISSN: 1039-0073
ISBN: 0 642 27354 5

THE LOWER DARLING REGIONAL STEADY STATE GROUNDWATER FLOW MODEL

Ross S. Brodie
Australian Geological Survey Organisation, Canberra

EXECUTIVE SUMMARY

A groundwater model has been constructed for the northwest quadrant of the Murray Basin, north of the Murray River and containing the reach of the Darling River south of Wilcannia. The Lower Darling model was developed to predict the changes in the watertable and salt fluxes to the rivers due to broad scale management practices, such as clearing of native vegetation, expansion of irrigation or changes to river regulation. At this stage, a steady state three-dimensional model simulating groundwater conditions observed in 1988 has been constructed using the MODFLOW modelling package.

The model consists of five layers, corresponding to the layered aquifers within the Murray Basin Cainozoic sediments. The basal layer 5 is the lower Renmark Group aquifer which consists of sands and silts deposited within the deeper troughs of the basin by large rivers. The overlying layer 4 is made up of a variety of sedimentary units, spanning the transition from land to sea. In the northeast, the clays, silts and sands of the middle Renmark Group were deposited in rivers, deltas and coastal swamps. Seawards, towards the centre of the model area, the clays and silts of the Geera Clay and Winnambool Formation indicate shallow marine and lagoonal settings. Persistent marine conditions further to the southwest resulted in a series of platform carbonates, collectively named the Murray Group Limestone. Overlying the middle Renmark Group sediments in the northeast, layer 3 consists of the upper Renmark Group and represents the continuation of fluvial conditions in this area. The extensive deposition of sands during the Pliocene is represented in layer 2, which consists of the fluvial Calivil Formation and the marginal marine Loxton-Parilla Sands. Layer 1 contains the mottled clays and silts of the fluvial Shepparton Formation, as well as the more recent alluvial deposits found in the Murray-Darling floodplain (the Coonambidgal Formation) and an extensive lacustrine clay (the Blanchetown Clay). These layers are subdivided into 7.5km x 7.5 km cells, resulting in 5341 active cells in 42 rows and 65 columns. The Lower Cretaceous sediments that underly the Tertiary sequence were indirectly represented in the model.

The basin structure of troughs and ridges tends to direct the regional groundwater flow within the model area to the southwest, towards the Murray River. Hydraulic gradients are low, with 5-10 cm/km typical for the basal lower Renmark Group. The flow is from the basin margins to the regional discharge zone defined by active salinas in the southern half of the model. In this area, upwards groundwater flow is driven by high heads in the deeper aquifers. Towards the southern model boundary, the density-corrected head in the Lower Renmark Group aquifer is over 20m higher than the watertable in the shallow Murray Group Limestone aquifer. Also, groundwater salinities increase down gradient, so that salinities exceed sea water concentration (35,0000 mg/L) near the discharge zone. The combination of upwards

leakage and high salinities contributes significantly to the salt loads entering the Murray River between Mildura and Morgan. This is particularly true of the Woolpunda Reach, necessitating the construction of a major groundwater interception scheme.

Model calibration resulted in about 93% of model cells having simulated heads within 5m of observed heads, and about half within 2m. Layer 5 was the most successfully calibrated layer with over 90% of cells within 3m of observed heads. The standard deviation of the head residual was 2.25m over the entire model domain. This is a good result considering the paucity of reliable water level data for the area. In some parts of the model, the error margin for the observed head arrays can exceed five metres because of the lack of properly surveyed boreholes. The fact that simulated salt loads into the Murray River is compatible with previously documented estimates, lends further support for the veracity of the model.

In terms of input into the groundwater system, recharge from rainfall is the largest contributor. Although recharge represents less than 0.1% of rainfall, it adds over 26 ML/d to the groundwater system due to the large model area. Conversely, the irrigation areas cover less than 0.5% of the model area, but provide accessions of 12.5 ML/d. Leakage also occurs from the major storage systems of Menindee Lakes (10.7 ML/d) and Lake Victoria (2.6 ML/d). Upwards leakage from the Lower Cretaceous accounts for 14% or 9.7 ML/d of input into the Tertiary aquifers. This water enters the Lower Cretaceous in the northeast, where the aquifer progressively shallows and becomes the watertable aquifer outside the model area.

The Murray River loses about the same volume of water to the groundwater system (4.1 ML/d) as the Darling system (4.5 ML/d). The difference is that leakage only occurs in a small minority of Murray cells (9 out of 51) compared to the vast majority of Darling cells (102 out of 113). These river losses from the Murray tend to occur at or immediately upstream of the locks where the river stage is artificially high. The river leakage of 0.4 ML/d predicted upstream of Lock 6 at Chowilla is a good example, as it corresponds to a flushed zone of low groundwater salinity along the floodplain. Hence, the broad scale impacts on the groundwater system of regulating the Murray River can be identified by the model.

Although the Darling is a losing stream for most of its length, most of the leakage (94%) occurs along the reach upstream of Menindee. This reflects the extensive weir pool and the corresponding freshening of the alluvial aquifer with salinities around 600-700 mg/L. In comparison, the rest of the Darling cells, in particular along the Anabranch, have low losses to the shallow aquifer (< 0.01 ML/d) expressed by higher salinities in the floodplain aquifer of 1500-4000 mg/L.

As expected, the Murray River is the major sink for groundwater in the region, with seepages totalling 28 ML/d. The highest inflows of 1-2 ML/d occur in cells peripheral to the irrigation areas, particularly Berri, Renmark and Mildura. With the Woolpunda North bores extracting 10 ML/d, the groundwater seepage from the north to the Woolpunda reach is limited to 1.2 ML/d. In comparison, the groundwater inflows into the Darling River are insignificant, totalling about 0.04 ML/d downstream of Burtundy.

The Lower Cretaceous is a significant sink for groundwater from the Tertiary aquifers in the northeast half of the model where downward leakage prevails. About a quarter of the 20

ML/d lost to the Lower Cretaceous occurs near the Menindee Lakes. Groundwater also exits out of the model layer (0.7 ML/d) where flow in the lower Renmark Group continues southwards under the Woolpunda Reach. In addition, the active salt lakes are predicted to be evaporating over 12 ML/d out of the shallow aquifer. There may also be a component of diffuse upward leakage in areas adjacent to the salinas which has not been explicitly modelled.

A sensitivity analysis indicated that the model was most responsive to changes in rainfall-derived recharge. For example, a 5-fold recharge increase caused river gains (thereby salt loads) to increase 4-fold. Changes in hydraulic conductivity arrays, either in a horizontal direction as conductance terms, or in a vertical direction as leakance terms, also significantly changed model output. The model was not particularly sensitive to changes to the conductance term for the river bed and for the linkage between the Tertiary aquifers and the underlying Lower Cretaceous.

The model predicted significant changes to the groundwater system due to clearing of all the mallee for grazing. The scenario used a conservative estimate for the anticipated increase in recharge (0.25-0.5% of rainfall) and assumed that the Woolpunda Interception Scheme was fully operational. In this situation, salt loads to the Murray River increased from a baseline of 632 t/d to 821 t/d, distributed along the whole reach between Mildura and Morgan. If post-clearing recharge amounts to 1% of rainfall, a figure commonly used in other models, then salt loads to the Murray River were estimated to increase to 1047 t/d. This equates to an 80 EC increase in the salinity of the Murray River at Morgan. The other streams also experienced increased groundwater seepage, with salt loads to the Darling rising from 0.6 t/d to 2.7 t/d. Parts of the Anabranch switched from a losing stream to gaining groundwater with a salt load of 0.9 t/d. This would have dire consequences for water quality in the series of small dams constructed in the channel. The scenario also suggests a similar problem for Lake Victoria, where groundwater seepage may develop along the margins of the lake, contributing 0.7 t/d of salt into the water storage.

The watertable rise associated with the mallee clearing can exceed 10 metres, particularly under the cleared areas north of the Murray in South Australia and the extreme west of New South Wales as well as east of the Darling. Areas with shallow watertables where salinas may be reactivated or expanded include the Darling floodplain downstream of Burtundy, the central reach of the Anabranch around Lake Popiltah, the northern margin of the regional discharge zone north of Lake Victoria such as the Scotia and Huntingfield complexes, and the Chowilla floodplain.

Other scenarios dealt with the infrastructure used in river regulation and salinity mitigation within the model area. Removal of the Woolpunda Interception Scheme bores north of the river resulted in salt loads to the Woolpunda Reach increasing from 22 t/d to 145 t/d. The recovery of the watertable in the Murray Group Limestone resulted in a 6-12 m increase in heads near the bores and a 32 EC increase in salinity at Morgan.

The effect of decommissioning the Menindee Lakes storages was investigated. Downward leakage from the lakes is a significant contributor to the underlying aquifers, indicated by the watertable mound and associated dilution effect. Removal of the water storage resulted in a

general decrease in heads in all model layers, radially outwards from the lakes. In the shallow aquifer, this head decrease was 7-11m within 20km of the lakes, decreasing to 1m about 100 km away. The overall inputs into the groundwater system were reduced by about 10 ML/d, including a decrease in leakage from the Darling River by 0.6 ML/d with the removal of the main weir. Only a small decrease in salt loads to the Murray occurred (632 t/d to 629 t/d). This probably relates to the vast distance between the Menindee Lakes and the Murray River, so that the head decrease does not greatly effect the regional hydraulic gradient.

A number of strategies can be implemented to improve the model. Due to the variation in groundwater salinity, ranging from <1000 mg/L near the Darling River to >100,000 mg/L under the salt lakes, density effects need to be taken into account as MODFLOW assumes freshwater conditions. Density corrections may change simulated heads by over 1m, and may partially offset the tendency of the model to overestimate heads. There is also scope to optimise sensitive input arrays such as conductance and leakance using available automated calibration packages. There is also a need to link the Lower Darling model with the flow and salinity models constructed for the Murray River. The output of one model can be used in the calibration of the other, and vice-versa.

TABLE OF CONTENTS

List of Figures

List of Tables

1. INTRODUCTION

The Murray Geological Basin is a large but relatively shallow basin containing Cainozoic aeolian, fluvial, marine and marginal marine sediments. The Murray Basin is also a strategic agricultural region for Australia. Over the last century, clearing of native vegetation and development for pasture, cropping and irrigation has created an imbalance in the hydrologic regime. Deep rooted native vegetation which are efficient interceptors of rainfall have been replaced by shallow rooted perennials and annuals, drastically increasing the volume of water infiltrating beyond the root zone. As the basin sediments are relatively thin and mostly water-saturated, there is limited additional groundwater storage capacity. Hence, the increases in recharge rates have caused rapid rises in groundwater levels. Subsequent waterlogging and salinisation of land and increased salt loads to surface waters have had serious repercussions to the sustainability of agricultural production as well as to the natural environment.

Salinisation in the Murray Basin is a groundwater-related problem. In 1989, the Murray Darling Basin Ministerial Council endorsed a basin-wide regional groundwater modelling program, as proposed by the MDBC Groundwater Working Group. The program involved subdividing the basin into five model areas - Southern Riverine Plain (Gutteridge, Haskins and Davey Pty Ltd, 1992), Lower Murrumbidgee (Punthakey *et al*, 1994), Lachlan Fan (Kellett, 1997), South Australian/Victorian Mallee (Sinclair Knight Merz Pty Ltd, 1995) and Lower Darling (Figure 1.1). The models are designed to provide a predictive capacity in terms of long term regional groundwater responses to land and water management strategies.

In this context, the objectives of the Lower Darling Groundwater Model are;

(i) Construct a steady state three dimensional model simulating the regional groundwater system in the area as evident in 1988,
(ii) Predict the likely effect to regional groundwater dynamics, in terms of watertable levels and salt fluxes to surface water features, of various regional land and water management strategies. These include issues such as broad scale clearing of mallee vegetation, revegetation initiatives and river regulation.

This report documents construction of the steady state Lower Darling regional groundwater model as part of NRMS Project D5039 - *Murray Darling Basin Groundwater Modelling*.

1.1 Location

The Lower Darling groundwater model covers the northwest quarter of the Murray Basin, in the Mallee geomorphic region of western New South Wales and South Australia (Figure 1.1). The model is about 425km along a northeast axis, 150-250km wide and has an area of 78,525 km^2 The 1:250,000 scale topographic map sheets which the model partially or wholly covers are indicated on Figure 1.2.

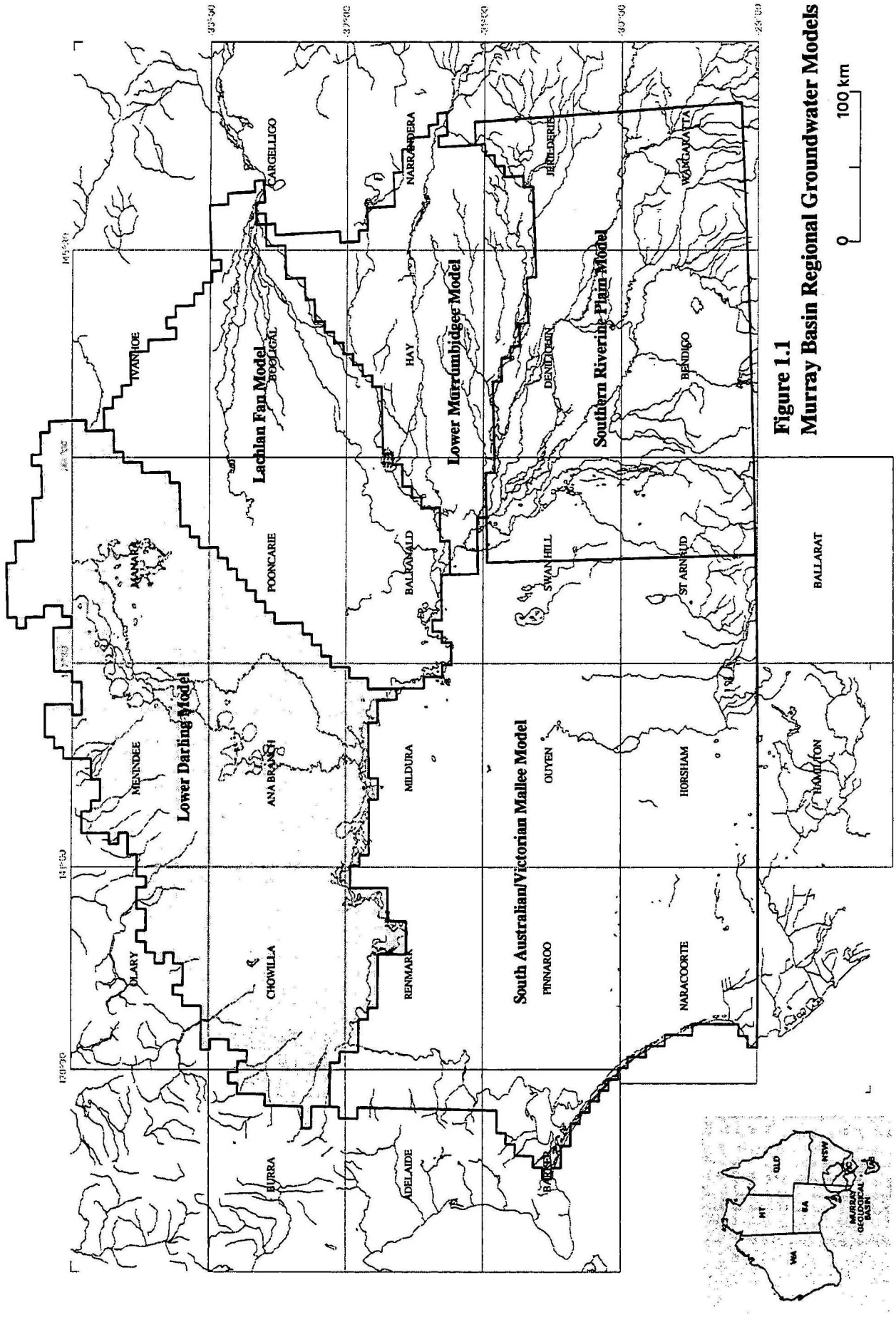

Figure 1.1
Murray Basin Regional Groundwater Models

Figure 1.2

Location Map for Lower Darling Model

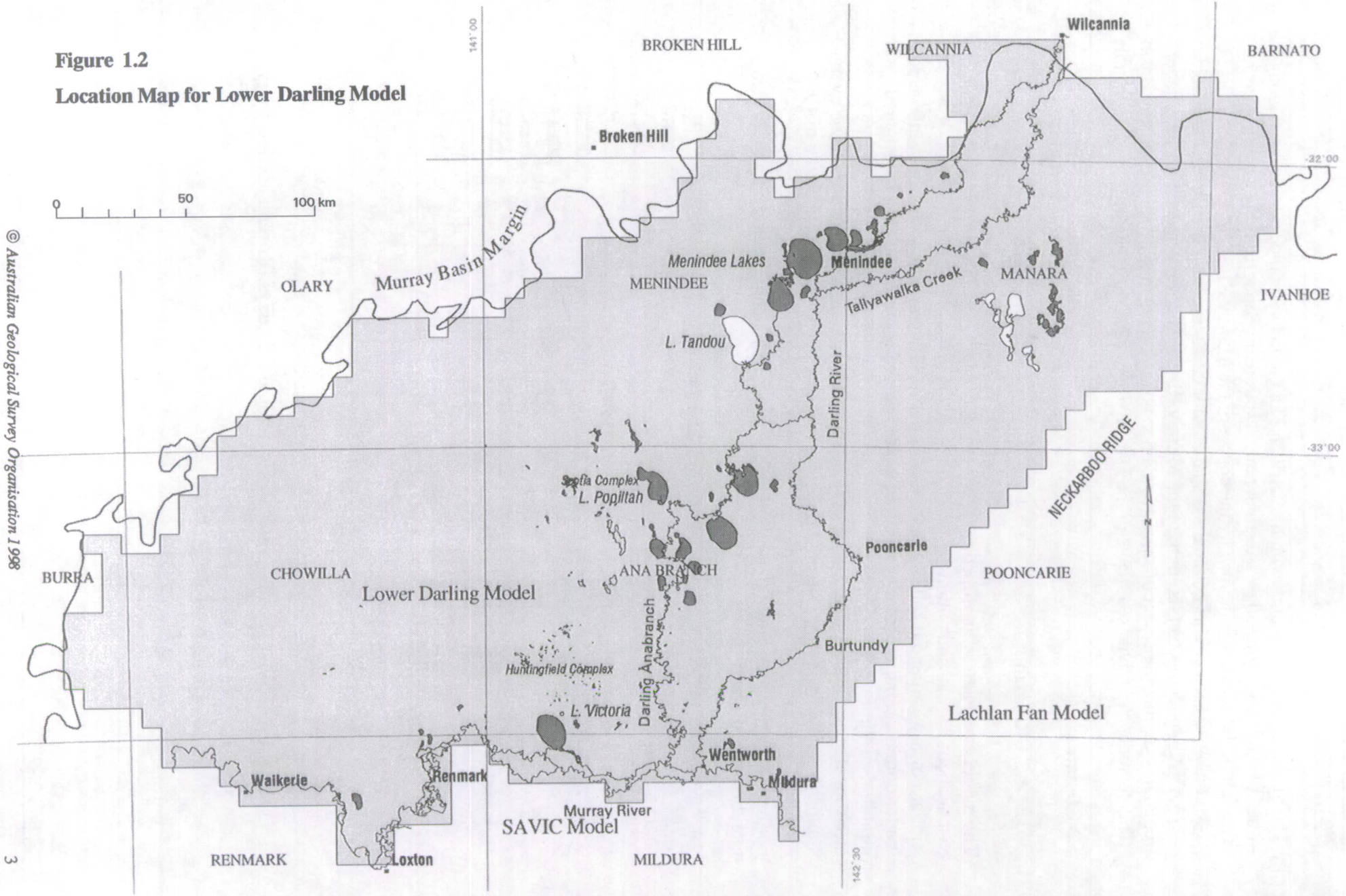

The model shares a boundary with the Lachlan Fan groundwater model to the east, along the trace of the Neckarboo Ridge, a distinct northeast trending topographic feature (Figure 1.2). The southern boundary is defined by the course of the Murray River from Mallee Cliffs, near Mildura to Morgan. This boundary is shared with the South Australian/Victorian Mallee (SAVIC) model, which is south of the Murray River. The western and northern model boundary defines the extent of saturated Cainozoic sediments making up the Murray Basin. This includes the fluvial sediments of the Darling River south of the township of Wilcannia.

1.2 Climate

1.2.1 Rainfall

The model area has a semi-arid climate, with median annual rainfall highest in the south and east at about 275mm and diminishing to the northwest to less than 200mm (Figure 1.4). A similar north-west trend is followed in the seasonality of the rainfall where the southern part is winter dominant, influenced by prevailing westerlies and associated fronts. Northwards, rainfall distribution becomes more uniform over the year, reflecting the overprinting of the monsoonal air streams of northern Australia generating summer thunderstorms. The average number of annual rain days (where > 0.25 mm fell) also decreases from about 80 to 40. Figure 1.3 illustrates these trends of increasing aridity and seasonal uniformity in a northwesterly direction found in the Bureau of Meteorology annual rain days and median monthly rainfall data.

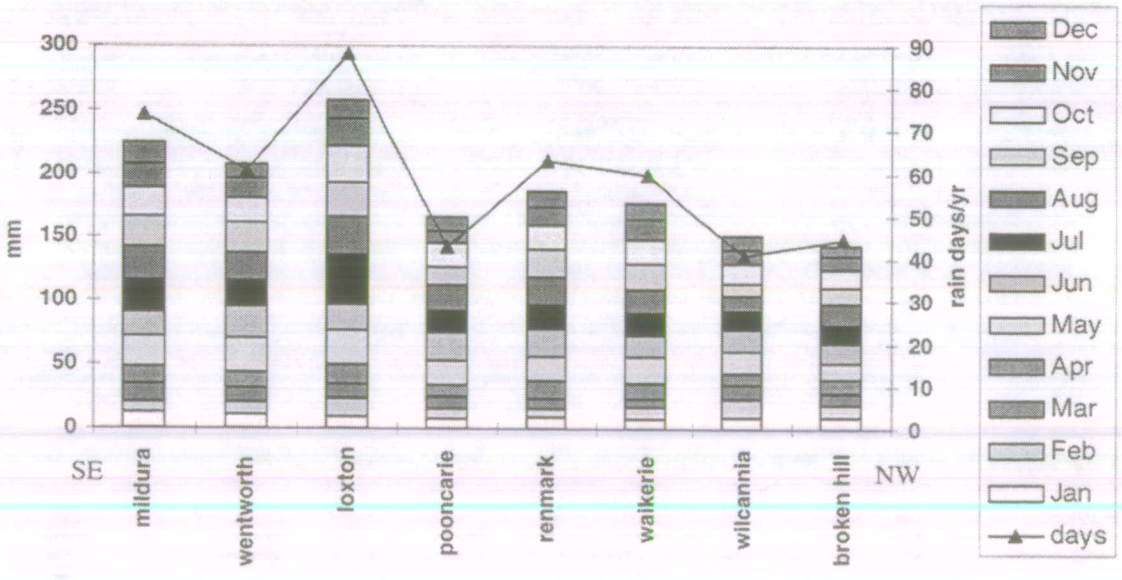

Figure 1.3 Median monthly rainfall and annual rain days (Bureau of Metrology)

Figure 1.4

Lower Darling Model
Average Annual Rainfall (mm/yr)

Source: Bureau of Meteorology data Processing by NRIC

Figure 1.5

Lower Darling Model
Average Annual Pan Evaporation (mm/yr)

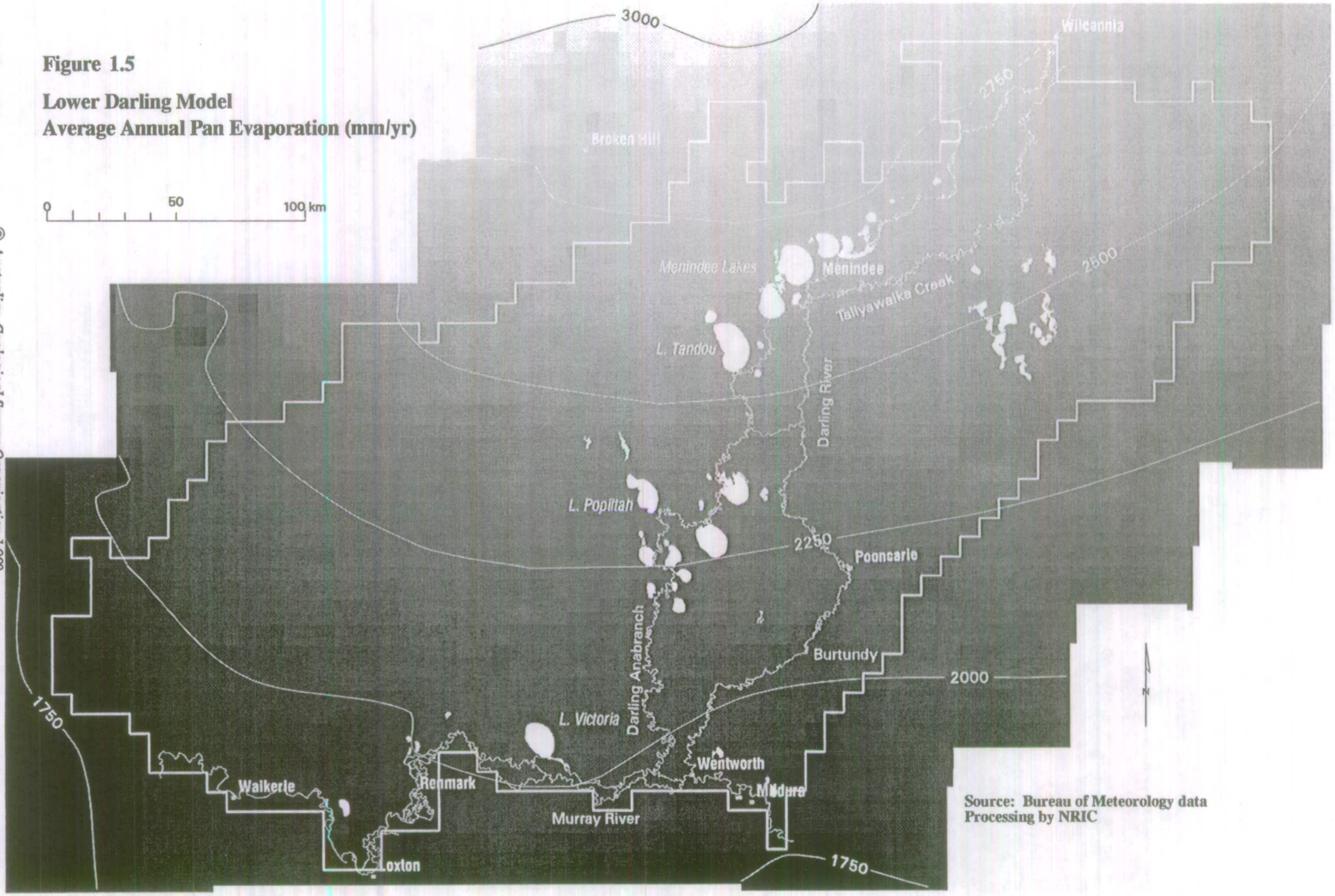

Source: Bureau of Meteorology data
Processing by NRIC

Rainfall is also highly variable, with dry years having annual rainfall less than 100 mm contrasting with exceptionally wet years with rainfall exceeding 700 mm. This variability is illustrated by the broad range between monthly 10, 50 and 90 percentile values for Pooncarie (Figure 1.6). For example, rainfall at Pooncarie has varied from zero to exceeding 60 mm for the month of January. Prolonged dry conditions are relatively common, with major drought events occurring in 1939-45, 1965-67 and 1982-83 (Scriven, 1988).

1.2.2 Evaporation

Average annual pan evaporation follows an inverse relationship with rainfall, increasing from about 1750 mm/yr to over 2750 mm/yr in a northerly direction (Figure 1.5). Monthly potential evaporation exceeds rainfall throughout the year, with the deficit obviously reaching a maxima during summer. The data from Wentworth is typical of this, with the seasonal evaporation peak in January of 251mm and a minima of 43mm in July (Figure 1.7). The residual between rainfall and evaporation is the main determinant for plant growth, where soil moisture indices as plotted on Figure 1.7, infer that rainfall is more effective in the winter months (Edwards, 1979).

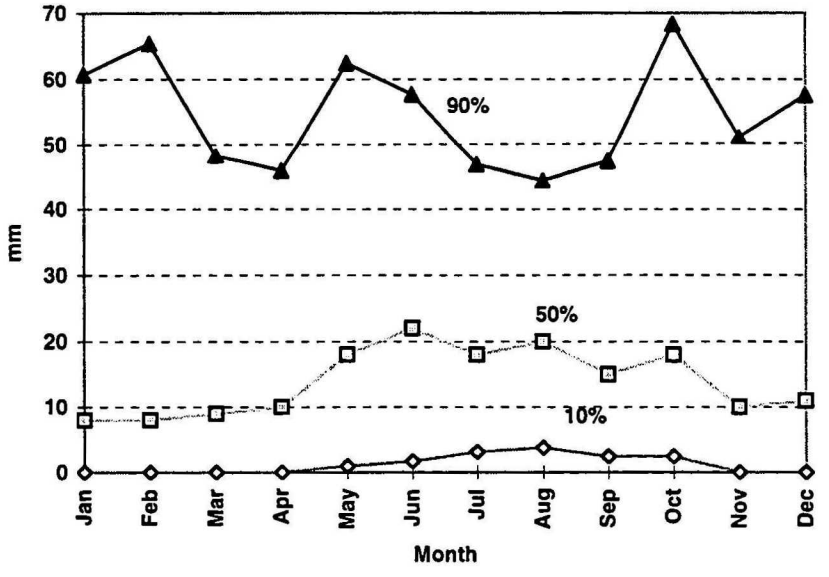

Figure 1.6 Variability in monthly rainfall for Pooncarie (Scriven, 1988)

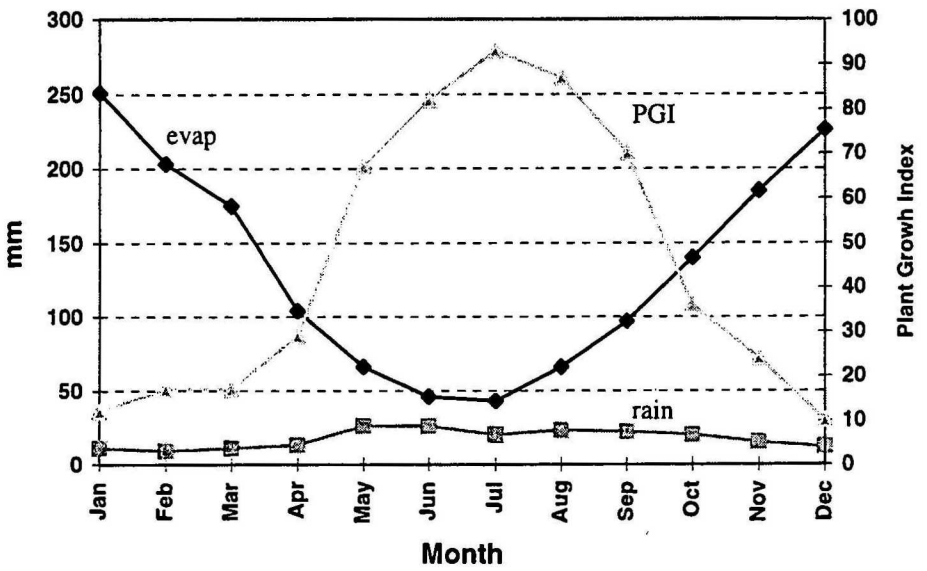

Figure 1.7 Average monthly rainfall and pan evaporation for Wentworth (Scriven, 1988)

1.2.3 Temperature

The model area experiences hot summers and mild winters. Daily temperatures tend to increase northwards, with mean summer daily maxima increasing from 32 °C to 36 °C, mean summer daily minima from 14°C to 20°C, mean winter daily maxima from 17 °C to 20 °C and mean winter daily minima from 2°C to 5°C. The average number of hours of daily bright sunshine is 10-10.5 in summer and 6-7 in winter.

1.3 Geomorphology

The landscape features of the model area which are characteristic of the Mallee province, are due to a combination of aeolian, lacustrine and fluvial processes (Figure 1.8). These morphostratigraphic units are described in detail in a major synthesis of Murray Basin geology by Brown and Stephenson (1991a).

1.3.1 Aeolian Landforms

The aeolian dune fields are the most extensive landscape feature (Figure 1.8) and can be subdivided on the basis of lithology and dune form into:

Woorinen Formation (Qdw), a large dune field system consisting of discontinuous chains of east-west trending longitudinal dunes. Typically, individual dunes are 100-3,000 metres long, up to 100 metres wide and have subdued and rounded crests 2-3 metres high. These are largely stabilised by vegetation and separated by broad swales. The dominant lithologies are red-brown siliceous sand, red calcareous silty clay and sandy clay. In profile, well developed brecciated sheets of calcrete as well as palaeosols are characteristic, reflecting episodes of dune mobilisation and stabilisation.

Figure 1.8

Lower Darling Model
Geomorphological Units

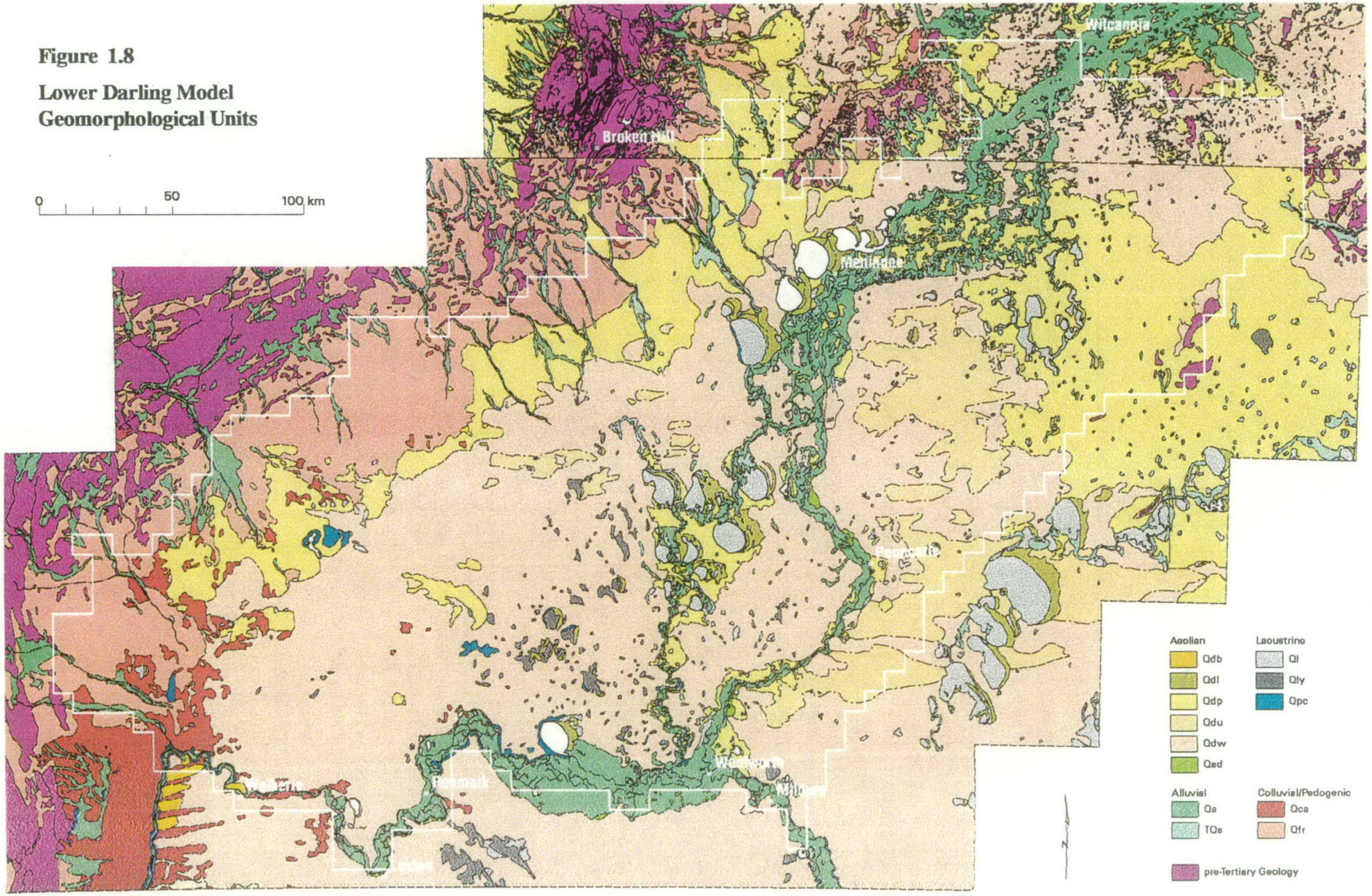

Brown & Stephenson, 1991a

Unnamed Quaternary Aeolian Dune Deposits (Qdu) form elongate easterly-trending dune fields with an irregular to sub-parabolic pattern, particularly east of the Darling River. Individual dunes tend to have sharp crests and are relatively close together, converging down-wind to form high, steep apices, pointing in an easterly direction. This implies deposition with seasonal westerly winds, similar to current conditions. The dunes are largely stabilised by mallee, but as the soil cover is poor the dunes are susceptible to erosion and are locally mobile. The unit consists mainly of red-brown to pale orange siliceous sand and lacks the clay and carbonate content characteristic of the Woorinen Formation.

Unnamed Quaternary Aeolian Sand Plain (Qdp) forms flat to gently undulating, internally draining plains between the dune fields proper and the footslopes of the basin margins, as well as adjacent to the river systems. Irregular sand accumulations as roughly circular hummocks 100-3,000 metres in diameter, as well as numerous local fluvio-lacustrine depressions are characteristic of the plain. The unit contains red or brown clayey siliceous sand, clay pellet aggregates, loamy soils and calcrete hardpans. Adjacent to the northwest foot slopes, the unit is mainly silty sand and sandy silt while near the Darling River system, more clay pellets, gypsum and salt are evident. The thickness of the unit is in the order of 2-3 metres.

Undifferentiated Quaternary Lacustrine-Derived Aeolian Lunette Deposits (Qdl) are the crescentic transverse dunes found along the down-wind (eastern) margins of many lakes. Lithologies are variable and dunes may be composite bodies of well-sorted siliceous sand, silty clay, clay pellet aggregates, gypseous clays and gypsite. These lithological variations are interpreted to reflect changes in hydrological conditions within the accompanying lake over geological time. The sands were deposited by deflation of beach deposits of relatively deep freshwater lakes during wetter climes. As the climate became drier and lakes became dominated by a shallow saline watertable, clay pellets were mainly deposited on the lunette. The relative proportions of these lithologies varies from lake to lake - for example, the Lake Victoria lunette has a high content of fine grained sand, while the Nulla Lake lunette, twenty kilometres to the northeast, is clay dominant. Lake deflation may form a large single dune, or a series of flanking dunes of varying age, such as at Popio Lake.

Bunyip Sand (Qdb) forms elongate mobile dune fields adjacent to river channels, where prevailing winds blow fluvial sands out of the valley and onto the surrounding plain. The main deposit in the model area is along the northern margin of the Murray River near Waikerie. Individual dunes of well-sorted light red to brown quartz sand are of variable shape - sub parabolic, irregular or linear. Similar source-bordering fluvial-derived sand dunes *(Qad)* are found localised along the Darling River.

1.3.2 Lacustrine Landforms

Entrenched within the aeolian landscape are lakes, which are mostly dry in the semi-arid climate. The lake deposits are classified based on two geological end members determined by the relative dominance of either saline groundwater processes or fresh surface water processes during their recent history:

Yamba Formation and other Saline Lake Deposits (Qly) are found in ephemerally active and fossil saline lakes, which are particularly prevalent in low-lying areas in the southern central part of the model area. Lithologies include gypsite, halite, friable gypseous clay, grey pelletal gypsum-quartz sand aggregates and black sulphide rich mud, found in lacustrine bed deposits typically a few metres thick. Sometimes, mounds and sheets of ferricrete, calcrete and silcrete-cemented sand are evident. The lithological variation reflects the seasonal influences of wind, rain and groundwater. However, the dominant process is evaporative, mostly from discharged groundwater with contributions from local surface run-off. The playas typically occur as irregularly shaped lakes lying 1-2 metres below surrounding older lake floor sediments or dune field sands. Deflation by wind of the lake bed has formed the characteristic lunettes (Qdl) along the eastern margins.

Undifferentiated Quaternary Lacustrine Deposits (Ql) are typical of lakes where discharge of saline groundwaters is not the dominant process. These include the large flood-plain lakes and swamps found along the Darling (eg Menindee, Tandou), Anabranch (eg Travellers, Popiltah), Talyawalka (eg Teryaweynya) and the Murray (eg Victoria) as well as smaller terminal lakes, ox-bow lakes and interdune hollows. These lakes are round or kidney shaped and range in size from a few to several hundred square kilometres. The lake floors tend to contain finely laminated to massive grey clay, silty clay, silt, humic clay and grey palaeosols. Minor sand and gravels can be found in lacustrine deltas at the entrance points to the lakes. The sediment profile can also contain the saline and gypseous clays indicative of former groundwater discharge. The lacustrine deposits are of variable thickness, but generally 2-5 metres.

1.3.3 Fluvial Landforms

Incised into the aeolian dune field by some 10-40 metres are the floodplains of the Darling and Murray River systems, where a range of fluvial landforms are apparent. For example, in the New South Wales part of the model area, the Murray River is expressed as a wide floodplain due to the high erodability of the underlying Pliocene Sands. The large meanders within the broad trench have a wavelength of about four kilometres. Downstream in South Australia, more competent limestone restricts the river which forms the relatively linear and narrow Murray Gorge.

The geomorphology of the Darling River also changes along its length. From Wilcannia to the junction of the Anabranch, the sinuous Darling occupies a wide floodplain (20-50 km) with Talyawalka Creek and numerous smaller distributaries. Some of the outer boundaries between the fluvial sediments and surrounding sand plain are strikingly linear, implying structural control (refer Figure 1.13). Downstream, the Darling flows in a narrow (2-3 km) and more linear floodplain. A similar trend is evident for the Anabranch, where the number and size of floodplain lakes decreases southwards.

The differences in river geomorphology along the Darling River, reflects two generations of channel diversion (Bowler *et al*, 1978). The current anabranch systems of Talyawalka Creek and the Great Anabranch define the palaeo-Darling channel of the Late Pleistocene (Figure 1.9). These channels contain a large meander scroll pattern and a relatively coarse bed load.

The present course of the Darling was initiated 11,000 BP and tends to be confined within a narrower trench and have smaller meander wavelengths and clayey bed loads.

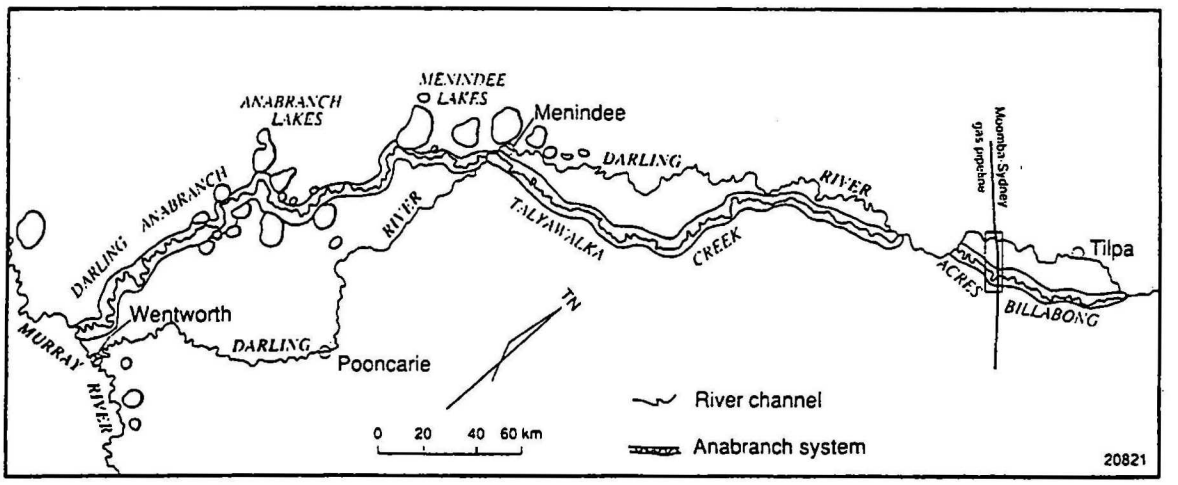

Figure 1.9 Relationship between modern Darling River and older anabranch systems (from Bowler *et al*, 1978)

Coonambidgal Formation (Qa) are the alluvial deposits of the recent river systems, consisting of grey or red-brown silt, silty clay and poorly sorted sand and gravel. Two alluvial terraces have been mapped for the Coonambidgal Formation along the Darling trench (Cameron, 1996). The younger terrace contains the modern river channel and has a poorly developed soil profile. The older, higher alluvial terrace has a well-developed soil profile, typically with carbonate nodules. In turn, the unit is entrenched in older aeolian-modified alluvial terraces of the floodplain. A series of alluvial terraces is also evident within the Murray River floodplain. In the Murray Gorge, a coarser grained quartz sand and gravel basal layer about 20-25 metres thick has been defined as the *Monoman Formation (Qa)*. Alluvium is also associated with ephemeral streams which drain the surrounding basement ranges and terminate into the aeolian terrain.

1.3.4 Residual Landforms

Along the margin of the Murray Basin (and the model area), the aeolian landscape is replaced by the lower slopes and outwash areas of the surrounding ranges. This is geomorphologically expressed as moderate to low-angle sloping or broadly undulating stony plains with sparse dendritic drainage. The deposits form residual lag deposits around outcrops of pre-Tertiary rocks, including Proterozoic sediments of the Benda Range, the Precambrian high grade metamorphic complex of the Barrier Ranges and the Devonian sandstones of the Manara Hills. The *Pooraka Formation (Qfr)* is the composite unit making up these colluvial and high-level alluvial deposits, and consists of diverse lithologies - gravel, sand, red brown poorly sorted clayey sand and clay. Localised, the unit may be cemented by a ferruginous or silicified matrix.

Calcrete Deposits (Qca) in the form of massive, strongly cemented, pale grey, resistant sheets and calcrete rubble, are the dominant geomorphological feature along parts of the western margin of the basin, in South Australia.

1.4 Vegetation

The predominate soil type developed over the various geomorphological units is the main factor influencing vegetation cover over the model area. Figure 1.10 simplifies this relationship between vegetation and land form for an idealised transect from river channel, floodplain, lake bed to sand plain and dune field (Fox, 1991). The relationship is also used in classifying land systems mapping into a coarser regional rangeland classification (Walker, 1991). In reality, there are mixing of these vegetation communities with many mapped boundaries being transitional. This is mainly due to subtle differences in soil type at a local scale.

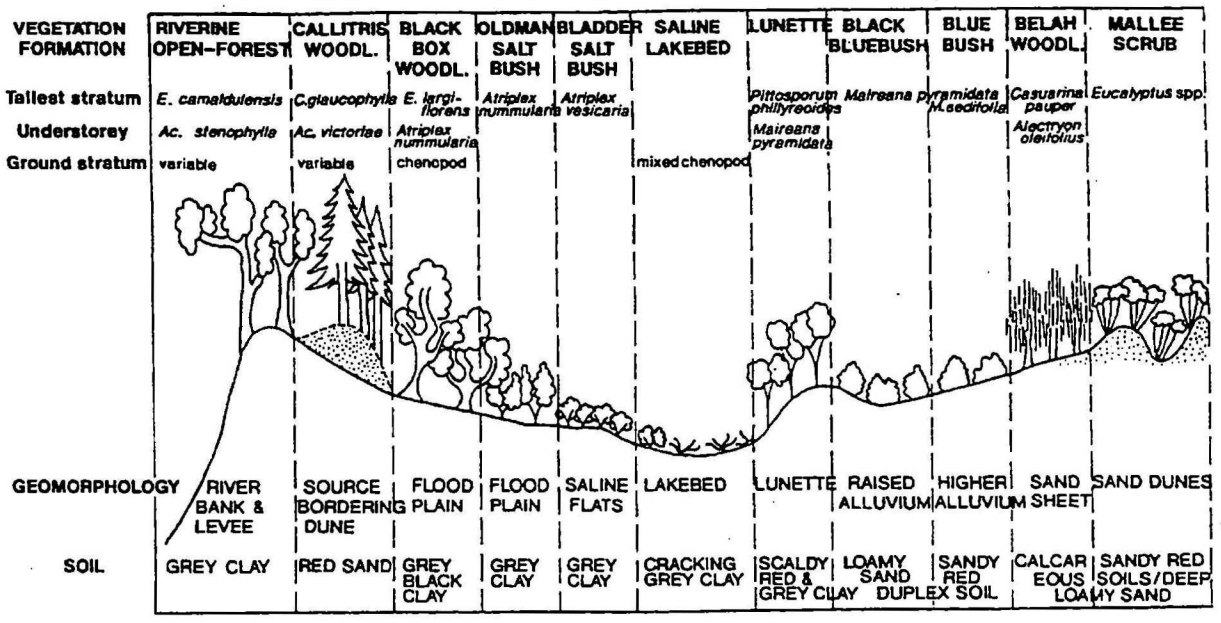

Figure 1.10 Idealised relationship between vegetation and geomorphology (from Fox, 1991)

Along the river banks and levees can be found stringers of eucalypt forest consisting of river red gum (*E. camaldulensis*) and black box (*E. largiflorens*) with an understory of river cooba (*Acacia stenophylla*) and nitre goosefoot (*Chenopodium nitrariaceum*). The river red gum are constrained along the river corridor as it relies on the episodic prolonged flooding to successfully propagate. Away from the river channel, in areas of the floodplain subject to periodic inundation, reasonable grazing country of low open woodlands dominated by black box prevail. An understory of nitre goosefoot, old man saltbush (*Atriplex nummularia*) with abundant annual forbs and grasses is typically found. The river red gums and black box are mapped as scattered eucalyptus woodland along a river corridor in preliminary National Forestry Inventory (NFI) mapping (Figure 1.11)

Figure 1.11

Lower Darling Model
Vegetation Mapping
Preliminary NFI Data

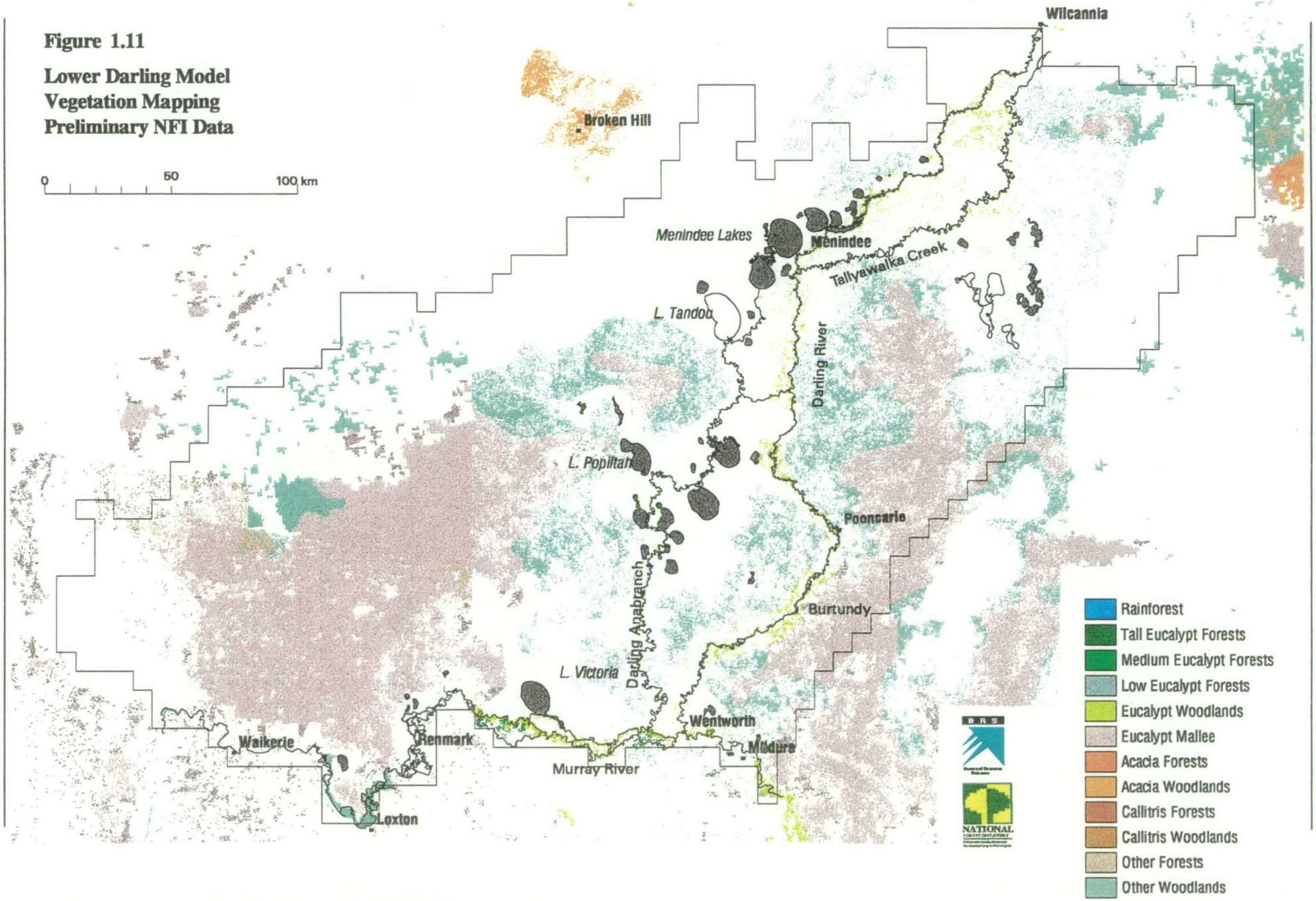

An open mixed woodland of white cyprus pine (*Callitris glaucophylla*), needlewood (*Hakea leucoptera*), sugarwood (*Myoporum platycarpum*) with clumped prickly wattle (*Acacia victoriae*), hopbush (*Dodonaea spp*) and bluebush (*Maireana spp*) is found over the deep loose sandy soil of the source bordering dunes (Qad). In a landscape with limited resource of useable timber, the larger tree species have been selectively cleared.

The vegetation cover of the lake beds is largely defined by soil salinity. In depressions near the rivers subject to intermittent flooding, grasslands of canegrass (*Eragrostis australasica*) and lignum (*Muehlenbeckia cunninghamii*) form important wildlife habitats. Sedge swamps dominated by spike rushes (*Eleocharis spp*) also occur, particularly in the Murray floodplain near Lake Victoria. In many larger floodplain lakes, the typical original herbland of glasswort (*Scleristegia Tenuis*), saltbush (*Atriplex spp*) and pigface (*Disphyma spp)* have been cleared during opportunistic cropping. Herb cover becomes sparse with the extremes of soil salinity found in the active groundwater discharge lakes.

The alluvial flats also have a diversity of vegetation cover. A low shrubland of mostly bladder saltbush (*Atriplex vesicaria*) or old man saltbush (*Atriplex nummularia*) can be found on some tracts of grey clay alluvium. These are often heavily grazed and can be invaded by dillon bush (*Nitraria billardeiri*). The stands of old man saltbush have particularly been decimated by grazing pressure, rabbit plagues and caterpillar infestation. In contrast, the loamy flats surrounding the ephemeral streams draining the Barrier Range are mainly vegetated by mitchell grass (*Astrebla lappacea*) and other perennial grasses.

A low shrubland of black blue bush (*Maireana pyramidata*), thorny saltbush (*Rhagodia spinescens*), copperburr (*Sclerolaena spp*) and saltbush (*Atriplex spp*) with sparse trees is typical of the sand plain adjacent to the riverine environment (Qdp). This is gradually replaced upslope by an assemblage of pearl bluebush (*Maireana sedifolia*), crowfoot (*Erodium spp*), (*Tetragonia tetragonioides*) and copperburr.

In turn, the bluebush grade into the tall shrubland species typical of the aeolian landforms. Mallee consisting of *Eucalyptus socialis*, *E. costata* and *E. dumosa* are the most extensive flora over the calcareous red sands of the dune fields (Qdw). Eucalypt mallee shrubland is found in a 50-100km wide belt commencing north of the Murray between Renmark and Morgan up to Lake Tandou, and a 25-50km wide belt between the Darling River and the Willandra Lakes-Tallyawalka Lakes system (Figure 1.11). The density and content of the understory varies over the model area (Scriven, 1988). The mallee near Ivanhoe supports dense broombush (*Melaleuca uncinata*), punty bush (*Cassia eremophila*), cactus pea (*Bossiaea walkeri*) and showy daisy bush (*Olearia pimeleoides*). Variable densities of pituri (*Duboisia hopwoodii*), spine bush (*Acacia coletioides*) and wilhelm's wattle (*Acacia wilhelmiana*) are evident in the mallee around Pooncarie. West of the Darling, intermingled dense stands of narrow leaf hopbush (*Dodonaea attenuata*) and turpentine (*Eromophila sturtii*) are found. Groundcover is usually porcupine grass (*Triodia irritans*), with copperburrs, *Beyeria opaca*, *Podolepis capillaris*, cottony saltbush (*Chenopodium curvispicatum*) and speargrass (*Stipa spp.*)

In the broad swales, the mallee is subordinate to a tall arid shrubland of belah (*Casuarina cristata*) and rosewood (*Heterodendrum oleifolium*) and scattered sugarwood and white cyprus pine. Bluebush, bladder saltbush, speargrass and copperburrs form the common understorey species. This assemblage is also typical of the extensive sand plain (Qdp) bordering the northwest margin of the basin. Local dense clumps of punty bush and turpentine as well as scattered stands of mulga (*Acacia aneura*) and nelia (*Acacia loderi*) are also found. The belah and rosewoods are mapped as 'Other Woodlands' peripheral to the mallee by the NFI (Figure 1.11)

Progressing up-slope and onto the stony rises (Qfr), the tall shrub species become less abundant, and can also include prickly wattle (*Acacia victoriae*) and dead finish (*A. tetragonophylla*). Dense to scattered black bluebush and pearl bluebush with variable speargrass, copperburrs, kerosene grass (*Aristida contorta*) and fuzzweed (*Vittadinia triloba*) prevail. Where little soil has developed, many of these talus slopes are essentially devoid of vegetation.

1.5 Topography

At the northern and western margins of the model area, ranges and hills of more resistant basement metamorphic and sediments form the prominent topographic features. Some of these highs (such as Scopes Range) reach elevations of 200-350 metres AHD, rising over 70 metres above the surrounding plain and mark the boundary of the Murray Basin (Figure 1.12). Off these ranges, ground slopes consistently away to the southeast for some 20 to 40 km, with the gradient slowly decreasing from 4m/km to <1m/km.

This consistency is disrupted towards the centre of the model area, being replaced by the subtle but complex topography associated with the major river systems. The Darling and Murray Rivers, with associated floodplain lakes and terraces are entrenched some 10-40 metres into the aeolian sand plain. This dissection is most apparent in the lower reaches of the Murray, which has created limestone cliffs up to 40 metres high. This river reach at Morgan is predicably also the lowest point in the model area (<10 m AHD). In terms of positive relief, the lunettes on the eastern margins of the major lakes are local arcuate landscape features reaching 10-20 metres in height.

West of the Anabranch, the subdued topography is also complex and undulating. Broad arcuate ridges, trending in a northwest direction, commonly reach an elevation of 80 metres AHD. These features are readily apparent in Landsat MSS imagery (Figure 1.13). These are surface expressions of relict beach strand lines in the underlying Pliocene marine sands. In the swales between these ridges occupy numerous salt lakes and clay pans which have deflated down to elevations of 20-30 metres AHD.

The eastern model boundary is marked by a broad (5-15 km wide) high called the Neckarboo Ridge. This feature reflects a pre-Tertiary structural high which extends from Mallee Cliffs (east of Mildura), northeast to the Manara Hills. The latter hills, with the Quamby Hills and Darnick Range are Devonian sandstone outcrops which reach elevations of 200 m AHD.

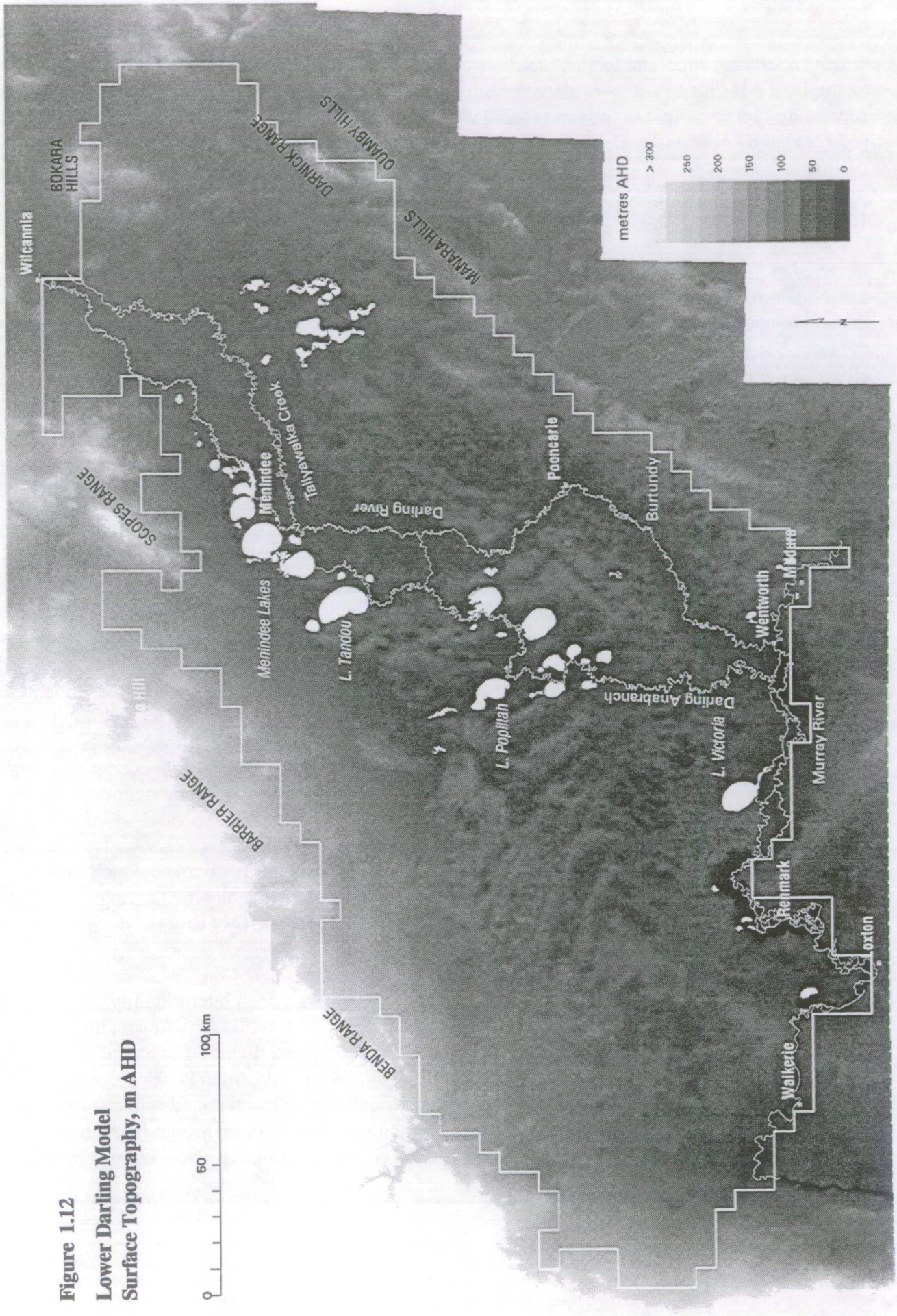

Figure 1.12
Lower Darling Model
Surface Topography, m AHD

Other underlying structural features are also expressed in the surface topography. For example, the Hamley Fault is evident trending northeast in the centre of the model area, separating higher ground to the west from lower country to the east. Similar structures are represented by northeast and northwest trending linearities in topographic highs and river drainage.

1.6 Land Use

In terms of area, pastoralism in the form of merino wool production is the main land use in the model area. Small cattle herds also augment the rural enterprise. Sheep stocking rates depend on the landform (Scriven, 1988), varying from one sheep to 8-20 ha in the mallee dunes to one sheep to 6 ha in the more open belah-rosewood plain. The bluebush country closer to the rivers can carry 3-5 sheep/ha in favourable seasons. Figure 1.13 shows the different stocking rates and vegetation cover apparent between paddocks, particularly northwest of Menindee. Large fire scars characteristic of the mallee country are also evident. Kangaroos and feral goats are commonly harvested for skin and meat.

The lake beds and alluvial floodplains can also be a valuable grazing resource. Opportunistic cropping of some of the large floodplain lakes takes place after major flood events (Birchall, 1991). Crop type depends on when the floodwaters sufficiently recede to plant, with wheat, barley, canola and safflower in winter or sorghum and sunflowers in summer. The crop relies on the residual soil moisture and natural fertility of the heavy self-mulching alkaline grey clays. Cultivation is permitted on over half or about 35 500 ha of the lake bed system.

Irrigation has developed along the Murray River and to a lesser extent, the Darling and evident as distinct clusters in Landsat MSS imagery (Figure 1.13). The Sunraysia District around Mildura and Dareton is dominated by vineyards producing wine and dried grapes. Other irrigated crops include citrus, stone fruit, vegetables, melons, almonds, olives, avocados and minor cereals and fodder. Downstream, the Riverland Districts between Renmark and Morgan form the strategic irrigation region in South Australia. Similar high value horticultural crops (vines, citrus, stone fruit, almonds) are grown. In recent years, establishment of vineyards for wine production has become particularly popular. Small scale irrigation of citrus and vine crops occurs as small dispersed holdings along the Darling, downstream of Menindee. An irrigation enterprise at Lake Tandou grows cotton, wheat, barley and sorghum on the lake bed (Figure 1.13).

Mineral resource development is limited in the area. Gypsum has been intermittently mined from some saline lake beds and lunettes, mostly for use as a soil conditioner with smaller, higher grade tonnages used in the manufacture of cement and plasterboard. For example, deposits have been defined at Morgan, Ramco West, Waikerie and Rotten Lake. Recent exploration has discovered heavy mineral deposits hosted in the Pliocene Sands which underlie the model area. This includes the significant 1.061 billion tonne Mount Massidon resource near the Scotia Lake complex, grading at 2.09% heavy minerals (NSW Dept Mineral Resources, 1996).

Figure 1.13 Landsat MSS imagery - red/green/blue, bands 4,3,1 respectively

Fishing from the inland rivers and lakes is important to the district. For example, an annual worth of $3m has been estimated for commercial fishing in the Darling River (Bellert, 1991). Minor rural industries include honey production, firewood collection, oil production from eucalypts and garden fencing material from broombush (*Melaleuca uncinatata*).

A number of reserves have been gazetted in the model area. Kinchega National Park incorporates the fluvial land systems between the Darling River and the Menindee Lakes. Nearie Lake, a small floodplain lake on the Anabranch, is a nature reserve. Danggali Conservation Park contains mallee habitat immediately west of the South Australia-New South Wales border.

Most of the towns in the region are located on the Murray River, servicing the local irrigation, cropping and pastoral industries. These include the main centres of Mildura, Wentworth, Renmark, Berri, Loxton, Waikerie and Morgan. Menindee, Pooncarie and Wilcannia, all located on the Darling River, are the only townships within the model area located north of the Murray River.

1.7 Management Issues

Removal of native vegetation for pastoral or cultivation purposes is a contentious land management issue in the model area, particularly in western New South Wales. Landholders are pressing for clearing approvals, to maintain and improve the viability of their farming enterprise. Local business and industry sectors tend to support further agricultural development, as a means of boosting investment. The aboriginal community need to protect their traditional heritage, recognising the importance of a stable and diverse natural environment. Conservation groups also have concerns on the impacts on biodiversity and habitat. A regional planning committee made up of representatives of key interest groups - landholders, the aboriginal community, conservation organisations, catchment management committees, local government representatives and government agencies - has been formed to develop an equitable and sustainable management plan (NSW Dept Land & Water Conservation, 1996a). Many other issues face managers of rangelands, including woody weed invasion, feral animal impacts, degrading soil quality and erosion

In 1989, the Murray Geological Basin Policy was introduced on the basis of the linkage between clearing native vegetation and enhanced recharge causing watertables to rise (NSW Dept Land & Water Conservation, 1996b). A Clearing Licence application will only be approved in the Murray Basin if it includes sufficient evidence that the proposal has no likely significant impact on the groundwater system.

Of major concern is the possibility of long-term increased accessions and salt loads to the river due to broadscale clearing. Modelling of the Mallee region south of the Murray River suggests that river salinity at Morgan will increase by 70 ECU, fifty years after watertables respond to historical clearing (Barnett, 1989). This study also concluded that the current watertable represents pre-clearing conditions and the pressure front due to clearing that started 50-80 years ago has not as yet reached the relatively deep watertable found over most of the region. Similar modelling for the current agricultural activity around Balranald suggested

increased salt loads to the river system of 50 tonnes/day after 50 years, increasing to 200 tonnes/day after 400 years (Cook *et al*, 1996). Scenario modelling involving clearing of the mallee in the western riverine plain of New South Wales, predicted increases of salt flows to the Murray and Murrumbidgee rivers by 85-140 tonnes/day (Kellett, 1997).

These accessions are additional to the salt load presently entering the Murray River floodplain. A significant management issue is the control of groundwater accessions to the river by hydraulic loading from irrigation mounds, evaporation basins, water storages and weirs. For example, outbreaks of land salinisation has occurred adjacent to Lake Victoria.

1.8 Previous Work

Early groundwater investigations in the model area concentrated on finding a reliable water supply in the semi-arid environment. For instance, Dixon (1891) highlighted the possibility of using the Murray Basin aquifers to supply water to an expanding Broken Hill. Early reconnaissance in the 1930s provided an important summary of livestock and domestic bores and wells operating in western New South Wales at that time as well as regional interpretations of watertables and salinity (Kenny, 1934; Mullholland, 1940).

In the 1980s, the South Australian Department of Mines & Energy drilled a series of observation bores as part of a regional hydrogeological investigation of the Murray Basin (Reed, 1980; Barnett, 1981). This was followed by a similar reconnaissance drilling program in western New South Wales by the NSW Department of Water Resources and AGSO. This data was used extensively in regional hydrogeology mapping at 1:250,000 scale compiled as part of the Murray Basin Hydrogeological Map Series (Barnett,1991,1994; Brodie,1992,1994; Kellett, 1991,1994a,1994b; Rural Water Commission,1991).

Recent groundwater studies in New South Wales have focused on the interaction between the groundwater system and the rivers. This has included investigations near Lake Victoria (Williams *et al*, 1993), the Menindee Lakes (Bish & Salotti, 1996) as well as the Darling River itself (Stannards, 1981; Williams 1991a,1991b; Williams *et al*, 1995; Jewell, 1993). Away from the river, work on the salinas north of Lake Victoria has provided insights into local stratigraphy and hydrodynamics (Ferguson & Radke, 1992; Ferguson *et al*, 1995).

Along the Murray, particularly in South Australia, the main objective of groundwater investigations has been to quantify and manage salt loads to the river. This includes work associated with the Woolpunda Interception Scheme (Telfer, 1987; Lindsay & Barnett, 1989; Watkins, 1993) as well as with specific irrigation districts (Howles, 1987;Watkins et al, 1995) and the Chowilla floodplain (Waterhouse, 1989). Previous groundwater modelling in the Lower Darling region has tended to be associated with these studies. The exception is a regional coupled economic and groundwater model constructed over most of the New South Wales part of this study area, investigating the salinisation impacts of dryland agriculture (Prathapar *et al*, 1994).

2. REGIONAL GEOLOGY

2.1 Pre-Cainozoic

Surrounding the model area, the Murray Basin is flanked by low hills and ranges consisting of Proterozoic and Palaeozoic terranes (Figure 2.1). In the west, in South Australia, mainly Late Proterozoic weakly metamorphosed fluvial to shallow marine clastics, carbonates and evaporites of the Adelaide Fold Belt form the Benda Range. Further to the northeast, Proterozoic migmatite, quartzofeldspathic metasediments, gneisses and basic intrusives constitute the Broken Hill - Willyama Block. The north east corner of the model is bounded by Darling Basin sediments made up of marine clastics and continental quartzose sandstones of mainly Devonian age. Isolated outcrops of Devonian sandstone also form the Manara Hills, Darnick Range and Quamby Hills which demarcates the structural high that is the eastern boundary to the model.

Regional aeromagnetic and gravity data indicate that these terranes also underlie the northwest quadrant of the Murray Basin as a northeast trending collage (Brown *et al*, 1988). The structural contours for the base of the Cainozoic sediments (Figure 2.1) shows this dominant northeast grain of the underlying basement. Differential subsidence of underlying basement elements has largely defined the geometry of the Murray Basin sedimentary sequence. A series of linear, northeast trending infrabasins including the Tarrara, Menindee and Wentworth Troughs have formed. These are embayments to the main depocentre for the Murray Basin, the Renmark Trough, located under the southern margin of the model. Here, over 600 metres of Cainozoic fill has accumulated. Smaller northeast trending depressions also separate structural highs, such as the Redan Embayment between the Broken Hill Block and Scopes Range as well as the Bunnerungee Trough between the Lake Victoria and Lake Wintlow Highs.

The troughs can be fault bounded and also disrupted by northwest trending cross faulting. For example, the Renmark Trough is bounded to the west by the Hamley Fault, separating it from a smaller depression, the Canegrass Lobe. The orthogonal faults bounding the Blantyre Trough are expressed as the abrupt linear bounds of the Tallyawalka Creek floodplain. The Wentworth Trough is displaced sinistrally along a northwest trending cross fault coinciding with a similar linear trend in the course of the Darling River.

Separating the troughs are basement highs of similar northeasterly trend. The Cambro-Ordovician sediments of the Scopes Range form a distinct ridge, extending 50km under the Cainozoic cover. The Lake Wintlow High is a regional structure coinciding with a linear belt having a high magnetic signature, interpreted to be due to Cambrian volcanics (Brown *et al*, 1988). The Neckarboo Ridge, along the eastern boundary of the model, is traceable on the land surface by elevated dune fields, 10-20km across. Abrupt changes in dip direction between outcrops of Devonian sediments along the ridge suggests extensive cross faulting (Kellett, 1994a). The ridge is separated from the main Devonian outcrops to the north, by the Baden Park Depression.

Figure 2.1

Lower Darling Model
Base of Cainozoic Sediments
structural contours, m AHD

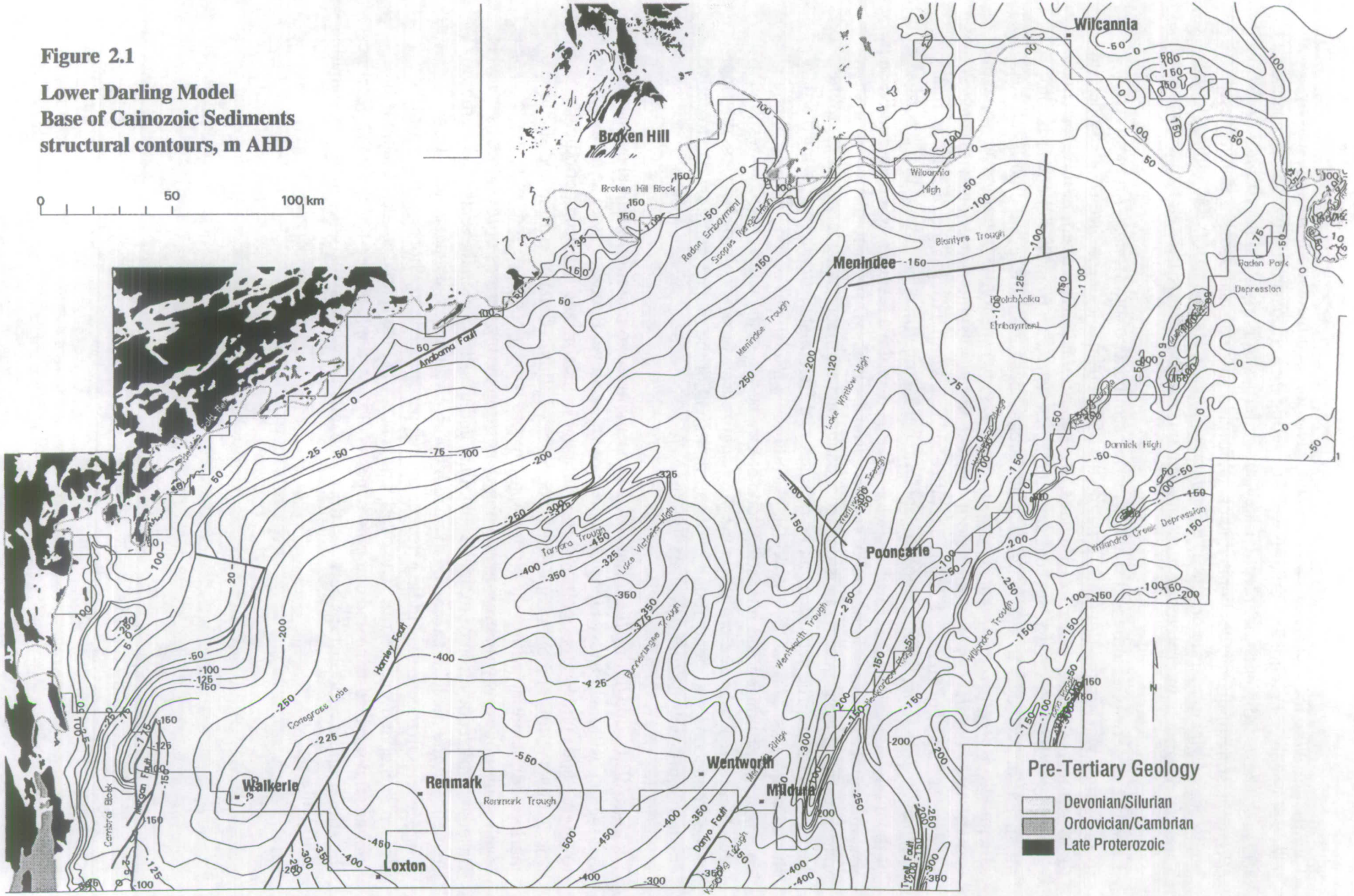

The troughs were the loci for Late Palaeozoic-Mesozoic sedimentation, as indicated by intersections in petroleum exploration wells targeting the infrabasins (Brown & Stephenson, 1991a). These sediments include the Late Carboniferous to Early Permian *Urana Formation (Pl),* consisting of diamictite, laminated claystone and siltstone and poorly sorted coarse sandstone of glacio-marine origin. The Permian sediments are about 300-450m thick in the Tarrara Trough and interpreted to be 800-900m thick in the Renmark Trough.

Lower Cretaceous fluviatile and shallow marine sediments of the *Monash Formation (Kl)* form a thin cover. In the Renmark Trough, the 350-500?m thick sequence is subdivided into three members. In the basal *Pyap Member,* the depositional environment of the grey friable sandstone with minor mudstone, coal and conglomerate grades from fluvial upwards into marine, as indicated by increasing glauconite, arenaceous foraminifera and dinoflagellates. The middle *Merreti Member* consists of marine mudstone, siltstone and minor sandstone and is overlain by the fluvio-lacustrine chloritic volcanolithic siltstone, sandstone and shale of the uppermost *Coombol Member.* In the Tarrara and Wentworth Troughs the Monash Formation is typically 100-150m thick and the upper Coombol Member may be absent. In the northeast of the model area, the Lower Cretaceous platform cover thins (usually to <80m) but extends past the infrabasins, onlapping the Devonian basement highs. Dominant lithologies are non-marine carbonaceous quartz sandstone, coal bands and argillaceous sand equivalent to the Merreti Member. The sequence can be difficult to differentiate from the overlying Tertiary fluvial sediments. Marine grey sticky clays and pyritic mudstones of the Pyap Member are less common. A prolonged and intense episode of weathering in the late Cretaceous resulted in a deep bleached, kaolinised profile on the pre-Cainozoic surface. The profile is less developed in the Cretaceous sediments found in the northern half of the model, possibly due to active erosion in the early Tertiary (Kellett, 1994b).

Tectonic disruption during the Cainozoic has been limited to minor differential subsidence so that the depositional history tends to relate more to sea level fluctuations. The area has had a low-lying and subdued topography throughout the Cainozoic and has been periodically flooded by shallow epicontinental seas. Sequences of fluvio-deltaic, paralic and shallow marine sedimentation within the stratigraphic record correspond to periods of high global sea-levels. This contrasts with erosion and non-deposition during periods of low global sea levels. Based on this recognition of major depositional and non-depositional events, the Tertiary sequence in the model area can be divided into three sequences - Palaeocene to Lower Oligocene, Oligocene to Middle Miocene and Upper Miocene to Pliocene (Brown, 1989, Brown & Stephenson, 1991a). The overlying veneer of Quaternary sediments include the aeolian, fluvial, lacustrine and colluvial deposits discussed in Chapter 1. Figure 2.2 describes the stratigraphic relationships between the Cainozoic terrigenous, marginal marine and marine sediments.

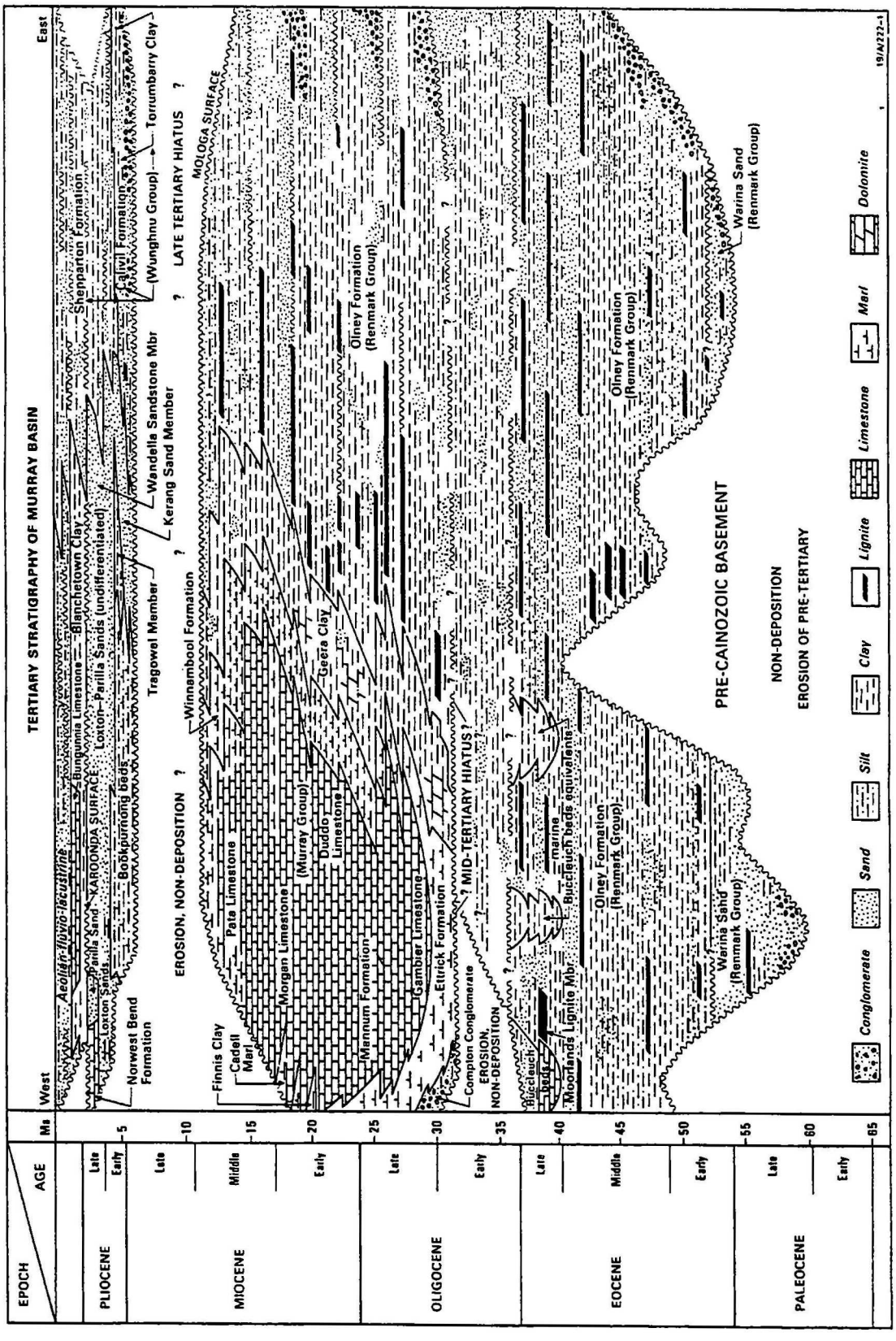

Figure 2.2 Tertiary Stratigraphy of the Murray Basin (from Brown & Stephenson, 1991a)

2.2 Paleocene to Lower Oligocene Sequence

2.2.1 Warina Sand (Tew)

In the model area, the Tertiary basal sediments are carbonaceous and fluvial showing minor marine influence. Deposition commenced in the Palaeocene-Eocene, around 60 Ma ago, with the partial infilling of the major troughs by medium to coarse quartz sands and minor interbedded carbonaceous fine sand, silt and clay of the Warina Sand. The sequence is thickest (150-250m) in the main depocentre, the Renmark Trough, and is absent over the basement highs. The sands are muscovite rich, implying that the metamorphic Broken Hill - Willyama Block had been a significant source of material. The sands also contain scattered pyritised wood fragments and can be partially lithified by siliceous or dolomitic cement. The thick, homogenous sand bodies indicate deposition by large, high discharge braided or anastomosed river systems.

2.2.2 lower Renmark Group (Ter1)

The lower Renmark Group sediments represent the continuation of fluvio-lacustrine deposition into the Late Oligocene. Like the Warina Sand, geometry is controlled by the depressions within the model area, with thicknesses reaching 150-200m in the Renmark and Tarrara Troughs and the unit absent over the basement highs. The top of the unit (Figure 2.3) tends to mimic the essential structural elements of the underlying basement. Lithologies include fine to medium quartz sands and carbonaceous silt and clay. Carbonised and pyritic plant remains, including fossil logs as well as interbedded lignite are characteristic. Palynological studies from this material place most of the sequence in the middle Eocene to early Oligocene *Nothofagidites asperus* zone (Kellett, 1989). Deposition of the silts and clays were in extensive floodplains and lakes, with sands deposited in meandering channels. Hence, the sequence contains more laterally discontinuous, finer grained units than in the underlying Warina Sands. However, in the Lower Darling region, the lower Renmark Group tends to be sandier than equivalent sequences found in the Riverine Plain, reflecting a coarser quartz-rich provenance.

2.2.3 Buccleuch Beds equivalents (Teb)

Late Eocene to Early Oligocene marginal marine sediments intersected in boreholes around Waikerie indicate a minor marine incursion into the lower Renmark Group sediments. Lithologies include glauconitic marls and carbonaceous sands with limestone bands. The unit has been tentatively correlated with marine sediments found in the equivalent stratigraphic position in the Buccleuch Embayment, found along the coastal margin of the Murray Basin.

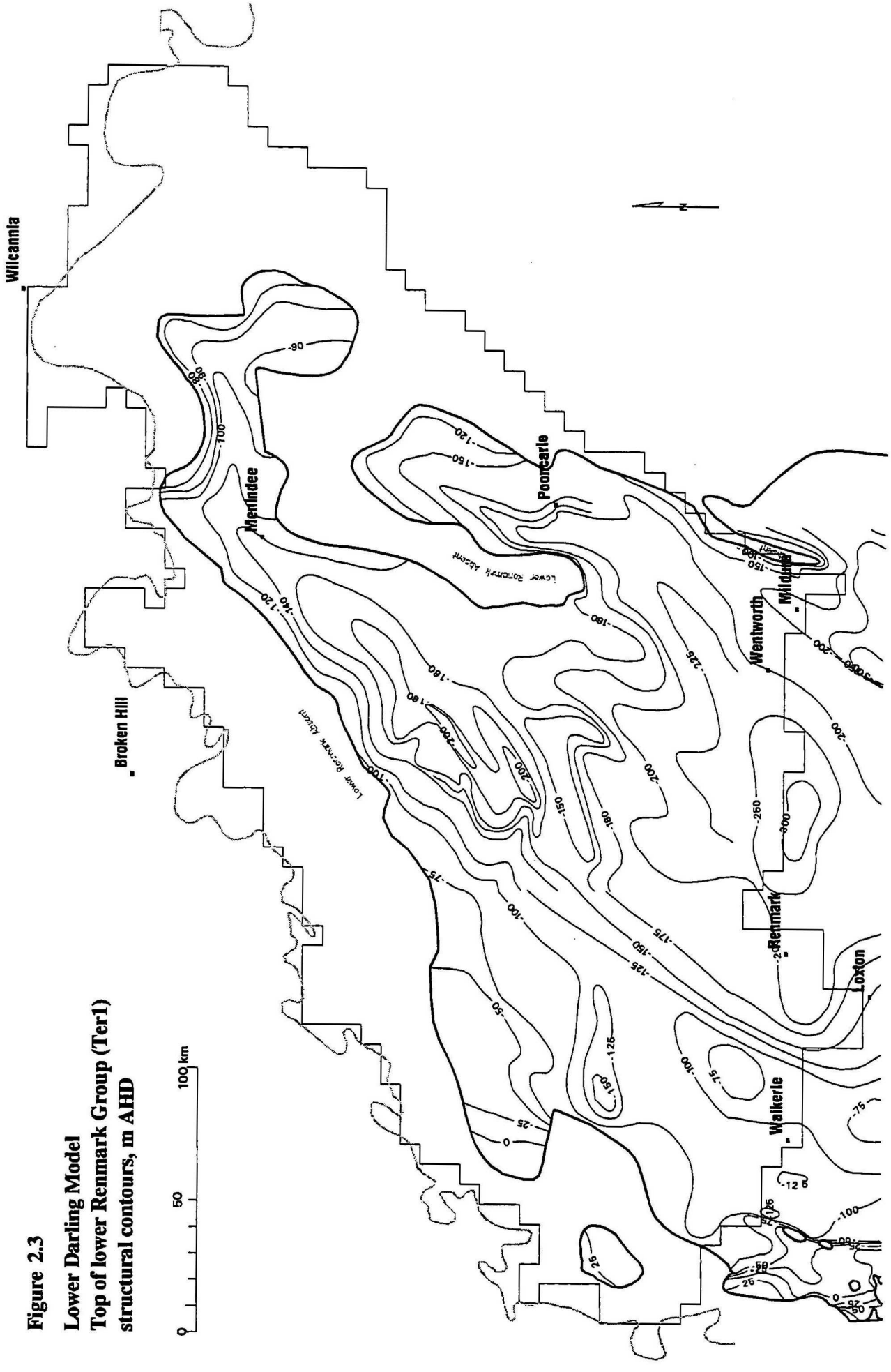

Figure 2.3
Lower Darling Model
Top of lower Renmark Group (Ter1) structural contours, m AHD

2.3 Oligocene- Middle Miocene Sequence

A possible Early Oligocene period of sub-aerial erosion and non-deposition was followed by a sustained period of marine invasion from the southwest, commencing about 32 Ma ago. This formed the glauconitic clays, marls and limestones of the Murray Group sequence which underlie the southwestern half of the model area.

2.3.1 Compton Conglomerate (Toc)

The initiation of the marine transgression deposited the Compton Conglomerate, a composite rock unit made up of partly cemented ferruginous quartz-pebble conglomerate, green glauconitic clay, brown humic clay and calcareous sandstone. The unit is limited to remnants along the western margin of the basin, in South Australia (Figure 2.4). Thickness is usually less than 20 metres, but can exceed 50 metres, particularly over structural highs.

2.3.2 Ettrick Formation (Toe)

Persistence of marine conditions is indicated by a continuous but thin layer of grey-green , glauconitic, highly fossiliferous calcareous clay, the Ettrick Formation, over the Compton Conglomerate and lower Renmark Group fluvial sediments. The unit is typically less than 25m thick. A maximum thickness of over 40m is found in the Renmark Trough and localised accumulations over 30m are found along the western margin of the basin (Figure 2.5). The sediments can be finely laminated or heavily bioturbated, contain dense micritic limestone and soft calcarenite interbeds and fragmented skeletal debris An abundant and diverse assemblage of bryozoans, molluscs, echinoids, foraminifera and dinoflagellates is characteristic. These lithologies are typical of a low energy shallow marine shelf environment. This ranges from deeper marine conditions in the southwest to restricted marine shelf and lagoonal conditions to the east and north. This is reflected in the carbonate content being highest towards the west, and with the formation becoming more argillaceous to the east and north.

2.3.3 Murray Group Limestone (Tml)

In turn, the Ettrick Formation is overlain by a series of Late Oligocene to Middle Miocene platform limestones, collectively named the Murray Group Limestone. The limestones are constrained within the lateral extent of the Ettrick Formation, in the southwestern half of the model. Two accumulations are apparent from the isopach map (Figure 2.6), the dominant depocentre of the Renmark Trough where thicknesses exceed 140m, and a subordinate accumulation centred around Waikerie where 100-120m of limestone is found. Localised thickening of the sequence is also apparent along the axes of the Tarrara and Wentworth Troughs. In the west, the limestone tends to be a skeletal calcarenite, becoming finer-grained and marly to the north and east. In South Australia, the sequence is subdivided into a series of limestone units (Mannum, Morgan and Pata) and is exposed along the walls of the Murray River gorge. The upper surface of the Murray Group Limestone shows a distinct ridge trending northeast from Woolpunda (Figure 2.7). For the purposes of the model, this is called the Woolpunda Ridge. To the west of this ridge is a depression centred over the Renmark Trough.

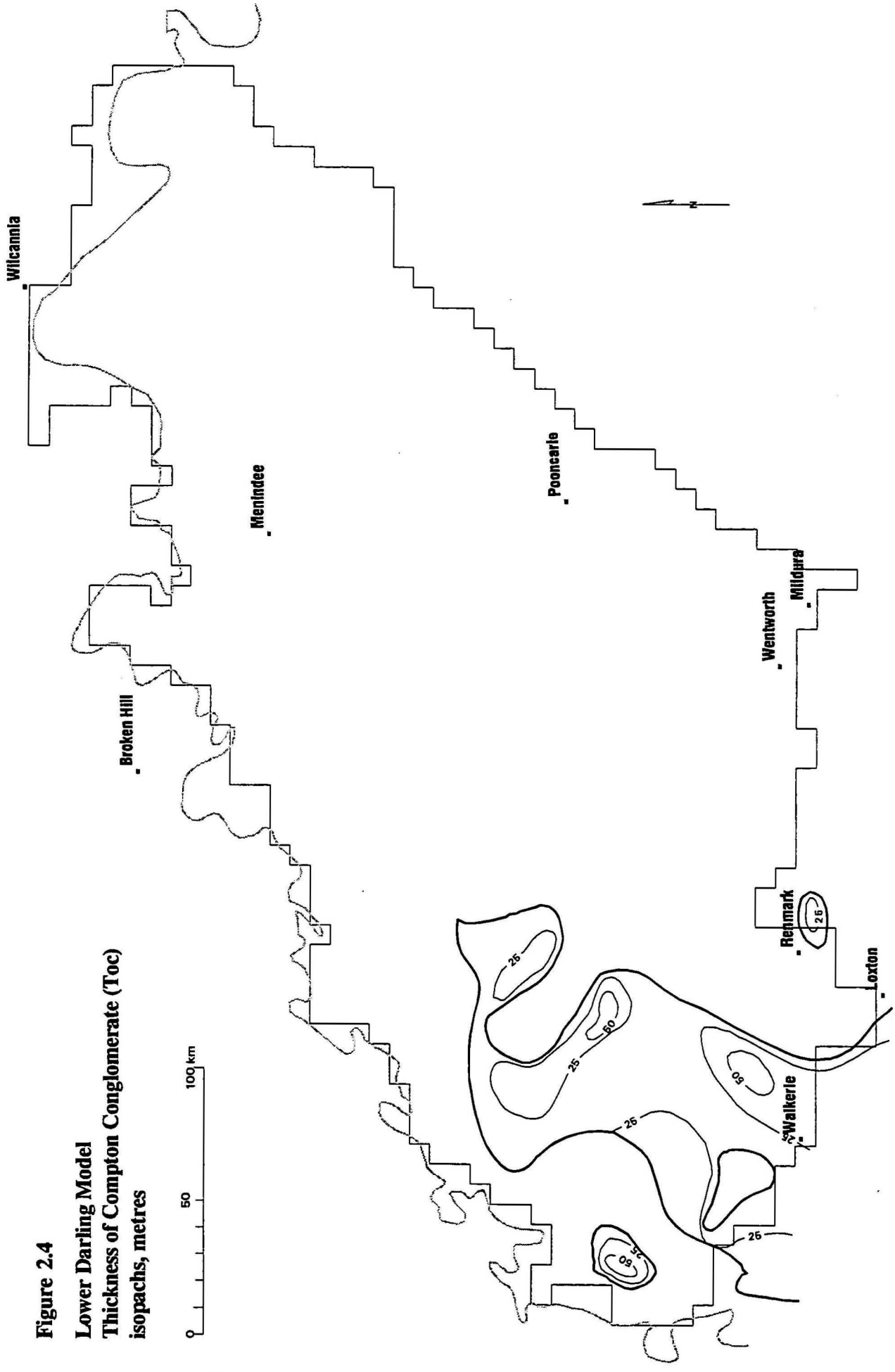

Figure 2.4
Lower Darling Model
Thickness of Compton Conglomerate (Toc) isopachs, metres

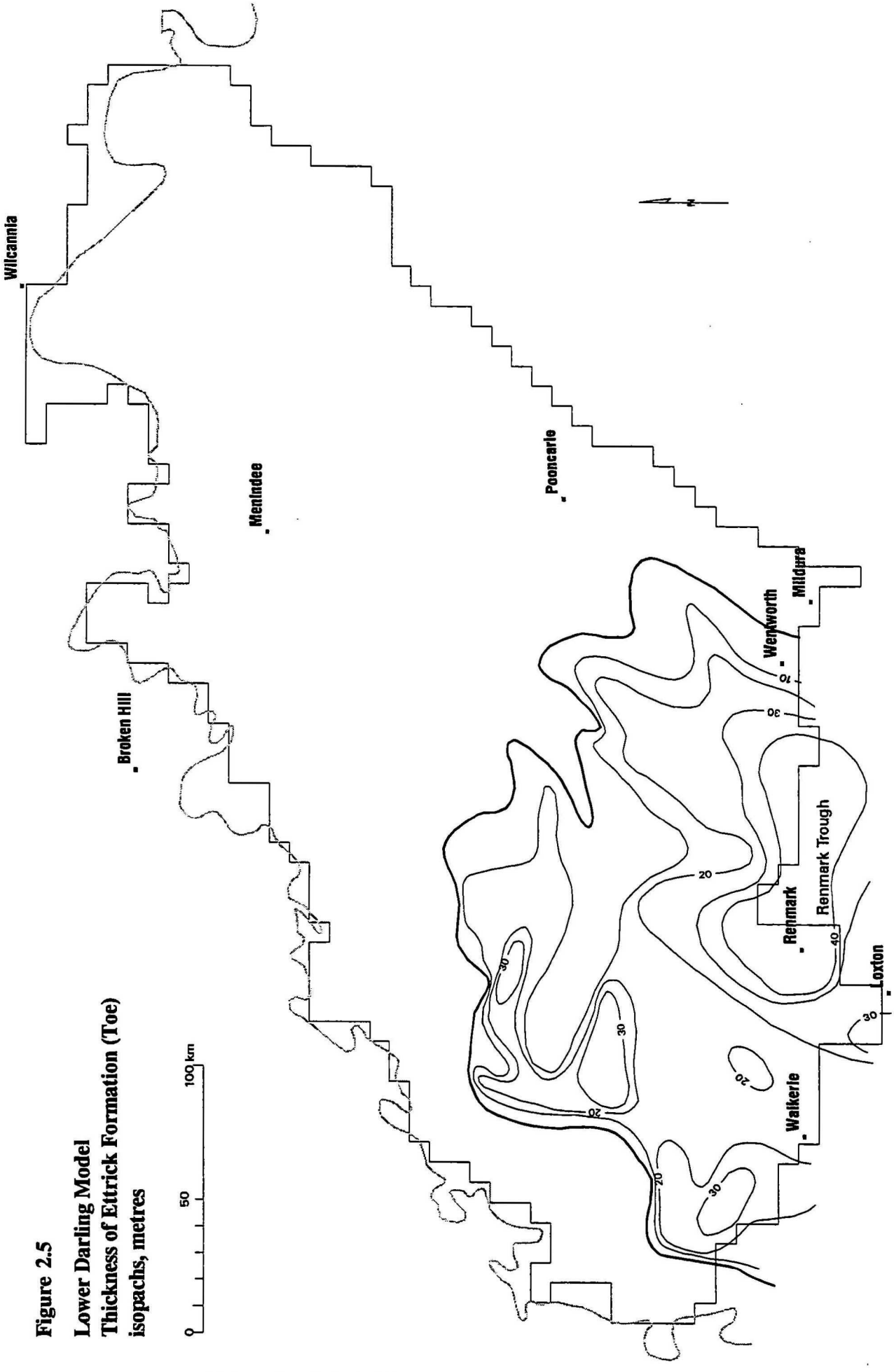

Figure 2.5
Lower Darling Model
Thickness of Ettrick Formation (Toe) isopachs, metres

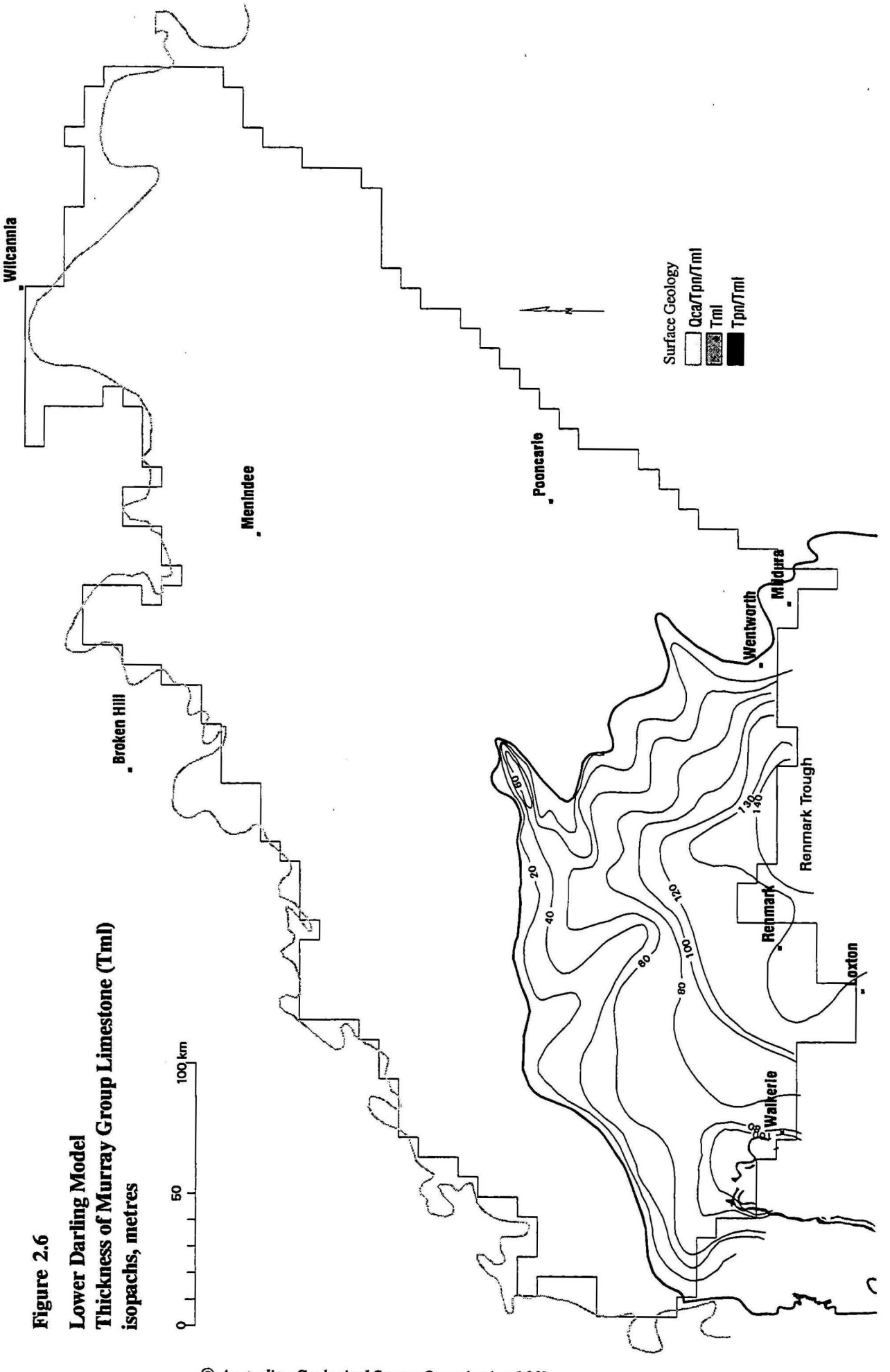

Figure 2.6
Lower Darling Model
Thickness of Murray Group Limestone (Tml) isopachs, metres

2.3.4 Winnambool Formation (Tmw)

Contemporaneous with the formation of the platform limestones during the Late Oligocene to Middle Miocene was landward deposition of the Winnambool Formation in shallow restricted marine and lagoonal environments. This is the richly fossiliferous glauconitic calcareous clay and silty clay with minor limestone interbeds that flank the Murray Group Limestone to the north and east. The unit forms a zone mostly 70-100km wide, commencing west of Morgan, arcing north and east past Mildura (Figure 2.8). Pods 60-100m thick are aligned along the central axis of this arc. The formation is the younger depositional equivalent to the Ettrick Formation, which pre-dates and underlies the platform limestone sequence. Due to the subdued topography, minor fluctuations in sea level resulted in large lateral movement in the boundaries between the shallow marine facies. This is indicated by extensive interfingering between the Murray Group Limestone and the Winnambool Formation.

2.3.5 Geera Clay (Tmg)

The Winnambool Formation grades laterally and interfingers with the Geera Clay, made up of dark sticky muds, silt, clay and minor sand and dolomite. The silt and clay are quartz-rich, glauconitic, pyritic and locally calcareous. The dark colour is attributed to abundant organics and disseminated iron sulphides. The unit is typically massive and bioturbated with minor fine laminations and cemented zones. Towards the north and east the silty muds become increasingly carbonaceous and interbedded with peat and ligneous sands. The lithologies indicate that the Geera Clay was deposited in shallow to marginal marine environments, grading landwards towards estuaries and deltas. The distribution of Geera Clay shows a similar pattern to that of the Winnambool Formation, but displaced to the northeast (Figure 2.9) An arcuate zone 50-150km wide spans across the centre of the model area, containing localised accumulations 60-100m thick. The isopachs indicate offshoots up into the Redan Embayment and the Tarrara Trough. These are part of the maximum extent of the Oligocene-Miocene marine transgression into the Murray Basin. The northeast trending zone of thinning apparent in the isopachs corresponds to the Lake Wintlow structural high.

2.3.6 middle Renmark Group (Ter2)

In the northeastern half of the model area, fluvio-lacustrine conditions persisted through to the Middle Miocene. Hence, the middle Renmark Group are the terrigenous carbonaceous clays, silts and quartzose sands deposited by river systems, deltas and coastal swamps during the period when the Murray Group Limestones were being formed. This has resulted in a wedge of sediments constrained by the basin margin to the northwest and north, by marine deposition to the southeast and partially covering the Neckarboo Ridge structural high (Figure 2.10) The stuctural contours of the top of the middle Renmark Group mimic the underlying basement with a major low superimposed over the Tarrara, Menindee and Blantyre Troughs as well as a similar feature over the Wentworth Trough. The thickness of the unit is usually 40-80m, increasing to 100-160m in the troughs. Due to high base levels during this time, a low energy depositional environment has resulted in the middle Renmark Group being the finest grained sequence in the Renmark Group sediments. Grey carbonaceous micaceous silts, black humic clays, lignites and fine quartzose sands are typical lithologies. The early Oligocene to early Miocene *Proteacidites tuburculatus* zone occurs within these sediments (Kellett, 1989).

Figure 2.7

Lower Darling Model
Top of Murray Group Limestone (Tml)
structural contours, m AHD

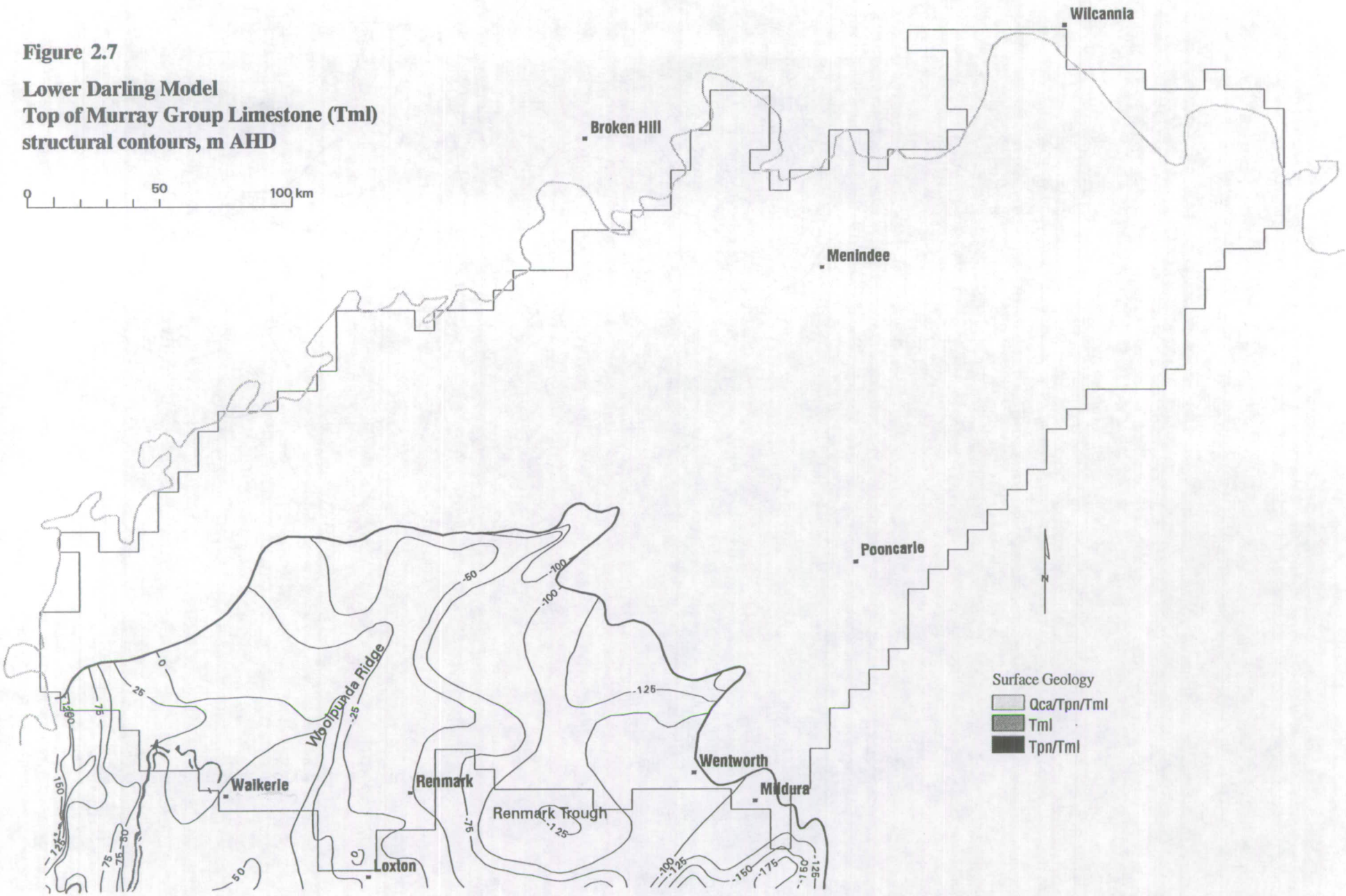

Figure 2.8

Lower Darling Model
Thickness of Winnambool Formation (Tmw) isopachs, metres

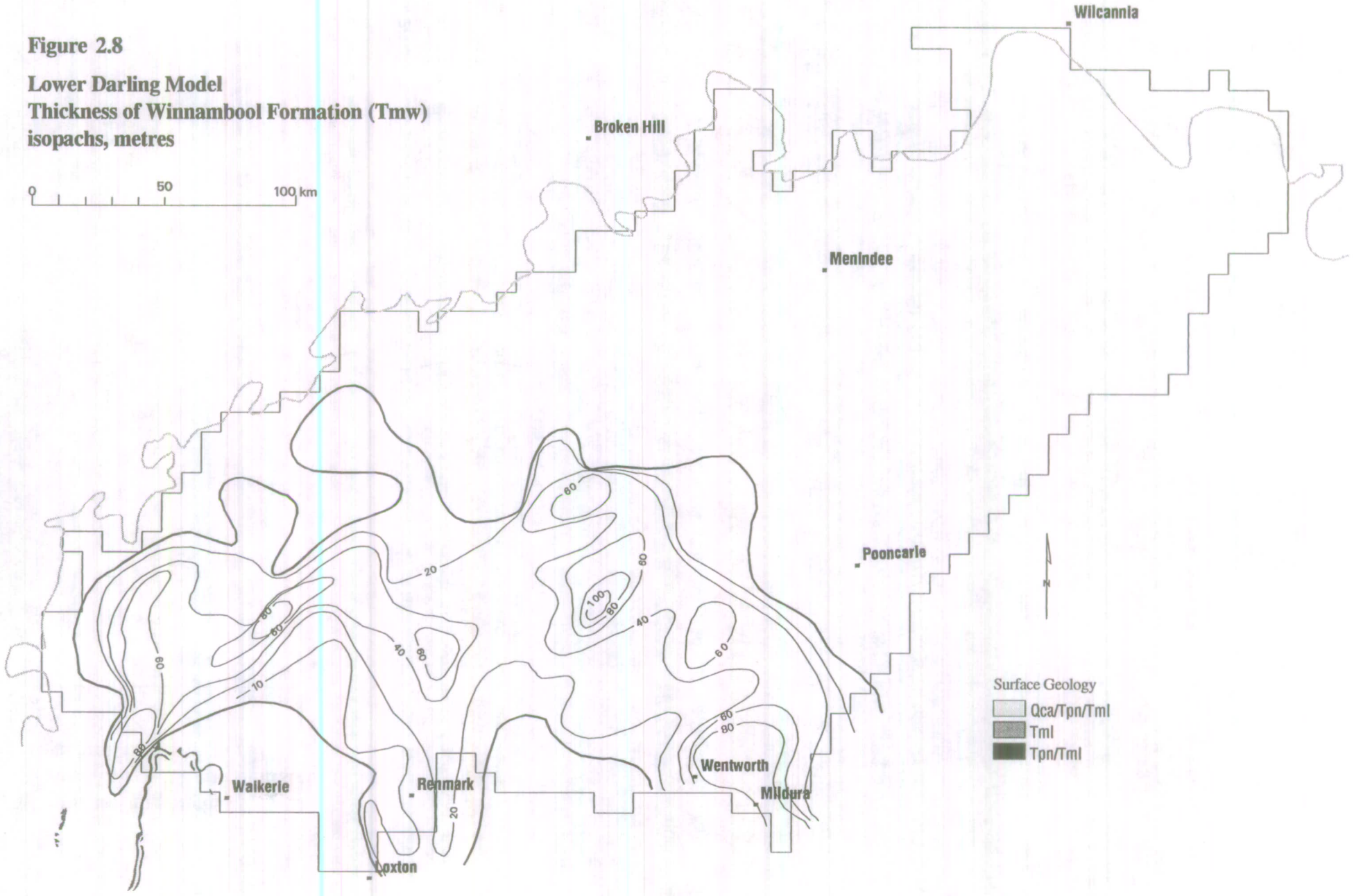

Figure 2.9

Lower Darling Model
Thickness of Geera Clay (Tmg) isopachs, metres

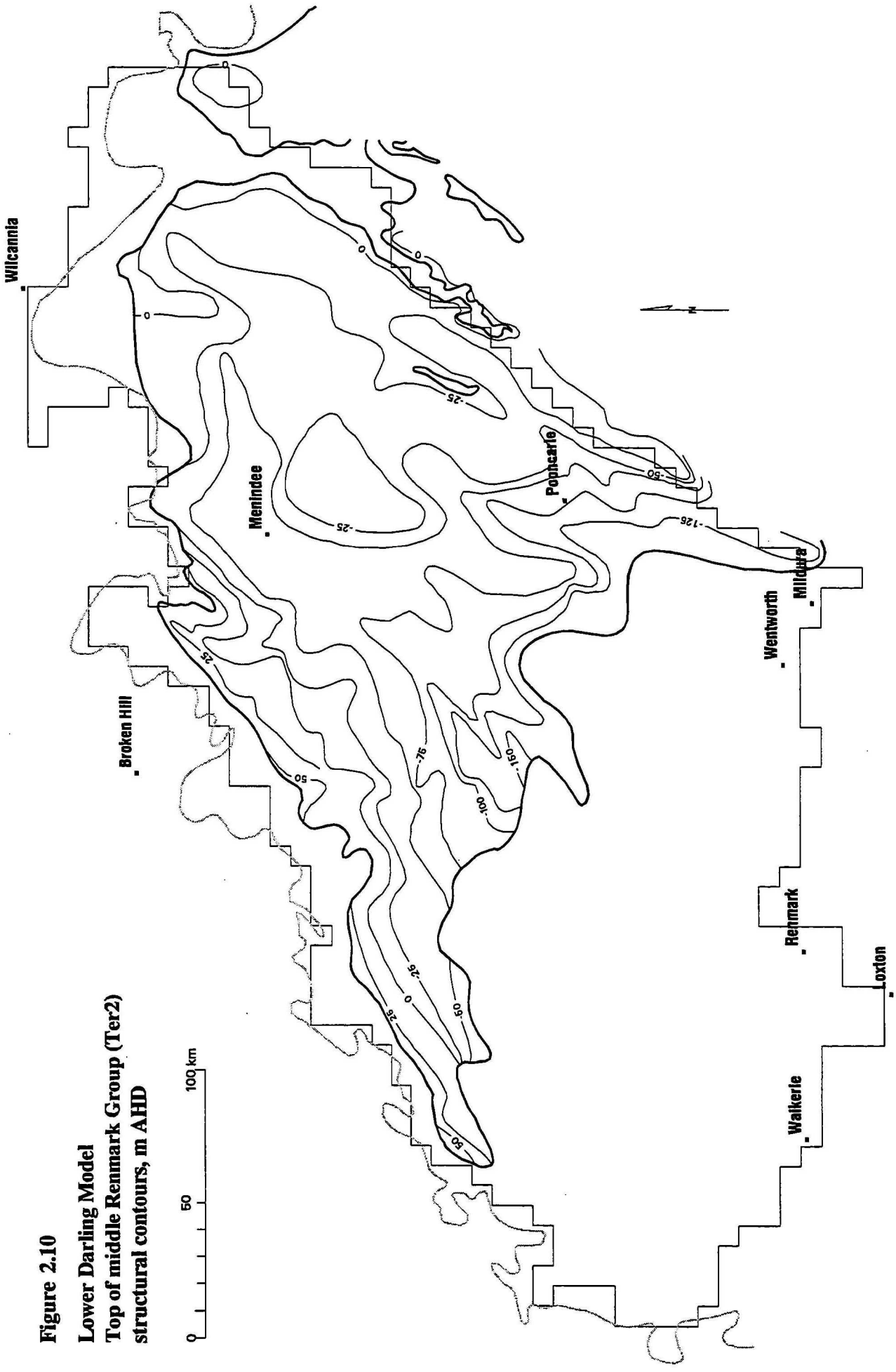

Figure 2.10
Lower Darling Model
Top of middle Renmark Group (Ter2) structural contours, m AHD

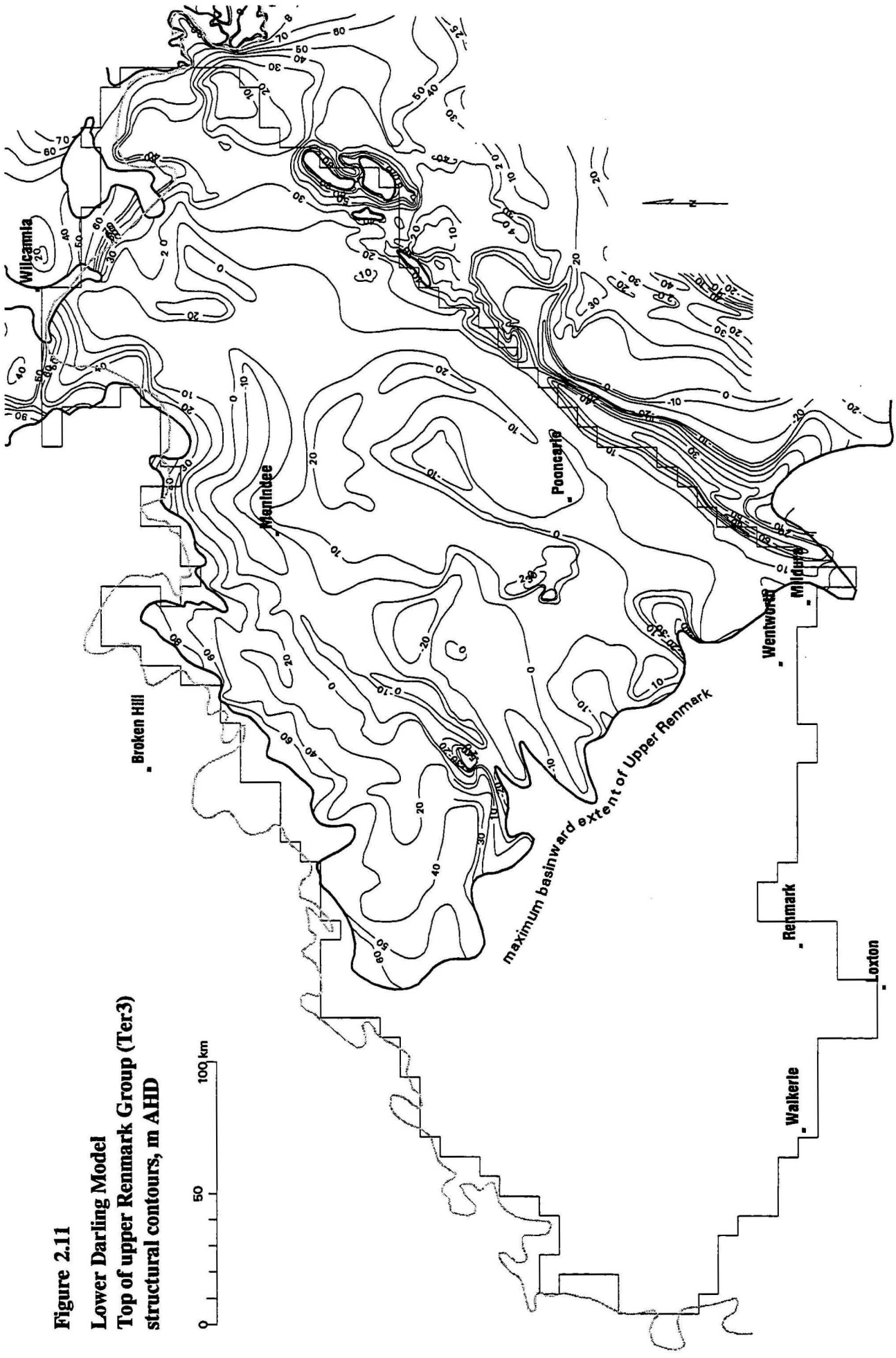

Figure 2.11
Lower Darling Model
Top of upper Renmark Group (Ter3) structural contours, m AHD

2.3.7 upper Renmark Group (Ter3)

The subsequent retreat of the sea during the mid-Miocene resulted in the Geera Clay and Winnambool Formation extending southwestwards back over the top of the Murray Group Limestones (refer Figure 2.2). Similarly, the youngest part of the Renmark Group sediments , the upper Renmark Group, progrades over the Geera Clay. The maximum basinward extent of this is shown in the structural contours for the top of the upper Renmark Group (Figure 2.11). The sequence pinches out towards the northwest onto the basement highs but, with the exception of around scattered Devonian outcrops, covers the Neckarboo Ridge. Similar Miocene fluvial sediments also extend northwards up into the Darling floodplain. Thickness varies from 40-60m in the Wentworth and Tarrara troughs to <20m over structural highs. The sediments are generally coarser grained than that of the middle Renmark Group and consist of grey fine to medium ligneous quartz sands, micaceous silts and green-grey plastic clay. The sequence corresponds to the mid to late-Miocene *Triporopollenites bellus* zone (Kellett, 1989).

2.3.8 Geera Clay equivalent (Tmge)

Sandy clays found laterally between the Geera Clay and both the middle and upper Renmark Group have been informally named the Geera Clay equivalent (Macphail *et al*, 1993). The unit is difficult to differentiate from the fluvio-lacustrine sands and clays, but contains marine dinoflagellates and chitonous remains of foraminifera. The sequence is generally upwards coarsening and like the upper Renmark Group, progrades over the Geera Clay. Hence the unit is interpreted to have been deposited during periods of marine retreat. The marginal marine unit has been dated as early to mid-Miocene.

The final retreat of the sea in the late Miocene was followed by a period of non-deposition and weathering of the basin sediments. This resulted in the Mologa Surface, typically represented as reddish-brown mottling and ferrugenisation of the uppermost 5-10m of the upper Renmark Group sands, silts and clays. The preferred timing for this hiatus is 10.5 Ma (Macphail *et al*, 1993).

2.4 Upper Miocene - Pliocene Sequence

2.4.1 Bookpurnong Beds (Tpb)

The upper parts of the Tertiary sequence in the model area relate to a marine incursion and subsequent retreat during the late Miocene to Pliocene, commencing about 6 Ma ago. The initial sea level rise deposited the Bookpurnong Beds, a sequence of glauconitic fossiliferous clays and marls, in the southern-central part of the model area (Figure 2.12). Over the northwest trending Miocene structural highs in this area the beds are absent or thin to <10m. Maximum thicknesses of 30-50m correspond to the Tarrara and Renmark Troughs. The sediments contain a distinctive shelly macrofauna dominated by bivalves, with gastropods and scaphopods. These are typical of low-energy marine shelf conditions.

2.4.2 Loxton-Parilla Sands (Tps)

The Bookpurnong Beds are flanked laterally to the east and north by the basal late Miocene component of the Loxton-Parilla Sands. The sands were also later deposited as an extensive sheet over the Bookpurnong Beds during the marine regression in the early Pliocene. The dominant lithology is yellow brown, weakly cemented, fine to coarse, well sorted quartz sand containing trace molluscs and pelecypod casts and bioturbation features. The sands also contain disseminated heavy minerals, and host economic deposits of zircon, tourmaline, ilmenite, leucoxene and rutile. Poorly sorted micaceous quartz sand, silt and clay are minor lithologies. Clay constitutes less than 15% of the lithologies but tends to increase at depth (Ferguson & Radke, 1992).

The unit is interpreted to have been deposited in various shelf to strandplain settings, such as shallow marine, beach , barrier bar and estuarine with crosscutting entrenchment by younger river systems. Regressive upward-coarsening sequences with lenses of disarticulated shells and heavy minerals support these depositional environments (Ferguson & Radke, 1992). The top surface of the Loxton-Parilla Sands is characterised by northwesterly arcuate ridges, which are the remnants of former coastal ridges, with intervening swales (Figure 2.13). The Millewa Ridge, south of Lake Victoria, is the largest of these strand lines in the area with an elevation of over 50m. The sands form an extensive cover up into the Menindee and Blantyre Troughs and over the southern half of the Neckarboo Ridge. The average thickness is 40-50m, increasing to 70-80m in the Renmark Trough and decreasing to 10-20m over Miocene structural highs.

2.4.3 Calivil Formation (Tpc)

During the marine transgression which deposited the Bookpurnong Beds in the late-Miocene to early Pliocene, fluvial-lacustrine environments prevailed in the northeast of the model area. This resulted in the deposition of the Calivil Formation along the margins of the basin, up into the Darling floodplain and over most of the northerly half of the Neckarboo Ridge (Figure 2.13) The top surface of the formation is characterised by palaeochannels draining the surrounding basement ranges. Some of the major floodplain lakes along the Darling (Menindee, Tandou, Cawndilla) are positioned where major drainage lines intersect the margin of Loxton-Parilla Sands deposition. Typical lithologies are pale yellow, white or brown kaolinised fine to coarse quartzose sand with interbedded clays and silts. The bleached, kaolinitic material may reflect active erosion of basement which was deeply weathered in the late Miocene (Mologa Surface). The sands can be partly to strongly ferrugenised and silcrete hardpans are evident. The sediments are lithologically similar to the underlying upper Renmark Group, but have a lower lignite content and a higher coarse sand content. The unit has an average thickness of 30-40m, with greater deposition (50-60m) in a large palaeochannel system down the trace of the Blantyre and Wentworth Troughs.

2.4.4 Norwest Bend Formation (Tpn)

In the extreme southeastern corner of the model area, a resistant capping of between 1 to 12m of Norwest Bend Formation sediments is found over the shallow Murray Group Limestone. This is a pale grey to yellow coquinoid calcarenite, made up of oyster shell detritus in a localised quartz sand matrix. The oyster beds were formed in a high energy estuarine setting within a drowned valley of the ancestral Pliocene Murray River.

2.4.5 Shepparton Formation (TQs)

During and after the early Pliocene regressive phase which deposited the marginal marine Loxton-Parilla sand sheet basinwards, fluvial and lacustrine deposition was maintained in the northeast half of the model area. This resulted in Shepparton Formation sediments overlying the Calivil Formation and Loxton-Parilla Sands. The sequence consists of poorly consolidated clay and silts with lenses of polymictic fine to coarse sands. The multicoloured, mottled clays, numerous palaesols and hardbands indicated modification by pedogenesis. The sequence is typically 30-40m thick, ranging from 10-20m over Miocene highs to 50-60m in the palaeochannel tracing the Blantyre and Menindee Troughs. Channel fill and alluvial fans can be found on the margin of a local high centred over the Lake Wintlow High.

2.5 Quaternary Sequence

2.5.1 Blanchetown Clay

A late Pliocene uplift of the Pinnaroo Block resulted in the tectonic damming of the ancestral Murray River, forming the freshwater megalake, Lake Bungunnia, about 2.5 Ma ago. The Blanchetown Clay represents the silty to sandy clays, micrite lenses and dolomitic limestones deposited on the lake bed. The distribution of sediment is patchy and largely controlled by the late Pliocene topography (Figure 2.14), reaching northwards to the Menindee Lakes and eastwards to the margins of the Neckarboo Ridge. The lake covered over 33,000 km^2 and had a maximum depth of 70m (Stephenson, 1986). The unit is typically <10m thick but several depocentres where thickness exceeds 20m are apparent. The isopachs also indicate where Pliocene highs had formed islands and ridges into the lake system. Post-depositional erosion, such as deflation within saline lakes, has also altered geometry. The clays are green-grey or brown and can contain calcareous nodules, ostracod debris and gypsum. Increased gypsum levels at the top of the sequence relate to when the system retreated to a series of smaller hypersaline lakes with the onset of aridity about 0.6Ma ago. Sedimentological studies of the Blanchetown Clay at Nulla Spring Lake supports the progressive increase in lake salinities from fresh to hypersaline, punctuated by rapid fluctuations (Ferguson & Radke, 1992). The Yamba Formation (Qly) in ephemeral and fossil salt lakes found in local depressions represent more recent lacustrine deposition under groundwater discharge conditions. The onset of aridity is also evident in the deflation and remobilisation of the Loxton Parilla Sands by prevailing westerly winds to form the extensive Quaternary dune fields (refer Figure 1.8, Chapter 1.3).

Deposition of alluvial sediments also prevailed through the Quaternary, manifested as the Coonambidgal Formation (Qa) of the floodplain of the Murray and Darling river system. These sediments are entrenched into aeolian modified terraces of Shepparton Formation.

To the southwest a weathering profile consisting of ferricrete duricrusts, silcrete cements, limonite pisolites and a kaolinitic matrix was developed over the top 5-15m of the Loxton Parilla Sands. This Karoonda Surface produced the calcrete deposits (Qca) along the basin margins in South Australia.

Figure 2.12

Lower Darling Model
Thickness of Bookpurnong Beds (Tpb) isopachs, metres

Figure 2.13

Lower Darling Model
Top of Pliocene Sands (Tps/Tpc) structural contours, m AHD

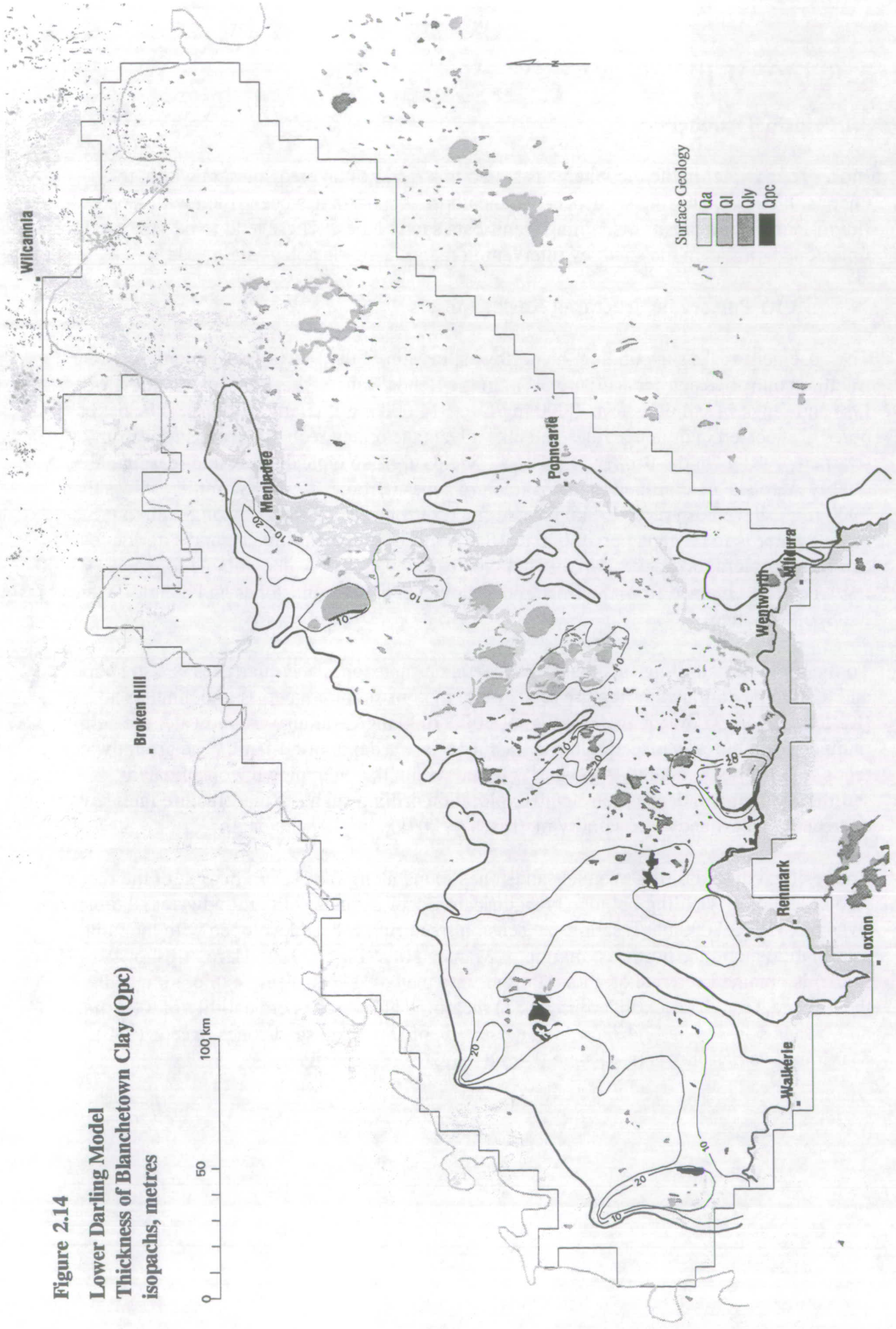

Figure 2.14
Lower Darling Model
Thickness of Blanchetown Clay (Qpc) isopachs, metres

3. REGIONAL HYDROGEOLOGY

3.1 Principal Aquifers

Most groundwater in the model area is stored in a series of layered aquifers within the unconsolidated Cainozoic sequence. To the north, the basin has been filled with mostly fluvio-lacustrine deposits containing significant sand bodies. These tend to be separated from limestone aquifers in the south by intervening marginal marine clays and marls.

3.1.1 Palaeozoic Fractured Rock Aquifers

The basement rocks surrounding the northwest margin of the Murray Basin contain minor fracture controlled aquifers (Figure 3.1). In the Benda Range, these are low yielding (<0.5 L/s) and range in salinities from 3000 mg/L to >14,000 mg/L (Barnett, 1994). The better bores are located in drainage lines and take advantage of any recharge from surface run off (Barnett, 1981). On the Broken Hill Block, yields are also typically low and reasonable quality supplies are confined to major fracture zones (Brodie, 1994). Salinities of less than 3000 mg/L have been recorded in isolated fracture zones along the Hillston Fault, but most groundwater is in the range of 10,000 to 18,000 mg/L. Elevated sulphate and fluoride levels can be a problem for stock. Variable but mostly low yields of water suitable for stock (<3000 mg/L) can be obtained from the fractured Ordovician quartz sandstones and conglomerates of the Scopes Range.

To the northeast, drilling success in the Devonian sandstones and quartzites is also sporadic and tend to be confined to fracture sets around major structures such as anticlinal axes (Kellett, 1994a). Low yields (<0.5L/s) of 3000-7000 mg/L salinity groundwater are being pumped from bores intersecting these fracture sets at a depth of 50-80m. The groundwater tends to be of better quality than what is found within the onlapping unconsolidated sediments. Limited deeper petroleum exploration drilling suggests that fracture intensity decreases and groundwater salinity increases (> 20,000 mg/L) with depth.

The residual outcrops of Devonian sandstones found along the eastern margin of the model also contain low yielding but locally significant fracture zones with groundwater suitable for livestock (3000-7000 mg/L salinity). Tension fracturing is best developed with the fault termination along the northeast margin of Manara Hills (Figure 3.1). Here, fresh water (750 mg/L) is obtained at a rate of 2 L/s. Further into the basin, petroleum exploration drilling in the Tarrara Trough (A.O.G Tarrara No. 1) measured an average permeability of .007 m/d and an average porosity of 13.4% for the intersection of Devonian sandstones (Reed, 1980). Maximum values encountered were 0.4m/d and 20.8% respectively.

3.1.2 Permian Aquifer/Aquitard

The Urana Formation (Pl), with a dominance of argillaceous glacial sediments, constitutes a confining bed. However, interbedded aquifers made up of poorly sorted coarse sandstones are found. For instance, drill stem tests on the Permian basal sand intersected by Monash No 1 in the Renmark Trough indicated good permeability (Reed, 1980). The groundwater in the formation was saline and under artesian conditions.

3.1.3 Cretaceous Aquifer/Aquitard

The fluvial to marine friable sandstones of the basal Pyap Member of the Merreti Formation (Kl) found in bores drilled into the Renmark Trough also have aquifer properties with measured porosities ranging between 26 to 41% (Reed, 1980). Groundwater is saline, at about 30,000 mg/L. The middle Merreti Member and upper Coombol Member, are dominated by mudstones and siltstones, particularly in the deeper troughs towards and including the main depocentre, the Renmark Trough. Hence, these sequences tend to confine the underlying basal Pyap Member and any Lower Permian sands. In Loxton No 1, ten kilometres southeast of its namesake, groundwater with a salinity of 4760 mg/L was intersected within coarse sands of the Coombol Member (Reed, 1980).

The weathering surface developed over the Upper Cretaceous can form an effective permeability barrier between the Cretaceous aquifers and the groundwater system in the overlying Renmark Group sediments. However, to the northeast, a degree of hydraulic conductivity is afforded by thinning or absence of this weathering profile. The hydrogeology for the Cretaceous sediments has only been mapped in any detail for the IVANHOE and WILCANNIA topographic mapsheets. Figure 3.1 shows some of this mapping in the northeast corner of the model. Here, around the Devonian outcrops of the Cobar Block, the Cretaceous sediments form a low-yielding but locally significant shallow aquifer. Groundwater useable for livestock with salinities of about 9000-11,000 mg/L are found in a 10-30km corridor along the basin margin, where the aquifer is unconfined and subject to episodic recharge from ephemeral streams (Kellett, 1994b). In this zone, the aquifer can be stratified with deep groundwater separated from shallower, more saline groundwater by silicified hard bands. Down basin, the aquifer is higher yielding but also has higher salinities (>35,000 mg/L). Groundwater flow is to the west and northwest, constrained by components of the Neckarboo Ridge such as the Manara Hills. Near Ivanhoe, the Cretaceous aquifers in the Murray Basin proper also receive westwards flow from unconfined equivalents in a smaller basin to the east, the Hampton Sub-Basin, via two disruptions or chokes in the intervening basement high.

Figure 3.1

Lower Darling Model
Pre-Cainozoic and lower Renmark Group Aquifers
Salinity/Yield & SWL

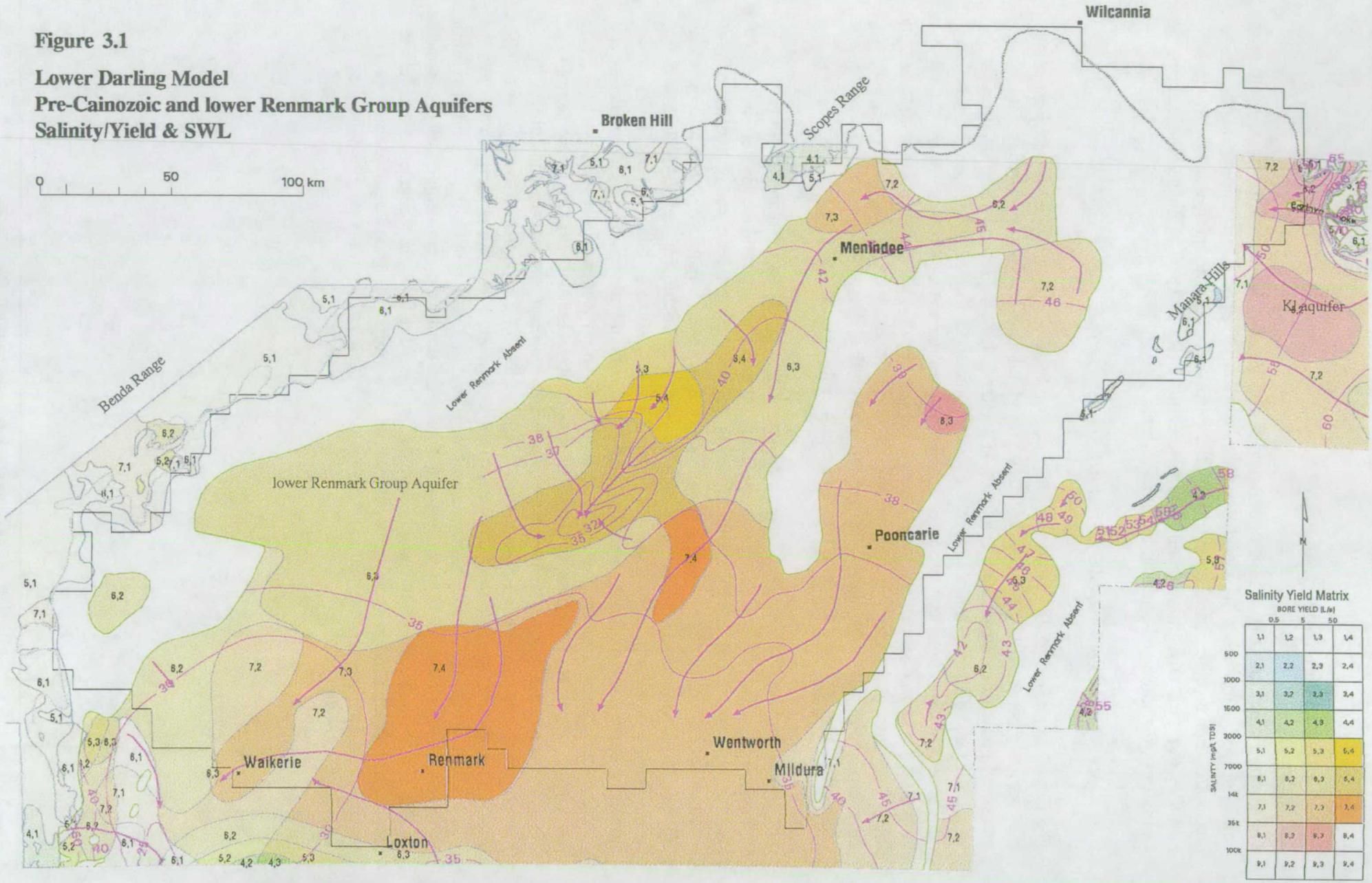

3.1.4 lower Renmark Group Aquifer

The basal aquifer of the Tertiary sequence, the lower Renmark Group aquifer, is confined to the major troughs in the model area (Figure 3.1). In the Blantyre, Menindee and Tarrara Troughs, groundwater tends to flow down-basin to the west and southwest, parallel to the trough bounds. Hydraulic gradients in this area are low, around 5-10 cm/km. Along the northwest margin of the sediment pile, the flow direction is initially to the south or southeast, orthogonal to the aquifer margin. Coupled with a relative freshening of the groundwater (about 6000 mg/L), this suggests downward leakage from the overlying aquifers along this corridor. The main locus of flow is the southwestern corner of the model area, near Woolpunda. Here, the groundwater continues to flow southwards and out of the model. Limited water level measurements in the area suggest that the Tarrara Trough also acts as a localised groundwater sink. Artesian conditions prevail in the southern half of the model area, particularly for bores located in topographic depressions.

Useable groundwater is limited to a 5-60km zone parallel to the northwest margin of the aquifer (Figure 3.1). Here typical salinities are 11,000-13,000 mg/L with isolated fresher pods with salinities < 6000 mg/L. To the north of this zone, in the Wentworth and Blantyre troughs, the groundwater is more saline, ranging 14,000-40,000 mg/L. This may relate to the finer grained nature of the sediments, lessening the flow through of groundwater. In this area, most of the recharge is thought to be via bed leakage of the Darling River system further to the north (Kellett, 1994a). The lower Renmark Group aquifer in the upper parts of the Wentworth Trough also has saline groundwater found in a relatively finer grained sequence.

Aquifer yields are generally very good and exceed 5 L/s. This reflects the significant interbeds of fine to medium micaceous quartz sands found in the fluvial sequence. Sustainable aquifer yields of over 50 L/s are reached in the central axes of the basins, particularly the Menindee, Tarrara and Renmark Troughs. This is accounted for by the partial filling of the troughs by medium to coarse quartz sands of the Warina Sand.

3.1.5 middle Renmark Group Aquifer

The middle Renmark Group aquifer extends over the lower Renmark Group aquifer in the northeast half of the model area, pinching out down basin by a thickening marginal marine sequence (Figure 3.2). Like the lower Renmark Group aquifer, groundwater flow is to the southwest and directed by the basin structure of troughs and ridges. In the northwest, groundwater flow is off the margins of the Broken Hill Block and the Scopes Range and down the axis of the Redan Embayment. The regional flow system is also overprinted by a groundwater mound under the Menindee Lakes storages. Along the eastern model boundary, groundwater flows initially to the west and northwest off the flank of the Neckarboo Ridge, which acts as a groundwater divide.

Groundwater salinity increases southwards down the flow path. The freshest groundwater, with a typical salinity of 2000 mg/L is found along the western margin of the Scopes Range. A dilution effect by the Darling River system is apparent for the middle Renmark Group aquifer. The main factor controlling the increase in salinity down gradient is the increasing thickness of interbedded and overlying Geera Clay. For example, the northern part of the

aquifer abutting the Broken Hill Block has no Geera Clay overlying it and has groundwater suitable for livestock (3500 mg/L). Southwards along the margin where Geera Clay becomes progressively thicker, salinity increases to around 10,000 mg/L. Sulphate levels can also exceed 1000 mg/L and borehole corrosion can be a problem. The salinity exceeds 35,000 mg/L along the basinward margin of the aquifer.

Sustainable aquifer yields are typically low (<0.5 L/s) where the aquifer thins out over the basement margins. This not only reflects a reduction in aquifer thickness but also a decrease in grain size of the sediments. The sediment pile becomes coarser and thicker with the development of significant fluvial systems along a corridor defined by the Blantyre, Menindee and Tarrara Troughs. This is indicated by higher aquifer yields (5-50 L/s) in this area.

3.1.6 Murray Group Limestone Aquifer

The Murray Group Limestone is limited in extent to the southern third of the model area (Figure 3.2). The Geera Clay and Winnambool Formation form a lateral permeability barrier between the Murray Group Limestone aquifer and the middle Renmark Group aquifer to the northeast. Not only are these marginal marine sediments finer grained, but also a significant store of salt. The Ettrick Formation forms a thin (10-30m) aquitard between the limestone and the underlying lower Renmark Group aquifer.

Groundwater flow in the Murray Group Limestone is directed towards the southwest margin of the model, basically the reach of the Murray River between Renmark and Morgan. West of the Hamley Fault in this area, the limestone platform is elevated and the aquifer becomes unconfined. Natural groundwater mounds have developed on both sides of the Woolpunda Reach of the river between Waikerie and Overland Corner, induced by upward leakage from the lower Renmark Group aquifer. The main mechanism for this is the dramatic thinning of the deeper aquifer on the upthrown western block of the Hamley Fault (refer Figure 3.7). The Ettrick Formation also thins to <10m over the structural high, allowing greater upward movement of groundwater from the lower Renmark Group aquifer. The groundwater mounds have steepened the gradients towards the river from a regional average of 20cm/km to 1-2 m/km, resulting in inflows of 200 tonnes/day of salt (Barnett, 1991). The Woolpunda Interception Scheme operates to remove saline groundwater before it reaches the river, pumping it to the Stockyard Plain Disposal Basin.

Irrigation development along the riverine corridor has also created localised groundwater mounds in the unconfined limestone aquifer. For example, the irrigation development around Berri and Barmera has elevated the watertable by over six metres, steepening hydraulic gradients towards the floodplain and Lake Bonney. An interception scheme located between the groundwater mound underlying the Waikerie Irrigation Area and the river, removes 105 tonnes/day from the aquifer.

Figure 3.2

Lower Darling Model
middle Renmark Group/Murray Group Limestone
Salinity/Yield & SWL

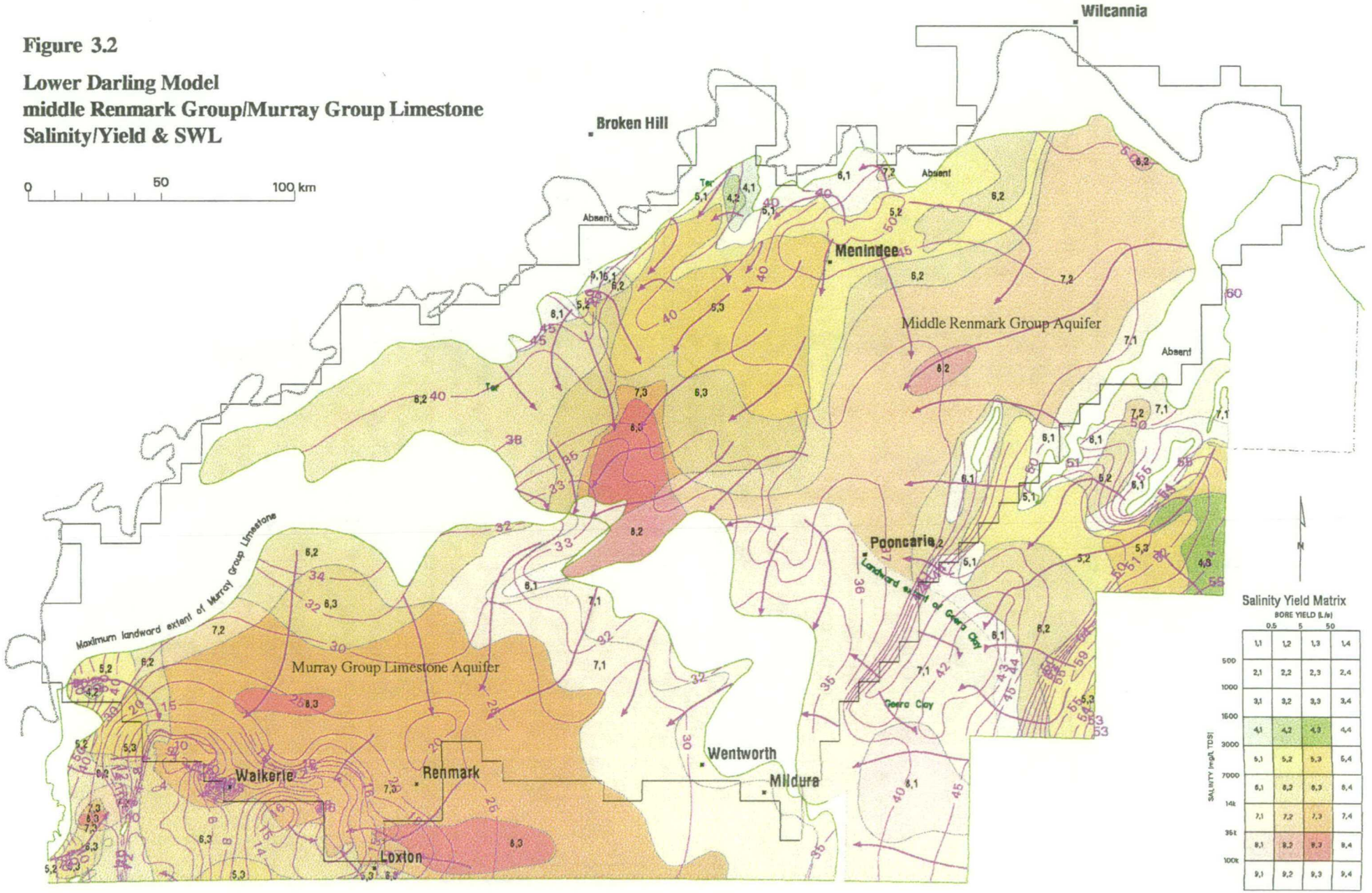

Most of the groundwater in the Murray Group is too saline for use, typically over 20,000 mg/L. However, ephemeral recharge from the Burra and Newikie Creeks has freshened Murray Group Limestone groundwater in the southwestern extreme of the model area, allowing it to be used for livestock (Barnett, 1994). Also, a marginal resource (<14,000 mg/L) is found along the northern bounds of the aquifer where the enveloping marginal marine sediments are relatively coarser, allowing leakage from shallower aquifers.

Sustainable aquifer yield increases down basin with thickening of the platform limestone unit. The aquifer is particularly low yielding (< 0.5L/s) along the eastern landward margin where the limestone is interbedded with marginal marine clays. Most of the aquifer has a yield exceeding 5 L/s.

3.1.7 upper Renmark Group Aquifer

The upper Renmark Group is the thinnest of the Renmark Group aquifers. However, it is laterally extensive, onlapping the basin margins and extending down basin over the Geera Clay (Figure 3.3). Groundwater flow is to the southwest, following the structural grain and topographic gradient of the basin. Along the eastern model margin, only the southern half of the Neckarboo Ridge forms a groundwater divide, where the aquifer is unconfined. The ridge is breached to the north, particularly with through flow in the Baden Park Depression which separates the Manara Hills from the Cobar Block. Under the Menindee Lakes and nearby floodplain, groundwater flows radially from a mound generated by enhanced recharge. A similar radial pattern is evident to the south, between the Darling River and Travellers Lake. This is not anthropogenic but reflects flow off a ridge structure, the Lake Wintlow High.

Groundwater useful for livestock is found along the northwest margin of the aquifer where it receives recharge from basement run off. Here, the middle and upper components of the Renmark Group are difficult to differentiate and act as a single aquifer with a typical salinity of 3500 mg/L. Similar salinities of about 5000 mg/L are found under the Menindee Lakes storage. Dilution aureoles are also apparent in the aquifer, under the Darling River floodplain upstream of Burtundy (4000-7000mg/L), and to a lesser extent, for the Anabranch floodplain and lake system north of Bunnerungee. In the lower reaches of these rivers, the aureoles are surrounded by very saline (> 35,000 mg/L) regional groundwater. In the extreme northeast of the model, periodic outflow from Sandy Creek onto the sand plain has resulted in localised freshening of groundwater to about 6000 mg/L.

Aquifer yields tend to be low (< 0.5 L/s) along the basin margins due to the fine grained nature of the upper Renmark Group sediments. In addition, a tongue of low yielding aquifer protrudes into the basin from the northwest margin. This corresponds with finer silts and clays deposited over a southeast trending pre-Miocene ridge. Basinwards, the upper Renmark Group also thins and becomes interbedded with marginal marine clays. This results in a low-yielding belt along the southwest margin of the aquifer.

Figure 3.3

Lower Darling Model
upper Renmark Group Aquifer
Salinity/Yield & SWL

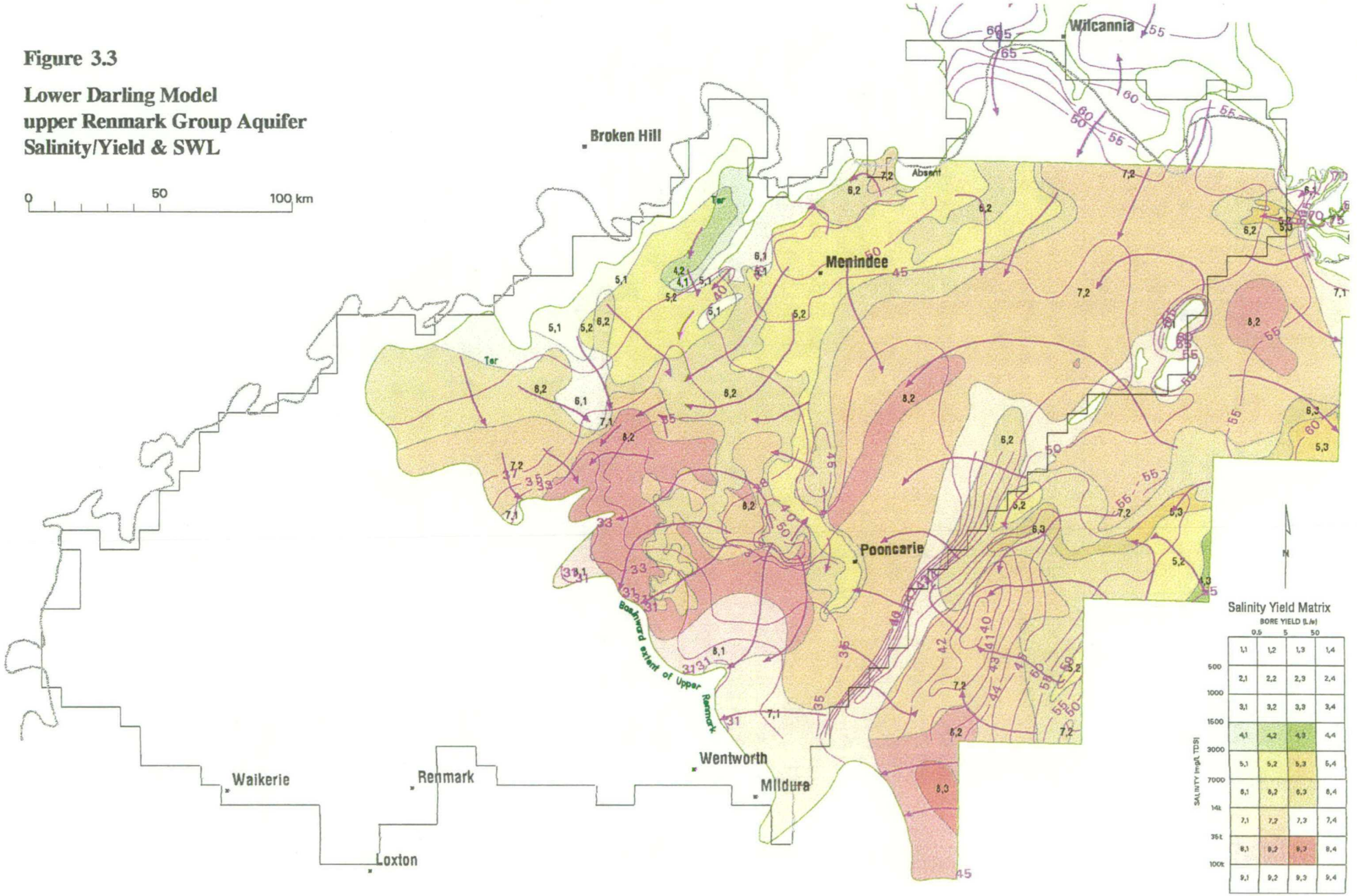

3.1.8 Pliocene Sands Aquifer

The Pliocene Sands aquifer is a composite of the marginal marine Loxton-Parilla Sands and the fluvial Calivil Formation (Figure 3.4). The aquifer extends over most of the model area. To the west, the sand sheet becomes unsaturated due to a combination of upwarping over the Hamley Fault and deeper watertables. In the southwest, the aquifer is underlain by the Bookpurnong Beds which impedes connectivity with the deeper Murray Group Limestone aquifer. Much of this area is also covered by a thin mantle of Blanchetown Clay which can act as an upper confining layer. Along the eastern model margin, the unit is dry over the southern half of the Neckarboo Ridge and also around the Devonian outcrops further to the north. To the east and north, the depositional history was mostly fluvial and the aquifer tends to be hydraulically connected with the underlying upper Renmark Group aquifer.

Like the deeper aquifers, groundwater flow is predominantly to the southwest, directed along the structural depressions. Along the northwest margin, flow is initially to the southeast orthogonal to the aquifer boundary. A major palaeochannel/deltaic system overlying the Blantyre, Menindee and Tarrara troughs captures this flow and directs it to the southwest. Likewise, off the Neckarboo Ridge groundwater flow is initially to the northwest, perpendicular to the structural high. Groundwater subsequently flows to the southwest, down the axis of the adjacent Wentworth Trough. Although the Neckarboo Ridge is a groundwater divide in the south, the aquifer receives groundwater across the northern half, particularly in the Baden Park Depression. The Lake Wintlow High, the ridge separating the two major depressions, the Blantyre-Menindee-Tarrara Troughs and the Wentworth Troughs, acts as a local groundwater divide. The most obvious effect of this ridge is the two groundwater mounds on either side of the Darling River in the centre of the model. A linear mound has developed over the Menindee Lakes and the Darling River upstream, which is maintained by enhanced leakage. Irrigation development along the Murray River, specifically at Mildura, Loxton and Berri-Barmera has also caused significant rises in local groundwater levels. The Berri-Barmera area is also the sink for regional groundwater in the Pliocene Sands aquifer.

The most distinctive feature of salinity mapping for the aquifer is the dilution effect due to recharge along the Darling River system. The freshest groundwater (600-900 mg/L) is found in a 2-10 km corridor centred along the Darling River channel upstream of Burtundy Weir. In a broader zone defined by the surrounding floodplain, Tallyawalka Creek and the upper reaches of the Darling Anabranch, salinities are not as low (1300-2500 mg/L). This reflects the lower frequency in which these outer parts of the river system are flooded. For example, outliers of higher salinity water (5000-7000 mg/L) are found within the floodplain on higher terraces which are rarely flooded. The dilution aureole dramatically decreases in width from 40-50 km at Menindee to 10-15 km at Pooncarie. This is a function of geomorphology where the width of the floodplain decreases downstream. In the northwest of the model area, the aureole borders groundwater freshened by periodic run off from the Broken Hill Block and Scopes Range. Here, salinities ranging between 2500-5000mg/L can be found. Useable water can also be found underneath Sandy Creek and as isolated pods along the Neckarboo Ridge. The raising of the Murray River by Lock 6 has also caused localised flushing of the aquifer in the Chowilla floodplain (Barnett, 1994).

Figure 3.4

Lower Darling Model
Pliocene Sands Aquifer
Salinity/Yield & SWL

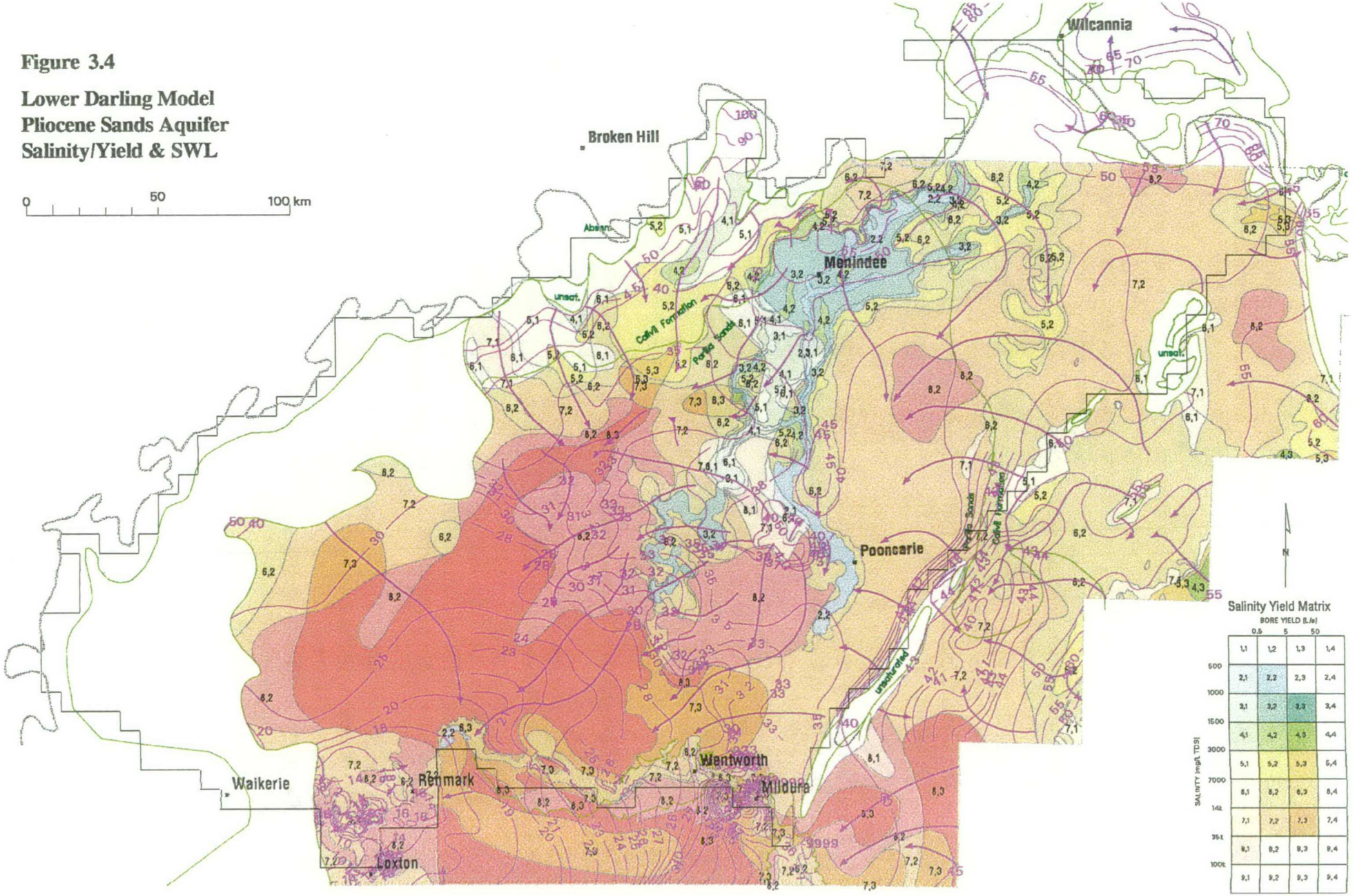

The remainder of the aquifer has salinities above the 14,000 mg/L threshold for livestock use, commonly exceeding 20,000 mg/L. Hundreds of bores have been drilled in these areas, but have been abandoned due to excessive salinities. Some boreholes have encountered thin freshwater lenses overlying the saline regional groundwater (Kellett, 1994a). These are located in sandy depressions, where collection and rapid infiltration of overland flow occurs. The mixing of the freshwater lens with the underlying saline groundwater is minimised due to the density contrast and cemented horizons found on top of the aquifer. The lenses are usually less than 5 m thick and sensitive to overpumping. Towards the lower end of the flow path in the southeast, salinities exceed sea water concentration (35,000 mg/L) and can become hypersaline (>100,000 mg/L) under salt lakes. The groundwater in the aquifer can be highly stratified, particularly underlying salinas. For example, near Nulla Lake east of Lake Victoria, salinity increases from 72,000 mg/L at 29m, to 94,000 mg/L at 39m and 106,000 mg/L at 59m depth. Hydrochemical studies of the aquifer suggests three stratifications - a saline lower Parilla, an upper Parilla and a low salinity uppermost lens (Ferguson & Radke, 1992).

Sustainable aquifer yield increases down basin. The aquifer is low yielding (<0.5 L/s) along its margins, as the unit is thin and finer grained. Low yields are also found associated with silts and clays deposited on the western margin of the Lake Wintlow High. To the northeast, most of the aquifer consists of kaolinitic fine to coarse quartzose sands with interbedded clays and silts of the Calivil Formation, yielding <5 L/s. However, yields exceed 5 L/s in the thicker and coarser grained sediments found within the trough structures. Higher yields are also found within the apex of the alluvial fan developed by Sandy Creek. Down basin, the Loxton-Parilla Sands is relatively clean and well-sorted and yields commonly exceed 5 L/s.

3.1.9 Shepparton Formation Aquifer

The Shepparton Formation spans the northern half of the model area, extending northwards up the Darling floodplain (Figure 3.5). However, the unit is only saturated in the deeper parts of the post-Pliocene land surface, namely the Darling River palaeochannel, a corridor connecting the Neckarboo Ridge with the Tallyawalka Creek system and the Baden Park Depression. In the centre of the model the aquifer is found in discrete northerly trending alluvial fans flanking a remnant of the Lake Wintlow High.

Groundwater flow is contiguous with that found in the underlying Pliocene Sands aquifer, indicating a degree of hydraulic connectivity. The groundwater mound underlying the Menindee Lakes and nearby floodplain significantly disrupts the regional flow to the southwest. River regulation and the long term maintenance of surface water storage in the lakes has elevated groundwater levels by over 10 metres.

Figure 3.5

Lower Darling Model
Shepparton Formation Aquifer
Salinity/Yield & SWL

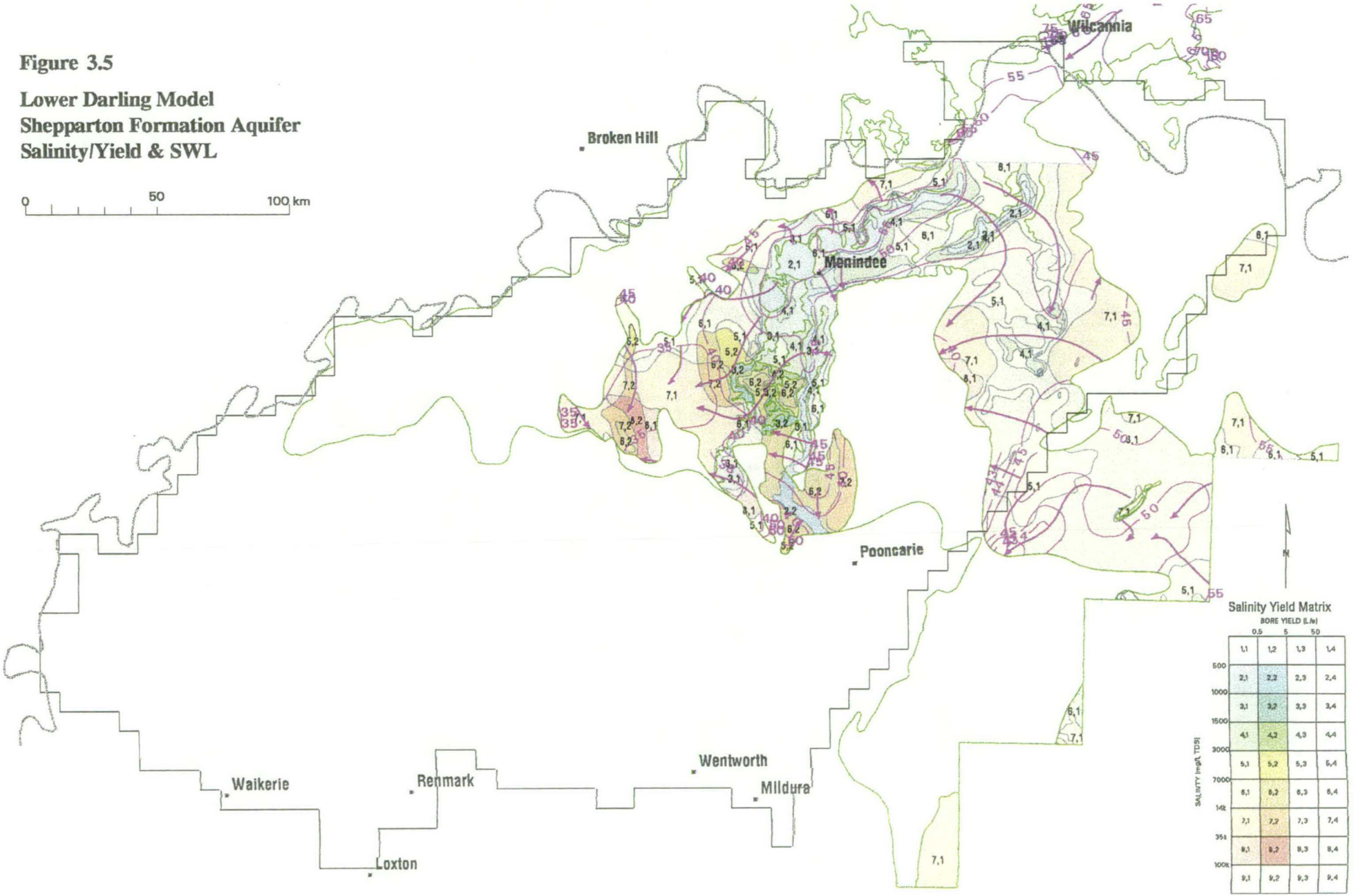

The aquifer also has a similar salinity distribution to that of the underlying Pliocene Sands aquifer. Groundwater is relatively fresh (700 mg/L) near the channel of the Darling River, but salinity increases rapidly away from the current watercourse, from good livestock quality to saline. In topographically higher terraces of Shepparton Formation within the floodplain where flooding is less common, the salinity is about 7000 mg/L. Occasional overflow into Teryaweynya Creek is the recharge mechanism for the aquifer found under the chain of lakes to the south of Tallyawalka Creek. Here, groundwater salinities are about 2000 mg/L, with bicarbonate and sulphate being the dominant anions (Kellett, 1994a). Away from the floodplain, the regional salinity varies from 7000 mg/L close to the northern basin margins, to >20,000 mg/L in the south. Aquifer salinities exceed 14,000 mg/L within the Baden Park Depression in the east, where influence of Sandy Creek is marginal.

Due to the silty nature of the Shepparton Formation, aquifer yields are generally less than 0.5 L/s. However, higher yields occur in thicker accumulations of coarser material found along palaeochannels.

3.1.10 Coonambidgal Formation Aquifer

The Coonambidgal Formation is the Quaternary alluvial deposits associated with the Murray-Darling drainage system. As such, these sediments are limited to the floodplain environment. Groundwater salinity is less than 1000 mg/L in the aquifer underlying the Darling River channel, the Menindee Lakes and parts of the Tallyawalka Creek channel. Within the upper terraces bordering the main watercourse, the salinity increases but tends to be still good livestock quality. Likewise along the Darling Anabranch, salinity increases downstream from 900 mg/L to 4000 mg/L, reflecting the reduced frequency of flooding in the lower reaches. As the saturated thickness of the aquifer is commonly less than 10 m, sustainable yields tend not to exceed 0.5 L/s.

3.1.11 Shallow Aquifer

The geological unit hosting the shallow watertable varies across the model, due to variations in watertable depth and the geometry of the basin (Figure 3.6). The watertable in the riverine floodplains is generally within 10 m of the ground surface and hosted in the Coonambidgal Formation. The watertable is found in remnant inliers of Shepparton Formation in the floodplain where the modern river has not incised into the older alluvial terraces. In the north, the Shepparton Formation is also the shallow aquifer in a corridor adjacent to the Darling River where the watertable depth is typically less than 30m, and the alluvial sequence is relatively thick. This situation also occurs in a regional depression centred on the lake system south of Tallyawalka Creek and in the Baden Park Depression.

Progressing up basin, the aquifers thin and their basal surfaces rise in elevation in accordance with the underlying basement. The watertable also deepens away from the influence of the river, with depths exceeding 70m near some of the basin margins. The net result is that the watertable is hosted in progressively deeper aquifers. For example, eastwards towards the Cobar Block, the watertable is in the Shepparton Formation, then the Pliocene Sands, then the upper Renmark Group and finally in the Lower Cretaceous Monash Formation. Along the Neckarboo Ridge the Pliocene Sands becomes unsaturated with the watertable occurring in

the underlying upper Renmark Group aquifer at depths exceeding 60 metres. This change in the watertable aquifer from the Pliocene Sands to the upper Renmark Group is also apparent along the northwest margin of the model area. In parts, a thick sequence of Quaternary colluvium and high level alluvials is evident adjacent to the Broken Hill Block and this tends to host the watertable.

Under the sand plains and dune fields of the southern-central part of the model, the Pliocene Sands is the shallow watertable aquifer. Here, the watertable is relatively shallow (< 30m). In the lower parts of the landscape, particularly around the salt lakes, the watertable is close to the surface (<10m) and is hosted in the Blanchetown Clay or Quaternary sediments.

West of the Hamley Fault, the sediments have been up-thrown and the watertable is deeper (40-60m). Here, the shallow watertable aquifer is the deeper Murray Group Limestone. Towards the basin margin, this changes to the lateral equivalents of the Winnambool Formation and Geera Clay where it is typically low yielding and saline.

3.2 Groundwater Flow Regime

For all of the layered aquifers in the Cainozoic sequence, groundwater flow is from the basin margins and structural highs to the southwestern corner of the model. Basin geometry, particularly the Blantyre-Menindee-Tarrara and Wentworth Troughs, has a role in directing that flow. Figure 3.7 is a cross section from recharge zone to discharge zone along the main axis of the model. The location of this profile is shown on Figure 4.19. The section indicates the lower salinities in the northeast caused by downward leakage from rivers, and the progressive increase in groundwater salinity down gradient. The discharge areas in the southwest are characterised by upward flow and high groundwater salinities.

3.2.1 Downwards Groundwater Flow

The basin margins are important sites of aquifer recharge. The surrounding elevated basement rocks are relatively impermeable and a significant component of a large rainfall event becomes surface run off. This is channelled by small dendritic drainage into the Murray Basin. Many of the larger creeks have sandy bed loads and are losing streams along their length when they flow. In the northwest, near the Broken Hill Block and Scopes Range, the shallow sediments are fluvial and sand-dominated, allowing rapid infiltration which would reduce evaporative loss. The drainage off the surrounding basement supplements the direct infiltration of rainfall in the area. The extent of this recharge mechanism is reflected in the relatively low salinities (3500 - 5000 mg/L) found in a corridor bordering these basement highs (Figure 3.8). Isotopic data supports recharge from surface water flow following summer thunderstorms (Evans & Kellett, 1989). Further to the southwest, the shallow sediments adjacent to the Benda Range are mostly marginal marine and clay-dominant. Here, infiltration is not as great, and the shallow aquifer is saline (> 14,000 mg/L).

Figure 3.6

Lower Darling Model
Geology of Shallow Aquifer
Depth to Watertable, m

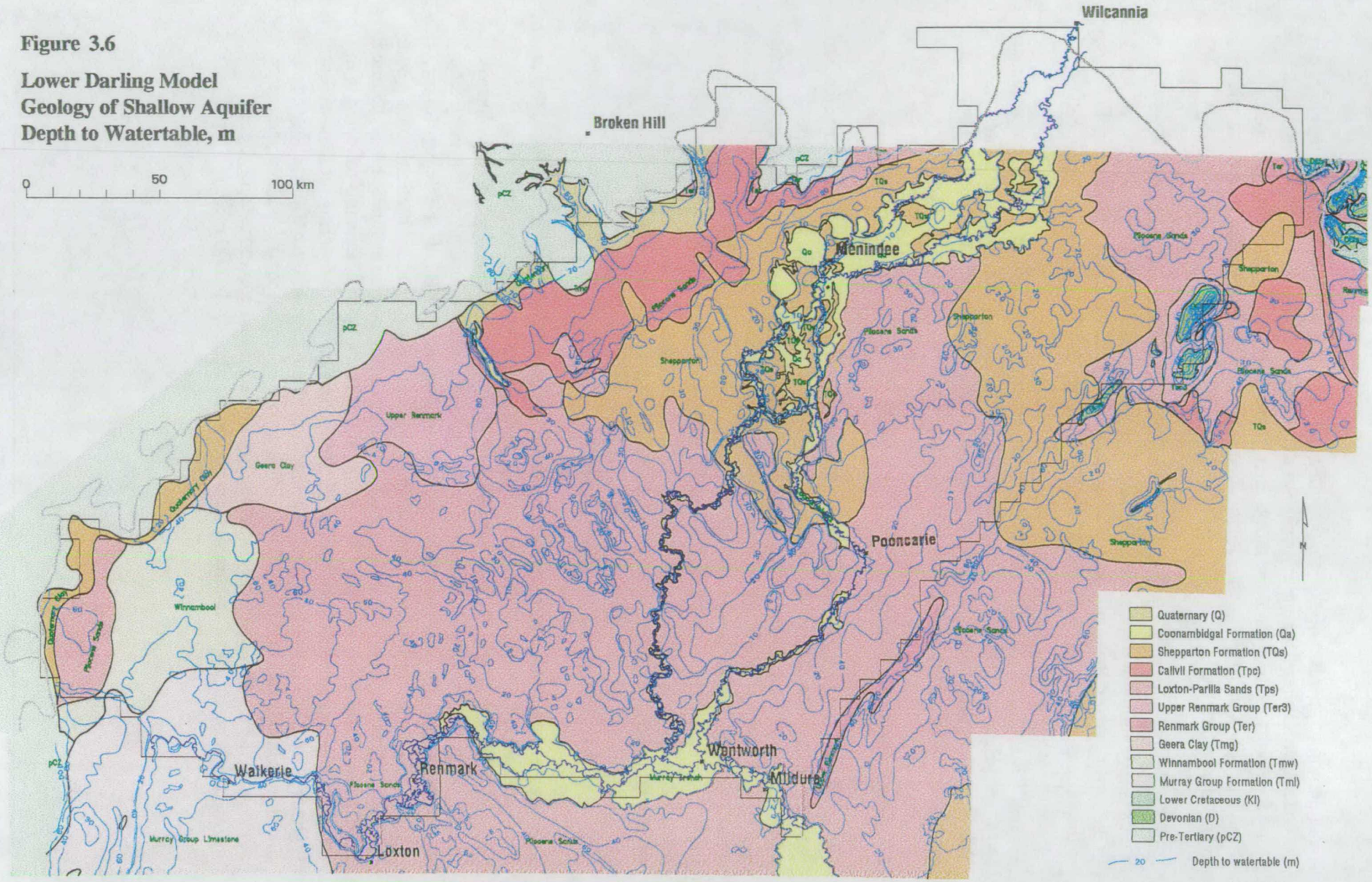

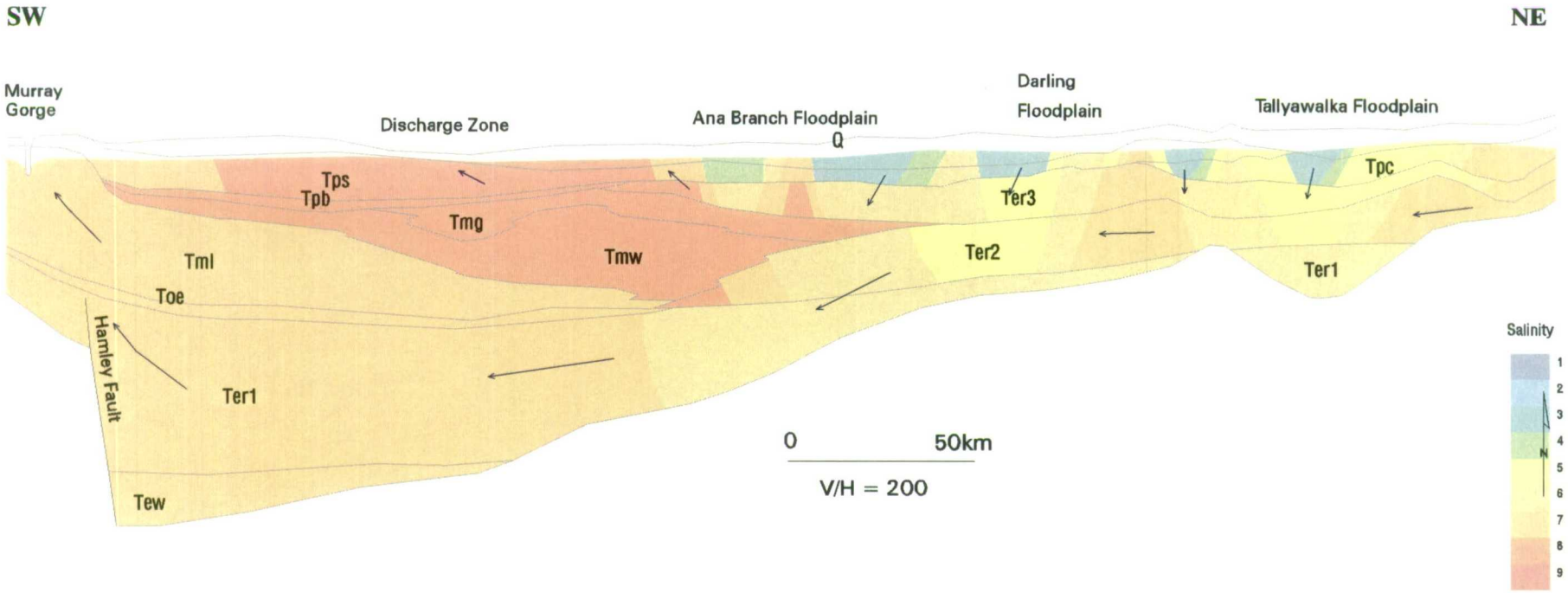

Figure 3.7 Cross section along a groundwater flow line

Figure 3.8

Lower Darling Model
Indicators of Downwards Groundwater Flow

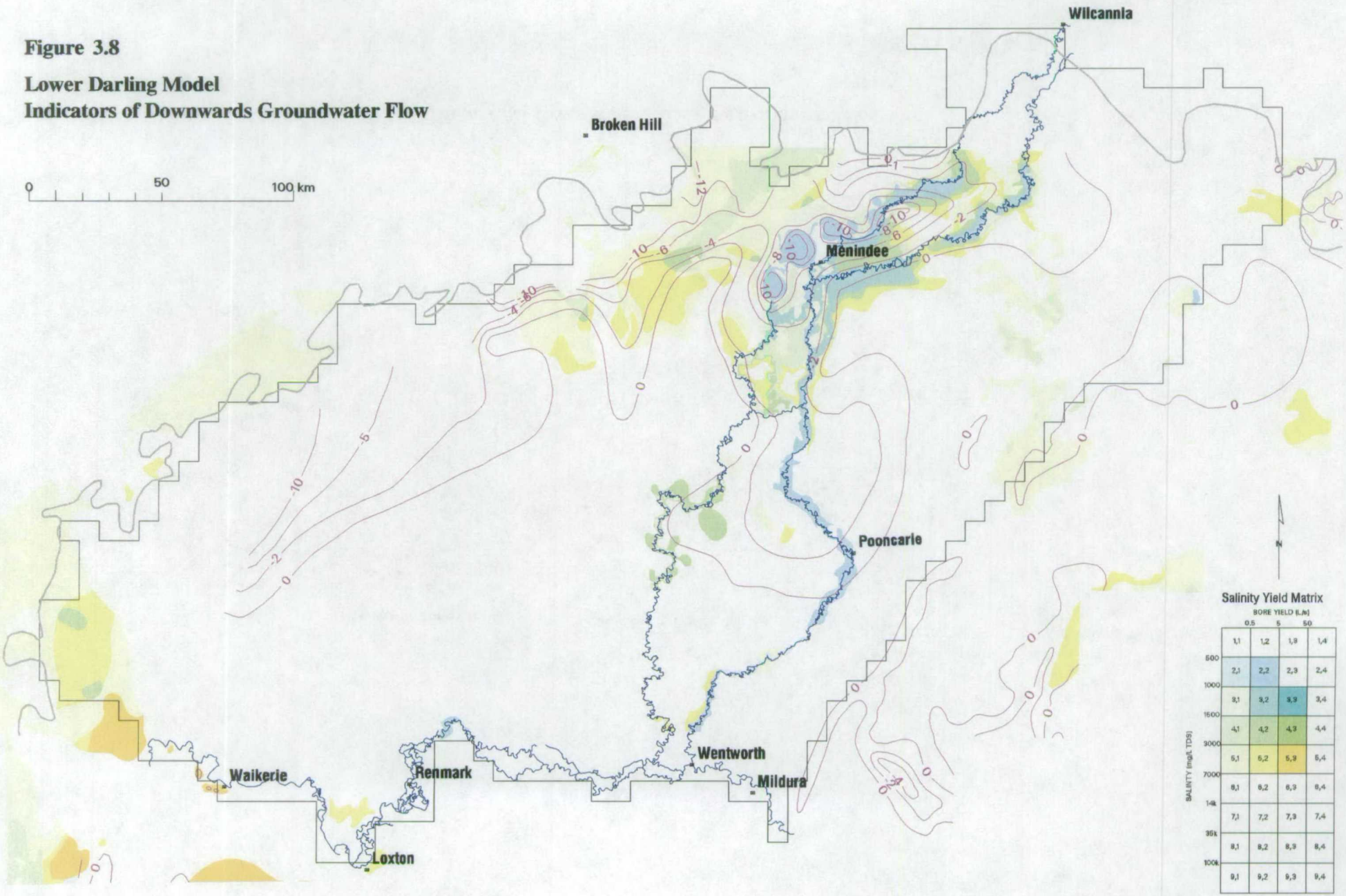

A corollary to this run on contribution is the possibility of changes in the amount of recharge due to changes to the environment in the basement hinterland. For example, there is anecdotal evidence that increased vegetation cover over the Broken Hill Block in the last few decades has reduced the run off generated from large rainfall episodes.

A downward groundwater flow regime is evident along the 20-50km wide zone paralleling the northwest basin margin as the shallow watertable is higher than the head in the deepest aquifer (Figure 3.8). The resulting negative head difference commonly exceeds -10m after correction of density effects due to salinity and temperature. The vertical hydraulic conductivity of the sediments determines the rate of downward inter-aquifer flow. The equivalent freshwater head difference is also negative over the Lake Wintlow High in the centre of the model. Here , recharge is concentrated at the apices of two alluvial fans developed over the structural high

Although upwards flow conditions prevail in the central-southern part of the model, groundwater recharge does occur at a local scale. For instance, sandy swales can be sites of internal drainage, receiving localised run off after significant storm events. Rapid infiltration can maintain a thin fresh water lens buoyed over the saline regional groundwater. Also, groundwater mounds developed under the irrigation districts are extreme examples of enhanced recharge in this environment.

Hence, areal recharge occurs to varying degrees across the whole of the landscape. Around the basin margins, where the vertical groundwater gradient is downward, infiltrating water tends to become part of the larger regional flow system. To the south, upwards gradients prevail and the effects of areal recharge are more localised (but no less significant). A comparison of areas where recharge has greatly been enhanced but are located in different vertical flow regimes lends evidence to this. The Menindee Lakes are close to the basin margin where the vertical flow potential is downward. Hence, lake bed leakage has had a major impact on the underlying aquifers. Dilution effects are evident for at least the Shepparton, Pliocene Sands and upper Renmark Group aquifers. Likewise, the basal lower Renmark Group aquifer appears to be the only aquifer which does not have flow lines perturbed by the lakes. In comparison, the aquifer response to the effects of enhanced recharge due to irrigation development around Berri-Barmera is very different. Here, the vertical flow potentials are upwards. A raised watertable and dilution aureole is found in the unconfined Pliocene Sands . However, the salinities and potentiometry of the deeper Murray Group and lower Renmark Group aquifers show no response to the substantial increase in local recharge. Rather than downward and into the regional flow system, because of the prevailing upwards flow regime, groundwater has flowed laterally and subsequently into the Murray River.

The proper estimation of areal recharge is critical for the model. This is based on the established links between clearing of native vegetation, enhancement of recharge, watertable rise and salinisation. Field measurements of recharge under native vegetation, including the mallee, belah-rosewood and pine woodland assemblages, indicate very low rates of < 0.3 mm/yr, or about 0.1% of mean annual rainfall (Cook *et al*, 1996). Potential recharge can increase dramatically following agricultural development. The magnitude of the change is largely dictated by the land use and soil type. Where mallee vegetation has been cleared for cropping or annual pastures, recharge through sandy soils (<10% clay) has been measured at

20-40 mm/yr (Cook *et al*, 1996). The recharge is typically less than 5 mm/yr when the clay content of the soil exceeds 20%. However, recharge rates seem not to diminish linearly with further increases in clay content (Kennett-Smith *et al*, 1994). This is due to percolation between peds, cracks or root channels in clay soils.

The magnitude of recharge is also dependent on the amount of rainfall. Field data suggests that potential recharge of <1 mm/yr exists for non-cropped sites, regardless of soil type, where mean annual rainfall is less than 250 mm/yr (Kennett-Smith *et al*, 1994). The threshold for cropped lands will be lower.

The introduction of native perennial pasture lessens the impact of clearing. For these agronomic practices, recharge rates are about 2 mm/yr for sandy soils and do not alter greatly for clay-dominant soils. In contrast, poor pasture management can increase groundwater recharge. At some field sites, where overgrazing by rabbits has caused the replacement of native perennial grasses with annual species, recharge rates are higher than that of nearby cropped land (Kennett-Smith *et al*, 1994). For cropping, elimination of fallow and introducing lucerne into rotations can decrease recharge.

There is a time lag between the clearing of native vegetation and the response by the regional watertable. The start of enhanced recharge can be seen as a distinct change in the chloride content of soil water in the unsaturated profile (Jolly *et al*, 1989). The solute front demarcates the relatively saline pre-clearing soil water from the fresher soil water introduced from enhanced recharge (Figure 3.9). Lower down the profile, a pressure front is marked by a distinct change in matric suction. This represents the displacement of pre-clearing soil water ahead of the solute front (Jolly *et al*, 1989). The watertable will rise when the pressure front reaches it, and water will be added at the post-clearing recharge rate. The velocity of the pressure front is determined by the new recharge rate and the soil water content and can be highly variable (Cook *et al*, 1996). For example, the water table may start to rise within 50 years of clearing mallee vegetation off sandy aeolian soils.

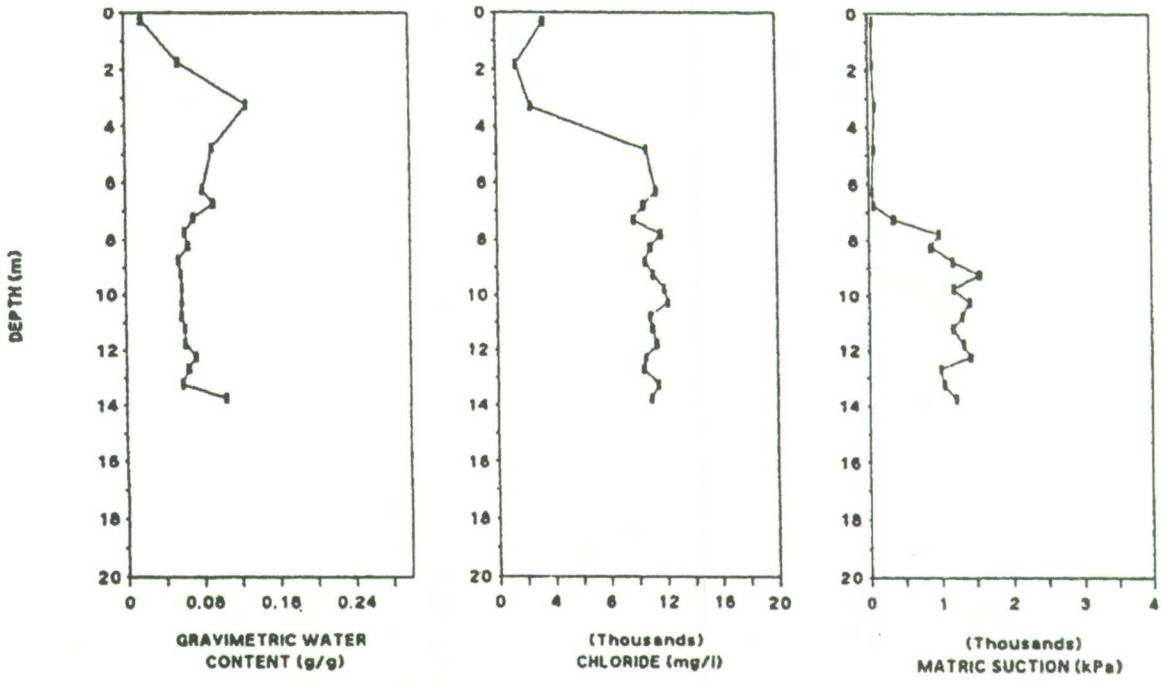

Figure 3.9 Profiles of gravimetric water content, chloride in soil water and matric suction of a corehole drilled in a field cleared of native Eucalyptus vegetation in 1980, near Kulkami, South Australia (from Jolly *et al*, 1989)

3.2.2 Upwards Groundwater Flow

Groundwater flows from the basin margin to the regional discharge zone located in the southern half of the model area. Here, the potential vertical groundwater flow is upwards, driven by high heads in the deeper aquifers. This is defined by a positive equivalent freshwater head difference which progressively increases down the flow path, mapped by the contours in Figure 3.10. This reaches a maxima in the southwest corner of the model where the head in the basal lower Renmark Group aquifer is over 20m higher than that in the shallow Murray Group Limestone aquifer. In this region, bores located in topographic lows and tapping the confined aquifer are commonly artesian.

Hydrostatic loading is likely to be contributing to the pressurising of the deeper confined aquifers. Groundwater in the lower Renmark Group flows from recharge zones along the northern margins, down basin and underneath a thickening sequence of marginal marine clays and marls of the Geera Clay and Winnambool Formation (Figure 3.7). These units are a store of highly saline and therefore relatively dense groundwater, representing a significant load which compresses the underlying elastic aquifer. This mechanism was used to explain the concomitant rise in pressures in the Murray Group Limestone aquifer and the lower Renmark Group aquifer recorded in piezometers east of Lake Victoria (Barnett, 1995).

Figure 3.10

Lower Darling Model
Indicators of Upwards Groundwater Flow

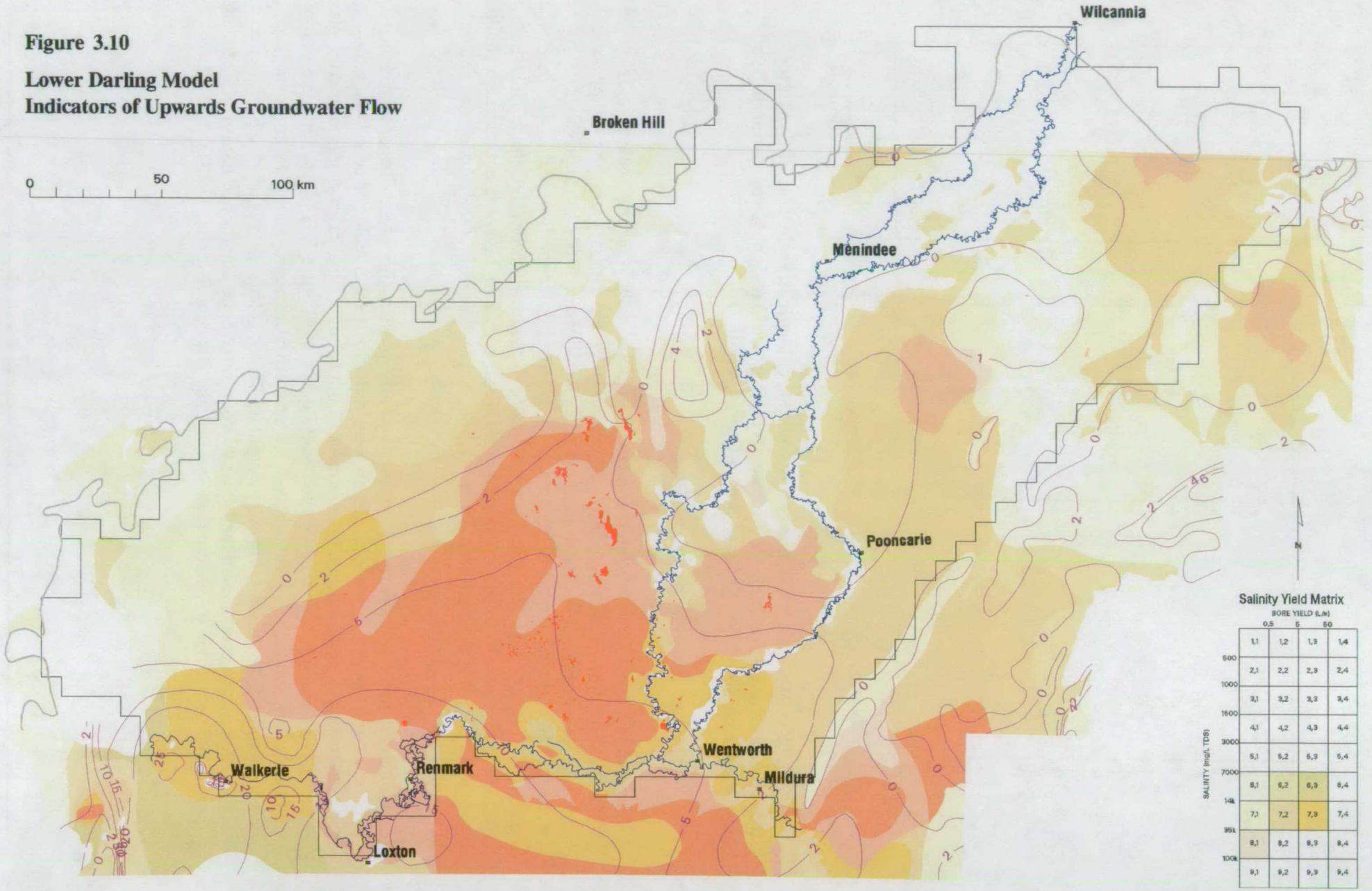

Figure 3.7 also shows another mechanism whereby the Geera Clay pressurises the underlying aquifer. The transgressive deposition of Geera Clay up basin has caused the dramatic thinning of the laterally equivalent fluvial middle Renmark Group aquifer. The marine clays form an effective permeability barrier and due to their onlapping geometry tends to divert the southwards flowing groundwater downwards and into the basal lower Renmark Group aquifer. The upper Renmark Group aquifer similarly pinches out basinwards. However the aquifer is typically in hydraulic connection with the overlying Pliocene Sands. Taken as a package, these units do not have the same rapid variation in thickness as seen in the middle Renmark Group.

Regional discharge conditions are manifested as numerous salinas entrenched into the sand plain. These are represented as red polygons in Figure 3.10 and are particularly evident in a 50km wide corridor north of Lake Victoria to Lake Popiltah and bounded to the east by the Darling Ana Branch. This low-lying region overlies the regional depocentres, the Renmark and Tarrara troughs which have been focii of tectonic subsidence and differential compaction. The control on the distribution of these salt lakes in this area is two fold. Firstly, they are located in depressions within the swale and ridge style topography. This topography reflects the deposition during the Pliocene of Loxton-Parilla Sand beach ridges, separated by broad swales and local palaeochannels . In these lows, the regional watertable intersects the land surface and discharge conditions prevail. Secondly, the discharge zones tend to occur near the basinward edge of the marginal marine deposits. Here, the Geera Clay and Winnambool Formation thin, allowing greater opportunity for upwards leakage from the pressurised basal aquifer to occur. This spatial relationship between the thinning marine clays and the salinas is evident in cross section (Figure 3.7). Salinas are also found where the Geera Clay is relatively thin (< 30m) along the northeast trending Lake Wintlow High.

Local geological structures may also facilitate upward leakage of groundwater. Nulla Spring Lake, for example, is fault bounded to the west with the underlying Blanchetown Clay displaced by nearly 10m (Ferguson & Radke, 1992). The Scotia complex is located on the upthrown side of the Hamley Fault where the upwarped Parilla Sand and Blanchetown Clay are relatively thin.

The groundwater discharge complexes in the area have been active since the arid phase which dried Lake Bungunnia, beginning 0.7 ma ago. The current saline lakes are superimposed over the isolated hypersaline remnants of the Lake found in the lows of the post-Pliocene land surface. These salinas have since been generating brines by evaporative concentration and refluxing of salts. These brine pools can migrate in response to the regional groundwater gradient and density effects and have contributed to the high regional salinity found in the Pliocene Sands aquifer (Jacobson *et al*, 1994). Isotopic data indicate two main sources of salt in the groundwater (Ferguson & Radke, 1992). In the upper levels of the Pliocene Sands, $^{36}Cl/Cl$ and $^{87}Sr/^{86}Sr$ ratios indicate modern marine aerosols as the principal source. In the basal part of the aquifer, the groundwater contains much older salt thought to be derived from the underlying marine sediments.

Advective sinking of the brine is determined by a critical Rayleigh number which largely depends on the ratio between the hydraulic conductivity of the lake floor sediments and the evaporation rate as well as the density difference between the brine and the regional groundwater (Jacobson *et al*, 1994). Reflux of the brine may occur if the density difference between the brine and the groundwater overcomes the upwards flow gradient. This tends to operate in salinas with high evaporation rates and a dominance of sand in the lake deposits. The Scotia discharge complex fit these criteria where refluxing has increased the salinity of the upper Renmark Group aquifer under the lake from a regional 28,000 mg/L to 54,000 mg/L (Figure 3.11). Where the salt lake is hosted in clay-dominated sediments, such as at Nulla Spring Lake, the hypersaline brine is more stable and contained (Figure 3.12).

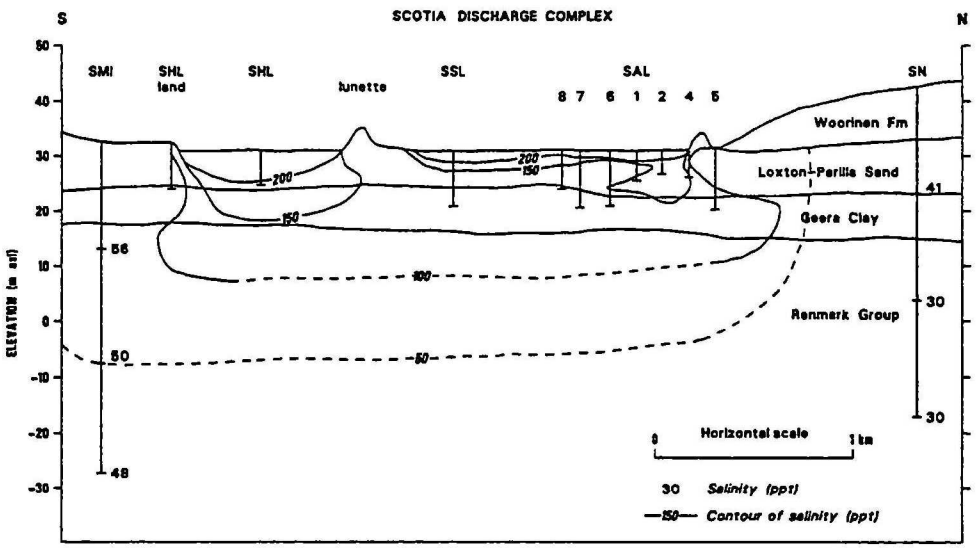

Figure 3.11 Transect showing brine salinity in the east Scotia salina (from Jacobson *et al*, 1994)

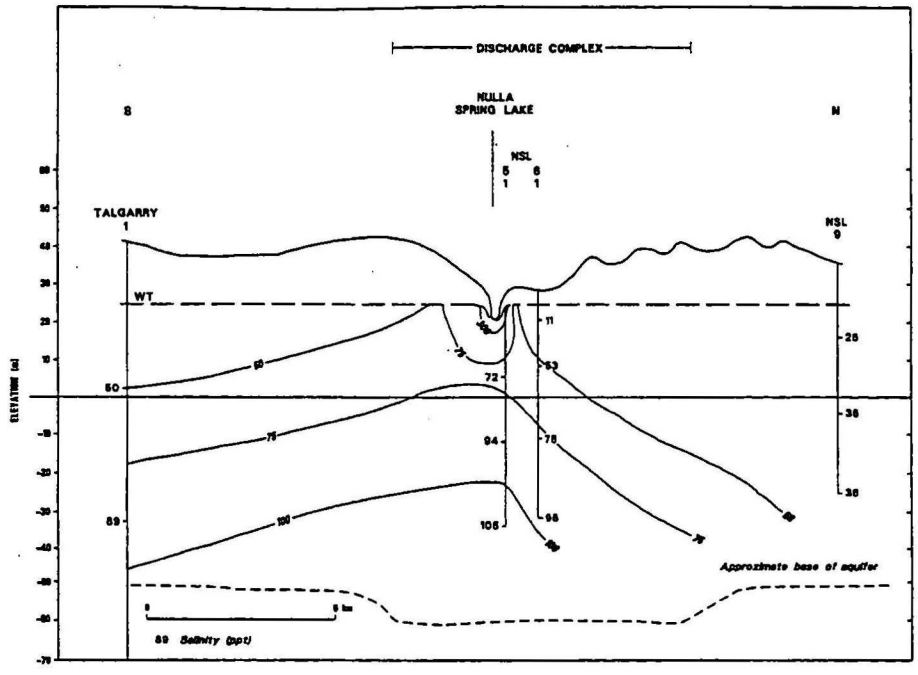

Figure 3.12 Transect showing fossil brine pool beneath the Nulla discharge complex (from Jacobson *et al*, 1994)

3.3 Surface Water - Groundwater Interaction

The interaction between the shallow groundwater system and the Murray-Darling drainage system is an important component of the modelling effort. The Darling River is a losing stream for most of its lower reaches, as indicated by freshening of the shallow groundwater within the immediate floodplain. In contrast, the Murray River traverses a regional discharge zone and is mostly gaining salty groundwater. River regulation, irrigation development and the practice of maintaining off-river storages in adjoining riverine lakes have resulted in significant changes in flow dynamics.

3.3.1 Murray River

The Murray River from Mildura to Morgan forms the southern boundary of the Lower Darling model. Natural flows in the Murray tend to have a seasonal pattern of peaking in winter-spring and ebbing in late summer-autumn. However, the magnitude of river flow varies markedly from year to year. These annual fluctuations are represented by the record of flows to South Australia from 1902 to 1987 (Figure 3.13) This plot shows the flood events of 1917, 1931 and 1974 as well as the largest recorded flood for the Lower Murray in 1956, caused by the synchronous flooding of the Upper Murray and Darling River.

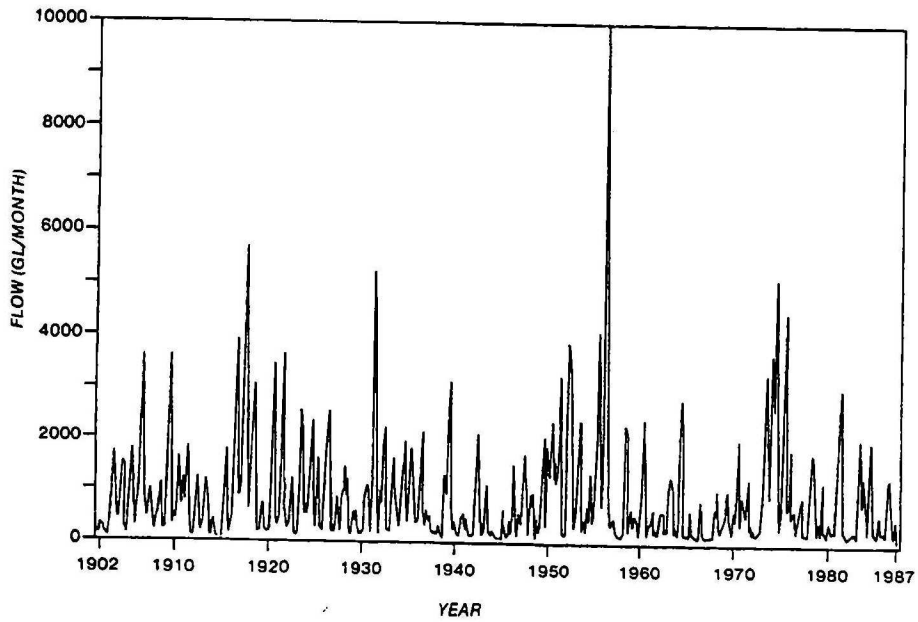

Figure 3.13 Actual flow in the Murray River to South Australia, 1902 to 1987 (from Mackay & Eastburn, 1990)

River regulation, particularly with the construction of large storages, has subdued the seasonal pattern by redistributing flows and mitigating floods. Also, a series of locks and weirs (Lock 2 to Lock 11) constructed along this reach have altered river water levels (Table 3.1). These weirs were initially installed to allow permanent navigation for 970km upstream of the river mouth, but now also play a role in directing water for irrigation and off-river storage. This has resulted in a stepped effect where modal river levels are maintained by the

locks, with the pool of one lock more or less reaching the next lock upstream. Major flood events are the only significant perturbations to river levels over time.

The weirs have also had the effect of increasing the frequency of flows into nearby distributaries which previously only received water from sporadic flood events. For example, the maintenance of elevated river levels by Lock 6 has resulted in groundwater flushing in the Chowilla floodplain (Barnett, 1994). Subsequent displacement of saline groundwater has also caused extensive vegetation decline.

Table 3.1 Locks on the Murray River in model area (MDBC, 1990)

Lock	Location	Km from Murray Mouth	Upper Pool Level (m AHD)	Weir Type	Year of Completion	Operator
1	Blanchetown	274	3.30	Boule	1922	SA
2	Waikerie	362	6.10	Boule	1928	SA
3	Overland Corner	431	9.80	Boule	1925	SA
4	Bookpurnong	516	13.2	Boule	1929	SA
5	Renmark	562	16.3	Boule	1927	SA
6	Murtho	620	19.25	Boule	1930	SA
7	Rufus River	697	22.10	Boule	1934	SA
8	Wangumma	726	24.60	Boule	1935	SA
9	Kulnine	765	27.40	Boule	1926	SA
10	Wentworth	825	30.80	Boule	1929	NSW
11	Mildura	878	34.5	Dethridge	1927	Vic

The section of the Murray River within the model area traverses the regional groundwater discharge zone for the Murray Basin. As such, it gains saline groundwater (over 20,000 mg/L) from the shallow aquifer, resulting in substantially increased salt loads. These accessions are caused by return flows off irrigation-induced groundwater mounds as well as high heads in the deeper confining aquifers driving upwards flow. Table 3.2 summarises various estimates of salt loads into the Murray River and floodplain environment from natural, river regulation or irrigation processes.

Irrigation around Mildura has caused the shallow watertable to rise by over 10 metres, resulting in significant displacement of saline groundwater into the river (Rural Water Commission, 1991). A series of bores (the Mildura-Merbein and Buronga interception schemes) along both sides of the river operate to reduce the impact. Similar groundwater mounds have developed under the irrigation districts in South Australia (Barnett, 1991). An average daily salt return to the river is estimated at 104 tonnes at Waikerie/Golden Heights, 146 tonnes at Berri/Cobdogla and 80 tonnes at Loxton (Smith & Watkins, 1993). Hydraulic loads, causing displacement of saline groundwater, are also imposed by water storages (eg Lake Victoria), the river locks and evaporation basins located within or near the floodplain.

The Woolpunda Reach , between Waikerie and Overland Corner, is a locus of regional saline groundwater inflows. Here, upwarping and thinning of the deeper confined aquifer has contributed to significant upward leakage into the shallow aquifer and ultimately, into the Murray River (Lindsay & Barnett, 1989). The Woolpunda Groundwater Interception Scheme,

consisting of 49 extraction bores located along transects on both sides of the river, delivers 15 ML/day of saline groundwater to the Stockyard Plain disposal basin. The scheme is designed to reduce river salinity by 40-50 ECU, equating to a saving for downstream users of over $1m per year.

Table 3.2 Estimated salt loads to the Murray River in the model area

Location	Average Salt Load *tonnes/day*	Principal Cause(s)
Merbein-Red Cliffs	44	irrigation mounds + direct drainage discharge
Border to Lock 6	59	natural accession + Lindsay River
Chowilla (Lock 6 to Templeton)	120	natural accession
Templeton to Lock 5	32	natural accession
	48	irrigation mound + Ral Ral Creek
Pike/Mundic	35	irrigation mounds
Berri East	13	irrigation mound
Berri to Cobdogla	146	irrigation mound
Remainder Lock 5 to Lock 4	19	natural accession
Bookpurnong/Lock 4	48	irrigation mound + lock induced
Loxton	80	irrigation mound + evaporation basin + direct drainage discharge
Pyap	14	direct drainage discharge
Gerard	18	irrigation mounds
New Residence	10	direct drainage discharge
Moorook/Kingston	23	irrigation mounds
Woolpunda	193	natural accession
Waikerie/Golden Heights	145	irrigation mound + direct drainage discharge
Sunlands/Qualco	25	irrigation mounds + natural accession
Lock 2	18	lock induced
Cadell	6	irrigation mound
Remainder Lock 2 to Lock 1	19	natural accession

Sources: Smith & Watkins (1993); Dudding *et al* (1989); Kellett (pers comm)

3.3.2 Lake Victoria

Lake Victoria is a large (118 km^2) floodplain lake of the Murray River, about 25 kilometres upstream of the New South Wales-South Australian border. Since 1928, the lake and connecting distributaries have been used as a water storage, mainly to provide entitlement flows for South Australia. With contributions from Menindee Lakes, these typically amount to 3000 ML/day in winter and 7000 ML/day in summer. The nominal capacity of the lake is 680 GL at a operating level of 27 m AHD, equating to a maximum lake depth of about 7 metres. Intake is from the Lock 9 pool via Frenchmans Creek.

Using Lake Victoria and Frenchmans Creek as artificial storages has altered the dynamics of the underlying groundwater system. The elevated heads in the lake and connecting creeks have laterally displaced highly saline shallow groundwater, causing salinisation problems in the surrounding landscape (Williams *et al*, 1993). Degradation of the floodplain east of the lake became most apparent to landholders in 1990-91. Subsequent vegetation surveys indicated that 7010 ha of the 22520 ha studied (31%) were salinised (Figure 3.14). These

areas typically had a groundcover of samphire, pigface and glasswort with black box showing obvious signs of stress.

A piezometer network measures a groundwater mound under Lake Victoria and along the course of Frenchmans Creek. The smaller distributaries within the floodplain between Frenchmans Creek and the Murray River have a layered profile of saline water. To reduce the impact on return flows to the Murray River, a network of spear points intercept the groundwater along the Rufus River. The groundwater is then pumped to an engineered disposal basin complex to the southwest of Lake Victoria (Figure 3.14) Saline flows in Brilka Creek are also transferred to the disposal basin. On average, 4500 ML/yr of water with salinities of 25,000-30,000 EC is pumped to the five interconnected disposal basins The basins cover an area of 300 ha at a maximum operating level of 54.5 m AHD (Hostetler & Radke, 1995).

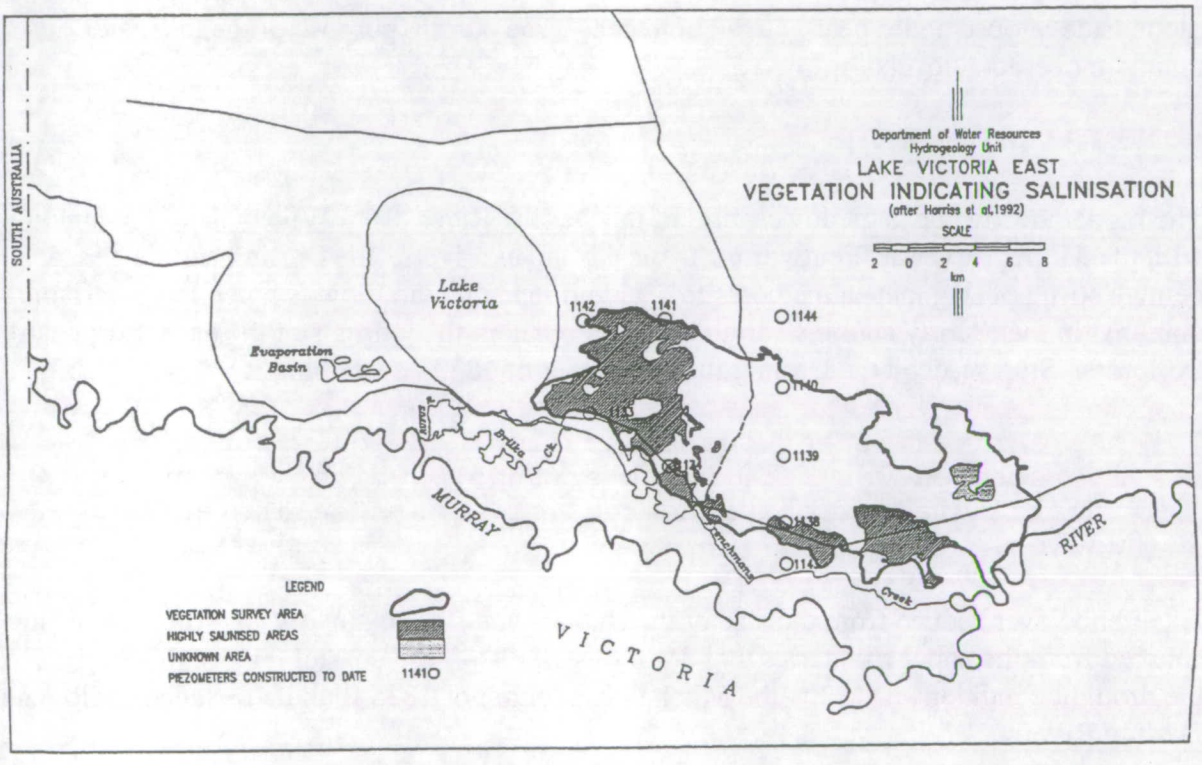

Figure 3.14 Vegetation indicating salinisation east of Lake Victoria (from Williams *et al*, 1993)

3.3.3 Lake Merreti

Lake Merreti, located 10km north of Cooltong, is also used to locally regulate flows in the Murray River. Since 1983, water is periodically released from the lake into Ral Ral Creek to supplement low river flows and maintain low salinities, servicing the Chaffey Irrigation Area downstream. With higher river levels, water is diverted back into the lake to replenish evaporative loss. The lake covers 370 ha and maintains a level of 16.30 m AHD when full (Hostetler & Radke, 1995). Regional groundwater levels are higher (16-18m AHD) and discharge conditions prevail.

3.3.4 Lake Bonney

Located immediately northwest of Barmera, Lake Bonney is a floodplain lake connected to the Murray River by Chambers Creek. The lake is 7km long and 3 km wide and with an area of 1650 ha, has a nominal capacity of 61 GL at a full surface level of 9.80 m AHD (Hostetler & Radke, 1995). The lake was used for supply of irrigation water until the 1930s, and until 1972, was used for disposal of drainage water. The lake receives groundwater inflow due to mounds developed under nearby irrigation areas. The current purpose of the lake is to maintain operating levels for Lock 3.

3.3.5 Darling River

The model area includes the lower third of the Darling River, from Wilcannia to the junction with the Murray River at Wentworth. Typical of inland rivers, the Darling can range from being a string of stagnant saline pools to a wide flooded plain. Flow is much more variable than that in the Murray and this variability is recorded in the journals of the early European explorers. Sturt reached the Darling in the summer of 1829, describing it

> "As a river it had ceased to flow; the only supply it received was from brine springs, which without imparting a current rendered its waters saline and useless.."

He did however deduce from the size of the channel and floodplain, the significance of floods sourced from the upper tributaries that drain westwards off the coastal ranges. In contrast to the drought conditions of 1829, the Mitchell expedition of 1835 found a fresher and flowing Darling River.

On average, significant flooding of the Darling system occurs every five years. This typically follows prolonged summer rains in southeastern Queensland. With regulation, this natural flow variability is reduced. Flow duration curves and the median monthly flow record (Figure 3.15) for Burtundy, show river flow is now always maintained at that point (Williams, 1991a). This reflects releases from the Menindee Lakes storage for downstream users, particularly in the high demand summer period. The duration curves also show that, on average, flows have been less after river regulation. This may be due to a number of factors including the flood mitigation role of the Menindee Lakes storage, allocation of water for upstream irrigators and rainfall variability.

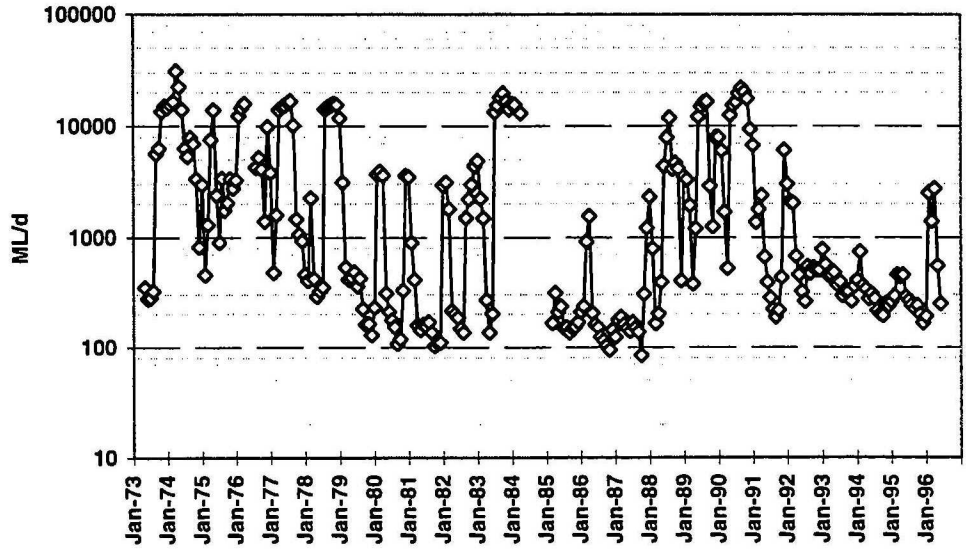

Figure 3.15 Monthly median flow for the Darling River at Burtundy, 1973 to 1996

The maintenance of flow in the river has effectively increased the modal river stage. This has altered the interaction between river and the underlying fluvial aquifer. A series of piezometer transects indicate that the river is losing water to the shallow aquifer (Stannard, 1981). A dilution aureole is found along most of the length of the river, where groundwater salinity is in the range of 400-4000 mg/L. This contrasts with salinities of about 20,000 mg/L, typical of the shallow aquifer away from the lower reach of the river. Downhole EM conductivity logging of piezometers indicate a distinct interface between an upper freshwater lens and the underlying saline regional groundwater (Williams & Beckham, 1995). The system appears to be dynamic, with the interface moving both laterally and vertically in response to changes in river levels (Jewell, 1993).

The dilution aureole was found along parts of the floodplain and lake system before the onset of river regulation. Mulholland (1940) records details of wells obtaining fresh to brackish groundwater flanking river channels and floodplain lakes in the Tallyawalka system. Large flood events allow overflow via Teryaweynya Creek into a chain of lakes to the south of the Tallyawalka. This has resulted in freshening of groundwater (<2000 mg/L) in the Shepparton Formation aquifer underlying these lakes (Kellett, 1994a). What has altered is the extent and longevity of this recharge mechanism. For example, downward leakage occurs in the lower reaches of the Darling where the river traverses a regional discharge zone so that vertical groundwater movement is regionally upwards. It is significant that water discharging from the Darling at Wentworth has bicarbonate rather than chloride as the dominant anion, implying relatively low levels of groundwater accessions (Mackay & Eastburn, 1990).

3.3.6 Menindee Lakes Storage

The Menindee Lakes storages represent the major infrastructure for regulation of river flow in the Darling system. The most upstream storage is Lake Wetherall created in the floodplain by a block bank and weir across the Darling River. This raises the river level to about twelve metres above the river bed, allowing impounded water to be then gravity fed to Lake Pamamaroo and in turn to the other floodplain lakes, Menindee and Cawndilla. This enables a nominal full supply capacity of 1680 GL over a surface area of 457 km^2. The capacities and operating levels of individual lakes are summarised in Table 3.3.

The scheme was constructed between 1949 and 1962, to secure a strategic water supply in semi-arid western New South Wales. Table 3.4 lists the major users of water stored in the scheme from 1990 to 1993. The impact that evaporation has on maintaining a long term water storage at Menindee is highlighted. Evaporation losses are very high as the lakes are very broad and shallow, ranging only 4 to 7m when full. The average net annual evaporation is 1.6 metres , equating to the loss of 460 GL/yr from storage.

Table 3.3 - Storage components of Menindee Lakes Scheme (Bewsher *et al*, 1994)

Lake	Bed Level *(m AHD)*	Full Supply Level (m AHD)	Full Supply Capacity *(GL)*	Surcharge level *(m AHD)*	Surcharge Capacity *(GL)*
Wetherall	49.6	61.67	267	62.28	343
Pamamaroo	55.3	60.45	270	61.93	377
Menindee	55.3	59.84	595	61.36	858
Cawndilla	53.0	59.84	547	61.36	706
TOTAL			**1678**		**2285**

Under the Murray Darling Basin Agreement, the Menindee Lakes meet a varying proportion of the annual entitlement flow for South Australia. This demand is determined by the capacity to provide any deficit in the entitlement not met by uncontrolled flows in the Murray River. If there is sufficient storage, an additional 3000 ML/day is released to reduce salinity levels in the Murray River as part of the MDBC Salinity and Drainage Strategy. Minimum flows to the Darling River are also needed to prevent algal development and eutrophication, and to maintain fish habitat. These flows vary with the season, typically set at 350 ML/day in summer and 200 ML/day in winter. Additional flushing releases may be needed with the onset of blue-green algae blooms. Other major users include irrigation on the lower reach of the Darling and at Lake Tandou and the annual replenishment flows for the Anabranch.

The use of these floodplain lakes as water storages have had an impact on the underlying groundwater system. A groundwater mound is evident over the lake system, creating a density-corrected head difference between the shallow aquifer and the deepest Tertiary aquifer of over ten metres (Brodie, 1992). Downward leakage is indicated by the level of dilution apparent in the deeper aquifers. There is potential for the watertables within depressions down-gradient from the storages (such as Emu Lake and Lake Tandou) to rise and cause salinisation problems (Bish & Salotti, 1996).

Table 3.4 : Water Use for Menindee Lakes Storage (NSW Dept Water Resources, 1994a)

Purpose	Allocation *(ML/yr)*	Nominal Supply *(ML/yr)*	Average Diversion 1990-93 *(ML/yr)*
Town Water	10120		6621
Irrigation - Lower Darling	20727		5694
Irrigation - Tandou Ltd	15567		40284
Livestock Supply	251		251
Domestic Supply	258		258
Recreation	91		0
Industrial - yabby farms	201		98
South Australian entitlement		720000	386000
Anabranch replenishment		50000	39067
Water quality flows			105250
Evaporation		440000	460000

3.3.7 Great Anabranch of the Darling River

The Great Anabranch is a relict channel of the Darling, abandoned after the river established its modern course to the east (refer Figure 2.16). Before river regulation, the Anabranch was an ephemeral stream, on average flowing two years out of three in its upper reaches (NSW Dept Water Resources, 1994a). Due to the large storage capacity in the floodplain lakes (Table 3.5), only major floods resulted in significant flows exiting the Anabranch into the Murray River. It has been estimated that under natural conditions a minimum annual flow of 50 GL was required to reach Nearie Lake, a situation which occurred in less than half of the years prior to river regulation.

Between 1869 and 1872, a channel was excavated from the Darling to the Anabranch by a consortium of downstream landholders (Withers, 1994). This allowed flow into the Anabranch when flows in the Darling River reached a threshold of 10,000 ML/day at the off take point. Previously, most flow was via Tandou Creek when river flow at Menindee exceeded 20,000 ML/day. A series of check banks have been constructed along the course of the Anabranch to provide storage for livestock and domestic use. Banks were also built across feeder creeks of the floodplain lakes to enable flow to be confined to the main channel.

Today, similar infrastructure exists and the Great Anabranch is essentially a stringer of small dams. Since 1961, an annual flow of 50,000 ML is released down the Anabranch to replenish these storages. This is usually released at a rate of 500 ML/day over a three-month period in winter. Flows of up to 2200 ML/day from Lake Cawndilla can be diverted down the Anabranch via a channel to Tandou Creek. Flooding of the Anabranch appears to be non-uniform where periods of near successive annual floods are followed by years with below-average flood frequency. For example, the time periods 1886-94, 1950-56 and 1974-78 are recorded as having a series of flood events. Figure 3.16 plots the recurrence interval for floods of various magnitude down the Anabranch based on an empirical study of the historical record (NSW Dept Water Resources, 1994b). Based on historical trends at Wycot between 1895 and 1993, natural flows exceeding 500 GL occur on average every three years.

Table 3.5 Potential storage capacities of Anabranch floodplain lakes (NSW Dept Water Resources, 1994b)

Lake	Area *ha*	~ Bed Level *m AHD*	~1890 Flood Level *m AHD*	~ Stored Volume in 1890 Flood *GL*
Tandou	18000	50.2	55.0	740
Mindona	9300	45.0	48.6	280
Travellers	11400	43.1	47.4	280
Popio	6100	41	47.1	300
Popiltah	9600	39.5	46.7	580
Nialia	2900	39.5	45.6	85
Yelta	3200	37.0	44.1	85
Nearie	2100	35.8	44.1	85
Nitchie	600	39.5	43.8	25
Milkengay	2300	36.1	43.8	140
Warrawenia	1200	35.2	38.9	30

The hydrological regime for the Anabranch is reflected in the underlying groundwater system. The groundwater salinity in the shallow fluvial aquifer of the Anabranch floodplain progressively degrades downstream from <1500 mg/L to over 5000 mg/L (Brodie, 1992). This is due to the tendency for only sporadic major floods reaching and hence recharging the bed of the lower reaches. At the turn of the century, numerous soakage wells were sunk along the main channel (Withers, 1994) to access this resource. These wells were typically 6 to 9 metres deep and were mostly used as a drought reserve.

Likewise, the sediments of the upper floodplain lakes (eg Mindona , Travellers) tend to contain better quality groundwater due to the greater frequency of flooding. Recharge from the advancing flood is mainly via the deep cracks developed in the dry heavy clay of the lake bed. Dixon (1891) had this to say in describing such a recharge event;

> "As the floods subside these immense flooded areas dry-up and crack in every direction with numerous deep interstices, which, when another flood advances, serve as conduit pipes for the water to flow-down into the underlying sand stratum. Some conception may be formed of the extent to which this occurs when we find that it has been observed that for a whole week the flood has poured-down into one such crack without being able to advance further."

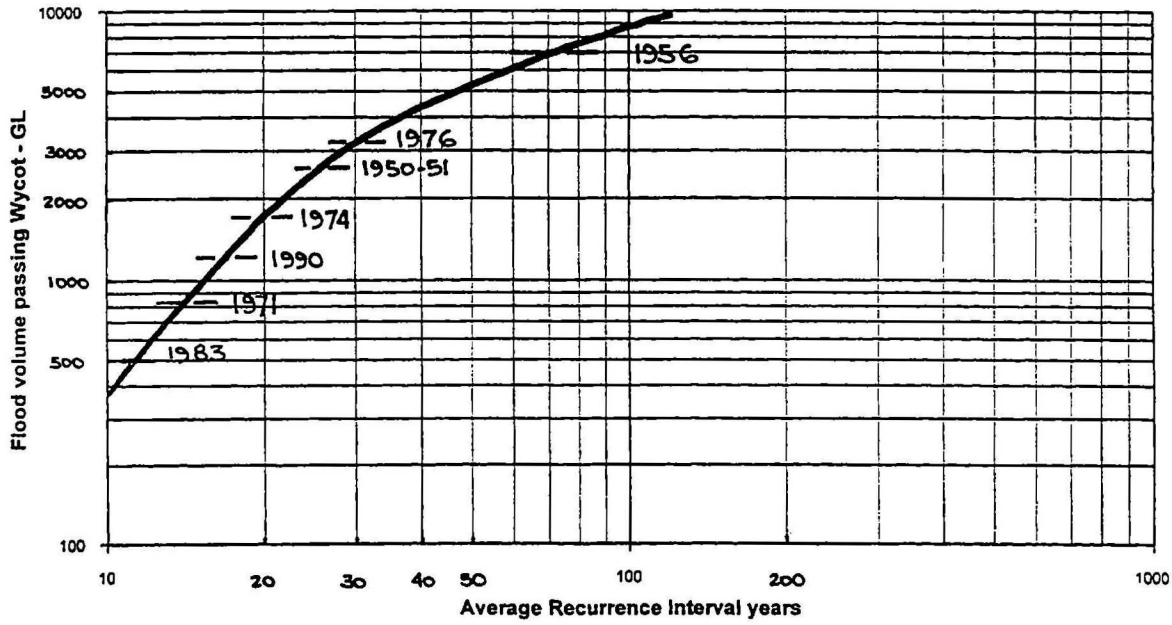

Figure 3.16 Frequency relationship for flood volumes entering the Darling Ana branch (from NSW Dept Water Resources, 1994b)

3.3.8 Ephemeral Streams

A number of ephemeral streams drain the southeast flanks of the Barrier and Benda Ranges which mark the western boundary of the model. These flow into the Murray Basin for 40-60 km into the sand plain, typically draining into a terminal lake. Some of the streams, such as Stephens Creek, Pine Creek and Turkey Plain Creek, have significant channels with a sandy bed. Flooding occurs intermittently and may not necessarily be synchronous with flooding in the Darling system which is determined by rainfall events high up in the catchment. For example, Woolcunda Lake which terminates flow from Turkey Plain Creek has been full four times this century, in 1921, 1938, 1989 and 1991. Water typically remained in the lake for about two years (Seekamp, pers comm).

Bores and shallow wells are found in or adjacent to the stream channel, accessing lower salinity groundwater than that found under the surrounding sand plain. The sporadic flooding is important in terms of groundwater recharge, with graziers reporting marked rises in groundwater levels in their livestock bores after such events.

4. MODEL DEVELOPMENT

4.1 Conceptual Model

For modelling purposes, the Cainozoic sequence in the Lower Darling region is subdivided into five layers (Figure 4.1):

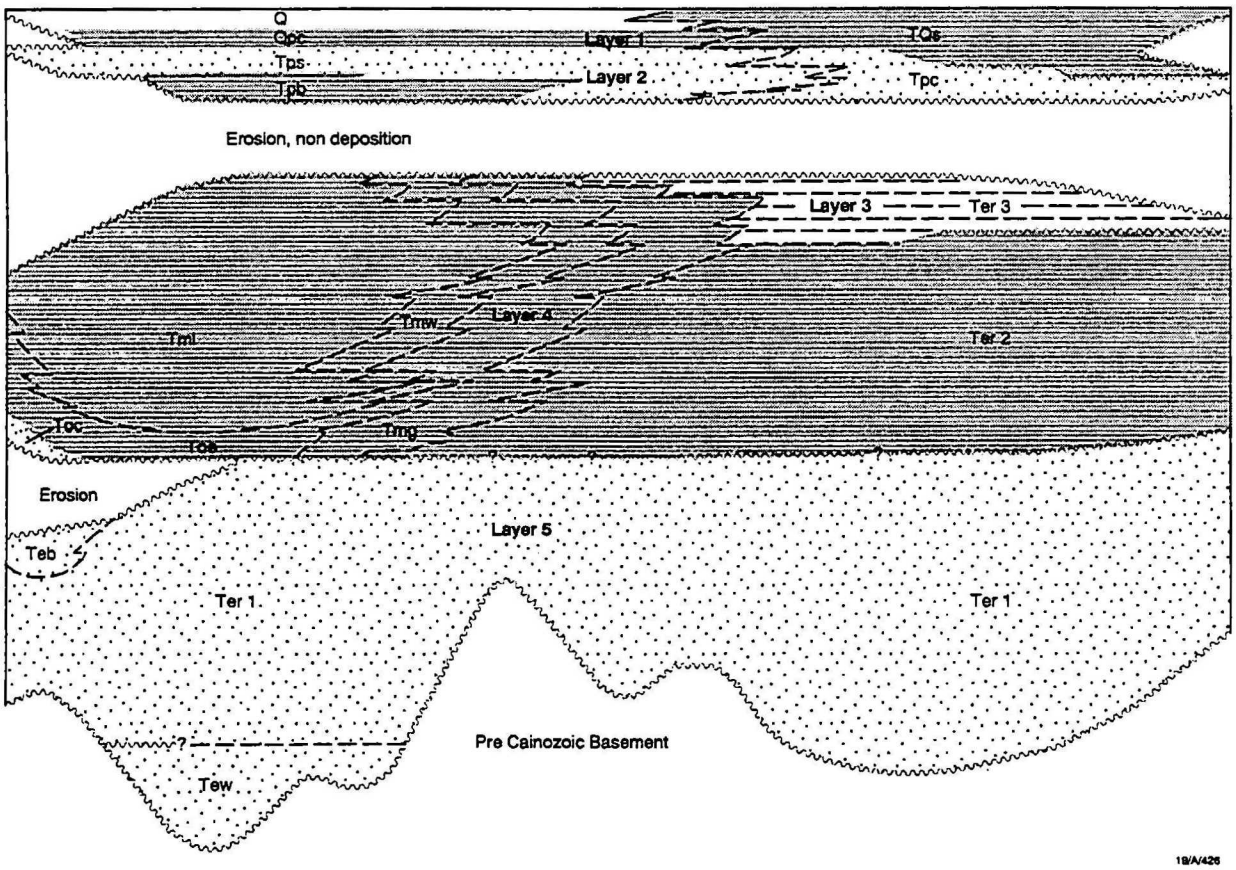

Figure 4.1 Subdivision of Cainozoic stratigraphy into model layers

Layer 1 - The mostly Quaternary sequence of fluvial Coonambidgal Formation (Qa) and Shepparton Formation (TQs) as well as the lacustrine Blanchetown Clay (Qpc) make up the uppermost model layer. The fluvial units are the shallow unconfined aquifer along the floodplain of the Murray-Darling river system and in landscape depressions. The Blanchetown Clay hosts the watertable in the low-lying discharge zone in the central-southern part of the model. Since watertable conditions persist for this uppermost aquifer it is defined as an unconfined layer (type = 1). This layer is particularly important in effectively modelling the interaction between groundwater and surface water features.

Layer 2 - The Loxton-Parilla Sands (Tps) and Calivil Sands (Tpc) are combined to form the second model layer, recognising the high degree of lateral hydraulic connection between the two units. The resulting Pliocene Sands aquifer is an important, laterally extensive system and is the shallow watertable aquifer in the broad intermediate area between the basin margins and the central basin lows defined by the Darling and Murray Rivers. Around the rivers the

Pliocene Sands is overlain by saturated alluvial sediments and towards the basin margins the unit becomes unsaturated. Hence, the layer is modelled as a mixed unconfined/confined aquifer where transmissivity varies (type = 3).

Layer 3: - The upper Renmark Group (Ter3) aquifer is separated out as the third model layer. The unit only occupies the northeast of the model area, lensing out against marginal marine sediments basinwards. The unit is the shallow watertable aquifer near the basin margins and along structural highs such as the Neckarboo Ridge, and is confined elsewhere. The upper Renmark Group is also treated as an unconfined/confined aquifer (type = 3).

Layer 4 - The Oligocene-Middle Miocene sequence is represented as the fourth layer. This layer is dominated by the middle Renmark Group (Ter2) aquifer in the northeast, marginal marine units such as Geera Clay (Tmg) and Winnambool Formation (Tmw) in the model centre with interbedded Murray Group Limestone (Tml) to the southwest. Due to the similarities in lithologies and hydraulic characteristics with the marginal marine clays and silts, the Ettrick Formation (Toe) and the Bookpurnong Beds (Tpb) are also included in the layer. Hence, the package of clays, marls and silts making up the mid-Tertiary permeability barrier (Brown & Radke, 1989) is defined by this layer. The Murray Group Limestone is the watertable aquifer bordering the Murray River Gorge in the southwest corner of the model. As the aquifer varies from being confined in the northeast to unconfined in the southwest, it is deemed a mixed unconfined/confined layer (type = 3).

Layer 5 - The basal model layer consists of the Palaeocene - Lower Oligocene sequence. This is dominated by the lower Renmark Group (Ter1) aquifer with minor Warina Sands (Tew), Compton Conglomerate (Toc) and Buccleuch Beds equivalents (Teb) to the southwest. The layer has a smaller spatial extent compared to the other layers, being limited to the troughs and depocentres of the basin. This deepest aquifer is confined (type = 0,) throughout the study area so that transmissivity cell values are fixed during model simulation.

This vertical discretisation is consistent with that of the neighbouring Lachlan Fan model (Kellett, 1997). This differs from the three-fold subdivision used for the SAVIC model, to the south of the Murray River. Here, a simpler conceptualisation with layers representing the upper unconfined aquifer (Pliocene Sands, Shepparton Formation), Murray Group Limestone and a composite Renmark Group was used. The separation out of the components of the Renmark Group as distinct layers in this modelling exercise is based on the significant head differences which can occur between these units. Near the basin margins, the Renmark Group sequence tends to be relatively homogenous and acts as a single aquifer system. However, basinwards, particularly with the interbedding of lacustrine to marginal marine clays and silts, the components of the Renmark Group become hydraulically separated (Kellett, 1989).

Another feature of the model conceptualisation is the incorporation of all of the stratigraphy into the model layers, including both aquifers and aquitards. This differs from modelling the aquifers only, with intervening aquitards defined by the vertical leakance arrays. This has advantages during compilation of aquifer properties based on the borehole record.

The Lower Darling Groundwater Model encompasses the northwest quarter of the Murray Basin (refer Figure 1.1). As such, the northern and western margins of the model are no flow boundaries defined by the extent of Murray Basin Cainozoic sediments. The eastern model boundary is defined by the Neckarboo Ridge, a structural high extending to the southwest into the basin. This mostly acts as a groundwater divide, however some lateral flow occurs in the shallow layers particularly in the Ivanhoe area, to the north. This represents the flux between this model and the neighbouring Lachlan Fan model. The Murray River acts as the southern boundary to the model. Here, the northwards flow regime found to the south of the river is met and the river demarcates a no-flow boundary for most layers. The exception is the basal layer, where there is evidence that flow in the lower Renmark Group aquifer continues further southwards past the river.

4.2 Model Definition

As prescribed by the MDBC Groundwater Working Group, the Lower Darling model uses the USGS MODFLOW code (McDonald & Harbaugh, 1988). This is a three dimensional finite difference package commonly used to simulate groundwater flow. The model uses the grid common to all of the regional groundwater models for the Murray Basin - namely one with a 7.5 km by 7.5 km cell size, generated from a false origin of 28500E, 586500N located in the Southern Ocean. The finite difference grid for the Lower Darling model comprises 42 rows and 65 columns, covering an area of 78,525 km^2 or about a quarter of the Murray Basin. The total number of active cells is 5341, consisting of 1322 cells in layer 1, 1285 cells in layer 2, 787 cells in layer 3, 1151 cells in layer 4 and 796 cells in layer 5.

As defined for the Murray Basin modelling project, Universal Transverse Mercator AMG Zone 54 was used as the standard projection. For the Lower Darling region, this entailed some minor reprojection of Zone 55 mapsheet data into the prerequisite Zone 54. Ideally, regional groundwater modelling should be based on an equal area projection (such as Albers) rather than a conformal or equal angle projection, as is AMG. This reduces errors associated with areal averaging of data to compile model parameters. Also, inaccuracies can develop when projecting spatial data in areas beyond the specified zone.

Modelling has only been carried out for steady state hydrogeological conditions due to data limitations. The hydrographic record for boreholes in the model area is sparse, both in time and in space. The bulk of the boreholes drilled are to supply water for livestock and drilling of a regional observation network consisting of nested piezometers, only commenced in 1987.

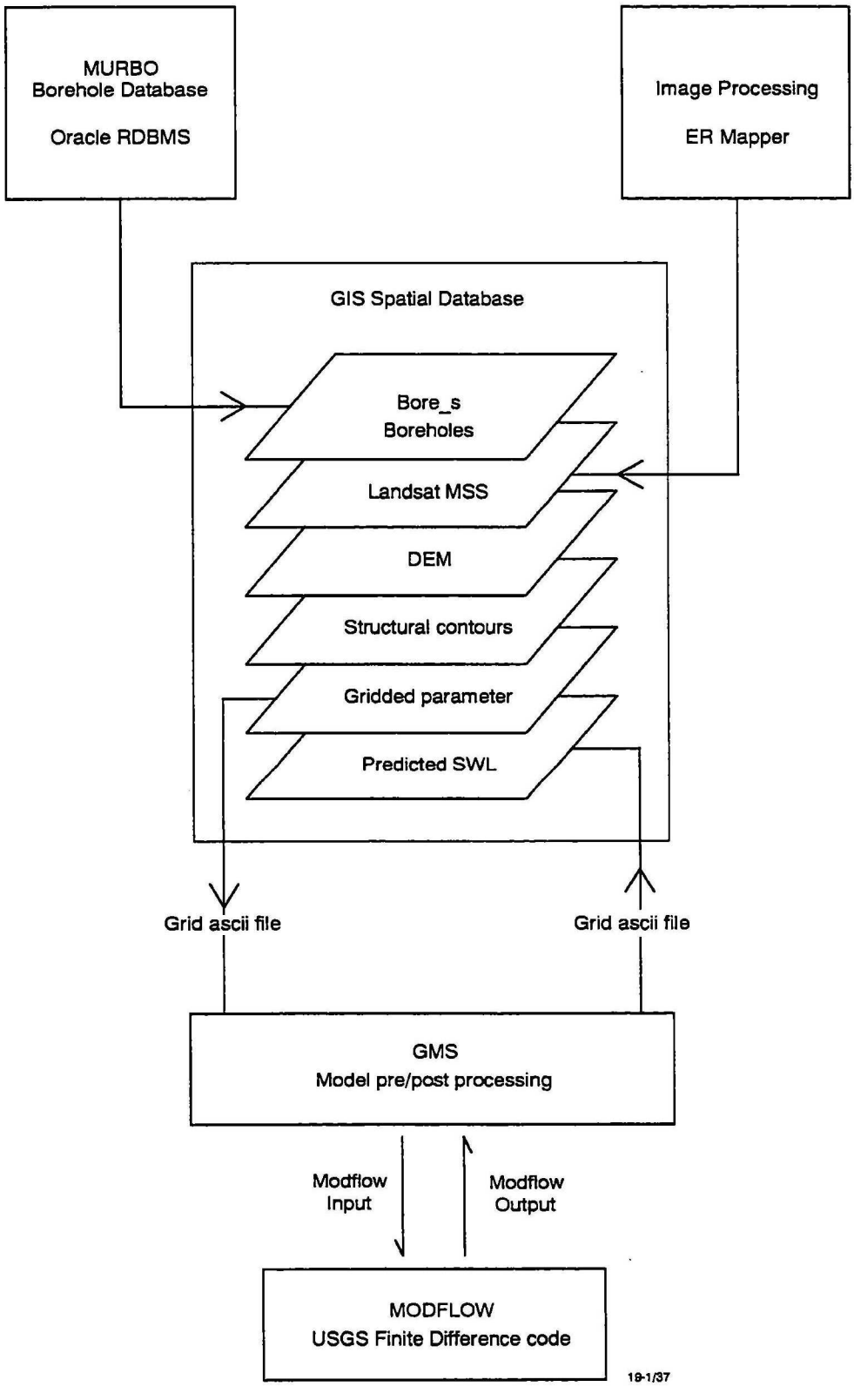

Figure 4.2 Working environment for compilation of Lower Darling Model

4.3 Working Environment

MODFLOW, as the name implies, is modular in design where components of the hydrogeological system are defined as independent packages. Conditions such as aquifer geometry and hydraulic characteristics as well as stresses such as wells, recharge and rivers are compartmentalised. A main program coordinates which modules are to be used in a model simulation.

Each of these modules require cell-by-cell averages of particular parameters, within a pre-defined file format. Figure 4.2 outlines the computing environment that was used to compile these MODFLOW files from the available data and to calibrate the model. A number of linkable software systems were used in the Unix environment to store, integrate and process the disparate datasets available for the model area. This included a relational database (RDBMS) to store key borehole data, a geographical information system (GIS) to maintain and analyse spatial data, image processing software and a model pre/post processor.

4.3.1 Borehole Database

An Oracle RDBMS is used to store key information for boreholes located within the model area. SQL-based queries can be made to access and process a range of borehole parameters. The MURBO schema, initially designed to support the regional hydrogeological mapping and modelling of the Murray Basin, was used to construct the tables (Brodie, 1993). The database structure contains the following data tables (Fig 4.3):

general- general borehole information such as name, location, elevation, drill depth, use, status and construction,
geophys - flags the existence of downhole geophysical logs,
pollen - palynological analyses of downhole lithological samples, including age estimates, predicted depositional environment, index and dominant pollen species and diagnostic pollen ratios,
foram- foraminiferal analyses of downhole lithological samples, analogous to the *pollen* table,
strat - downhole stratigraphy,
aqint - aquifer intervals intersected downhole, such as water cuts during drilling and final production intakes. Includes intake dimensions, construction and aquifer test data,
swl - standing water level measurements for particular aquifer intervals. Measurements may be relative to the top of casing or to the natural surface.
sample - data associated with field sampling of groundwater from particular aquifer intervals. Includes field measurement of pH, Eh, temperature, EC and dissolved oxygen,
majion - Major ion chemistry and routine lab measurements such as EC, pH and alkalinity for groundwater derived from particular aquifer intervals. Origin of sample stored in the *sample* table,
minion - Minor ion chemistry for groundwater derived from particular aquifer intervals,
isotope - Isotope chemistry for groundwater derived from particular aquifer intervals.

Authority tables are used to store attribute codes and definitions, linking to fields in the data tables. These tables ensure consistency in coding and that queries return the appropriate records. Examples include tables storing the relevant 1:250,000 and 1: 1,000,000 scale topographic maps (*sheet250* and *sheet1000*) , the standard geological units in the basin (*geol*) and codes for geological time periods (*age*).

The unique identifier for each borehole, typically the reference number assigned by the state water agency, is stored in the *boreid* field which is common to most of the data tables. This *boreid* field is used, with other fields, to link the data tables together providing the functionality of a relational database.

The majority of borehole data has been derived from the groundwater databases maintained by the agencies responsible for water resource management within each state. The relevant agencies are the New South Wales Department of Land & Water Conservation (DLWC) and Mines & Energy South Australia (MESA). Data was reformatted into the MURBO structure and codes, with a sequence of validation routines undertaken. Borehole information was also obtained from petroleum exploration archives and mineral exploration reports. In addition, data from about thirty nested piezometer sites that have been drilled in the western New South Wales part of the model as part of a recent AGSO-DLWC initiative have been incorporated.

Information for a total of 1982 bores in the vicinity of the model area are currently stored in the database, 1614 in New South Wales and 368 in South Australia. The majority of these boreholes (1378) are shallow, with depths less than 100 m. Only 19 bores have depths which exceed 500m. About 5000 stratigraphic intervals are stored in *strat*, 2750 aquifer intervals in *aqint*, 4750 water level measurements in *swl* and 1950 field chemistry samples in *sample*.

Additional tables were defined and populated to support the modelling effort. This included a table called *dwrdrill*, to store the lithological record of the boreholes. The definitions used in the groundwater database maintained by DLWC were emulated and includes fields for six description codes, four colour codes as well as grainsize, weathering, roundness and fossil attributes. The lithology of over 20,000 downhole intervals are described in the table and include data entered for the MESA bores in South Australia.

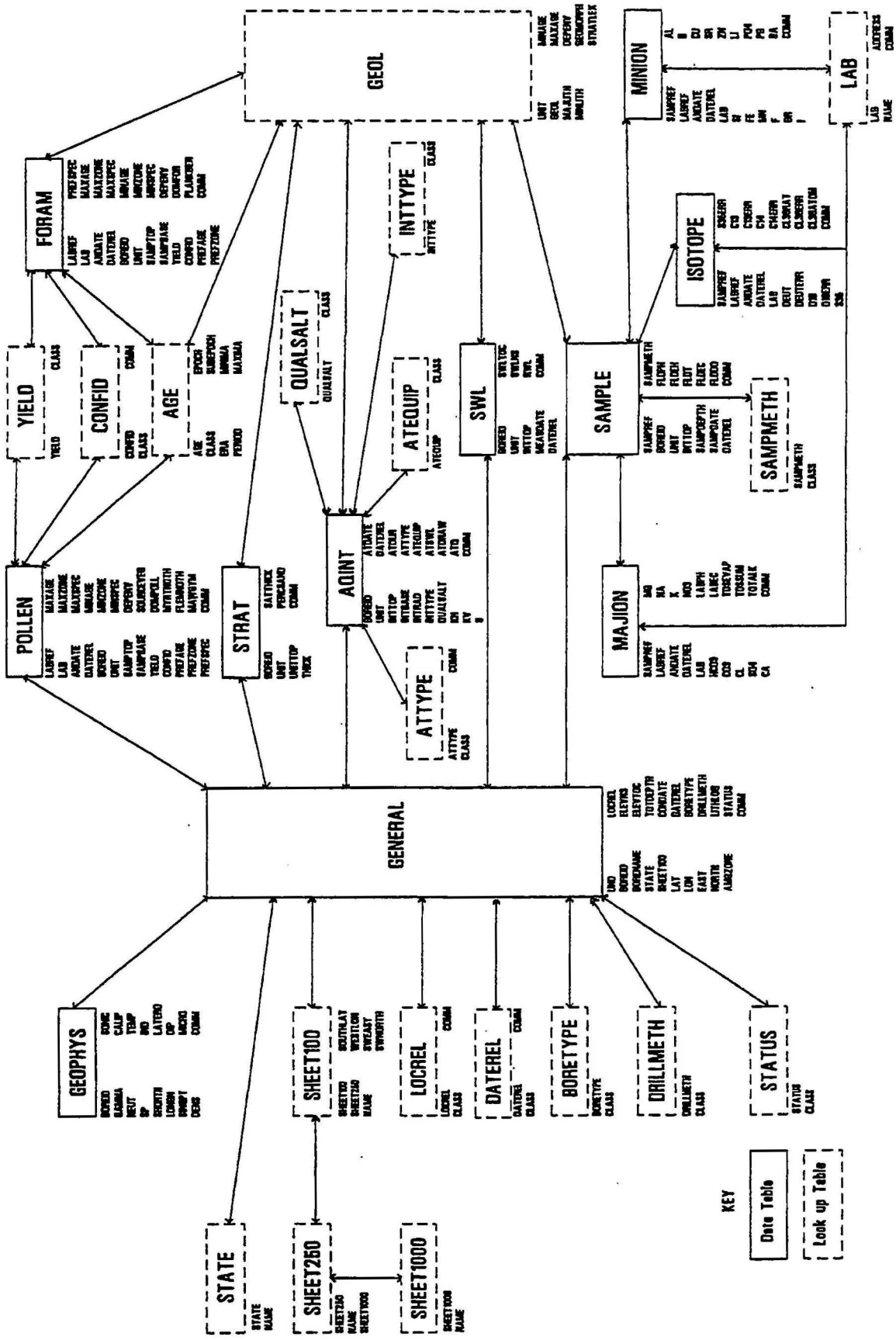

Figure 4.3 Schema for MURBO - Murray Basin borehole database (from Brodie, 1993)

4.3.2 GIS Spatial Database

Spatial data such as thematic mapping or digital elevation models (DEMs) are maintained in an Arc/Info geographical information system. Table 4.1 outlines the themes that are currently available over the model area. This involved the conversion of digital data from a number of federal and state government agencies.

Many of the hydrogeological datasets were derived from mapping undertaken for the 1:250,000 scale Murray Basin Hydrogeological Map Series. This involved the compilation of 26 mapsheets over the basin in a collaborative effort between AGSO and the water agencies of Victoria, New South Wales and South Australia. The mapping objectives were to show the influence of groundwater on salinisation, highlight present and potential salinity hazard, delineate useable groundwater resources and enhance community awareness of prevailing groundwater systems (Evans, 1992). Information on the depth to watertable, structural tops to aquifers, groundwater salinities, aquifer yields and potentiometry are displayed on the published maps. A GIS database was constructed for the Murray Basin from the digital data used in the publication process (Brodie *et al*, 1995).

Surface geology mapping, as well as lineaments, folds and faults, were derived from a basin-wide geological synthesis (Brown & Stephenson, 1991ab), supplemented with mapping information for the NSW part of the model area by the Geological Survey of New South Wales. Basic topographic and cultural information such as drainage, surface water features, roads, towns and homesteads was supplied by AUSLIG. This was supplemented by the national nine second DEM dataset recently published by AGSO and AUSLIG. Surface hydrology datasets were collected from different government agencies. These included surveys of the River Murray bed, the river level and flow data associated with gauging stations and locks. Climate data such as annual rainfall and evaporation were made available in raster form by NRIC. This involved meteorological station data being averaged and interpolated over the study area using an algorithm which considered surface topography. An important dataset is the *bore_s* point coverage containing the location of boreholes. This was generated from the MURBO database and as such is the spatial link to the attributes stored in the relational database (Figure 4.2). The attribute used to uniquely identify each borehole point in the GIS coverage is the same identifier which is used in the MURBO database, ie. the *boreid* field. In this way, the results of a SQL-based query on borehole attributes such as water levels, stratigraphy or chemistry within the relational database can be assigned to the appropriate geographical position.

Table 4.1 - Arc/Info GIS datasets available for Lower Darling Groundwater Model

Name	Theme	Type	Source
bore_s	boreholes	point	MURBO database
dem_g	9' digital elevation model of surface topography	grid	AGSO/AUSLIG
drainh_l	1:100 000 surface drainage	line, point	AUSLIG
drainm_l	1:1 000 000 surface drainage	line, point	AUSLIG
drainq_a	1:250 000 surface drainage	line	AUSLIG
evap_g	evaporation, mm/yr	grid	NRIC
gauge_s	Darling River gauging stations	point	NSW DLWC
geol_n	surface geology	polygon, line	AGSO
grav8.bil	gravity bouger anomalies	image	AGSO
home_s	homesteads	point	AUSLIG
irrig_p	irrigation districts	polygon	AGSO
klswl_l	potentiometry for Lower Cretaceous	lines, points	MB Hydro Series
klsy_n	salinity/yield for Lower Cretaceous	polygon, line	MB Hydro Series
klthk_l	thickness of Lower Cretaceous	line	author compiled
lakeh_p	1:100 000 surface water features	polygon	AUSLIG
lakeq_p	1:250 000 surface water features	polygon	AUSLIG
line_a	structural lineaments	line	AGSO
lndsys_p	land systems mapping	polygon	NSW DLWC, CSIRO
lock_s	locks on Murray River	point	MDBC
mbbnd_a	Murray Basin boundary	line	AGSO
pcztop_l	base of Tertiary structural contours	line, point	MB Hydro Series
qaswl_l	potentiometry for Coonambidgal Formation	line, point	MB Hydro Series
qpcthk_l	thickness of Blanchetown Clay	line, point	author compiled
rain_g	rainfall, mm/yr	grid	NRIC
reliab_p	reliability of hydrogeological datasets	polygon	MB Hydro Series
rivsabed_s	elevation of River Murray bed (SA)	point	SA Water
rivdem_s	spot heights near Murray River	points	MDBC
rivvicbed_s	elevation of River Murray bed (Vic)	points	MDBC
shalswl_l	Potentiometry for shallow aquifer	line, point	MB Hydro Series
shalsy_n	salinity/yield for shallow aquifer	polygon, line	MB Hydro Series
sheet100_p	1:100 000 mapsheets	polygon	AGSO
sheet250_p	1:250 000 mapsheets	polygon	AGSO
struct_a	geological structure - folds, faults	line	AGSO
swldep_l	depth to watertable	line, point	MB Hydro Series
swldiff_l	freshwater head difference	line, point	MB Hydro Series
ter1swl_l	potentiometry for lower Renmark Group	line, point	MB Hydro Series
ter1sy_n	salinity/yield for lower Renmark Group	polygon, line	MB Hydro Series
ter1top_l	top of lower Renmark Group	line, point	MB Hydro Series
ter2swl_l	potentiometry for middle Renmark Group	line, point	MB Hydro Series
ter2sy_n	salinity/yield for middle Renmark Group	polygon, line	MB Hydro Series
ter2top_l	top of middle Renmark Group	line, point	author compiled
ter3swl_l	potentiometry for upper Renmark Group	line, point	MB Hydro Series
ter3sy_n	salinity/yield for upper Renmark Group	polygon, line	MB Hydro Series
ter3thk_l	thickness of upper Renmark Group	line, point	author compiled
ter3top_l	top of upper Renmark Group	line, point	MB Hydro Series
mss.bil	Landsat MSS	image	AGSO
tmgthk_l	thickness of Geera Clay	line, point	author compiled
tmlswl_l	potentiometry for Murray Group Limestone	line, point	MB Hydro Series
tmlsy_n	salinity/yield for Murray Group Limestone	polygon, line	MB Hydro Series
tmlthk_l	thickness of Murray Group Limestone	line, point	author compiled
tmltop_l	top of Murray Group Limestone	line, point	MB Hydro Series
tmwthk_l	thickness of Winnambool Formation	line, point	author compiled
tocthk_l	thickness of Compton Conglomerate	line, point	author compiled
toethk_l	thickness of Ettrick Formation	line, point	author compiled
topo_l	topographic contours	line, point	AUSLIG
town_s	towns	point	AUSLIG
tpabase_l	base of Pliocene Sands	line, point	author compiled
tpaswl_l	potentiometry for Pliocene Sands	line, point	MB Hydro Series
tpasy_n	salinity/yield for Pliocene Sands	polygon, line	MB Hydro Series
tpatop_l	top of Pliocene Sands	line, point	MB Hydro Series
tpbthk_l	thickness of Bookpurnong Beds	line, point	author compiled
tqsswl_l	potentiometry for Shepparton Formation	line, point	MB Hydro Series
tqssy_n	salinity/yield for Shepparton Formation	polygon, line	MB Hydro Series
trans_l	transport - roads, rail	line, point	AUSLIG
veg_g	vegetation	grid	NFI
xsect_a	cross section lines	line	MB Hydro Series

AGSO - Australian Geological Survey Organisation
AUSLIG - Australian Surveying & Land Information Group
MB Hydro Series - 1:250 000 Murray Basin Hydrogeological Map Series
MDBC - Murray Darling Basin Commission
NFI - National Forest Inventory Preliminary data
NRIC - National Resource Information Centre

This capability was used extensively in the compilation of hydrogeological datasets to support the modelling. Relevant data was processed and extracted from the MURBO database and integrated with auxiliary spatial data in the GIS. This was used as a base to interpolate contours of the particular theme. For example, minimum thickness of the Lower Cretaceous was derived from the stratigraphic record for the deeper boreholes, as stored in the *strat* table. This included highlighting boreholes which drilled through the Tertiary but also where the Cretaceous was subsequently absent. This borehole data was placed in a spatial context by being integrated with existing GIS data such as the structural contours of the base Tertiary, and surface mapping of the Cretaceous and older units. Isopachs for the Lower Cretaceous were subsequently interpolated. Datasets such as thickness and structural tops of key stratigraphic units were compiled in this way.

4.3.3 Image Processing

ERMapper was used to rectify, clip and process imagery for use in the GIS environment. This included remotely sensed data, specifically Landsat MSS imagery which was used to indicate land use and vegetation clearing (refer Figure 1.13). Rasterised geophysical data, such as gravity bouguer anomalies useful in defining basin structure, were also processed. The software generated standard BIL files which could readily be incorporated into GIS displays.

4.3.4 Model Pre/Post Processor

Each of the MODFLOW modules requires input files in a predefined format. To produce these files, a graphical user environment for numerical modelling, the Department of Defence Groundwater Modelling System (GMS) was used (Brigham Young University, 1996). GMS has an interface to MODFLOW as well as to FEMWATER and MT3D modelling codes. This allows importing, visualising and editing of datasets into input arrays and the entering of model parameters via graphical displays. The final model input is also checked for logical errors by GMS, before the model is run using the standard MODFLOW code. In turn, head, drawdown or cell-by-cell flow model output can be loaded back into GMS for visualisation, reformatting or statistical analysis. GMS has a sophisticated range of visualisation tools including interactive rotation of 3D oblique views, hidden surface removal, contours and colour fringes, cross sections and iso-surfaces and animation sequences. A number of data formats can also be handled, such as triangulated irregular networks (TINs), boreholes, 2D & 3D meshes, grids and scatter points.

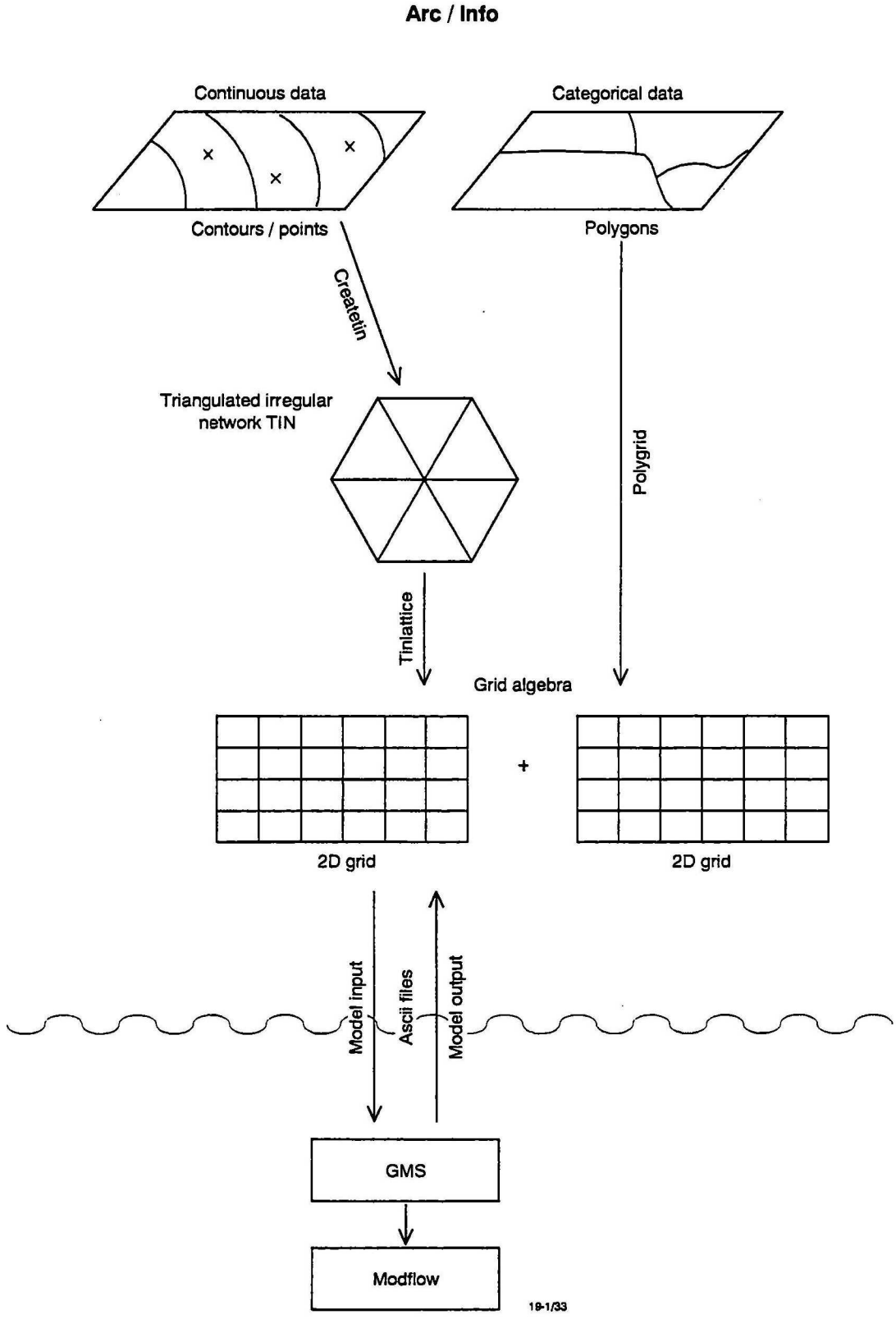

Figure 4.4 Data Processing for creation of MODFLOW input and calibration

The linkage between GMS and the Arc/Info GIS which stores the spatial information and in turn linked to the Oracle borehole database, is critical for the modelling process. Figure 4.4 summarises the data processing involved for the Lower Darling model in the creation of MODFLOW input. In Arc/Info, parameters were averaged for each model cell by creating a 2-D grid of the same dimensions and extent as the model. How this was achieved varied with the dataset.

Where a parameter had been mapped as a continuous surface by contours and point measurements, such as structural contours and spot heights, a triangular irregular network (TIN) was constructed. This involved forming the points which represent the vertices of the contours into a series of connecting triangles. Additional information such as spot heights, extra contours, or arcs depicting the axes of maxima (ridges) or minima (valleys) were added to better define the data surface. This was essentially an iterative process where contours or grids generated off the TIN were verified against the original contours for goodness of fit. The TIN input was then modified or added to and a new TIN is calculated. When the TIN adequately represented the data surface, it was resampled on the basis of the model grid.

Other parameters were mapped as polygons, and are termed discrete or discontinuous datasets. Categorical data such as soils or geomorphological mapping are examples of this type of data. For the model, layer conductivities and leakances were mapped in this way. These polygon coverages were simply resampled on the basis of the 2-D model grid.

Model parameters were also generated by algebraically combining grids. Examples include thickness grids where the layer base was subtracted from the layer top and transmissivity grids, where thickness was multiplied by the horizontal hydraulic conductivity. The use of grid algebra can become relatively sophisticated, for example the recharge array is generated by conditionally combining rainfall, geomorphology and vegetation grids.

Once the 2-D grid was generated in the GIS, it was exported as an ASCII file. In turn, this file was simply loaded into the relevant model array within GMS, allowing the MODFLOW input to be built up. The process could also operate in reverse. For example, the predicted heads from MODFLOW could be read into GMS for visualisation and statistics as well as the generation of an ASCII export file. In Arc/Info, this file was imported to generate a 2-D grid, allowing the predicted heads to be integrated with the available spatial datasets.

4.4 Basic (BAS) Package

The Basic Package coordinates the modelling process and stores fundamental parameters defining the model. These include model geometry (rows, columns, layers, active cells), the MODFLOW modules to be used, the standard units for time, the starting head arrays and model output options. The package also allocates memory and defines the location of input data.

4.4.1 Layer Boundaries

The spatial extent of each model layer is specified by the IBOUND array, with each cell defined as either a:

- variable-head cell (ibound > 0)
- constant-head cell (ibound < 0)
- or an inactive cell (ibound = 0) where no flow occurs

The bounds for layers 1 to 5 are depicted in Figures 4.5 to 4.9 respectively. In these arrays, cells where the layer is saturated were assigned a value of 1, and where the layer existed but is currently unsaturated was assigned a value of 2. This allows a cell where the layer exists to participate in the model simulation until it dries out and likewise allows a current unsaturated cell to be active and wet up during a predictive run where heads rise.

The boundary arrays are constructed from a polygon coverage developed within the GIS. Previous hydrogeological mapping such as structural or SWL contours, which define the boundaries of these aquifers were used as a base. These limits were checked and modified in a number of ways. Firstly, MURBO borehole data was used to plot locations where the geological units comprising the model layer were recorded in the *strat* table. Equally, boreholes which drilled deeper than the stratigraphic position of the layer but failed to intersect any relevant units, were also highlighted. This information was combined with surface geological mapping to edit the physical limits of the model layer. This was particularly useful in situations, such as in layer 4, which involved the combination of a number of different geological units. Secondly, grid analysis was used to validate the boundary of the saturated part of the layer. The elevation of the base of layer grid was subtracted from the grid representing the observed heads in the layer. Where the resulting grid was positive, the layer is saturated and conversely where the observed head is lower than the base of the layer, the layer is unsaturated.

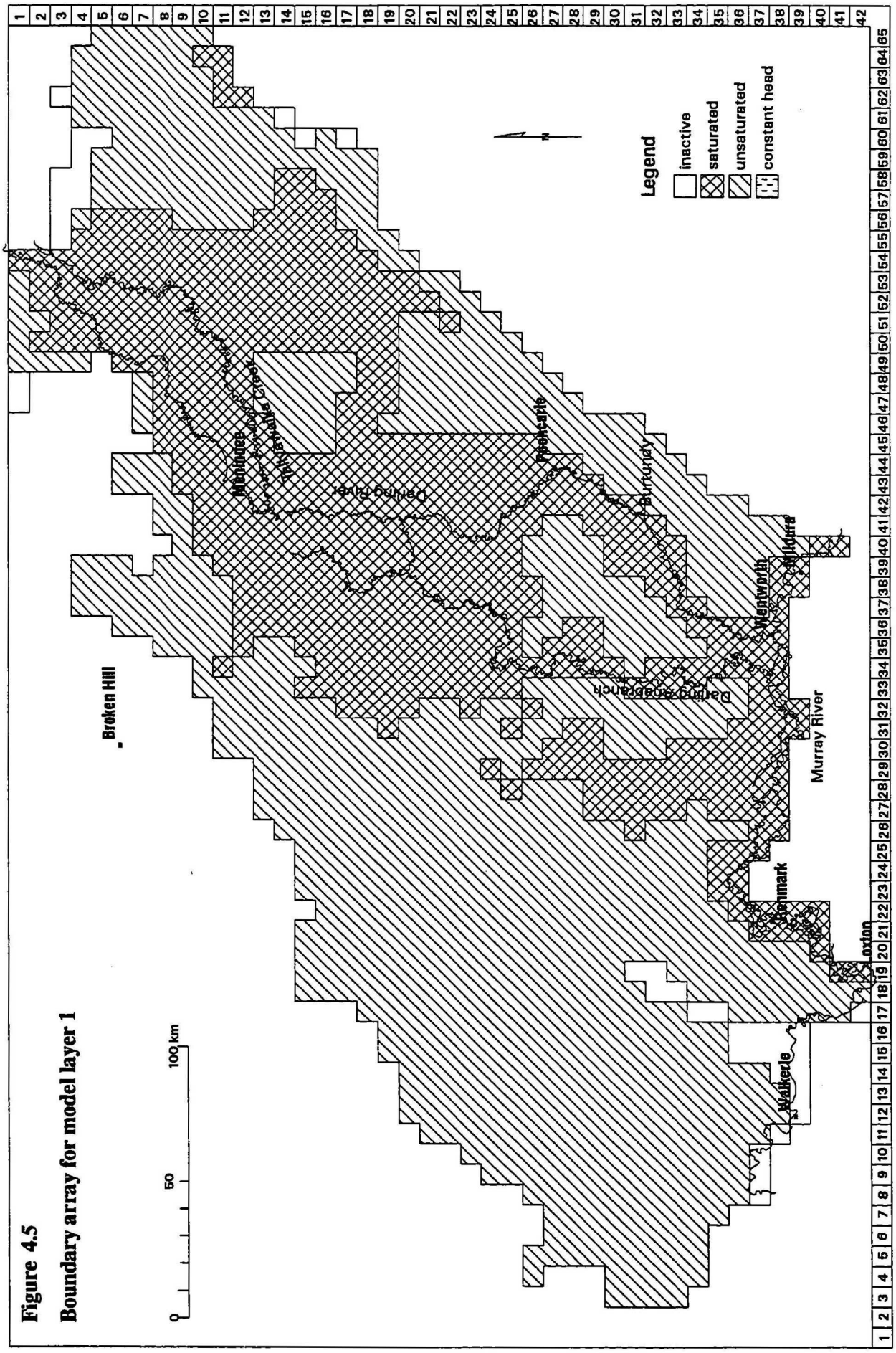

Figure 4.5
Boundary array for model layer 1

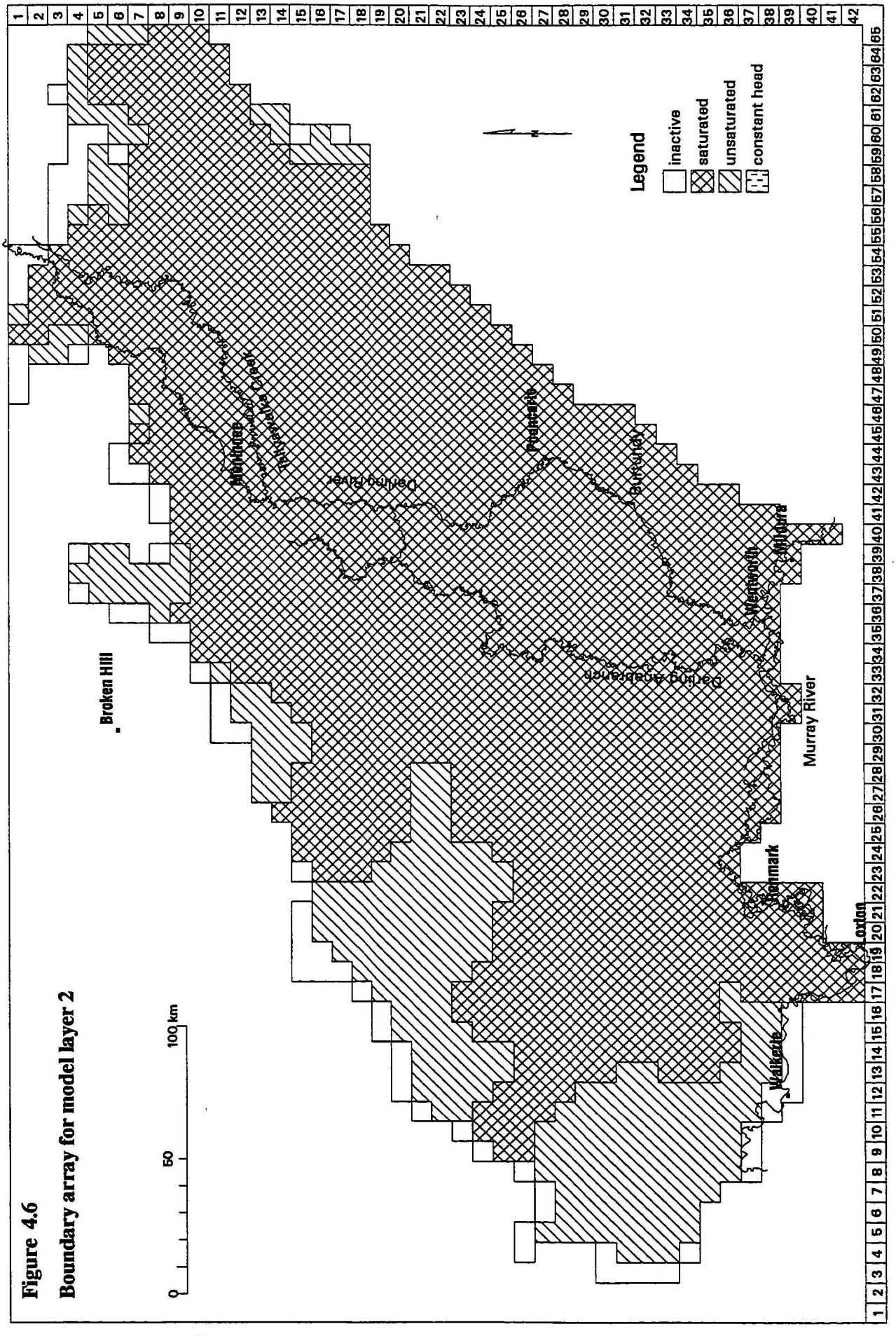

Figure 4.6
Boundary array for model layer 2

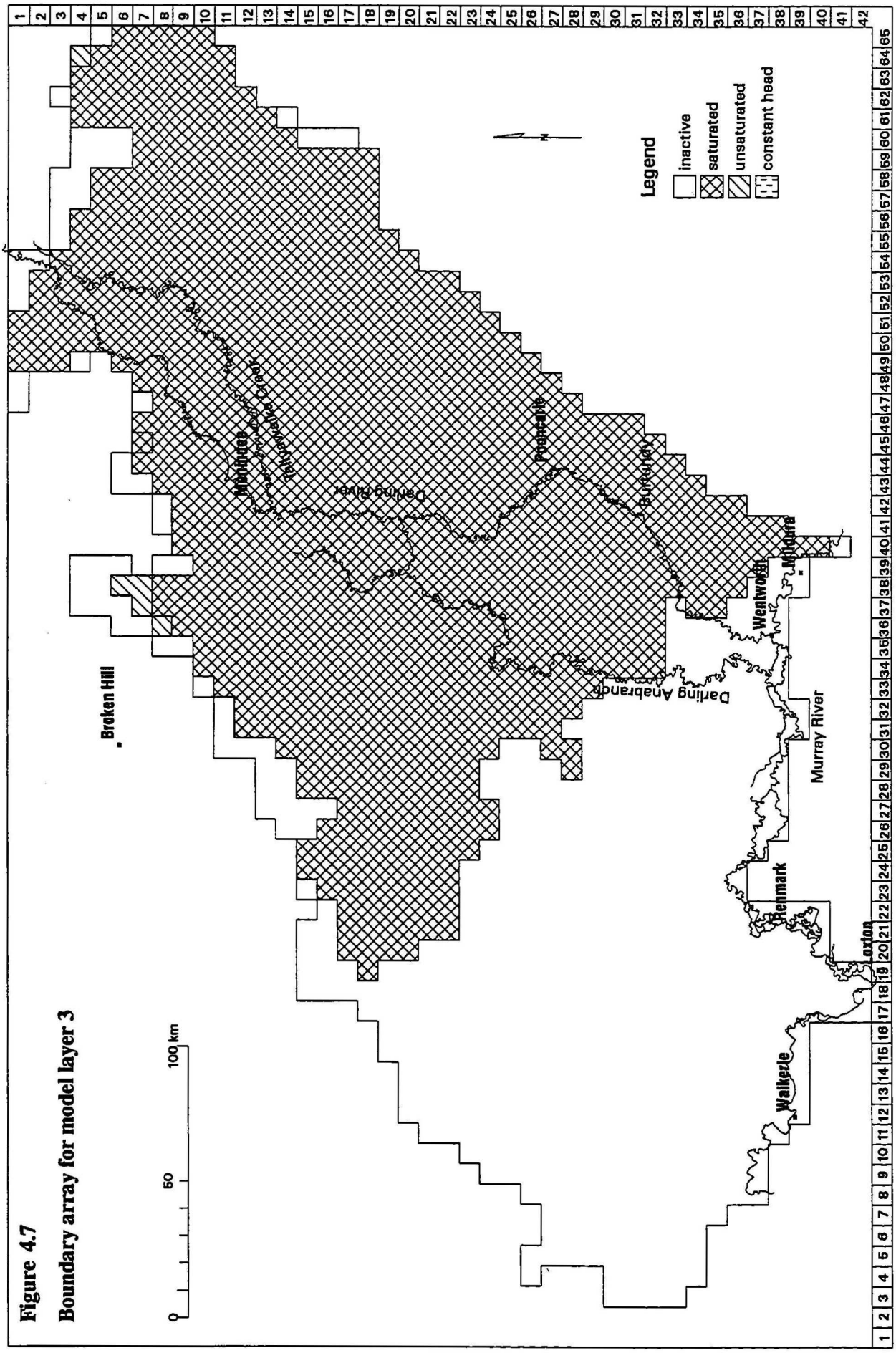

Figure 4.7

Boundary array for model layer 3

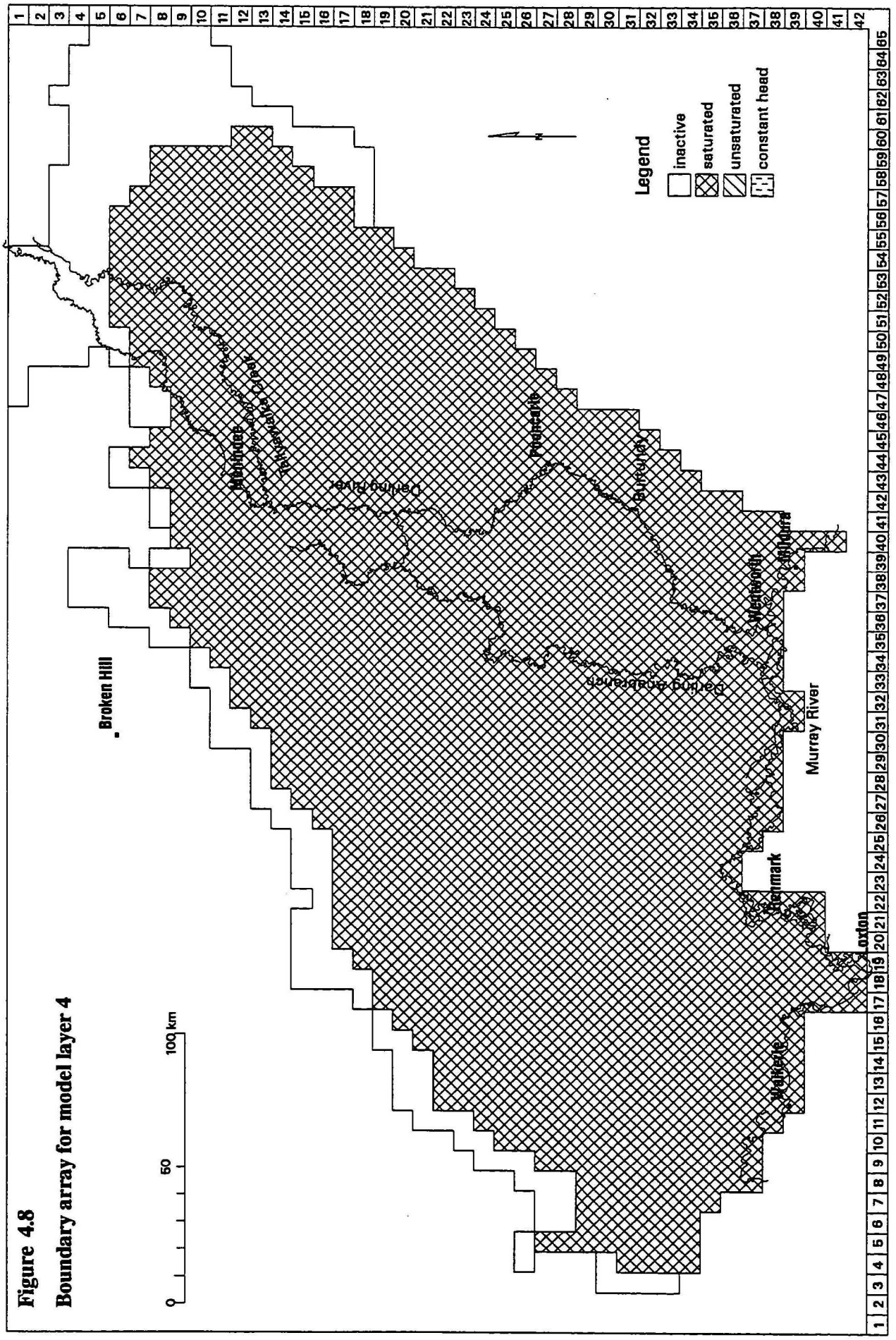

Figure 4.8
Boundary array for model layer 4

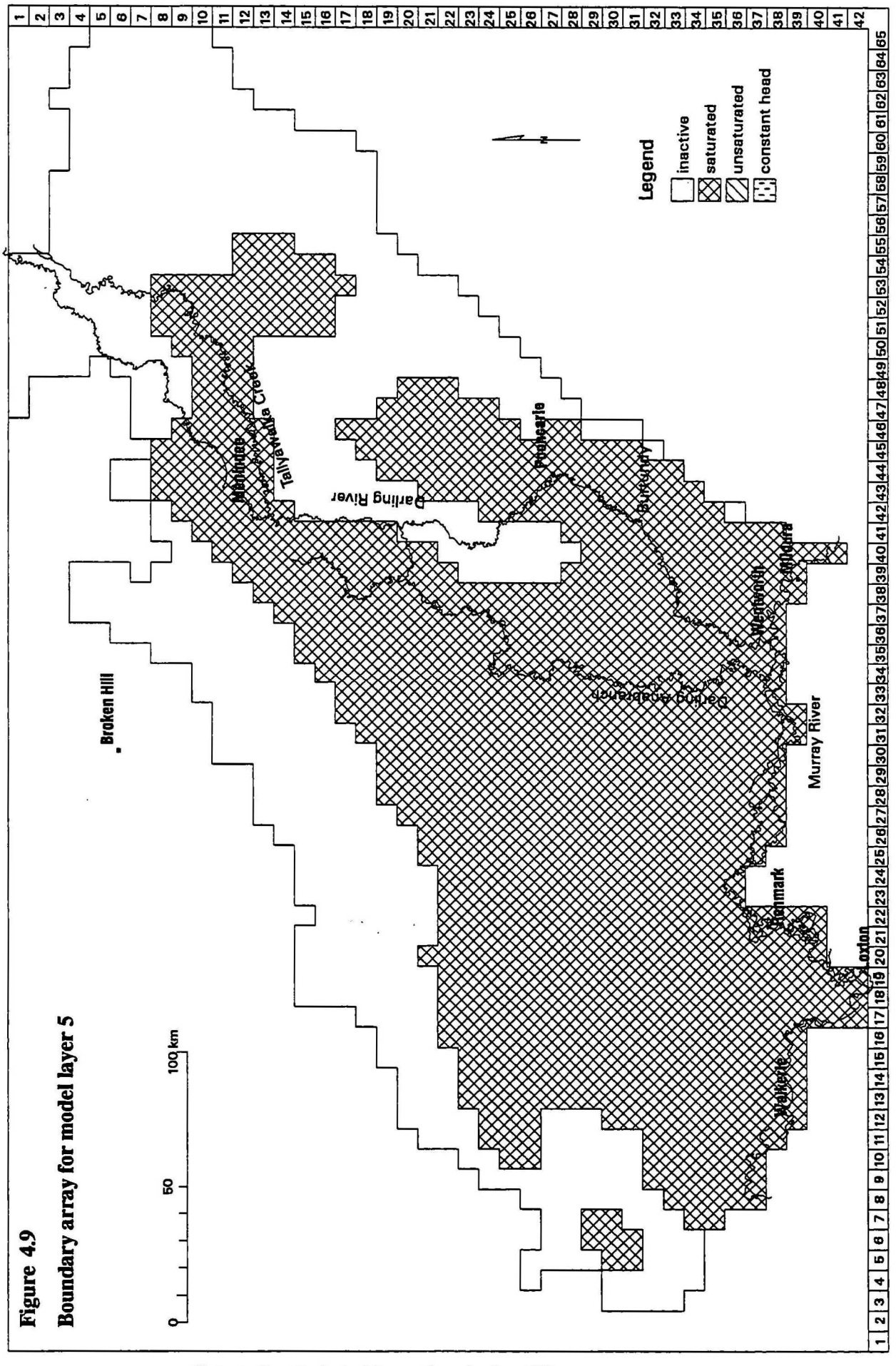

Figure 4.9
Boundary array for model layer 5

The boundary array for layer 1 is plotted in Figure 4.5. The Shepparton Formation spans the northern half of the layer where fluvial sediments dominate, as indicated in Figure 3.5. The Blánchetown Clay is a thin (10-20m) but laterally extensive unit in the southern half, reaching up into the Menindee Trough. The unit only partially covers the Woolpunda Ridge, shown by the inactive cells trending to the northwest of Waikerie. This model layer is only saturated (ibound = 1) in the deeper parts of the post-Pliocene land surface, close to the modern rivers. Here, the layer is thicker and the watertable is shallow due to the riparian influence. The Blanchetown Clay is also saturated in the low-lying central-southern discharge zone where watertables are also close to the surface.

The boundary array for layer 2 (Figure 4.6) shows the regional nature of the Pliocene Sands aquifer. The layer only becomes unsaturated near the basin margins, where the base of the layer rises up to the surrounding basement and the watertable is relatively deep. The incursions of unsaturated Pliocene Sands found along the western margin are largely defined by structural highs in the pre-Pliocene land surface.

In contrast, layer 3, the upper Renmark Group, is limited to the northern half of the model area, pinching out southwards against finer-grained marginal marine equivalents (Figure 4.7). The bulk of the unit is saturated, with occasional dry cells abutting the northern basin margin.

As layer 4 is a composite of mid-Tertiary aquifers such as the middle Renmark Group and the Murray Group Limestone as well as intervening aquitards such as the Geera Clay and Winnambool Formation, the active boundary array is extensive (Figure 4.8). As these units are deeper and relatively thick, the layer is invariably saturated.

The boundary array for layer 5 represents the confinement of the aquifer to the deeper parts of the basin (Figure 4.9). These include the large ovoid Renmark Trough in the south and the more linear Wentworth, Tarrara, Menindee and Blantyre Troughs to the north. A small outlier of lower Renmark Group sediments is found in the southeast corner of the model.

4.4.2 Initial Heads

MODFLOW uses an iterative process to find a solution to the system of governing finite difference equations. The code uses a backward-difference form of equations, so that a head distribution at the beginning of each time step is required to calculate the head distribution at the end of that time step. In theory, as this model is steady state, any head distribution can be used. In practice, the potentiometry interpreted for 1988 was used where the layer is saturated, while where the unit is deemed unsaturated a synthetic head was calculated by adding 10m to the base of the aquifer. This made validation of the model input easier, as GMS checks whether active cells are initially saturated. As the iterative process proceeds to a steady-state solution, the modelled head should decrease below the layer base where the layer is currently unsaturated.

The potentiometry observed in 1988 was also used as the basis to compare predicted heads. These heads were mapped as part of the Murray Basin Hydrogeological Map Series and stored as arc coverages in Arc/Info. The borehole water level measurements stored in the *swl* table

were used to verify the interpretation. Also, additional interpolation of contours had to be made outside the coverage of the published maps, particularly for the WILCANNIA mapsheet. The potentials for the saturated Blanchetown Clay component of Layer 1 used those mapped for the underlying Pliocene Sands. For layer 4, a composite coverage was constructed based on the potentiometric contours for the middle Renmark Group, Geera Clay and Murray Group Limestone.

From these arc coverages, TINs were constructed and grids emulating the model dimensions generated. These were then directly compared with the gridded predicted heads imported from GMS. For example, the modelled head grid could be subtracted from the observed head grid to derive the residual difference. Hence, problem areas where the model was either under or over predicting layer heads could be easily highlighted.

The observed head arrays are presented in Figures 4.10 to 4.14. The relevant potentiometric contours and flow directions are shown in Figures 3.1 to 3.5. The disruption of the general groundwater flow to the southwest by the Menindee Lakes is particularly evident in the observed heads for layer 1 (Figure 4.10). Here, river regulation and long-term water storage has increased the regional shallow watertable by over 10 m. Head varies in the shallow aquifer from > 60m AHD near the Cobar Block to < 5 m AHD along the Murray River, equating to an average hydraulic gradient of about 12 cm/km.

The Menindee Lakes also forms a significant groundwater mound in the observed heads for layer 2 (Figure 4.11). The regional groundwater flow is also to the southwest from >65 m AHD near the Cobar Block to a low of <10m AHD near Waikerie. Flow tends to be directed by the structural lows of the basin, with the high heads (~45 m AHD) in the model centre due to the Lake Wintlow structural high. The observed heads in layer 3 (Figure 4.12) are very similar, indicating the degree of connection between the Pliocene Sands and the upper Renmark Group.

Observed heads in layer 4 range from about 50m AHD in the middle Renmark Group north of Ivanhoe to <5 m AHD within the Murray Group Limestone along the Murray River (Figure 4.13). The groundwater mound under the Menindee Lakes is less prominent for this layer but does exist. High gradients of around 150 cm/km are evident in the southwest corner where recharge from Burra and Newikie Creeks flow along a relatively short flow path (50-60km) towards the groundwater sink along the Murray River.

Groundwater in layer 5 flows from a high of about 46 m AHD at the head of the Blantyre Trough to a low of 28 m AHD in the southwest corner of the model (Figure 4.14). Groundwater actually flows further southwards past the Murray River and beyond the model boundary. Flow also tends to be aligned with the structural elements of the basin with evidence suggesting that the Tarrara Trough acts as a local groundwater sink with heads at about 31 m AHD.

Figure 4.10

Observed head array for model layer 1

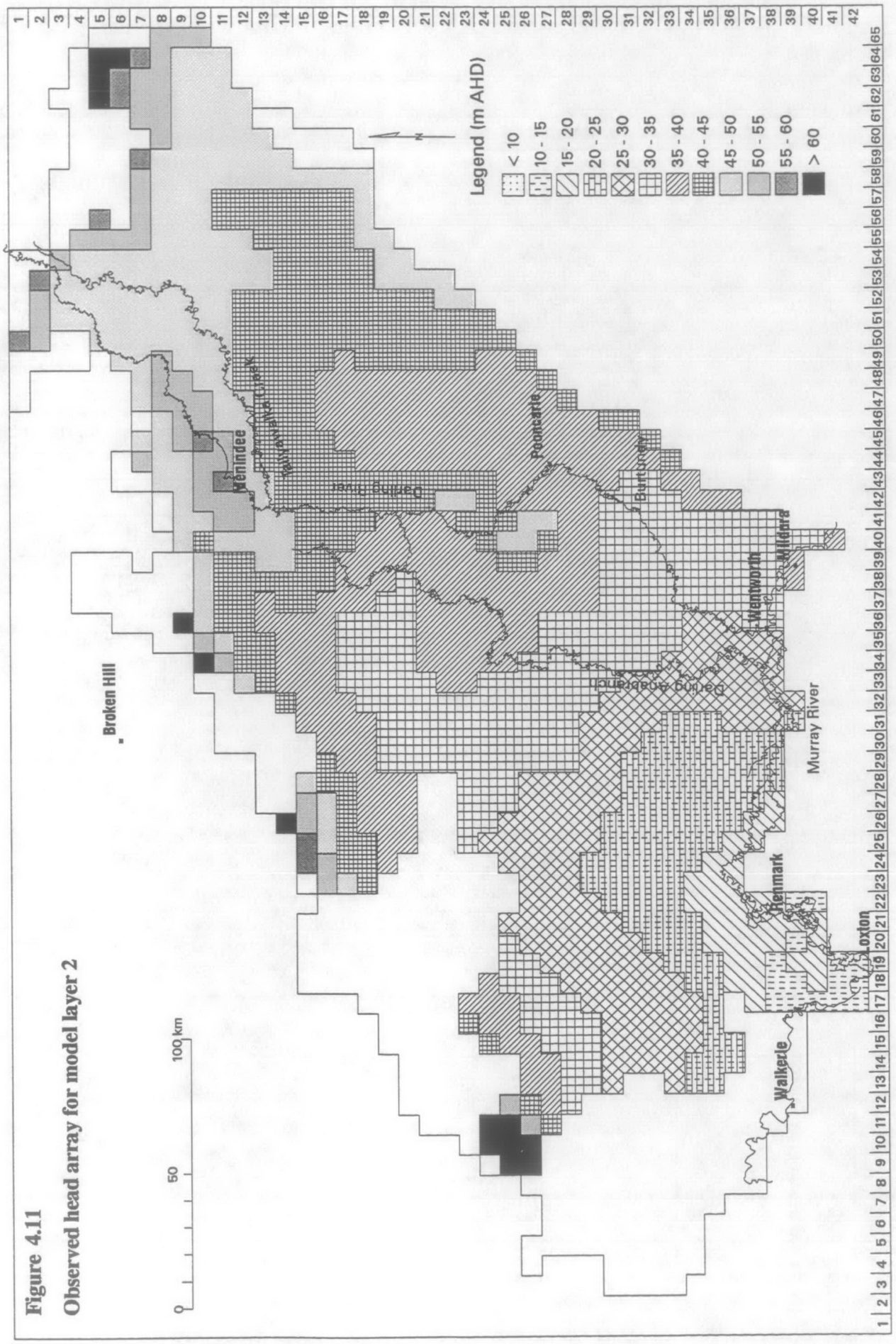

Figure 4.11

Observed head array for model layer 2

Figure 4.12

Observed head array for model layer 3

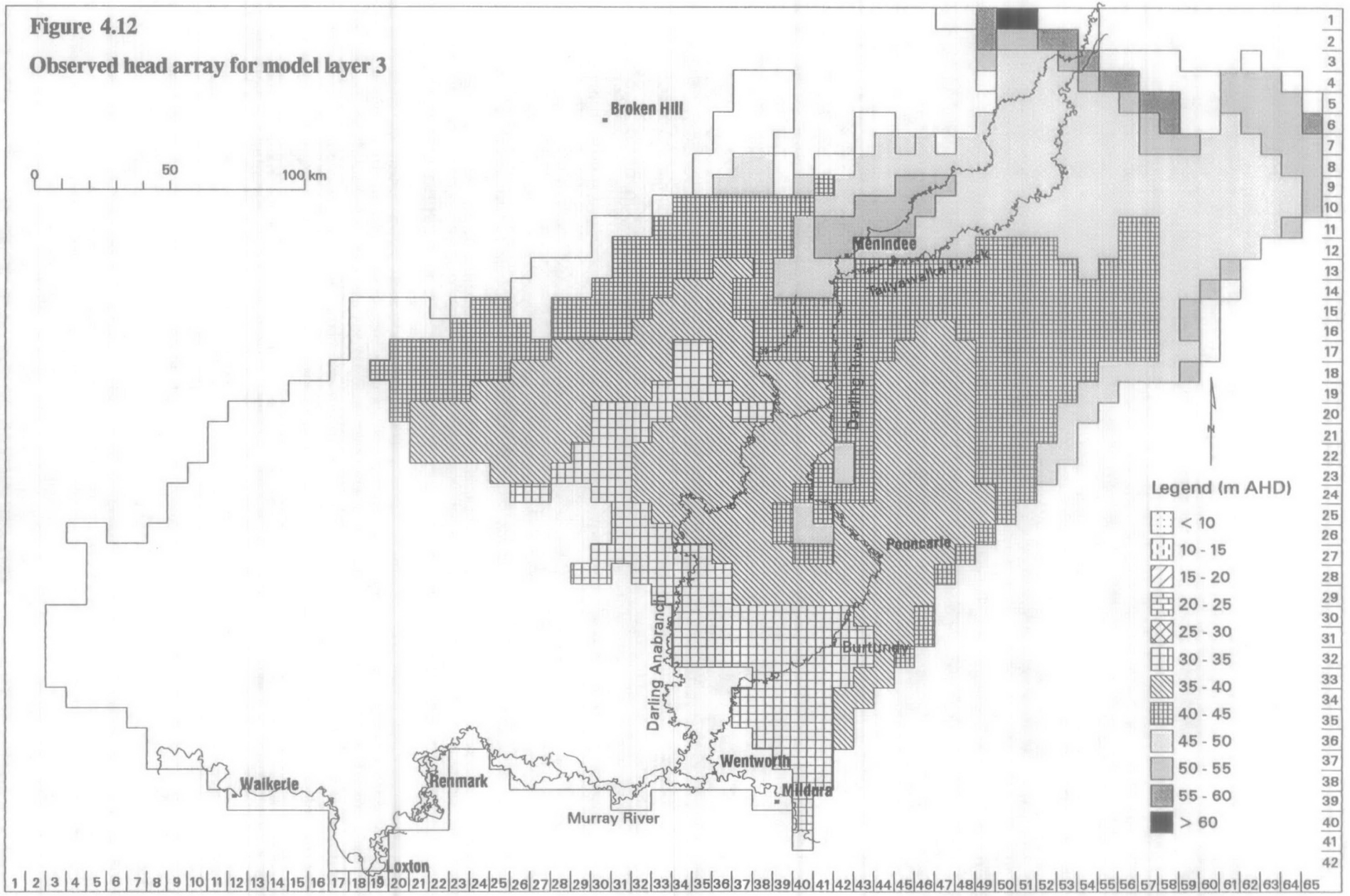

Figure 4.13

Observed head array for model layer 4

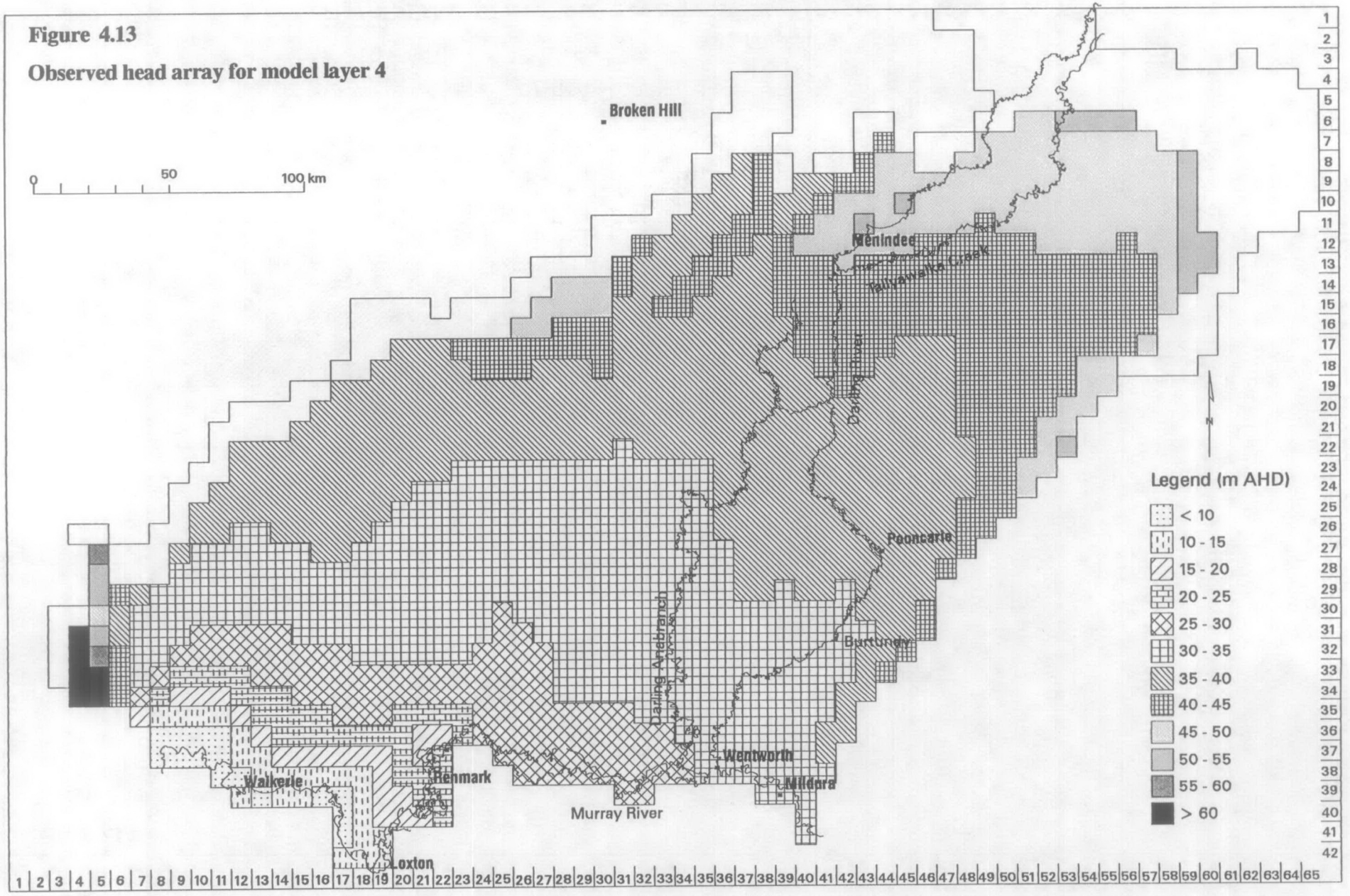

Figure 4.14

Observed head array for model layer 5

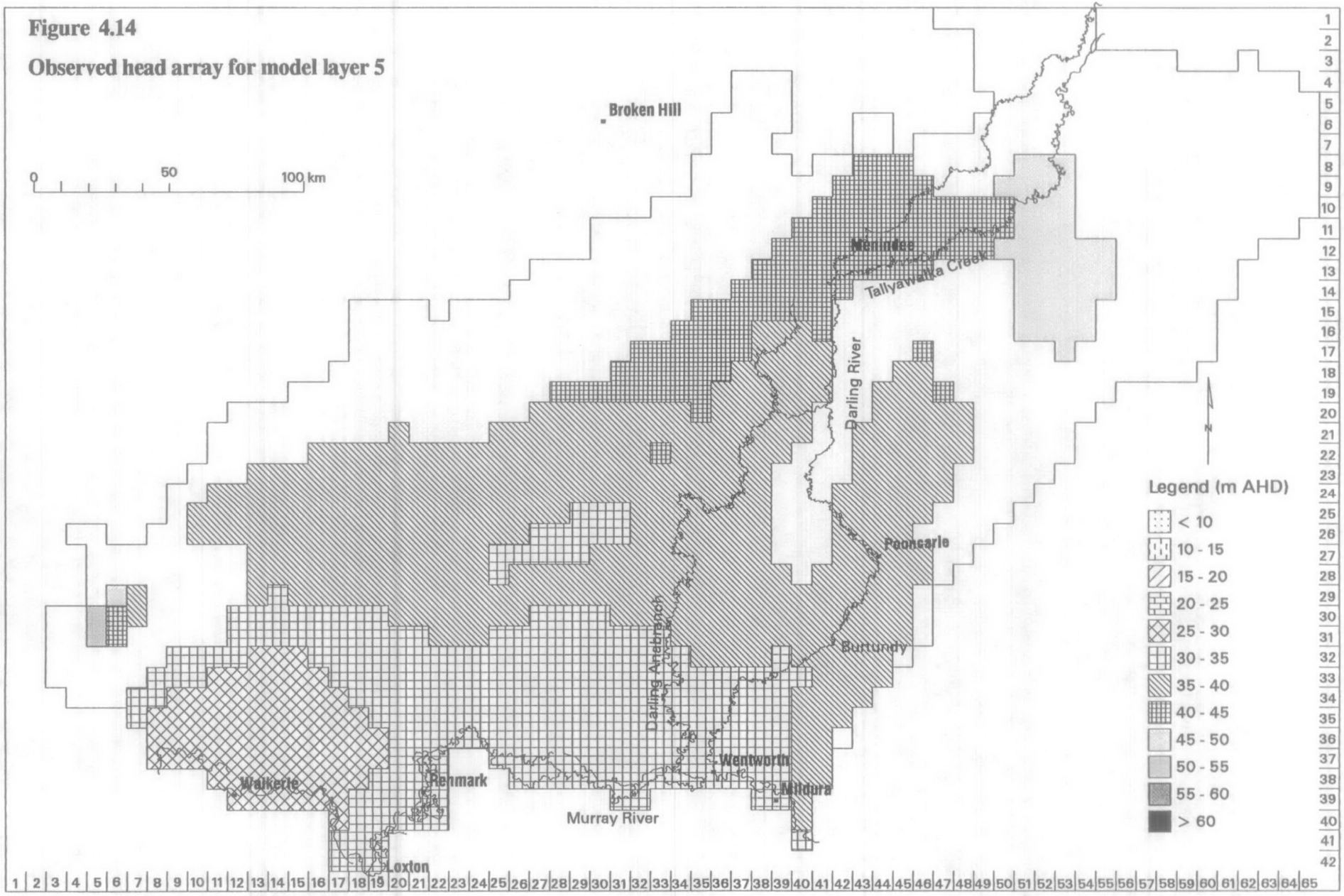

4.5 Block Centered Flow (BCF) Package

The Block Centred Flow package contains the fundamental parameters defining cell-to-cell flow and storage within the model, and as such is the core of the MODFLOW package. Groundwater flow is determined between the central nodes of adjacent cells; hence the term Block Centred Flow.

The three-dimensional movement of groundwater of constant density through a porous medium is described by the partial-differential equation;

$$\frac{\partial}{\partial x}\left(K_{xx}\frac{\partial h}{\partial x}\right) + \frac{\partial}{\partial y}\left(K_{yy}\frac{\partial h}{\partial y}\right) + \frac{\partial}{\partial z}\left(K_{zz}\frac{\partial h}{\partial z}\right) - W = Ss\frac{\partial h}{\partial t}$$

Where K_{xx}, K_{yy} and K_{zz} are hydraulic conductivity values along the x, y and z coordinate axes, h is the potentiometric head, W is the volumetric flux per unit volume and represents sources and sinks of water, Ss is the specific storage of the aquifer and t is time. This becomes a mathematical representation of an aquifer system when combined with boundary and initial head conditions.

For each model cell, this equation is used to describe the flow between a cell node and the nodes of the six adjacent cells. The notation is simplified by combining the grid dimensions and hydraulic conductivity into a conductance term (McDonald & Harbaugh, 1988). Specifically, conductance is the product of hydraulic conductivity (K) and the cross sectional area (A), determined by the cell dimensions, divided by the length of the flow path (L), the distance between nodes. This term is calculated for each of the internode prisms of aquifer between a cell node and its neighbouring six cell nodes. How this is calculated varies, depending on the aquifer type. For example, if the layer is the shallow watertable aquifer, horizontal conductances must be calculated dynamically as the saturated thickness changes with head fluctuations. Parameters such as hydraulic conductivity, the top and base of the cell need to be specified. The conductance in the vertical direction, the leakance (*vcont*) array, is also required as input. For basal confined aquifers where the saturated thickness is constant, only a transmissivity array is needed.

The data needs for the BCF package therefore vary with the type of aquifers modelled. For the Lower Darling Model, layer 1 is an unconfined aquifer type (type = 1) and layers 2,3 and 4 are mixed confined/unconfined (type = 3) requiring input of horizontal hydraulic conductivity, base and top arrays as well as vertical leakance. The basal layer 5 is modelled as a confined aquifer (type = 0), and only a transmissivity array is required. As the modelling is steady state, no storage terms (Ss) are needed in the governing equations.

4.5.1 Top and Base of Layers

The geometry of the aquifers need to be specified in the BCF package for the uppermost four model layers. Figures 4.15 to 4.18 are the relevant base of aquifer arrays for layers 1 to 4 respectively. As the model layers include all stratigraphic units, the tops of each layer match the base of the overlying layer. Many of these datasets were compiled as structural contours for the Murray Basin Hydrogeological Map Series (refer Figures 2.1-2.14). The available arc coverages such as the top of the Pliocene Sands, top of (upper) Renmark Group, top of Murray Group Limestone and base of Tertiary were updated and extended using the stratigraphic information stored in the *strat* table. Additional coverages, such as the top of the middle Renmark Group had to be specifically compiled for the model. For these, contours were manually interpolated from the stratigraphic information from the relational database, integrated in the GIS with data such as surface geology, interpreted aquifer boundaries, and structural contours of underlying units. These arc coverages were used to generate TINs, which were resampled to the model grid for transfer into GMS.

This process required a level of confidence on the stratigraphic interpretation stored in the *strat* table. To achieve this, a network of cross sections were drawn to visualise the stratigraphy in the vertical direction (Figure 4.19). This was semi-automated in the sense that the boreholes comprising the cross section could be selected within the GIS, relevant data accessed from the *strat* table and their downhole stratigraphy plotted. The stratigraphic boundaries were then manually interpolated between the plotted boreholes. A conceptual model could be built up for the regional geology and inconsistencies in the stratigraphic interpretation could be better highlighted.

The aquifer geometry could also be reconciled by using the gridded data. Thickness grids were generated by subtracting the layer base grid from the layer top grid. Potential errors were highlighted where the resulting grid was negative and the layer actually existed. These errors typically related to misinterpretations of the stratigraphy or in the TIN not adequately representing the data surface.

The base of layer 1 (Figure 4.15, Figure 2.13) depicts the post-Pliocene land surface following the deposition and erosion of the Calivil Formation in the northwest and the Parilla Sands to the south. Palaeochannels are a feature in the northwest where fluvial sedimentation prevailed, notably along the proto-Darling and off the Broken Hill Block. Elevated areas overly structural highs such as Lake Wintlow and the Neckarboo Ridge. The southeast trending dune and swale morphology characteristic of the Parilla Sands, is evident in the southern-central part of the model. The northeast trending Woolpunda Ridge, causing the absence of Blanchetown Clay, is a dominant feature in the southwest corner of the model. Elevations range from >150 m AHD along the northwest basement margin to less than sea level underlying Lake Victoria.

Figure 4.15

Base of layer array for model layer 1

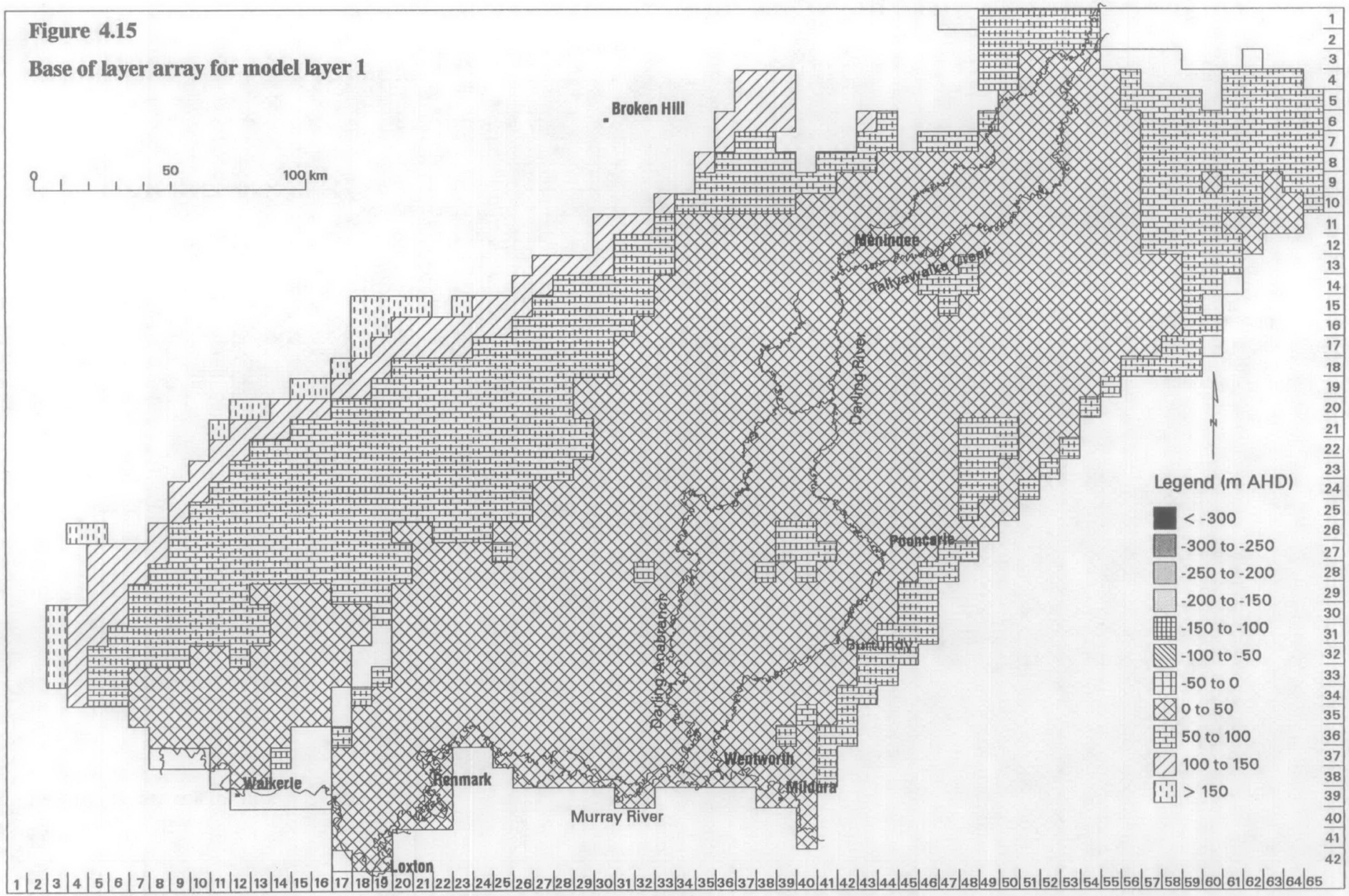

Figure 4.16

Base of layer array for model layer 2

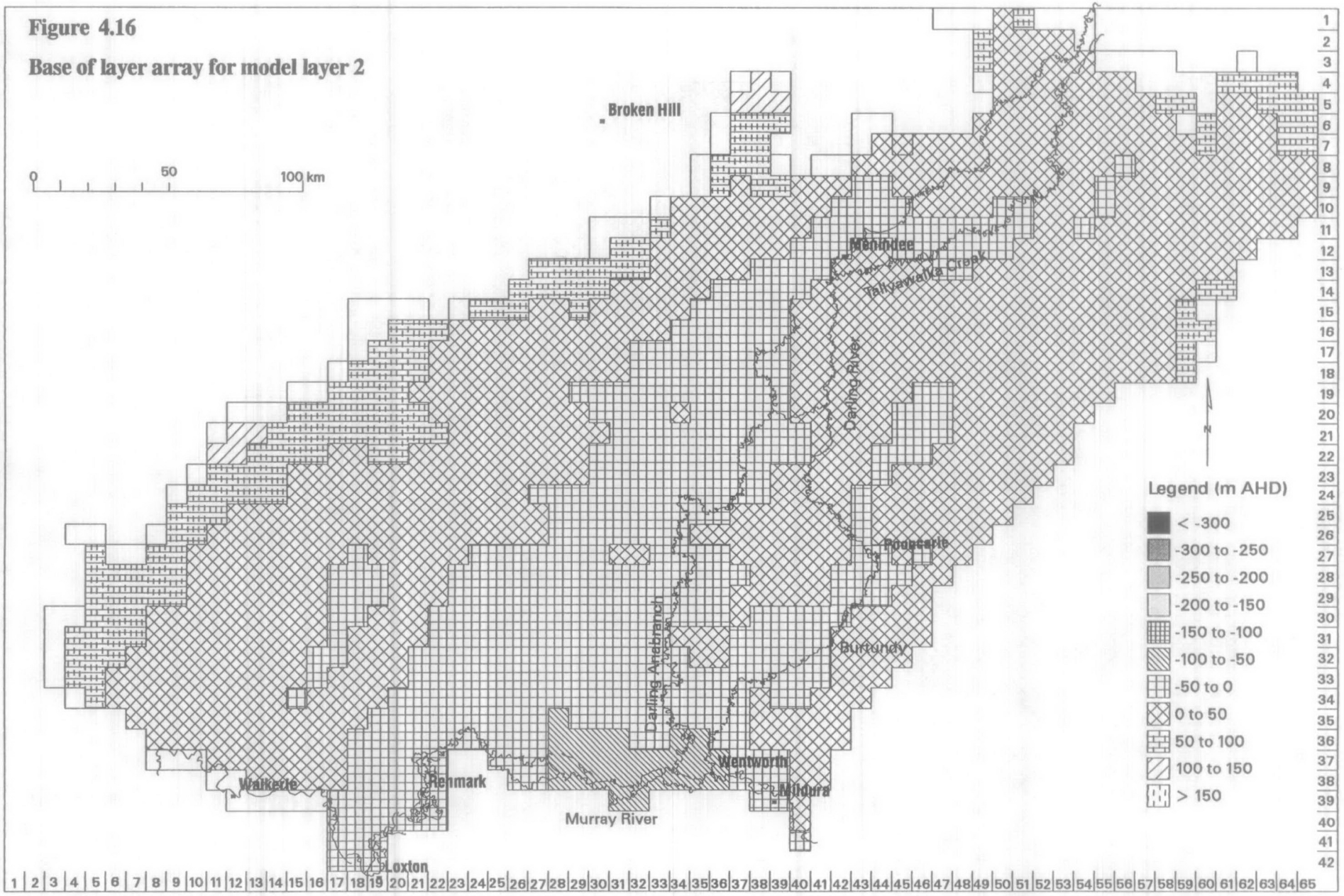

Figure 4.17

Base of layer array for model layer 3

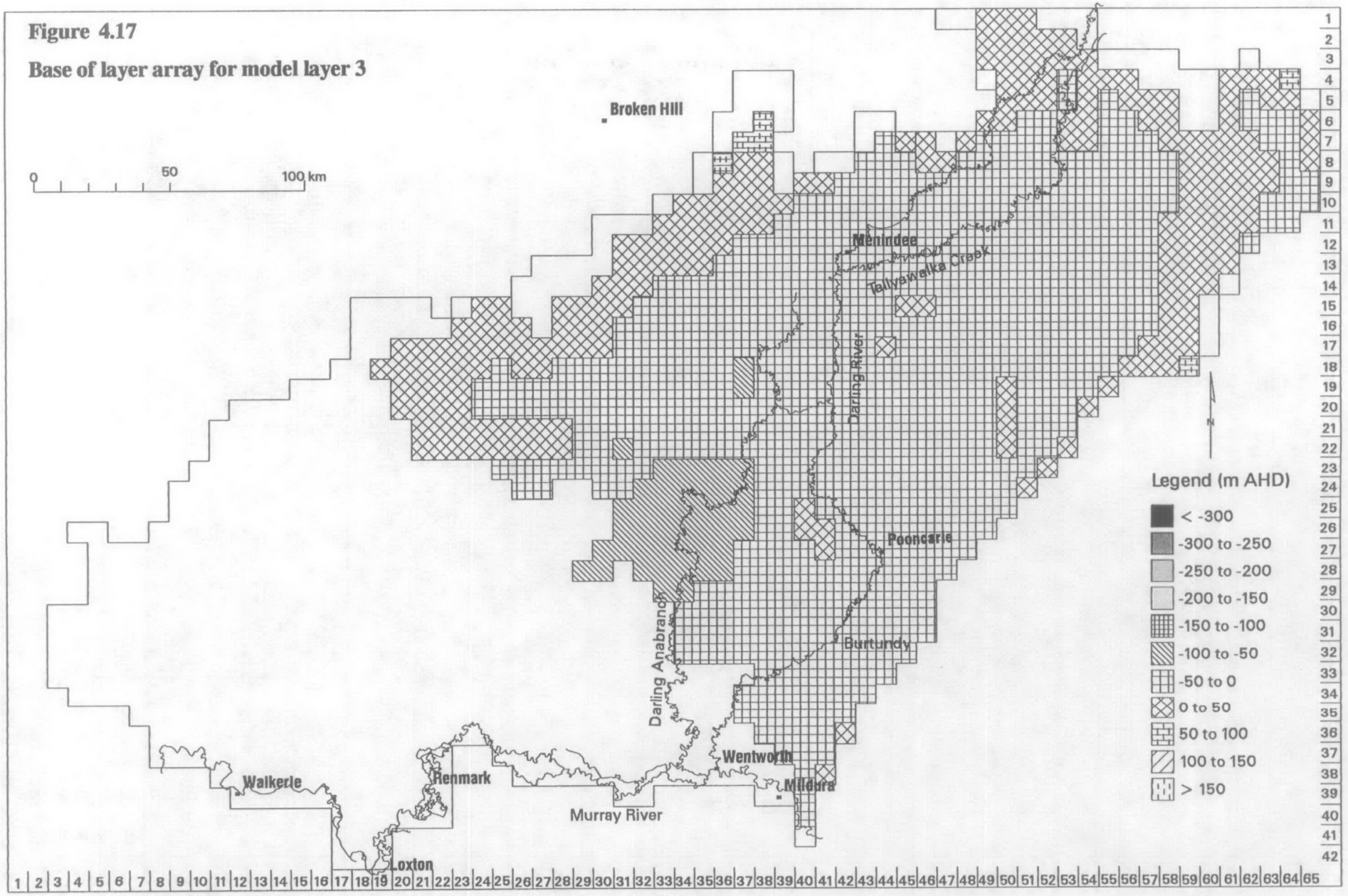

Figure 4.18

Base of layer array for model layer 4

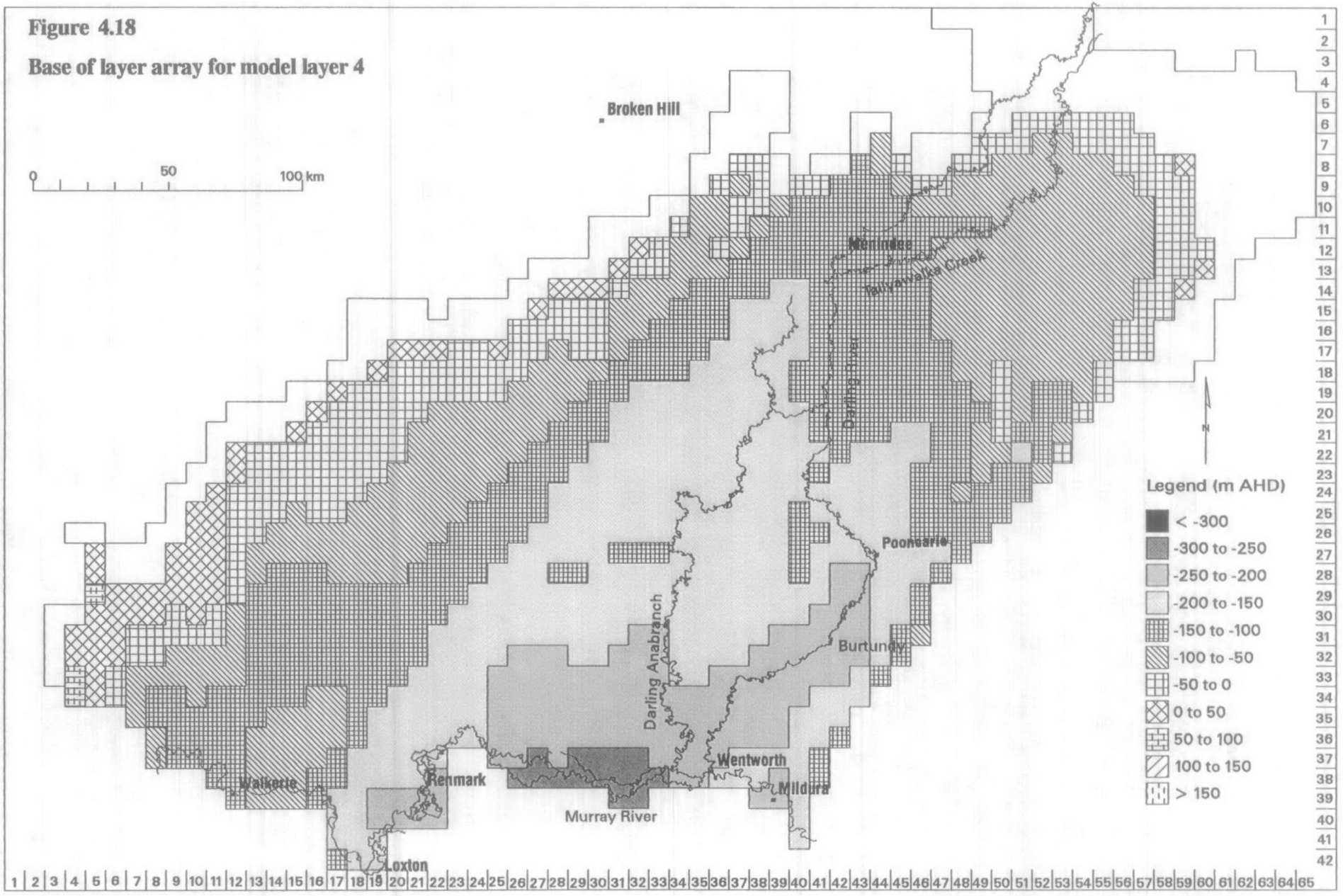

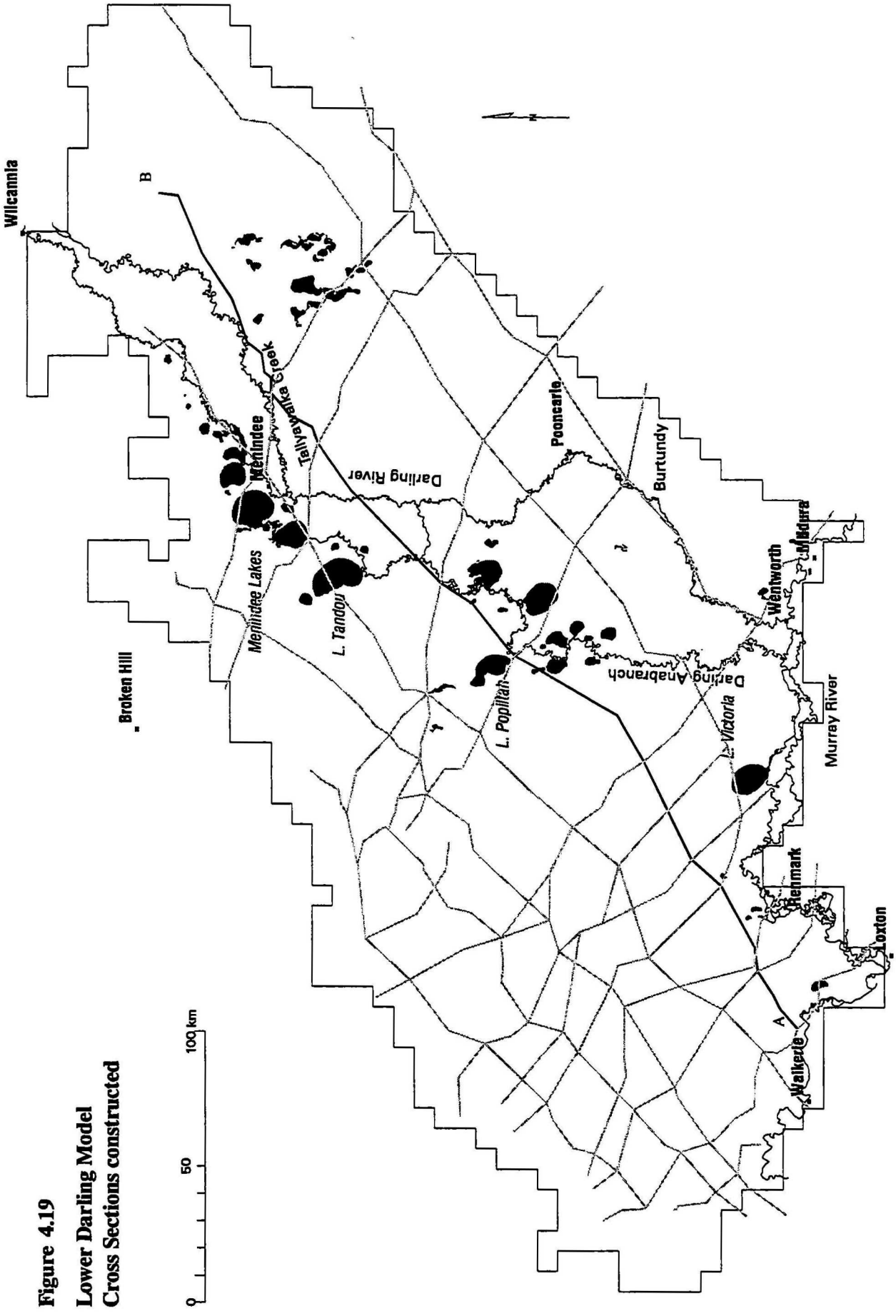

Figure 4.19
Lower Darling Model
Cross Sections constructed

The base of layer 2 (Figure 4.16, Figure 2.11) tends to mimic the main structural elements of the basin, varying from > 100 m AHD adjacent to the northwest margin to < -60 m AHD in the southern model margin. These structural elements include the Renmark and associated Canegrass Lobe in the south, and the Tarrara, Menindee, Wentworth and Blantyre Troughs to the north. A localised depression flanks the Lake Wintlow High in the model centre.

Similar geometry is displayed for the base of layer 3, characterised by a progressively deepening channel overlying the Blantyre, Menindee and Tarrara Troughs (Figure 4.17). Elevations are > 30m AHD along the edge of the Cobar Block, reaching a minima of < -70 m AHD in the Tarrara Trough area Elevation of the base of layer 4 (Figure 4.18, Figure 2.31) range from > 20 m AHD along the basin margins to < -300m AHD in the Renmark Trough. Again, the troughs and ridges making up the basin structure are recognisable.

4.5.2 Horizontal Hydraulic Conductivity

As parts of the uppermost four layers are unconfined so that the saturated thickness can potentially fluctuate, horizontal hydraulic conductivity arrays are defined for these layers to dynamically calculate conductance during model iterations. Figures 4.21 to 4.24 show the estimated horizontal hydraulic conductivity values for layers 1 to 4 respectively. These arrays are actually designated for calculating horizontal conductance in the row direction, and are multiplied by an anisotropy factor to calculate conductance in the column direction. For this model, the sediments are assumed to be horizontally isotropic so this factor is one.

Pump test data deriving reliable estimates of aquifer parameters are scarce for the model area and tend to concentrate along the Murray River. An average horizontal hydraulic conductivity of 2 m/d for the Loxton Sands was estimated from pump testing in the Sunlands and Qualco Irrigation Districts (Watkins *et al*, 1995). Single layer modelling in the area suggested a horizontal hydraulic conductivity of 0.5 m/d for the underlying Murray Group Limestone. Tests undertaken during the establishment of the Woolpunda Groundwater Interception Scheme, derived a horizontal hydraulic conductivity range for the Murray Group Limestone of 1 to 3.5 m/d (Telfer, 1987). For the purposes of flow net analysis, horizontal hydraulic conductivity zones of 1.5 and 2.2 m/d were used for the aquifer in the vicinity of the scheme. Further upstream, investigations into salinisation of the Chowilla floodplain assigned a value of 10 m/d for the alluvial sediments, 5 m/d for the upper part of the Parilla Sands aquifer, < 0.1 m/d for a clayey basal part, and 1-3 m/d for the underlying Murray Group Limestone (Waterhouse, 1989). The same horizontal hydraulic conductivity for the Parilla Sands was used in simulations of the groundwater interception scheme at Lake Ranfurly, near Mildura (Narayan & Armstrong, 1995). This model used a higher value of 25 m/d for the alluvial sands.

Due to the scarcity of test data, other methodologies for deriving conductivities are required. For the Lachlan Fan Model, an iterative algorithm based on the drawdown, duration and withdrawal rate from routine bailer tests was used to determine the transmissivity for the borehole intake (Kellett, 1997). This value was then integrated over the overall thickness of the sequence. For the Lower Darling model, the extensive lithological record was used to

obtain a de facto estimate of hydraulic conductivity. A similar approach was also used for the Lower Murrumbidgee groundwater model (Punthakey *et al*, 1994).

If the thickness of a model layer ($B_{i,j}$) is much larger than the thickness of an isotropic lithological interval ($b_{i,j}$) then the hydrologically equivalent horizontal hydraulic conductivity for the model layer $(Kx)_{ij}$ can be calculated using:

$$(Kx)_{i,j} = \sum_{k=1}^{m} \frac{K_{i,j,k} b_{i,j,k}}{B_{i,j}}$$

where $$B_{i,j} = \sum_{k=1}^{m} b_{i,j,k}$$

i = model row, j = model column, k = model layer,
m = total number of isotropic lithological layers in model layer

(Anderson & Woessner, 1992)

That is, the horizontal hydraulic conductivity of the model layer equals the sum of the hydraulic conductivity assigned to the lithological interval (K_{ijk}) multiplied by the thickness of the lithological interval divided by the total thickness of the model layer. The thickness of the model layer is equal to the sum of the thicknesses of the individual lithological intervals.

This approach was applied to the 20,000+ borehole lithology intervals recorded in the Oracle *dwrdrill* table. The process is summarised in Figure 4.20. The lithology table is derived from the groundwater database maintained by DLWC in New South Wales, and as such, only a borehole identifier and a depth (to base) physically located each interval. A thickness field was added and an internal join was used to update the field with the difference between the depth value and the depth value of the preceding interval in the hole. These values represent the $b_{i,j,k}$ in the horizontal hydraulic conductivity equation.

A nominal hydraulic conductivity $K_{i,j}$ needs to be assigned to each of the lithological intervals. In the *dwrdrill* table, the lithological description for each interval is defined by a lithological *name* field and six descriptor fields, *desc1* to *desc6*. In these fields are prescribed two to four letter codes used for the type and nature of the rock type eg. SDSN for sandstone, CLAY for clay, WTRD for weathered, SNDY for sandy. All of the 3728 unique combinations of these seven fields were imported from the table into an EXCEL spreadsheet and a nominal hydraulic conductivity value was assigned to each of these combinations (Figure 4.20). These values were based on the hydraulic conductivity ranges established for major rock types (Freeze & Cherry, 1979). These rock descriptors and assigned conductivities were loaded back into an Oracle table called *dwrk* and used to update the $K_{i,j}$ for each lithological interval in the *dwrdrill* table, by relating the common fields (*boreid, name, desc1-6*)

A weighted average of the lithological hydraulic conductivity values comprising each of the model layers in the boreholes needs to be calculated. This requires the depth to top and thickness ($B_{i,j}$) for each of the model layers within the borehole. A *layer* table was created to store this information and updated by using the stratigraphic information stored in the *strat* table. The layer top is the minimum stratigraphic top, and the layer thickness is the sum of stratigraphic thickness for all units comprising the model layer found in each borehole. For

example, any intersections of Bookpurnong Beds (Tpb), middle Renmark Group (Ter2), Geera Clay (Tmg), Winnambool Formation (Tmw) and Ettrick Formation (Toe) found in a borehole were combined to derive the top and thickness of layer 4 for that particular borehole.

With the essential elements of the horizontal hydraulic conductivity equation available (the assigned hydraulic conductivity $K_{i,j,k}$ and thickness $b_{i,j,k}$ of the lithological intervals in the *dwrdrill* table and the thickness of the model layers $B_{i,j}$ in each borehole in the *layer* table), the weighted average of horizontal hydraulic conductivity was calculated for the model layers intersected downhole. Any potential mismatch between the lithological intervals and the layer intersections were accounted for in the calculation. For instance, if the top of a model layer fell within a particular lithological interval, only the difference between the model top and the base of the lithology was used as a thickness term in the weighted average. The final product is a *layer* table which defines the model layers intersected for each borehole, with a horizontal hydraulic conductivity based on the lithological record assigned to these intersections.

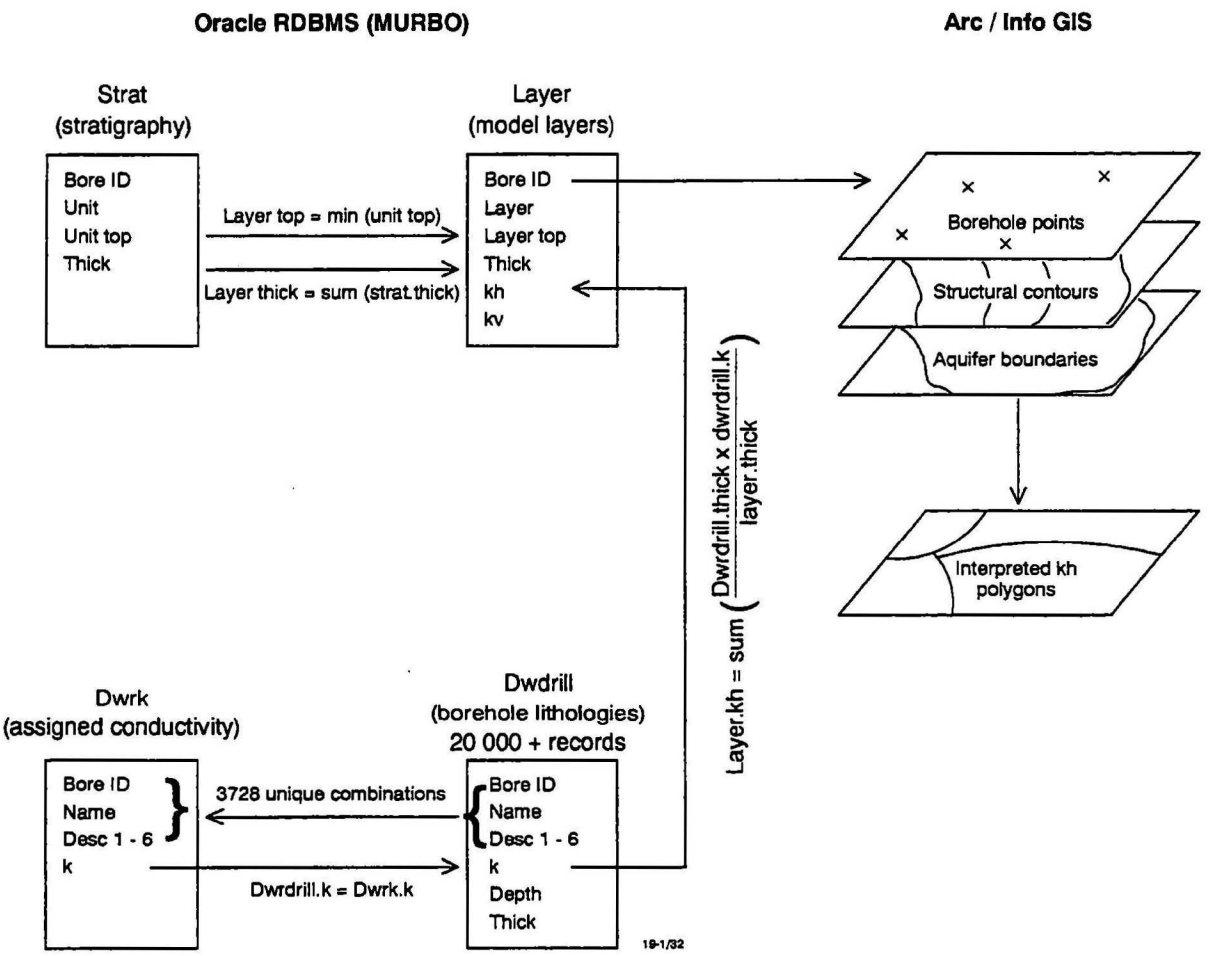

Figure 4.20 Estimation of horizontal hydraulic conductivity from lithological descriptions

This Oracle table was accessed from within the GIS to allow the horizontal hydraulic conductivity estimates to be placed in their spatial context. Boreholes which only partially penetrated the model layer and therefore had an estimated conductivity which was potentially misleading were differentiated. Mapping such as aquifer yield, geological structure and aquifer boundaries were overlain to assist in the manual interpolation. Horizontal hydraulic conductivity zones were then mapped into a polygon coverage which was subsequently gridded for input into the model (Figure 4.20).

This process was useful in obtaining relativities in horizontal hydraulic conductivity, rather than providing absolute values. That is, the process was used to demarcate regions of high, medium and low hydraulic conductivity This is due to the qualitative nature of assigning a notional $K_{i,j,k}$ value to the lithologies, and also to the variable reliability of the lithological record itself. However, the mapped zones do make sense geologically, and their horizontal hydraulic conductivity values were simply modified within reasonable limits during calibration.

The dominant feature of the horizontal hydraulic conductivity estimates for layer 1 (Figure 4.21) is the elevated values along the established drainage lines. Relatively coarse alluvial sands and silts of the Shepparton Formation and Coonambidgal Formation in the floodplains of the Darling and Murray Rivers have been assigned an average of 2 m/d. A conductive zone (1-10 m/d) also extends to the east, from the Darling-Tallyawalka system, initially following Teryaweynya Creek. This palaeochannel bifurcates, with one arm flanking the Neckarboo Ridge, and the other reaching Sandy Creek to the northeast. This implies that the modern Sandy Creek is a vestige of a larger feature which drained into the proto-Darling. To the west of the Darling, linear zones of highly permeable sands relate to palaeochannels flanking the Broken Hill Block. Away from the main alluvial channels, the layer is dominated by silts and clays of lower hydraulic conductivity (0.1-0.5 m/d). The Shepparton Formation in particular, is generally termed an aquitard/aquifer complex. To the south, the Blanchetown Clay is the major component of the layer and horizontal hydraulic conductivity is correspondingly low (.01 m/d). However, the unit appears to be coarser grained (0.1- 1 m/d) closer to the basin margins and also closer to the Murray River, particularly along structural highs. These elevated areas were essentially distant from the main sites of lacustrine clay deposition during Lake Bungunnia times.

The coarser grained nature of the Pliocene Sands is reflected in higher horizontal hydraulic conductivity estimates for layer 2 (Figure 4.22). In the north, where fluvial processes dominated, the zones of elevated horizontal hydraulic conductivity (4-20 m/d) represent the major drainage which deposited the Calivil Formation during the Pliocene. The main system follows the pre-Pliocene arcuate depression (refer Figure 2.11) defined by the underlying structural lows of the Blantyre Trough, linking southwards to the Menindee and Tarrara Troughs where the marine Parilla Sands were deposited. This palaeochannel extends eastwards following a much larger ancestor to the modern Sandy Creek. Lower conductivities (0.2-1 m/d) are evident over structural highs such as the Lake Wintlow High and along the basin margin where deposition was not as active or sustained. In the south, the hydraulic conductivity zones have a distinct southeast trending fabric. This matches the trend of the dune and swale morphology characteristic of the Loxton-Parilla Sands. Zones of high horizontal hydraulic conductivity (10 m/d) probably represent selective winnowing of sands.

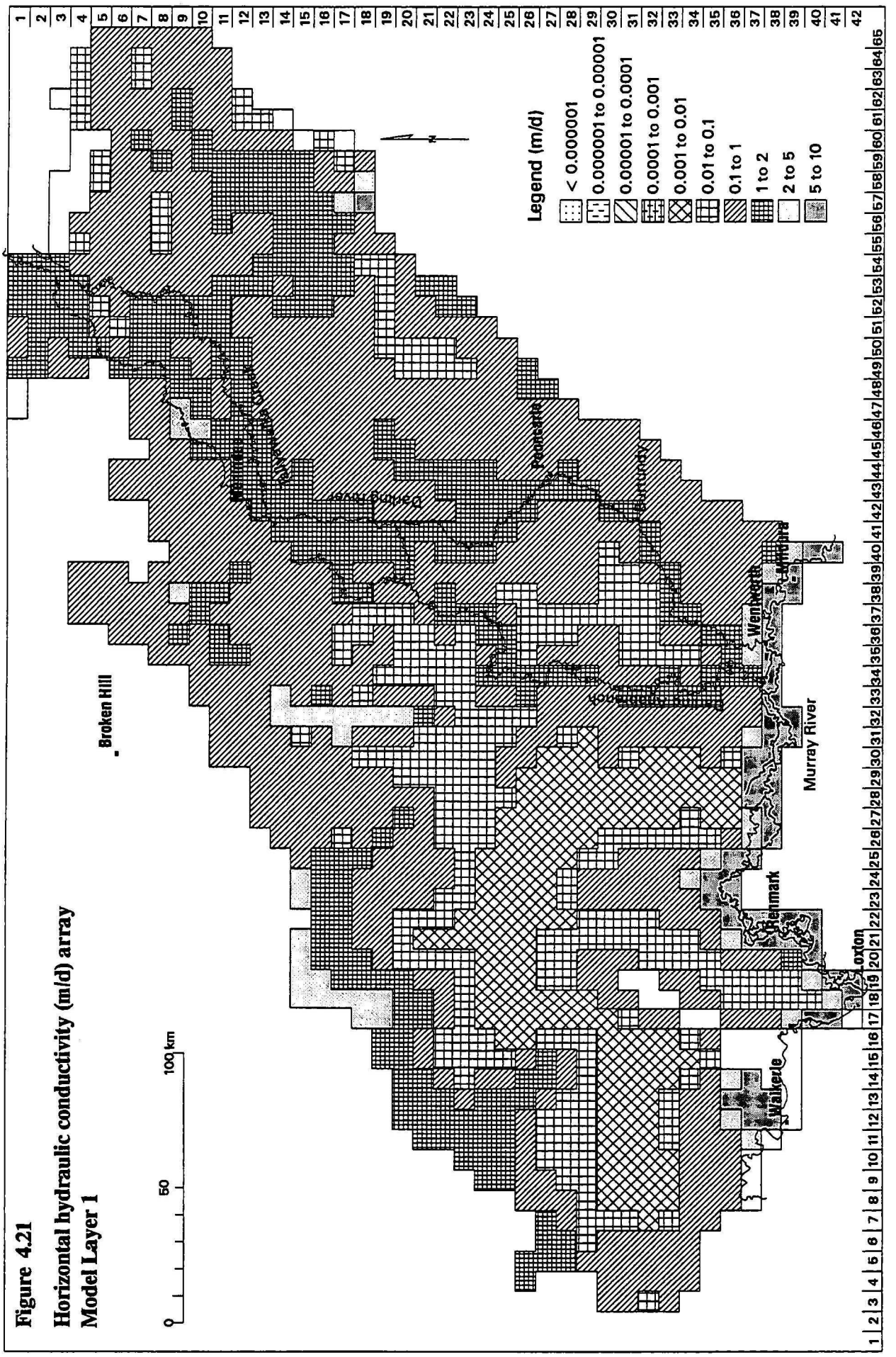

Figure 4.21
Horizontal hydraulic conductivity (m/d) array
Model Layer 1

Figure 4.22

Horizontal hydraulic conductivity (m/d) array
Model Layer 2

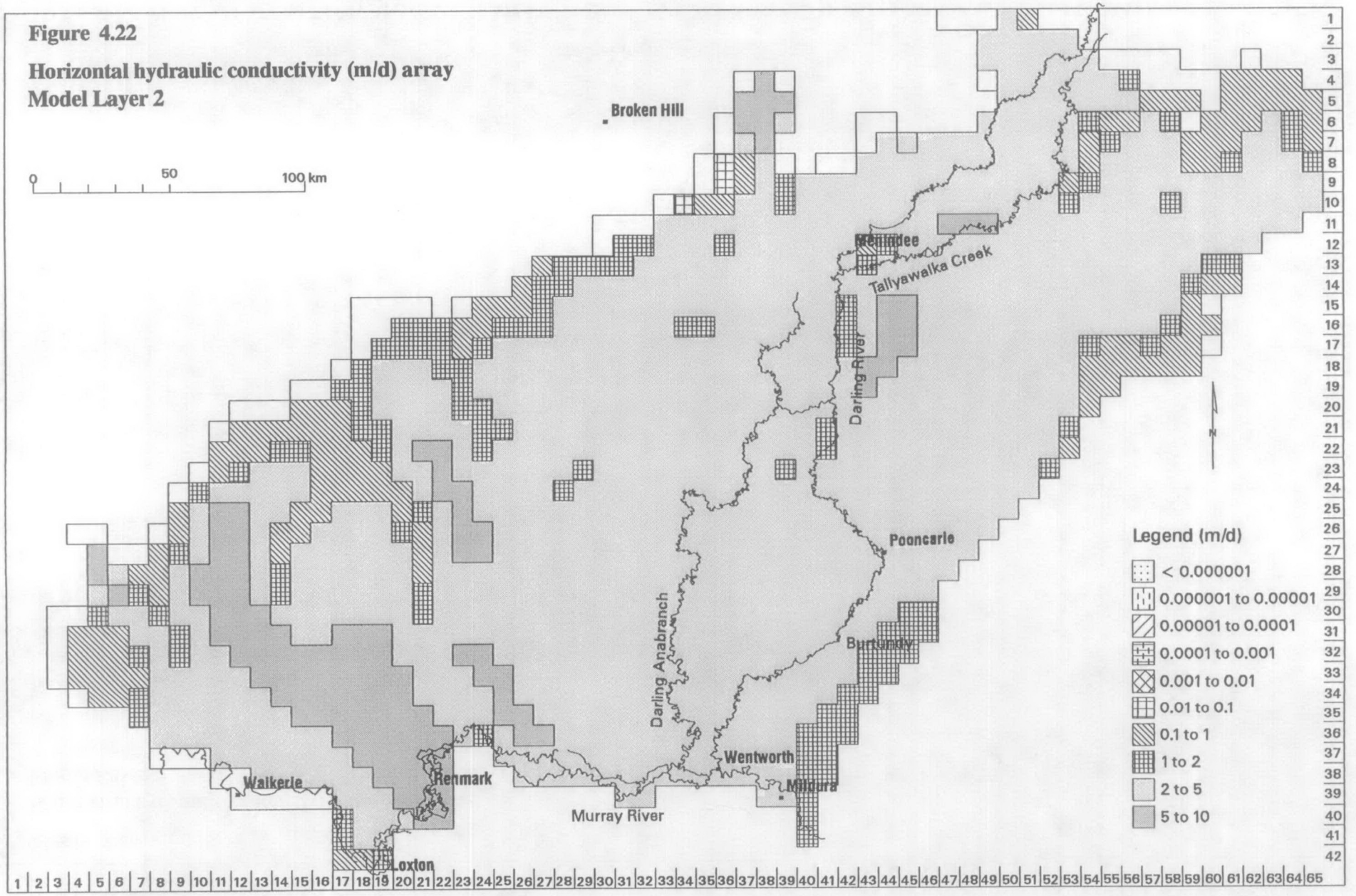

Figure 4.23

Horizontal hydraulic conductivity (m/d) array
Model Layer 3

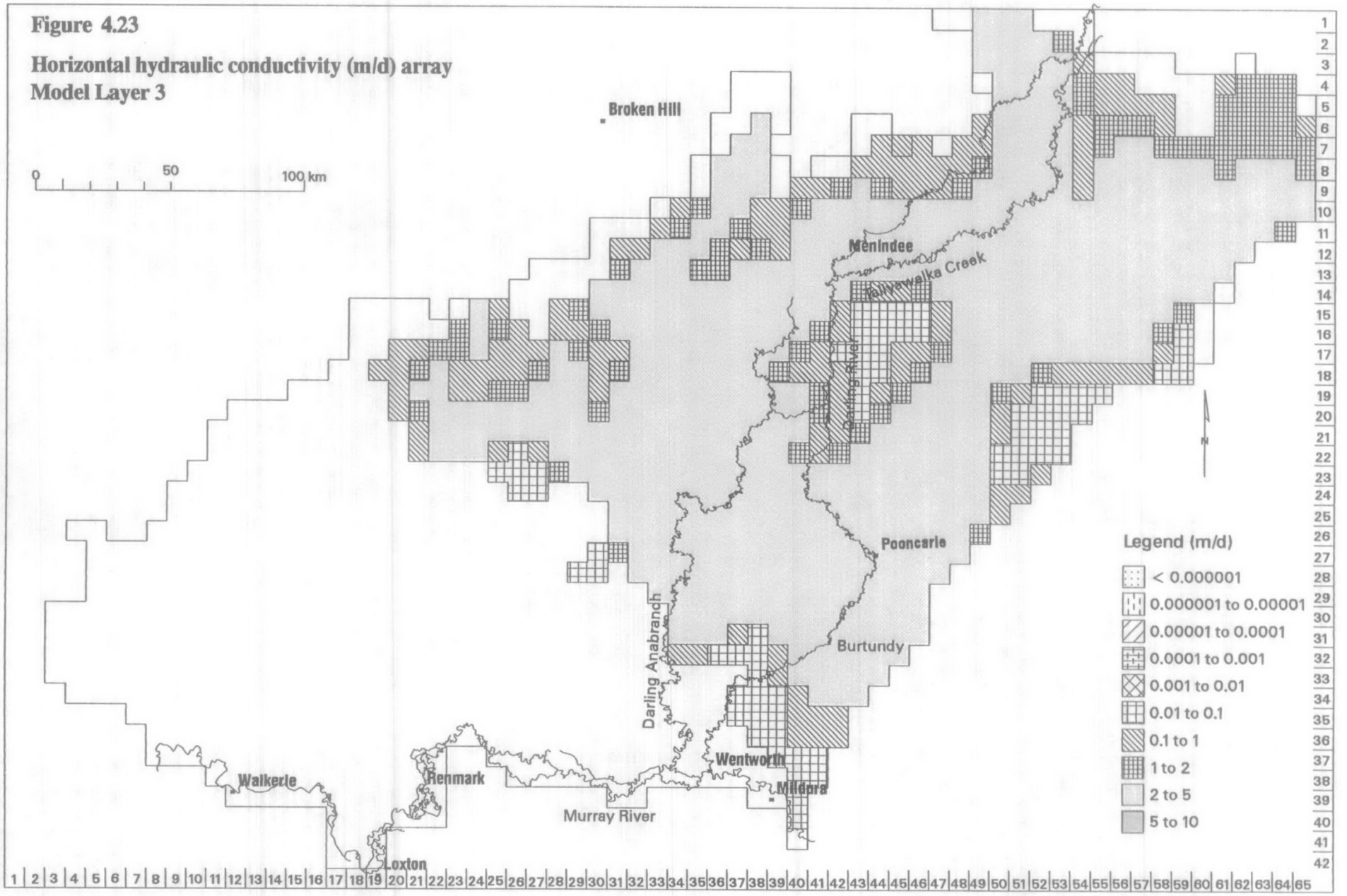

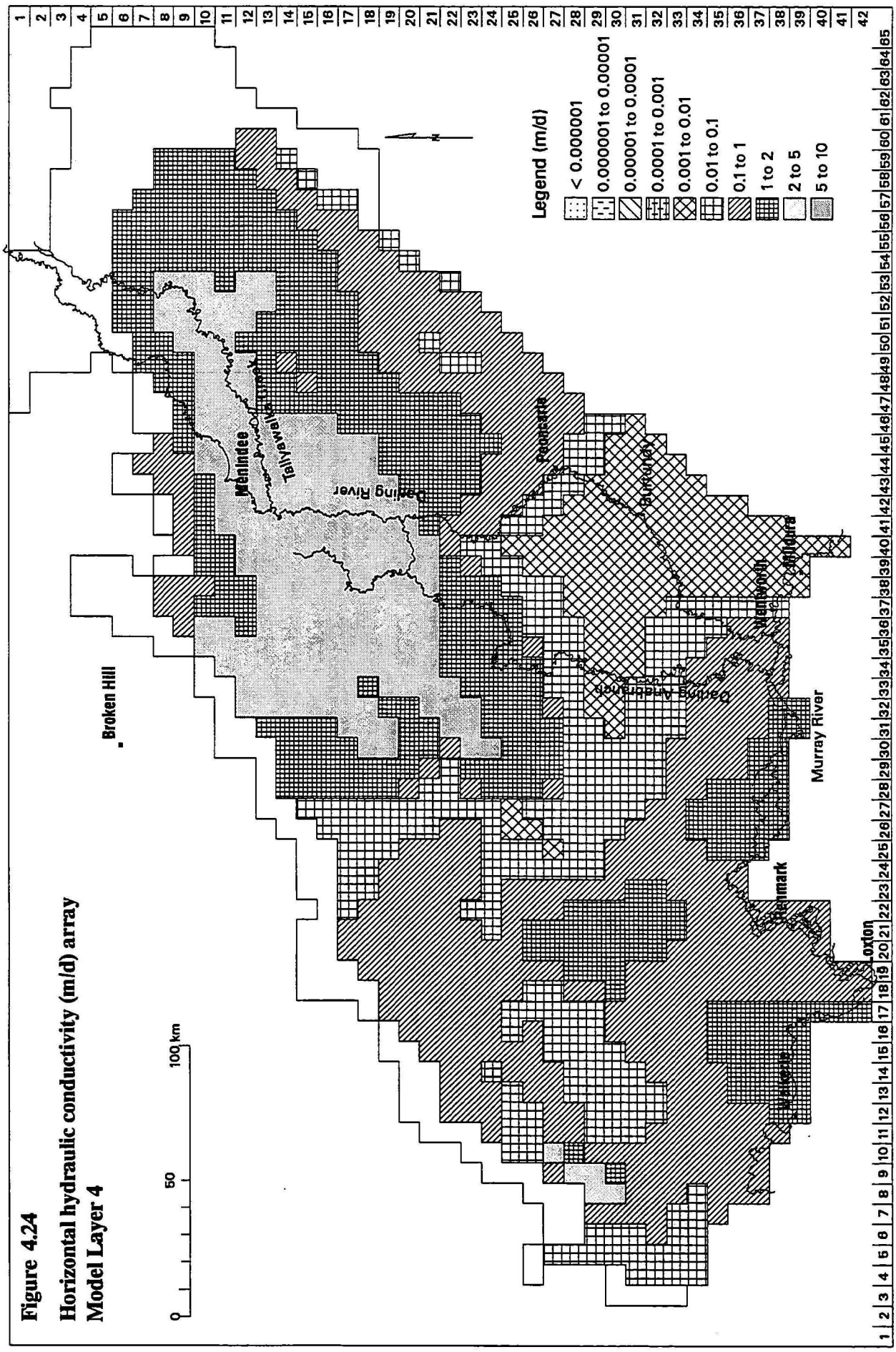

Figure 4.24
Horizontal hydraulic conductivity (m/d) array
Model Layer 4

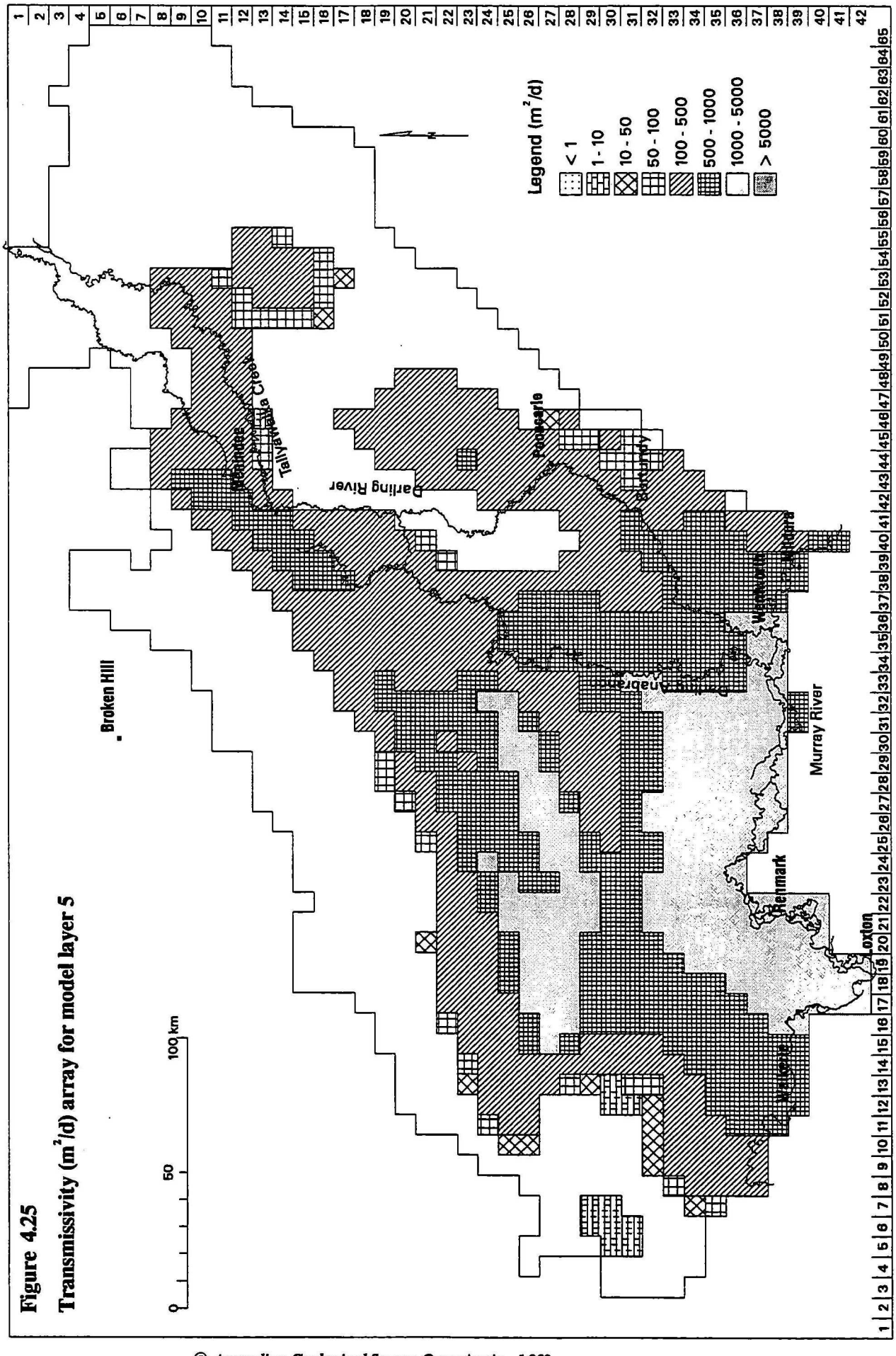

Figure 4.25
Transmissivity (m^2/d) array for model layer 5

The horizontal hydraulic conductivity for layer 3 (Figure 4.23) has features similar to the configuration found in the Pliocene Sands. Coarser grained sands and silts (3-5 m/d) are found in linear depressions defined by the underlying basin troughs. The connection between the ancestral Darling and Sandy Creek drainage is also evident in the fluvial deposition of the middle Miocene. Values of 0.1-0.5 m/d are typical for elevated areas, basin margins and along the seaward margin where the sequence thins out and is interbedded with the Geera Clay and its equivalents.

The variable horizontal hydraulic conductivity displayed in layer 4 (Figure 4.24) is largely due to the composite nature of the model layer. The fluvial sands and silts of the middle Renmark Group constitute the northern third, where horizontal hydraulic conductivity values are relatively high. A high permeability zone (4-5 m/d) is found in the lower-lying central Blantyre-Menindee Trough part of this area. These sediments are on average finer grained than the underlying lower Renmark Group sequence due to the high base levels and subsequent low energy depositional environment operating during the late Oligocene - early Miocene. This higher horizontal hydraulic conductivity zone is surrounded by carbonaceous silts and clays (0.1-2 m/d). Basinwards, the Geera Clay and Winnambool Formations are the dominant units in layer 4, represented by the low hydraulic conductivity band (.01 m/d) spanning the middle of the model. Further south, deposition of platform limestones of the Murray Group increase the overall hydraulic conductivity to 0.1-2 m/d.

Only a transmissivity array is required for the basal layer representing the lower Renmark Group (Figure 4.25). A horizontal hydraulic conductivity grid was created in the same manner as the other model layers and simply multiplied with a thickness grid, to derive estimated transmissivity. Due to the general thickness and coarse grained nature of the lower Renmark Group and Warina Sands, transmissivities are high. Values exceed 1,000 m^2/d in the basin troughs, with a maxima > 2500 m^2/d in the centre of the Renmark Trough. The unit is finer grained (1-2 m/d) along its margin and over structural highs, indicated by transmissivities < 200 m^2/d. This also holds true for the upper reaches of the Blantyre Trough.

4.5.3 Vertical Conductance

The water balance within each model cell also includes the vertical flux between the cell and its underlying counterpart. This requires a leakance term, which is essentially the vertical analogue of the horizontal conductance array. This deals with the vertical hydraulic conductivity of the aquifer prism between the model cell node and the node of the underlying cell. This parameter for aquifer material is usually poorly known and not often measured.

Field measurements in the model area are very rare. Laboratory permeability testing of cable tool samples of Bookpurnong Beds near Berri, reported a huge range in vertical hydraulic conductivity estimates from 10^{-3} to 10^{-7} m/d (Howles, 1987). Vertical hydraulic conductivity values of 10^{-4} to 10^{-5} m/d were assigned to the Ettrick Formation in a numerical model of the Woolpunda area (Watkins, 1993). For modelling around the Sunlands/Qualco Irrigation District, vertical hydraulic conductivity values of 5×10^{-4} and 2×10^{-4} m/d were assigned to the Blanchetown Clay and a finer-grained component of the Murray Group Limestone, the Cadell Marl, respectively (Watkins *et al*, 1995).

Due to this paucity of field data, methodologies are needed to extract an estimate for leakance arrays using the existing datasets. For the Lower Murrumbidgee Model, this was an inverse procedure to simultaneously estimate recharge and leakance from the hydrographic record and assumed aquifer properties (Punthakey *et al*, 1994). In contrast, an empirical relationships between horizontal and vertical hydraulic conductivity, using permeability tests of petroleum well cores, was developed for the Lachlan Fan Model (Kellett, 1997).

In the same vein as the methodology used in the Lower Darling model for horizontal hydraulic conductivities, vertical hydraulic conductivities were estimated using the lithological record stored in the *dwrdrill* table. Using the thickness ($b_{i,j,k}$) and assigned hydraulic conductivity ($K_{i,j,k}$) of assumed isotropic layers within the model layer, the hydrologically equivalent vertical hydraulic conductivity $(Kz)_{i,j}$ for the model layer of thickness $B_{i,j}$ can be calculated using the following equation:

$$(K_z)_{i,j} = \frac{B_{i,j}}{\sum_{k=1}^{m} b_{i,j,k} \,/\, K_{i,j,k}}$$

(Anderson & Woessner, 1992)

Hence, vertical hydraulic conductivity for a particular model layer is defined as the model layer thickness divided by the sum of the ratios of the thickness of the lithological layer divided by the hydraulic conductivity of the lithological layer, where the sum of the lithological layer thicknesses equals the model layer thickness. As such, the averaged vertical hydraulic conductivity for a model layer is largely defined by the K value of the finest grained and therefore least permeable lithological layer.

The leakance arrays deal with the prism of aquifer between the node of a model cell and the node of the underlying cell. This is a measure for the bottom half of a model cell in combination with the top half of the underlying model cell, rather than only using the model cell thickness as in the horizontal conductance term. Hence, lithological records for the borehole interval defined by the midpoint of the model cell as the top and the midpoint of the underlying aquifer as the base is used in the calculations. This simply involved adding two new fields to the *layer* table defining these midpoints, and using them in the vertical conductance equation, rather than the base and top of the model layer.

The calculation uses the nominal $K_{i,j}$ assigned to the individual lithological intervals making up the borehole record in the *dwrdrill* table as well as the intersections representing the midpoints of model layers, stored in the *layer* table. As in the horizontal conductance calculations, mismatches between the intervals defining the downhole lithology and the intervals defining the model layer midpoints were accounted for in the algorithm. The final vertical hydraulic conductivity estimate for the model layers for each relevant borehole, as stored in the *layer* table, was integrated with other spatial information such as aquifer boundaries, geological structure and geomorphology, within the GIS. Boreholes which only partially penetrated the model layers were specifically highlighted, as their vertical hydraulic conductivity value may not be representative. A polygon coverage defining vertical hydraulic conductivity zones was interpreted and resampled into a 2-D grid. This vertical hydraulic

conductivity grid is divided by the internodal distance, defined by the thickness of the model cell (Z_k) and the thickness of the underlying cell (Z_{k+1}) to derive the leakance (or *vcont*)array:

$$Vcont_{i,j,k+1/2} = \frac{Kz_{i,j}}{\frac{Z_k}{2} + \frac{Z_{k+1}}{2}}$$ (McDonald & Harbaugh, 1988)

These *vcont* grids were then transferred to GMS for input into MODFLOW. Due to the subjectivity of assigning nominal $K_{i,j}$ values to the lithologies, the arrays may not be correct in absolute terms. However, they define the geometry of vertical hydraulic conductivity zones for the model, assign relativities between these zones (high, medium, low) and proved useful in calibration.

The leakance array for layer 1 (Figure 4.26) relates to the basal half of the Shepparton Formation/ Blanchetown Clay sequence and the upper half of the Pliocene Sands. In this case, vertical flow resistance is largely defined by the silts and clays found in layer 1. In the Darling River floodplain, leakance values vary from $<1x10^{-6}$ d^{-1} north of Menindee to $2x10^{-5}$ d^{-1} downstream of Burtundy. This is due to a transition of vertical hydraulic conductivity from $1x10^{-5}$ m/d southwards to $5x10^{-4}$ m/d. The coarser and better developed fluvial deposits of the Murray River have higher leakance values of the range 2 to $10x10^{-3}$ d^{-1}, maximising in South Australia where the Parilla Sands thins significantly. Relatively high leakance values occur in the Sandy Creek system (5 to$15x10^{-5}$ d^{-1}) and analogous fluvial channels draining off the Benda Range to the west. With silts and clays more common in the uppermost layer away from the rivers, lower values (2 to10 x 10^{-6} d^{-1}) prevail.

The leakance grid for layer 2 (Figure 4.27) relates to the Pliocene Sands and the upper Renmark Group as the underlying layer 3 in the northwest, and components of layer 4 (Geera Clay, Winnambool Formation, Murray Group Limestone) as the underlying sequence to the south. The coarser fluvial sediment pile accumulated in both the Pliocene Sands and upper Renmark Group within the linear depression defined by the Blantyre, Menindee and Tarrara Troughs have relatively higher leakance values. These are typically 5 to $25x10^{-5}$ d^{-1} but peak at $1x10^{-3}$ d^{-1} overlying the Tarrara Trough. Relatively high values ($2x10^{-4}$ d^{-1}) are also assigned to the head of the Sandy Creek alluvial system. Away from these principle sites of deposition, a range of 1 to $5x10^{-5}$ d^{-1} is typical of the finer grained sediments. Down basin, the layer 3 upper Renmark Group pinches out and the clays, silts and marls of the layer 4 Geera Clay and Winnambool Formation dictate the leakance estimates. This is indicated by the broad arcuate 2 to $20x10^{-6}$ d^{-1} zone across the central-southern part of the model. Further south, the transition from the marginal marine clay sequence to the platform Murray Group Limestones, shows up as higher leakance values of 1 to $3x10^{-4}$ d^{-1}.

The connection between the upper Renmark Group and the underlying layer 4 sediments is displayed in the leakance grid for layer 3 (Figure 4.28). The underlying layer is the interbedded carbonaceous sands, silts and clays of the middle Renmark Group in the northeast half of the upper Renmark Group. As leakance is inversely related to the layer thickness, values are relatively higher high (3 to $20x10^{-5}$ d^{-1}) where the layer thins towards the northeast margin. This also occurs in the western margin, where combined with high vertical hydraulic conductivity values results in maximum leakance values of 4 to $5x10^{-4}$ d^{-1}. Localised higher

leakance (5 to $6x10^{-5}$ d^{-1}) occurs in the palaeochannel overlying the Menindee Trough. Away from the margins and local depressions, values of 5 to $10x10^{-6}$ d^{-1} are typical. Basinwards, the middle Renmark Group is progressively interbedded with Geera Clay. This causes the broad band of low leakance($1x10^{-6}$ d^{-1}) flanking the southern margin of the upper Renmark Group aquifer.

Figure 4.29 outlines the leakance array for layer 4, describing the layers' connection with the basal lower Renmark Group sediments of layer 5. The effect of the thinning of layer 4 is seen in the higher leakance values (2 to $3x10^{-5}$ d^{-1}) assigned to the northeast margin. Otherwise lower values a typical outside the limits of the underlying lower Renmark Group. As the lower Renmark Group consists of a relatively coarse sequence of sands, gravels and silts, the leakance is defined by the basal half of the layer 4 sequence. In the northeast along the Blantyre-Menindee Trough system, the middle Renmark Group predominates and the leakance is about 1 to $2x10^{-6}$ d^{-1}. Higher values of 1 to $2x10^{-5}$ d^{-1} have been assigned along the western rim of the lower Renmark Group. Very low leakance (4 to $8x10^{-8}$ d^{-1}) in the centre and south of the model relates to the accumulations of marginal marine clays. This increases near Woolpunda to 3 to $4x10^{-7}$ d^{-1} with the thinning and coarsening of the Ettrick Formation clays which separates the Murray Group Limestone from the lower Renmark Group. As the lower Renmark Group is the basal aquifer, no leakance array is required for layer 5.

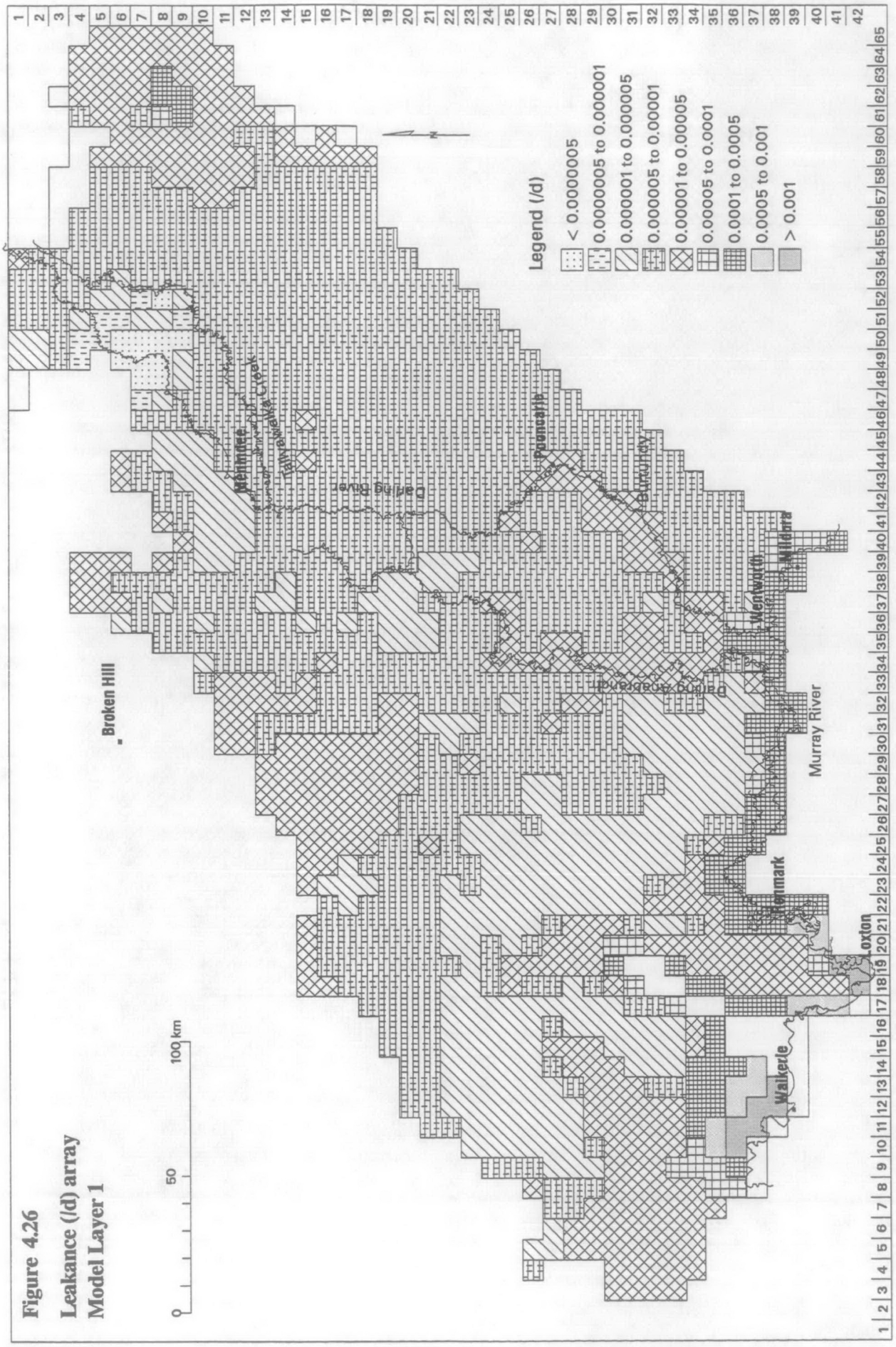

Figure 4.26
Leakance (/d) array
Model Layer 1

Figure 4.27

Leakance (/d) array
Model Layer 2

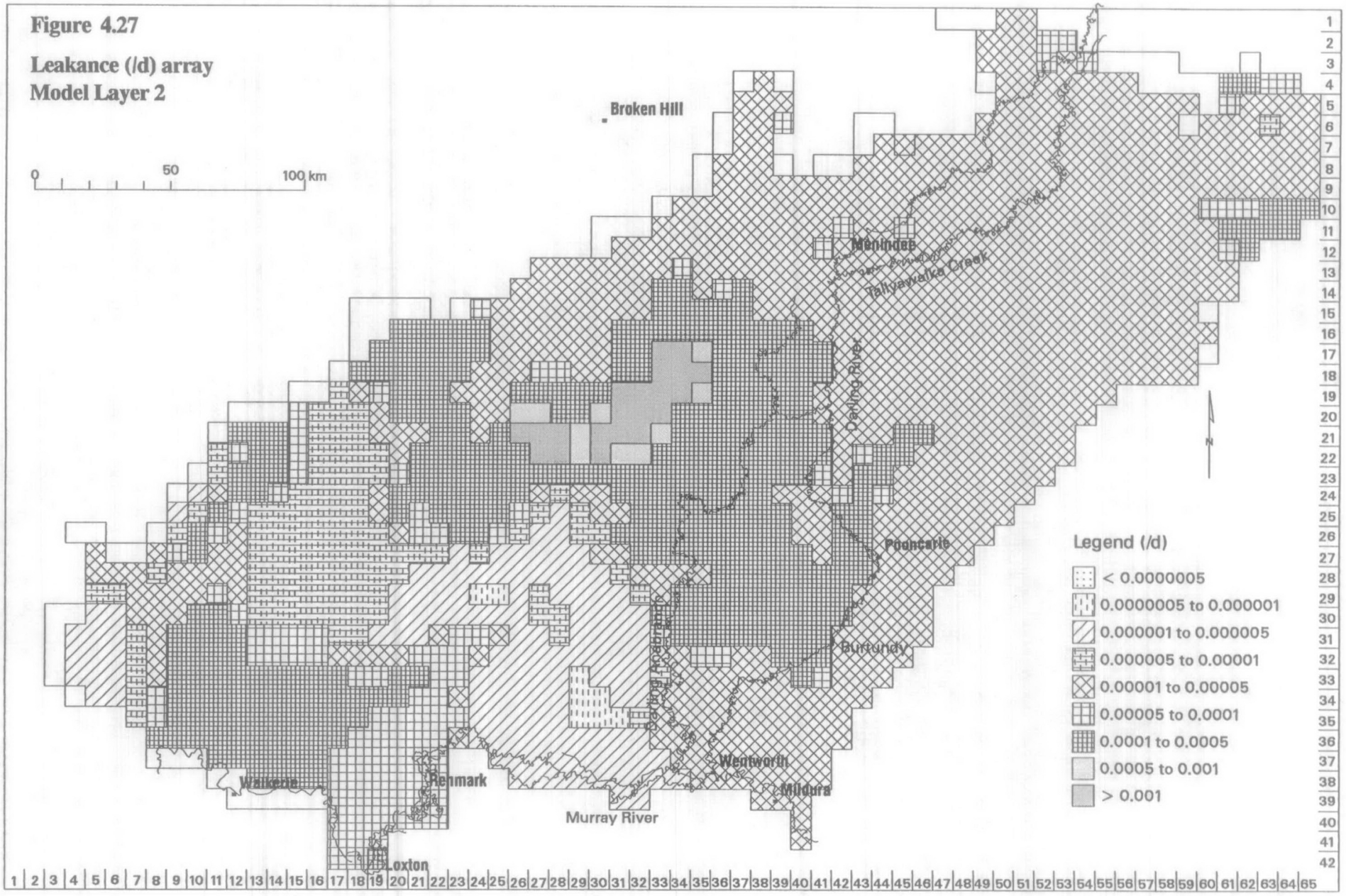

Figure 4.28

Leakance (/d) array
Model Layer 3

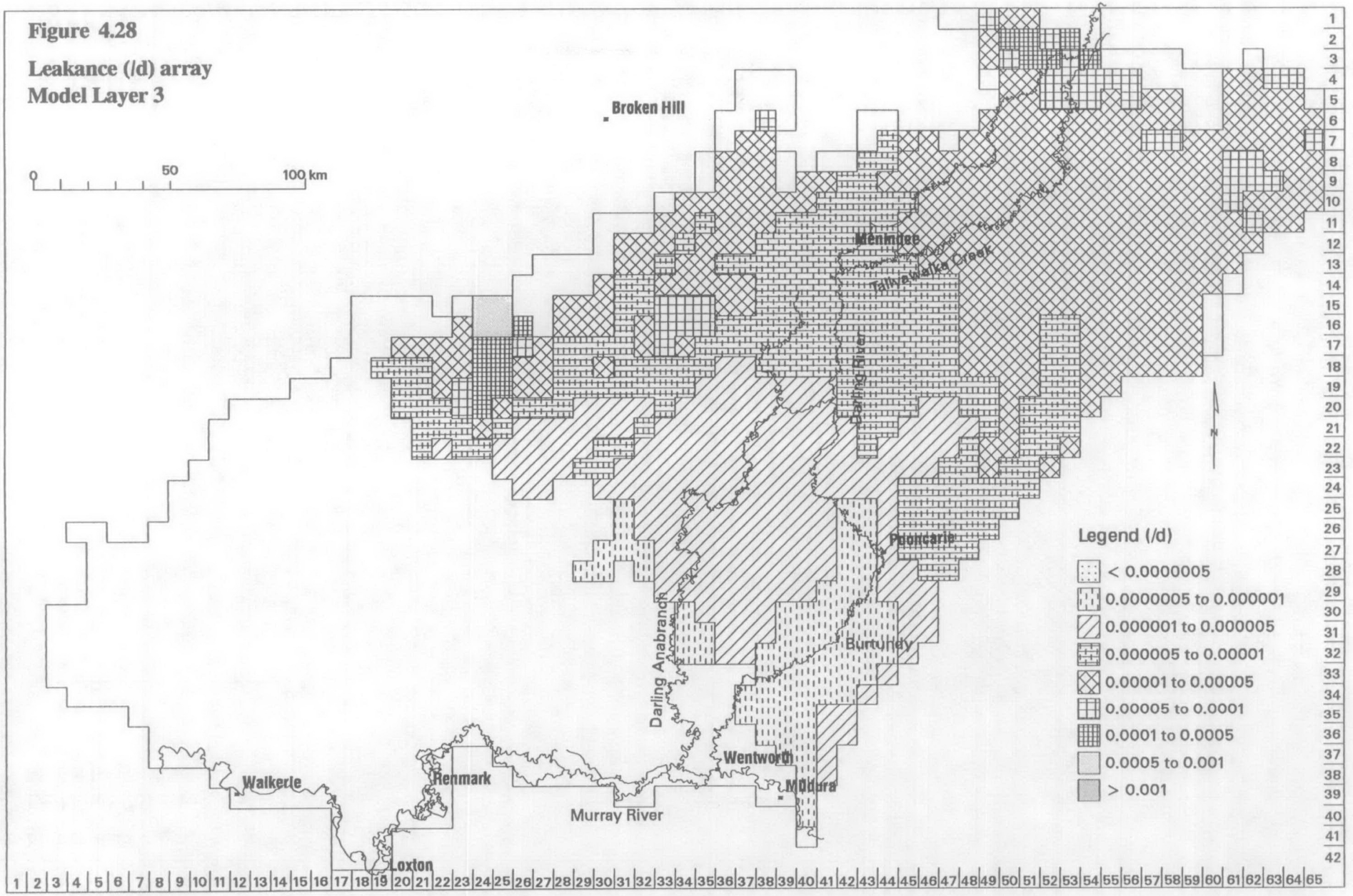

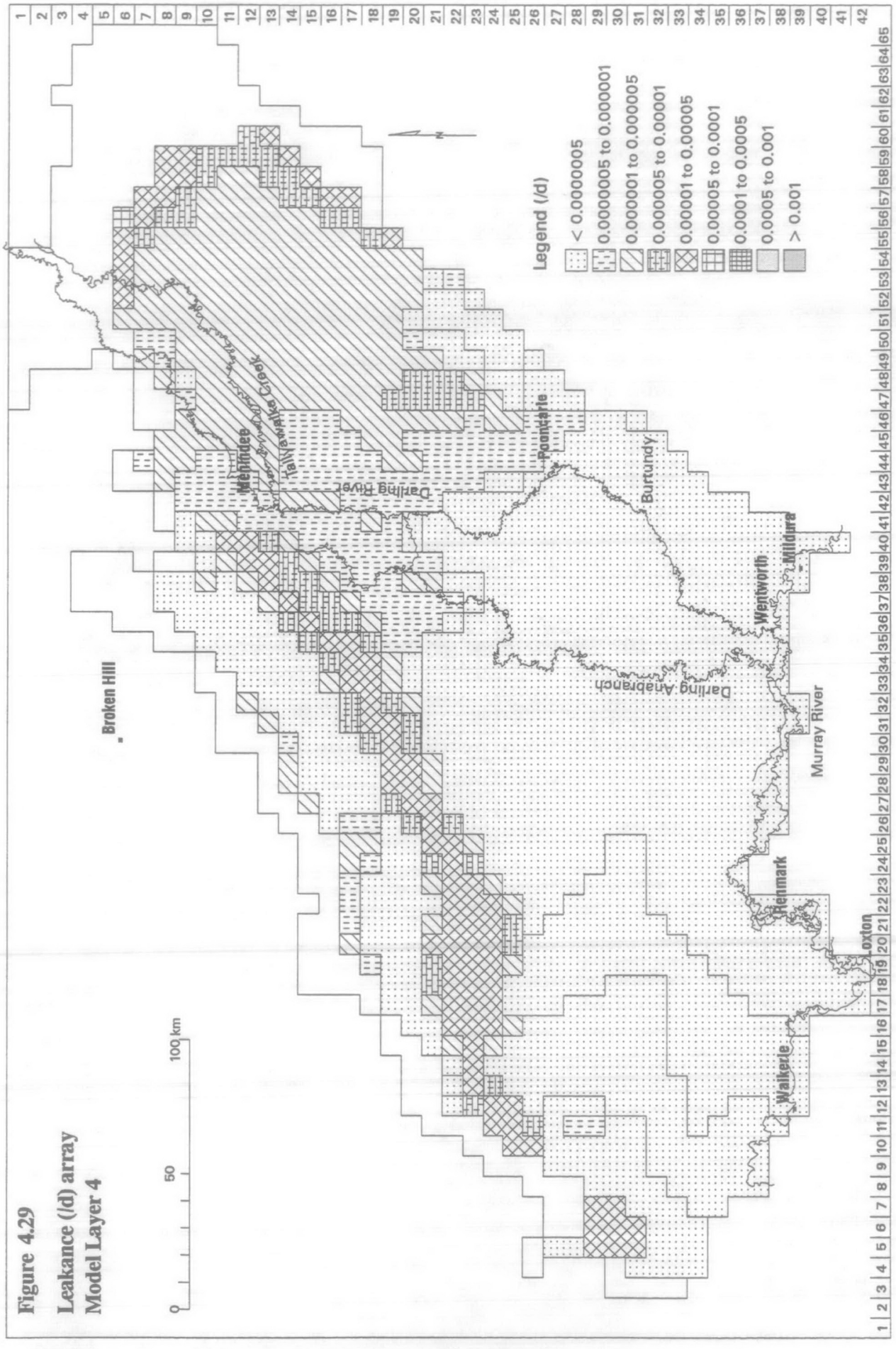

Figure 4.29
Leakance (/d) array
Model Layer 4

4.6 River (RIV) Package

The River package describes the interaction between the river system and the shallow aquifer. Rivers either lose to, or gain from, the groundwater system depending on the head difference between the river stage and the shallow watertable. In the model, a seepage term is added to the governing groundwater flow equation for each model cell traversed by the river. The degree of river-aquifer interaction is largely defined by the properties of the river bed. This bed is represented as a conductance term through which one-dimensional flow occurs (McDonald & Harbaugh, 1988). Analogous to the conductance arrays used in the BCF package, riverbed conductance (*Criv*) is defined for each river cell as:

$$Criv = KLW/M$$

where K is the vertical hydraulic conductivity of the riverbed material, L is the length of the river in the cell, W is the river width and M is the thickness of the riverbed. This assumes that the head loss across the riverbed defines the measurable head loss between the river and the aquifer. If the watertable is above the base of the riverbed, the flow between the river and the groundwater system (*Qriv*) varies with the aquifer head and is:

$$Qriv = Criv\ (Hriv - h_{i,j,k})$$

where *Hriv* is the river stage and $h_{i,j,k}$ is the head at the cell node (i,j,k) underlying the river reach. If the watertable is below the base of the river bed (*rbot*), the flow is essentially constant and defined by:

$$Qriv = Criv\ (Hriv - rbot)$$ (McDonald & Harbaugh, 1988)

The input file for the River package requires the layer, row and column number of the cell, the elevation of the river stage (*stage*), the river bed hydraulic conductance (*cond*) and the elevation of the bottom of the riverbed (*rbot*) for each designated river cell.

The configuration of river cells are maintained in an Arc/Info polygon coverage called *river_p* (Figure 4.30). This was created by intersecting the arc coverage *river_l*, representing the main channels of the Murray, Lindsay and Darling Rivers, the Darling Ana branch and Tallyawalka Creek, with the polygon coverage representing the model cells, *model_n*. This allowed automatic calculation of the row and column identifiers for each river cell. There are 164 cells depicting the main perennial drainage systems. The minor streams, such as those draining the Broken Hill Block, are not included in the package due to their ephemeral nature.

The layer attribute was defined by overlaying the boundary polygons for the model layers. To the east, layer 1 is the dominant watertable aquifer along the broad, shallow floodplains of the major rivers. Further down the Murray River in South Australia, these sediments become unsaturated and thin out, so that the Pliocene Sands (layer 2) is the regional shallow aquifer. Downstream, across the up thrown block of the Hamley Fault, the river cuts into a narrow gorge where the Murray Group Limestone of layer 4 is the surrounding watertable aquifer.

Figure 4.30

Lower Darling Model
Configuration of River cells

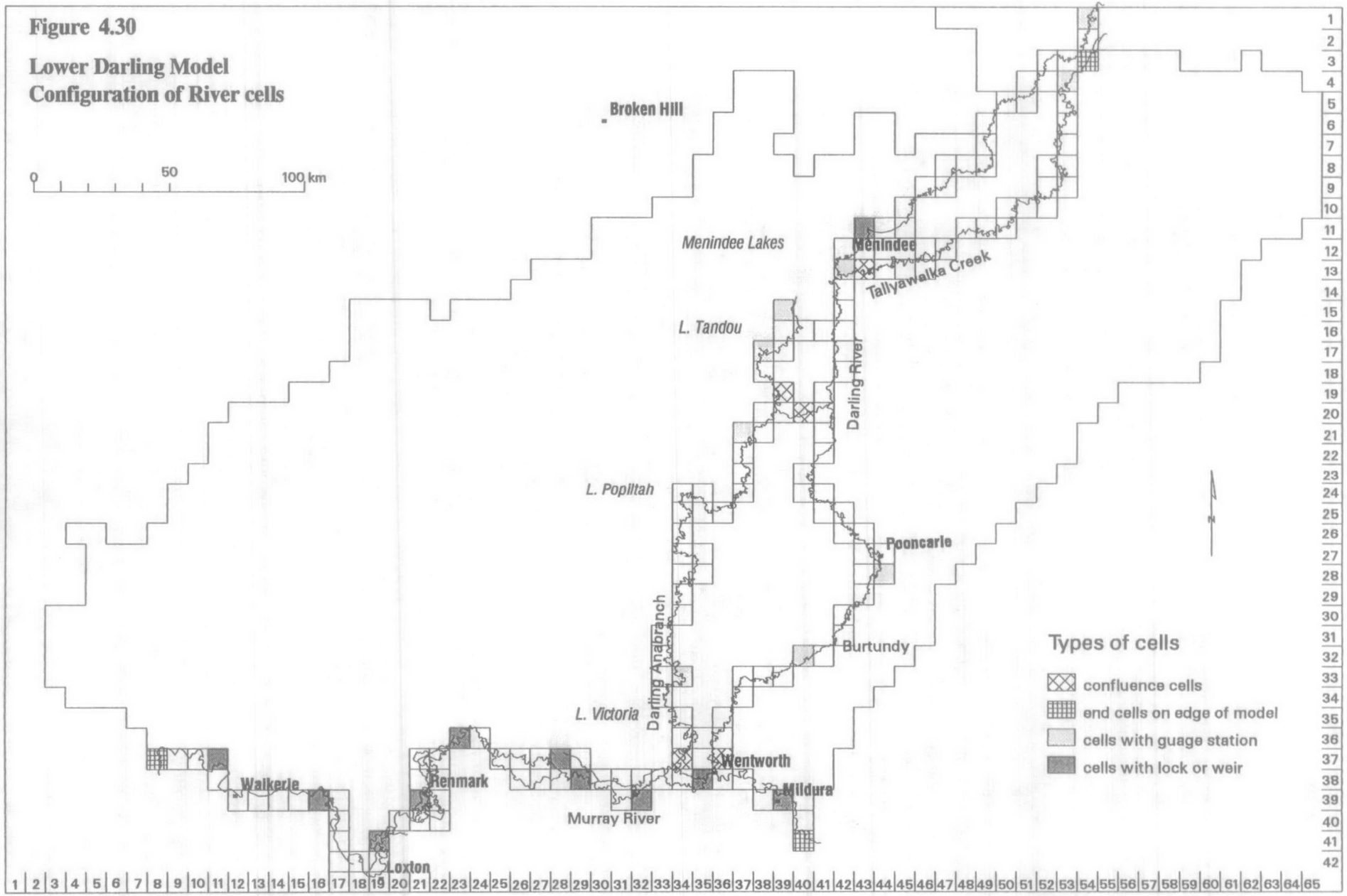

To assist in the assignment of parameters, river cells were classified into the following categories (Figure 4.30):

C - Confluence cells within which significant river channels meet
E - End cells at the margins of the active model domain
G - Gauge cells which contain a river gauging station
L - Lock cells where a lock was constructed.

These cells were particularly important as they either represent sites where specific information was collected (ie G and L cells) or where attention had to be paid (ie the C and E cells). Typically these cells became the end points containing the required information to interpolate the parameters for the intervening river cells.

4.6.1 River Stage

Estimation of the elevation of the head in the river, the river stage, was predicated by the available data and the degree of river regulation. For the Darling system, the recorded levels from gauging stations routinely collected by the NSW Department of Land & Water Conservation were used. Table 4.2 summarises these gauging stations and indicates the variability in the duration of the water level record. Some stations such as Burtundy and Bulpunga have a well maintained record spanning decades, while others have sporadic measurements taken over just a few years.

Table 4.2 Gauging Stations on the Darling/Tallyawalka

Station	River	Location	Gauge Zero AHD	River Bed AHD	Year From	Year To
425008	Darling	Wilcannia Main Channel	63.41	63.4?	1972	1996
425012	Darling	Weir 32	51.83	50.3?	1974	1976
425018	Tallyawalka	Barrier Highway	69.0	68?	1988	1991
425029	Tallyawalka	Kangaroo Waterholes			1976	1977
425007	Darling	Burtundy	32.40	30?	1973	1996
425005	Darling	Pooncarie	39.03	37.5?	1993	1994
425014	Cawndilla Channel	Cawndilla Outlet	53	53?	1992	1996
425013	Anabranch	Wycot			1981	1996
425019	Redbank Creek	Packers Crossing	49?	49?	1992	1996
425011	Anabranch	Bulpunga	32.04	32?	1955	1996

For the steady state model, a long term average of river stage is required. This is difficult considering the natural variability of river flow and the intermittent nature of the gauging record. The seasonal changes in the level of the Darling River is most apparent upstream of the Menindee Lakes, typified by the record near Wilcannia (Figure 4.31). Here, flood peaks have exceeded 11 metres and during drought periods the river has practically dried up. The Menindee Lakes storage has had a moderating effect on downstream water levels by absorbing major flood events and maintaining minimum flows during dry periods (Figure 4.32). The periodicity in the levels of the Anabranch reflects the policy of providing annual

replenishment flows from Menindee Lakes, interspersed with irregular natural flood events (Figure 4.33)

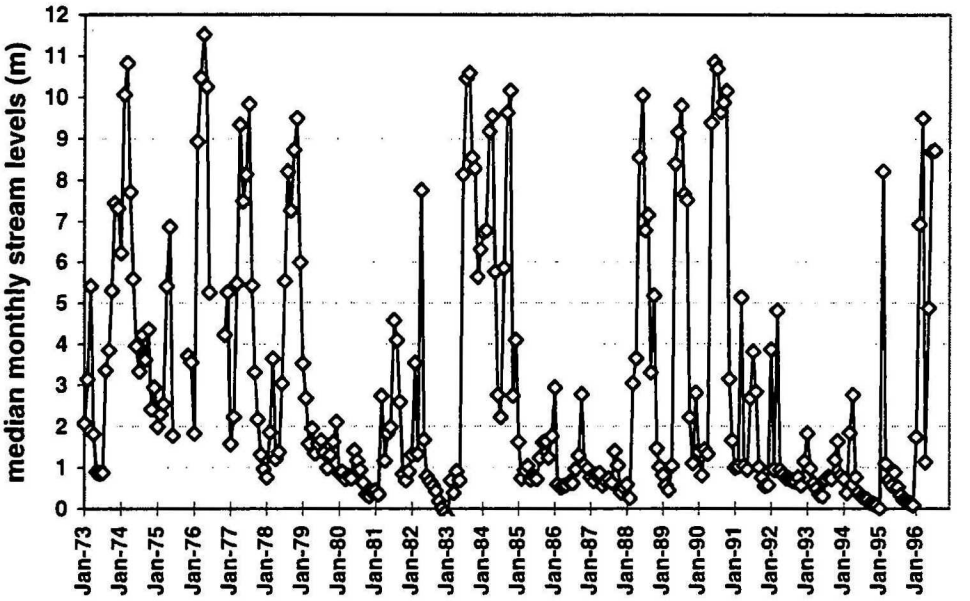

Figure 4.31 Monthly median water levels for the Darling River at Wilcannia Main Channel (NSW DLWC)

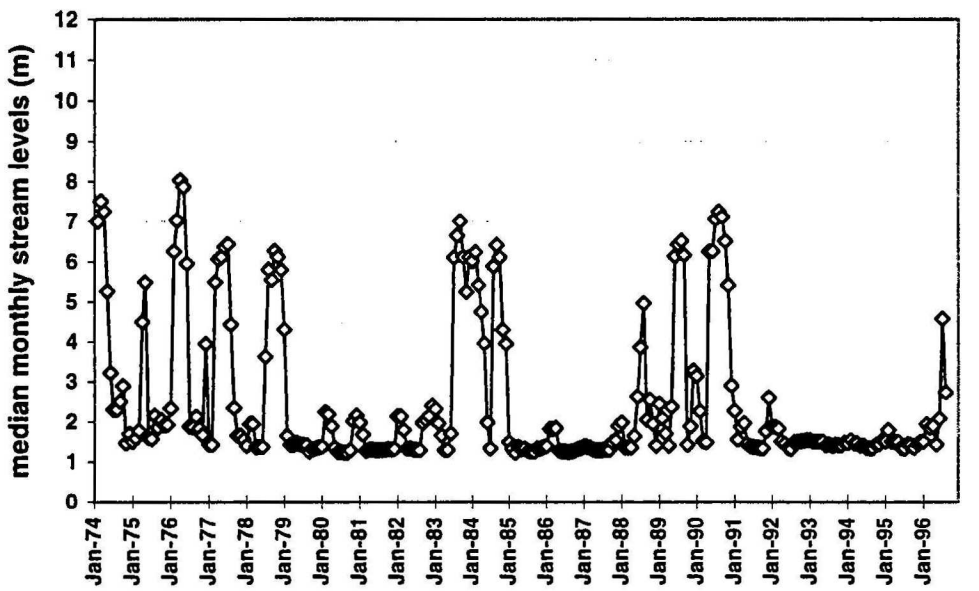

Figure 4.32 Monthly median water levels for the Darling River at Weir 32 (NSW DLWC)

Median values were calculated from the water level record of each of the stations and used for the steady state average stage. For the stations with limited data, this median was adjusted by comparing the record of nearby stations with a longer and better quality record. This was achieved by taking the median of the levels from the better station just for the time interval for which the measurements were taken for the station with the poor record. This was used in a ratio with the overall median of the better quality record to weight the median for the station with the limited record. For example, the median for the record at Pooncarie which spans 1993 to 1994, was multiplied by the ratio of the overall median for the Burtundy record divided by the median of the Burtundy record for the 1993-1994 time period.

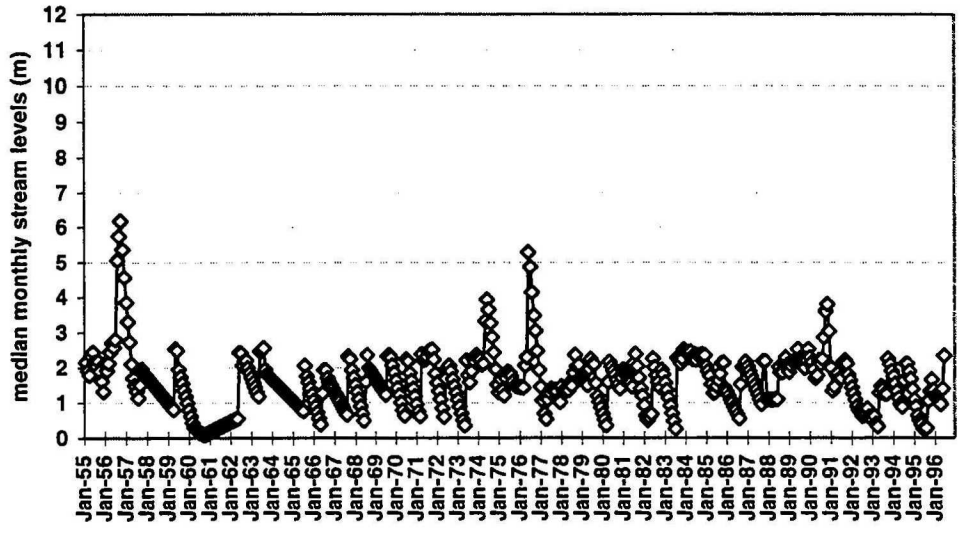

Figure 4.33 Monthly median water levels in the Darling Ana branch at Bulpunga (NSW DLWC)

These median values were then assigned to the relevant cells ('G' type) in the *river_p* polygon coverage, the cells which encompassed the gauging station. Using GIS functionality, the stage of the river cells between the gauging stations were simply calculated by linear interpolation.

The calculation of stage in the Murray River was approached differently. Seasonal fluctuations in river levels are subdued by the effects of the infrastructure of weirs and locks along the river. These locks force a stepped effect on the stage where the upstream pool of one lock practically reaches the next lock further up the river. The gauging record at Lock 11 near Mildura is an example of this river regulation (Figure 4.35). Here, the upstream pool is maintained at a near constant level of 34.4 m AHD, while downstream the modal level of 30.8 m AHD is only interrupted by flood events of varying magnitude. Operation of the lock will cease for the duration of the larger floods, represented by the fluctuations in the stage record at these times.

Table 4.3 summarises the modal averages of river levels both immediately upstream and downstream of the locks. These were derived from water level records maintained by the MDBC for the Murray River since 1986. The difference between the modal level of the

upstream pool and the modal level immediately below the next lock up the river is listed in the table. This gradient over the upstream river reach is less than 0.3 m for most of the locks.

This data was used in the stage calculations for the river cells making up the Murray/Lindsay drainage system. Within the *river_p* coverage, river cells containing these locks (type = 'L') had the average of the downstream and upstream modal values assigned as the stage. These lock cells were also used as end points to calculate the stage of intervening river cells by linear interpolation. The upstream modal average of the lower lock and the downstream modal average of the upper lock were used as the limits of this interpolation. For example, the cells making up the reach of the Murray River between Locks 3 and 4, have stage values ranging between 9.8 and 10.5 m AHD.

Table 4.3 Modal River Levels at Locks on the Murray River.

Lock	River Distance (km)	Upstream Mode (m AHD)	Downstream Mode (m AHD)	Stage Difference (m)
1	274	3.2	0.8	
2	362	6.2	3.4	0.2
3	431	9.8	6.3	0.1
4	516	13.2	10.5	0.7
5	562	16.3	13.4	0.2
6	620	19.3	16.5	0.2
7	697	22.1	21	1.7
8	726	24.6	22.2	0.1
9	765	27.4	24.6	0.0
10	825	30.8	27.7	0.3
11	878	34.4	30.8	0.0

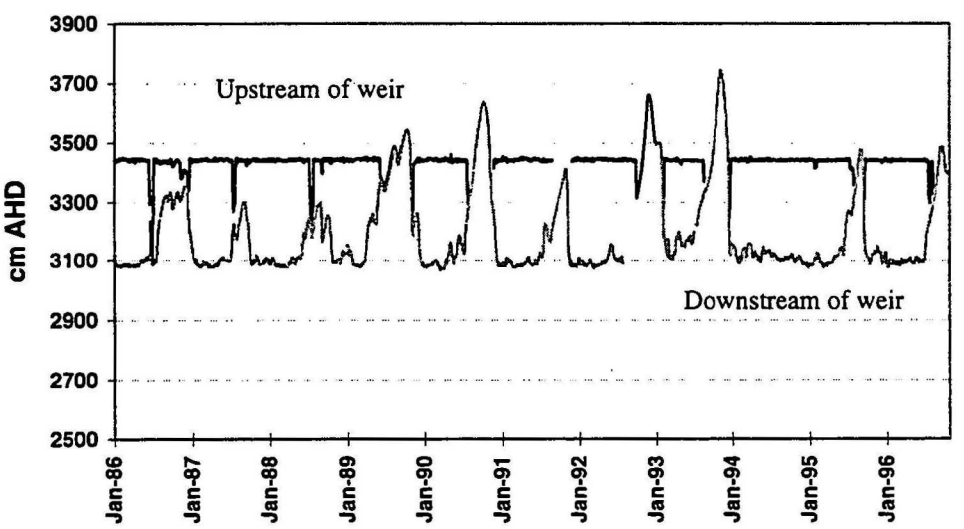

Figure 4.34 Gauging record for the Murray River at Lock 11, near Mildura (MDBC)

4.6.2 River Bed Conductance

The river bed conductance parameter requires the geometry of the river bed and an estimate for its hydraulic conductivity. Figure 4.35 outlines the GIS processes used to estimate the length (*L*) and width (*W*) of the river channel within each of the river cells. The arc coverage representing the main perennial drainage (*river_l*) was integrated with the model cell polygon coverage (*model_n*) to produce a combined identity coverage. In this coverage, the river arcs are split on the basis of the model cells, with the cell identifier, row and column assigned to the individual river reaches. As the length of each arc is a system-generated attribute, it is a simple matter of summing the lengths of all the river reaches belonging to a particular model cell to obtain the channel length parameter (*L*).

Estimation of channel width (W) is more problematic. The River Murray Digital Orthophoto Image Map Series produced by the MDBC and the South Australian Department Environment & Natural Resources was used as a base to measure the channel width at specific points. The black & white imagery is of 5 metre resolution and has been prepared to 1:25,000 scale cartographic standards. The photography was flown in May-June 1991 and according to the gauging station record, no anomalous conditions such as a flood prevailed at this time and the river levels were close to the median values used for modelling purposes. The dataset covers the floodplain of the Murray River and the lower Darling River system up to the Menindee Lakes. The generic BIL raster files were displayed as background and the width of the river channel measured off the image at a series of points using the distance measuring functions of the GIS. Over 2000 measuring points were created along the main rivers. These points were used in a near analysis with the identity coverage containing river reaches split on the basis of the model cells (Figure 4.35). This essentially allocated the measuring points to the nearest river reach. The width of each river reach within a model cell was calculated by averaging the measuring points allocated to that particular arc. In turn, the average width of the river channel for each model cell was calculated as the average for the river reaches within that cell, weighted on the basis of reach length.

The width of the Darling River is mostly in the 35-45 metre range, although it significantly widens (50-100+ m) upstream of the Menindee Lakes due to the main weir. Tallyawalka Creek has a similar average width of 35-45 m, thinning to about 20m in its upstream reach and widening to > 50 m near its confluence with the Darling. It is interesting that it appears that the lower reach of the ancestral Darling, the Ana branch, is slightly wider (50-60m) than that of its modern equivalent. The Murray is obviously a larger drainage system but tends also to have a greater variation in channel width. Within its extensive floodplain near Mildura, the river is about 90-130 m wide while downstream in the Murray Gorge, the channel is around 140-200+ m wide.

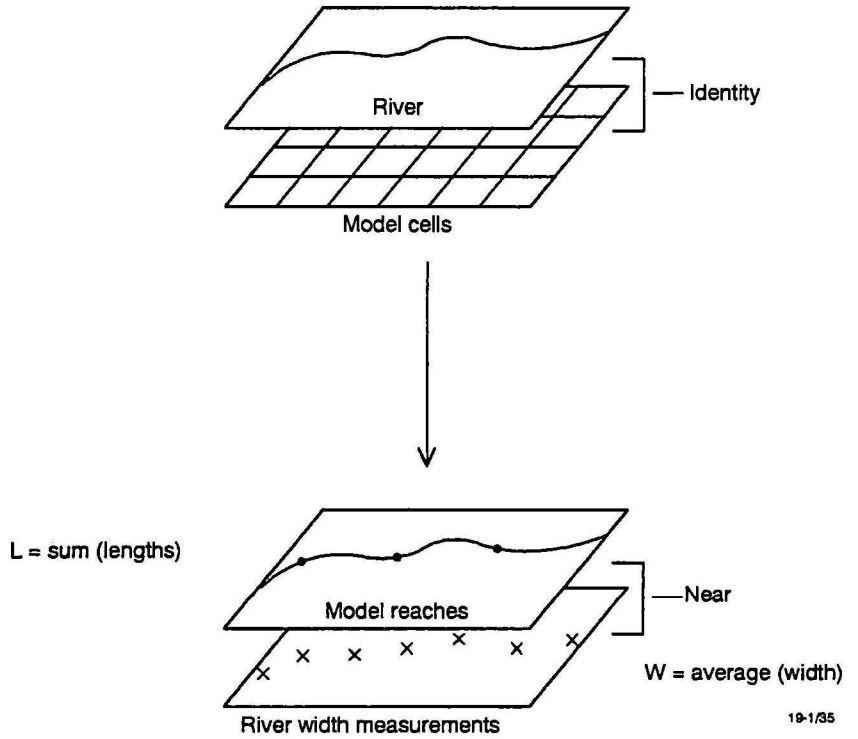

Figure 4.35 GIS methodology to calculate river length and width terms for river cells

The only remaining parameter required to determine the geometry of the river bed is its thickness (*M*). Field measurements for river bed thickness are rarely done, so nominal values were used, based on the experience of the other regional groundwater models. A value of 5m was used for the Murray system and 3m for the Darling and Tallyawalka/Anabranch. Likewise nominal K values were also assigned and this was the main variable which was altered during calibration. The vertical hydraulic conductivity was set constant for each of the major rivers. This differs from the approach taken for modelling of the Lachlan and Murrumbidgee systems, which allowed for a linear decay in hydraulic conductivity down the river (Punthakey *et al*, 1994). The Lower Murrumbidgee model captures the full extent of the river geomorphology from where the river enters the basin at the apex of an alluvial fan to where it finally reaches the Murray. In contrast, the Lower Darling model deals with only the lower reaches of the major rivers, where the lithology of the river bed is relatively constant.

4.6.3 River Bed Elevation

The elevation of the base of the riverbed (*rbot*) defines the threshold between when flow is constant or head variant. When the shallow watertable is below the river bed base, constant flow is defined by the difference between the river stage and the river bed base. When the shallow watertable is above the river bed base, the flow depends on the head difference between the river and the aquifer.

The methodology used to estimate *rbot* for the river cells varied, depending on the availability of river bed surveys. Available data varies from high density sampling to sporadic measurements. Figure 4.36 summarises the processes undertaken within the GIS to obtain cell-by-cell estimates of *rbot* in South Australia. Here, very detailed river survey involving a multitude of transects zigzagging across and up the river is available for the Murray River. This has produced a digital dataset of over 145,000 points measuring the elevation of the top of the river bed both laterally across the channel and longitudinally up, producing a convoluted trace (Figure 4.36). The average elevation of the deepest part of the channel for the river reach within each model cell had to be derived from this survey data.

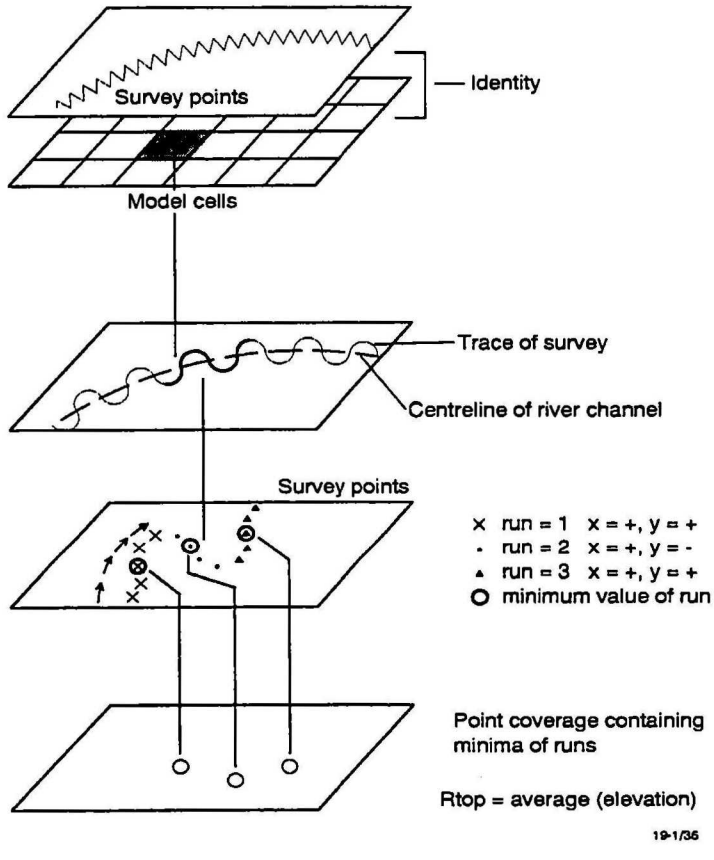

Figure 4.36 GIS methodology to process river bed survey data for the Murray River in South Australia

To achieve this, the survey points were integrated with the model cell polygon coverage. This produced an identity coverage with model cell, row and column numbers allocated to each survey point. Due to the magnitude of the dataset, subsets of the survey points were selected on a model cell basis and copied into separate point coverages, for individual processing. This processing involved differentiating each of the traverses across the river channel and allocating survey points to these traverses. This was completed in a batch process which acted on any changes in direction from one survey point to the next. This starts with the coordinates of the very first two points being derived and variables describing the trends in both the x and y direction defined. For example, if the second point was to the northeast of the first, indicated by higher x and y coordinates, a positive (+) was assigned to the two direction variables. This was repeated incrementally along the survey line, by comparing

point 3 with point 2, then point 4 with point 3 and so on. The points were assigned the same traverse or *run* number until a fundamental change in direction occurred, for example when the y-direction variable changed from a positive to a negative (-). The subsequent points were allocated the next *run* number until another direction change occurred, and so on.

After each survey point was allocated to a run, the point which had the minimum elevation was selected out for each of the lateral runs and copied into another point coverage. These points represent the deepest part of the channel for the lateral river profiles. The complication is that the survey tended to go across the river channel, then sample in the upstream direction close to the edge of the river, then go back across to the river. The survey points from this scenario would be subdivided into three runs, two lateral and one longitudinal. As the longitudinal run tends to be near the edge of the river and not representative of the deeper part of the channel, its minimum should not really be included in the statistics. This was achieved by selecting points in runs of three (ie all points belonging to run 1 to 3, then 4 to 6, and so on) and the minimum elevation determined for these subsets. The final result is a point coverage which received the minima for the majority of cross-channel traverses for all of the model cells. An *rtop* value was calculated by averaging these survey points representing the deepest part of the channel within each cell. Finally, the nominal thickness of the river bed was subtracted from the *rtop* parameter, to derive *rbot*. Due to spurious values in the survey data effecting the statistics, some *rbot* values assigned to cells had to be adjusted, based on the trends in neighbouring cells.

In 1986, the Victorian Rural Water Commission undertook an echo sounding of the Murray River bed east of the South Australian border to Wentworth. This involved a longitudinal profile based on the centre line of the river and cross sections spaced about 5 km apart. The profile data was digitised into an arc coverage where the y-coordinates represent elevation in metres AHD of the river bed and the x-coordinates represent river distance from the Murray Mouth in km. Along this stretch of the Murray, the bed drops gradually from about 25.5 m AHD to 14 m AHD over a river length of 190 km, equating to a gradient of 6 cm/km (Figure 4.37). To link this dataset with the model cells, the minimum and maximum river distances were assigned to the river reaches within the relevant model cells in the *river_p* polygon coverage. This was done manually by locating geographical features which had designated river distances and were marked on the river profile plots.

The vertices of the arcs defining the river bed profile were converted into points and stored in a new point coverage. The minimum and maximum river distances that describe the limits of a particular model cell were used as criteria to select out the subset of these profile points that were contained within that particular model cell. Statistics on these selected points derived the mean and standard deviation of the measured elevation of the river bed within the model cell. The extra complication was that the profile line contains short sharp perturbations caused by snags or local obstructions. To reduce the influence of these anomalies, any elevation data beyond two standard deviations of the mean were removed from the selected set of survey points. The mean of the remaining data was used as the elevation of the river bed top, the *rtop* parameter. The *rbot* value was derived by subtracting the nominal thickness value from this parameter. For the few remaining Murray River cells east of Wentworth, the base of river bed was simply extrapolated using the gradient defined by the river survey.

Similar surveys of the bed of the Darling River appear to be not currently available. The only survey control is that available for the gauging stations. The top of the river bed at these points were estimated by deducting the cease flow height from the gauge zero level. These values were used as end points for linearly interpolation of values for the intervening river cells. The nominal thickness was subtracted to obtain the final *rbot* parameter.

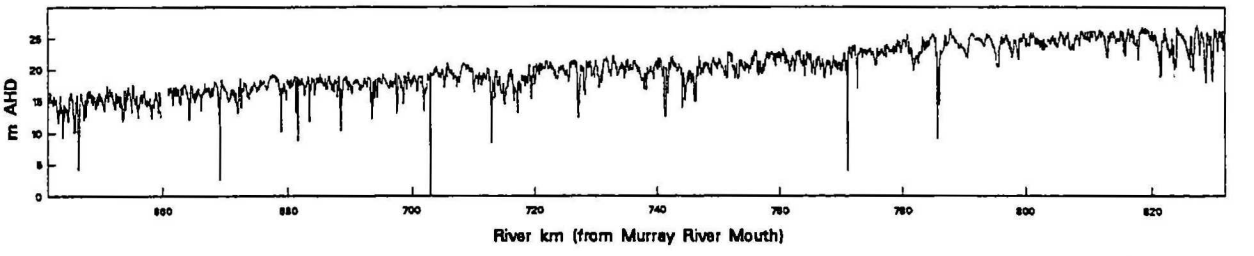

Figure 4.37 Profile of bed of Murray River from Wentworth to the SA-Vic border (RWC)

4.7 Recharge (RCH) Package

The proper estimation of recharge is critical to the modelling effort. One of the model objectives is to predict the long term effects of regional clearing of mallee on the watertable and river salt loads. This clearing is represented by a change in the recharge array from low infiltration rates under native vegetation (<0.1% rainfall) to significantly higher (1-5+% rainfall).

The other regional groundwater models in the Murray Basin have used differing approaches to characterise recharge. A chloride mass balance comparing rainfall and shallow groundwater established a 1% recharge rate for the eastern Riverine Plain (Kellett, 1997). Based on the published field measurements of recharge under undisturbed mallee, a value of 0.1 mm/yr was assigned to the mallee remnants within the Lachlan Fan Model. The recharge for model cells intermediate to these end points was calculated by linear interpolation using an empirical algorithm based on the proportion of undisturbed mallee and a soil properties index. In contrast, the net recharge for the Lower Murrumbidgee model was calculated within the same inverse procedure that was used to estimate leakance (Punthakey *et al*, 1994). For the SAVIC model, a water balance model to estimate drainage from the evapotranspirative zone and a soil water infiltration model to map deeper percolation were coupled to in an attempt to predict recharge through time (Jayatilaka *et al*, 1994).

Vegetation and the soil clay content are the dominant controls in the Mallee region in determining the percentage of rainfall that percolates past the evapotranspirative zone and becomes groundwater recharge. These parameters are somewhat interconnected as the predominate soil type tends to influence vegetation cover (refer Fig 1.10). The mallee assemblage prefers the sandy aeolian landforms, while low bluebush and saltbush shrublands dominate the clayey alluvial plains near the rivers.

Figure 4.38 outlines the GIS-based methodology used to estimate rainfall recharge for the Lower Darling model. The final recharge array is a function of land systems mapping as a de facto soils properties map, vegetation and rainfall, with consideration for areal recharge from other sources. This process relied upon the raster based functionality of the Arc/Info GIS, where grids with a 2.5km resolution, finer than the model cells, were generated and combined.

Due to the absence of a complete coverage of soil mapping at a suitable scale, the land systems polygon coverage was used to map regional changes in clay content. This coverage is based on the mapping undertaken by the Soil Conservation Service of NSW (Walker,1991), augmented by mapping in South Australia by CSIRO (Laut *et al*, 1977). These land system units tend to delineate the aeolian, fluvial and lacustrine surface geomorphologies across the landscape (refer Figure 1.8), and as such are a reasonable representation for gross soil properties. Each unit was assigned a nominal percentage sand value. For aeolian landforms for which sandy soils are characteristic, this value was high (> 80) and for lacustrine landforms with clay soils this value was naturally low (<20). This information was stored in an attribute in the coverage and used to translate the polygon coverage into an equivalent %sand grid. In turn, a second authority table translated these %sand values into a recharge rate expressed as a percentage of rainfall. The thresholds used in this translation are based on the published literature on field estimates of recharge in the basin. Recharge through sandy soils with a low clay content (<10%) has been measured at 20-40 mm/yr, or about 5-15% of rainfall (Cook et al, 1996). This rapidly reduces to less than 1% rainfall when the clay content approaches 20%. Recharge does not appear to diminish linearly with further increases in clay content , most probably due to the role of secondary permeability features such as soil fractures and root channels (Kennett-Smith et al, 1994). The product of this translation is a grid representing surface geomorphology expressed as equivalent recharge as a percentage of rainfall.

The land systems mapping was also categorised on the basis of the density of dominant vegetation. This was a simple binary classification where land systems described as having a proportion of dense woodland vegetation such as mallee, belah-rosewood, black box or cypress pine was assigned a value of 1. This includes the Scotia, Arumpo and Mandleman land systems in New South Wales and the Canopus, Pine Valley and Parcoola land systems in South Australia. The remaining land systems were assigned a value of zero. The wooded land systems correspond well with the generalised version of the National Forest Cover dataset made available for the model area by the National Forest Inventory (Figure 1.11). As such, the main areas of mallee north of the Murray in South Australia and between the Darling River and Willandra Lakes are delineated. The belah-rosewood assemblage is mapped peripheral to these areas and eucalypt woodlands are found scattered along the floodplains of the major rivers.

The resulting vegetation grid was used as a condition to create the coverage representing recharge as a percentage of rainfall (Figure 4.36). That is, if the grid cell was effectively vegetated by mallee, belah or acacia (value = 1) then recharge was evaluated as 0.05% of rainfall. Otherwise (value = 0) the percentage rainfall as designated by the %sand classification of the land system was used. The resulting %rainfall grid was simply multiplied

with the average rainfall grid (refer Figure 1.3) to calculate the recharge due to rainfall in mm/yr.

Additional sources of areal recharge are apparent over the model area. The relatively low groundwater salinities in the shallow aquifer adjacent to the Broken Hill Block and Scopes Range, reflect additional recharge due to drainage off the basement highs (refer Figure 3.10) This includes leakage from the ephemeral streams such as Sandy Creek and Turkey Plains Creek. Enhanced recharge also occurs due to irrigation accessions, such as in the Berri-Barmera area. These areas were delineated as polygons in a separate coverage and assigned a nominal recharge rate.

This polygon coverage was converted to an equivalent recharge grid in mm/yr, which was then used to increase the rainfall recharge grid that was previously generated from the vegetation and geomorphology. The resulting grid was resampled into a coarser resolution grid (7.5 km) matching the model cells and a conversion factor used to derive the final recharge grid in m/d. This was the grid which was exported into GMS for use in the Recharge package and is plotted in Figure 4.39.

Recharge via rainfall is estimated to be a low 3 to 3.5×10^{-7} m/d, equating to about 0.1 mm/yr, over most of the model area. The general decrease in recharge to the northwest follows the general trend in total rainfall. Scattered higher recharge rates of 6 to 12×10^{-7} m/d are particularly evident along the eastern margin of the model. These relate to aeolian landforms which have been assigned a marginally higher sand content. Recharge increases by several orders of magnitude over the irrigation areas, with typical values of 3 to 5×10^{-5} m/d.

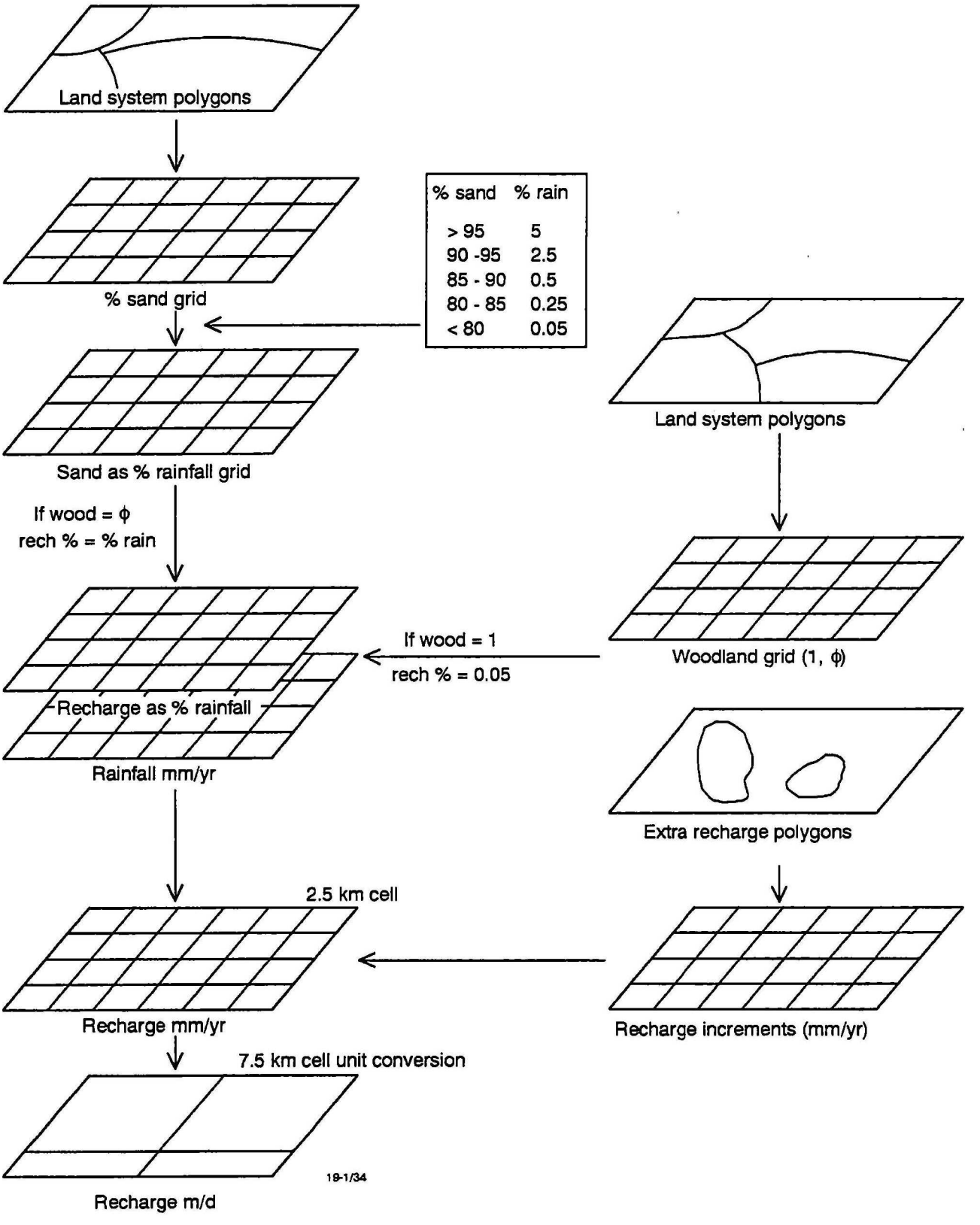

Figure 4.38 GIS methodology to estimate areal recharge

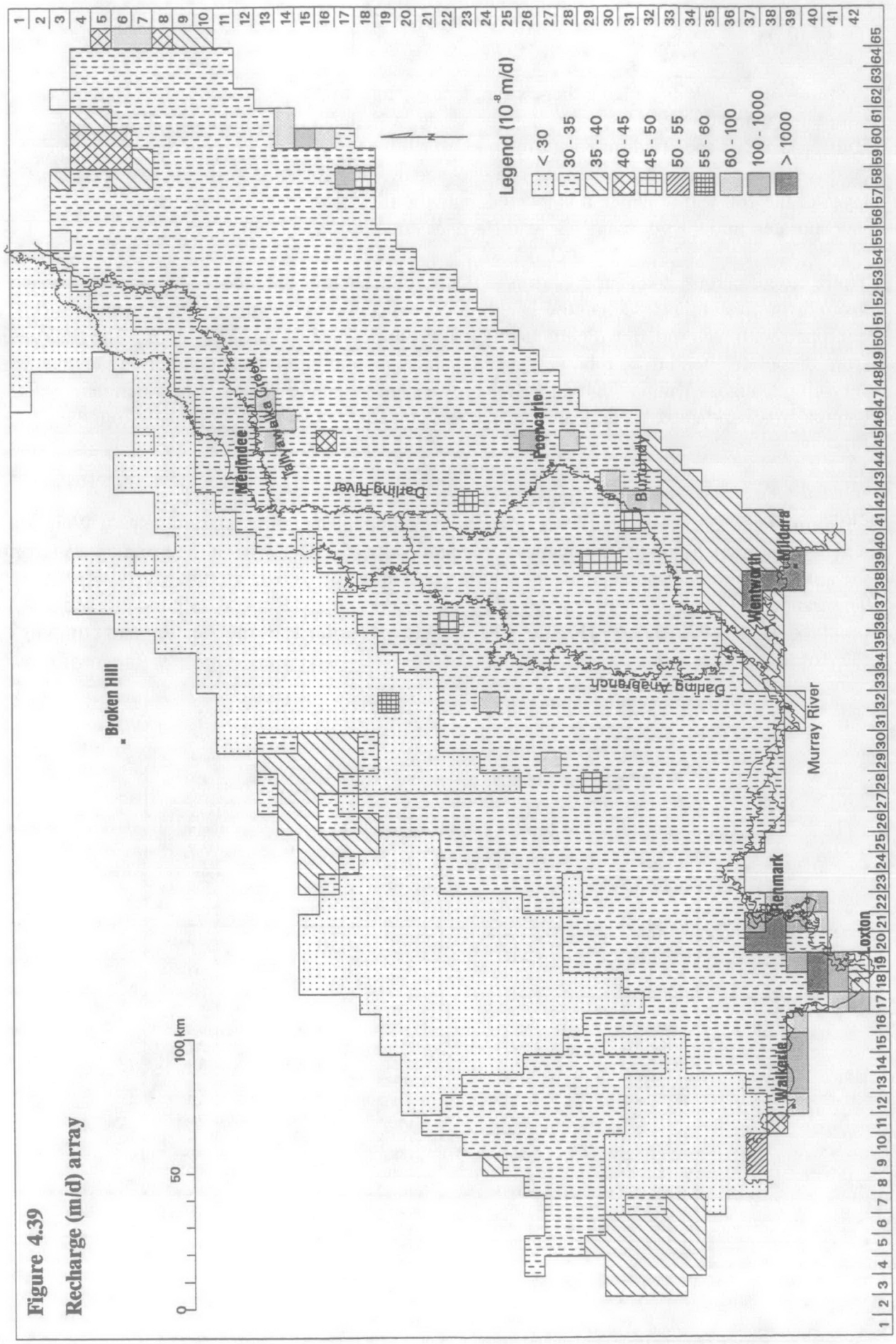

Figure 4.39
Recharge (m/d) array

4.8 Well (WEL) Package

Features such as wells which either extract from or inject into the groundwater system are simulated using the Well package. The flow rate, which is independent of cell area and aquifer head, is specified for each time period, with negative values indicating discharge and positive values indicating recharge. The package requires for each well, the row, column, layer of the cell within which it is located, and the flow rate, Q. The flow value is incorporated into the governing finite difference equations as a source term.

There are numerous stock supply bores in the northern half of the model, tapping groundwater salinities less than the 14,000 mg/L threshold for sheep. Most of these are equipped with windmills, with a minority using submersible or surface pumps. The flow rate from these bores tend to be relatively small (< 0.5 L/s) and intermittent, supplying tanks servicing troughs. Due to the relatively low water usage and low density of boreholes (typically > 2-5km apart), they are not likely to impact greatly on the regional groundwater flow system.

4.8.1 Woolpunda Interception Scheme

Of significance are the groundwater interception schemes operating continuously at Waikerie and Woolpunda. In the latter scheme, bores pump out 15 ML/day of saline groundwater from the shallow Murray Group Limestone aquifer, reducing accessions into the Murray River. The transect of boreholes constructed along the northern bank of the Woolpunda Reach is included in the Well package (Figure 4.40). Table 4.4 summaries the location and pumping rate for these bores.

Table 4.4 - Woolpunda North Interception Bores

Borename	Easting	Northing	Total ML 1995-96	Flow L/s
BORE NO . 25	438214	6221195	149	7.2
BORE NO . 26	437138	6220340	161	5.8
BORE NO . 27	436094	6219538	174	5.7
BORE NO . 28	434413	6218859	189	7.3
BORE NO . 29	432789	6219286	179	7.0
BORE NO . 30	431729	6219470	94	7.5
BORE NO . 31	430642	6219104	152	6.5
BORE NO . 32	429392	6219247	152	5.0
BORE NO . 33	428121	6219456	265	8.6
BORE NO . 34	427076	6220018	220	7.2
BORE NO . 35	426184	6220415	176	6.1
BORE NO . 36	425288	6220541.	173	5.9
BORE NO . 37	424371	6220750	161	5.4
BORE NO . 38	423754	6220585	153	5.1
BORE NO . 39	422976	6220517	100	3.7
BORE NO . 40	422207	6220313	104	4.2
BORE NO . 41	421269	6220153	99	3.3
BORE NO . 42	420349	6219754	102	3.4
BORE NO . 43	419464	6219292	90	3.0
BORE NO . 44	418621	6218831	52	1.9
BORE NO . 45	417722	6218503	32	1.2
BORE NO . 46	416743	6218473	28	1.0
BORE NO . 47	415538	6218579	31	1.0
BORE NO . 48	414326	6218671	28	1.0
BORE NO . 49	412943	6219119	44	1.0

Source: SA Water, Berri

4.8.2 Active Salinas

Groundwater flows from the basin margin to the regional discharge zone located over the basin depocentre to the south. Here, numerous active salinas are entrenched into the sandplain representing windows into the shallow groundwater system. The cumulative evaporative loss of groundwater from these salt lakes needs to be incorporated into the model. The simplest approach is to treat the salinas as pumping wells.

Within the GIS, a polygon coverage representing active salinas was combined with the model coverage. This subdivided the lakes on the basis of the model cells and allocated cell row and column numbers accordingly. The flow rate (Q) in m^3/d of groundwater discharge is based on the evaporation to rainfall deficit:

$$Q = -1 * A * (evap * mult - rain) * .001 / 365$$

where A is the area of the salt lake polygon within the model cell, *evap* is the average annual pan evaporation rate in mm/yr and *rain* is the average annual rainfall rate in mm/yr. The *mult* factor is used to obtain an actual evaporation rate from the pan measurement, and was set as 0.4. The relevant grids were sampled at the location of the lakes to derive the rainfall and evaporation parameters. The area A of each lake polygon is a system-generated attribute. The constants in the equation are used for unit conversion from mm/yr to m/d and to make the flow rates negative, indicating loss from the groundwater system.

4.9 General-Head Boundary (GHB) Package

Lateral and vertical fluxes between active model cells and external sources or sinks are simulated using the GHB package. A linear relationship between flow and head is established by

$$Q_{bi,j,k} = C_{bi,j,k} (h_{bi,j,k} - h_{i,j,k})$$ (McDonald & Harbaugh, 1988)

where $Q_{bi,j,k}$ is the flow into the cell i,j,k from the source, $C_{bi,j,k}$ is the conductance between the external source and the cell, $h_{bi,j,k}$ is the head of the external source and $h_{i,j,k}$ is the head in cell i,j,k. The corollary to this equation is that there is no limiting value for flow, and Q will indefinitely increase proportionate with increases in the head difference. This has the potential of causing unrealistic flows to be generated during model simulation. The GHB package requires the layer, column and row of the affected model cell, the head on the cell boundary and the hydraulic conductance of the interface between the model cell and the boundary. Deriving the first three parameters is simple as they are mandatory attributes of model cells. The head parameter used the value assigned to the external cell, as stored in the grid generated for the potentiometric surface of the relevant layer.

The conductance term is the parameter which is hardest to define and the one which was modified during calibration. The basic conductance equation is:

$$C = KA/L$$ (McDonald & Harbaugh, 1988)

where K is the hydraulic conductivity of the material in the direction of flow, A is the cross-sectional area perpendicular to the flow and L is the length of the flow. Hence, conductance is defined for a particular prism of aquifer and for a particular direction. For GHB cells representing horizontal fluxes, the cross sectional area is the vertical cell face defined by the layer thickness and the cell width (7.5km), and the flow length is the nodal distance between the GHB cell and the neighbouring external cell which equals the cell width (7.5km). For vertical fluxes, the area A is defined by the cell dimensions (7.5x7.5km) and the flow length L is the internode distance defined by half the layer thickness and half the thickness of the underlying external layer.

4.9.1 Boundary Fluxes

The GHB array for layers 1 to 4 is displayed in Figure 4.40. The Shepparton Formation receives groundwater from an external source in two areas in the northeast corner of the model. Firstly, the formation is saturated in the Baden Park Depression and receives westward flow. Secondly, two GHB cells along the northern boundary account for the downstream flow into the model within the saturated alluvial sediments of the Darling River floodplain. The arcuate structural high marking the edge of the Murray Basin between the Scopes Range and the Cobar Block enforces a groundwater divide within the Calivil Formation across the Darling River floodplain. Hence, no GHB cells are required for layer 2 in this area. However, groundwater flows into the model layer via the Baden Park Depression and a smaller gap between the Darnick Ridge and Quamby Hills. The Neckarboo Ridge forms a groundwater divide for the remainder of the eastern model boundary. The flow regime for the upper Renmark Group is very similar to that of layer 2, so layer 3 has the same configuration of GHB cells.

No GHB cells are required for the bounds of the layer 4 aquifers. The middle Renmark Group is absent along the northern half of the eastern margin and the Neckarboo Ridge structural high has created a groundwater divide along the southern half. The Murray River, which represents the southern layer boundary, acts as a drain so that the flow from the north tends to be matched with flow from the south of the river. Unlike the shallow aquifers, flow in the lower Renmark Group continues to the south of the river. Hence, GHB cells are required in the southwest margin to represent flux out of the active model (Figure 4.40).

As these GHB cells represent horizontal flow, the conductance term is basically the product of layer horizontal hydraulic conductivity and layer thickness. This is because the flow length matches the width of the cross sectional area (eg 7.5 km), thereby cancelling each other in the basic conductance equation. The layer horizontal hydraulic conductivity and thickness were parameters already estimated for the BCF package and available as gridded data. The average of grid values for the GHB cell and the neighbouring external cell were used in the calculations.

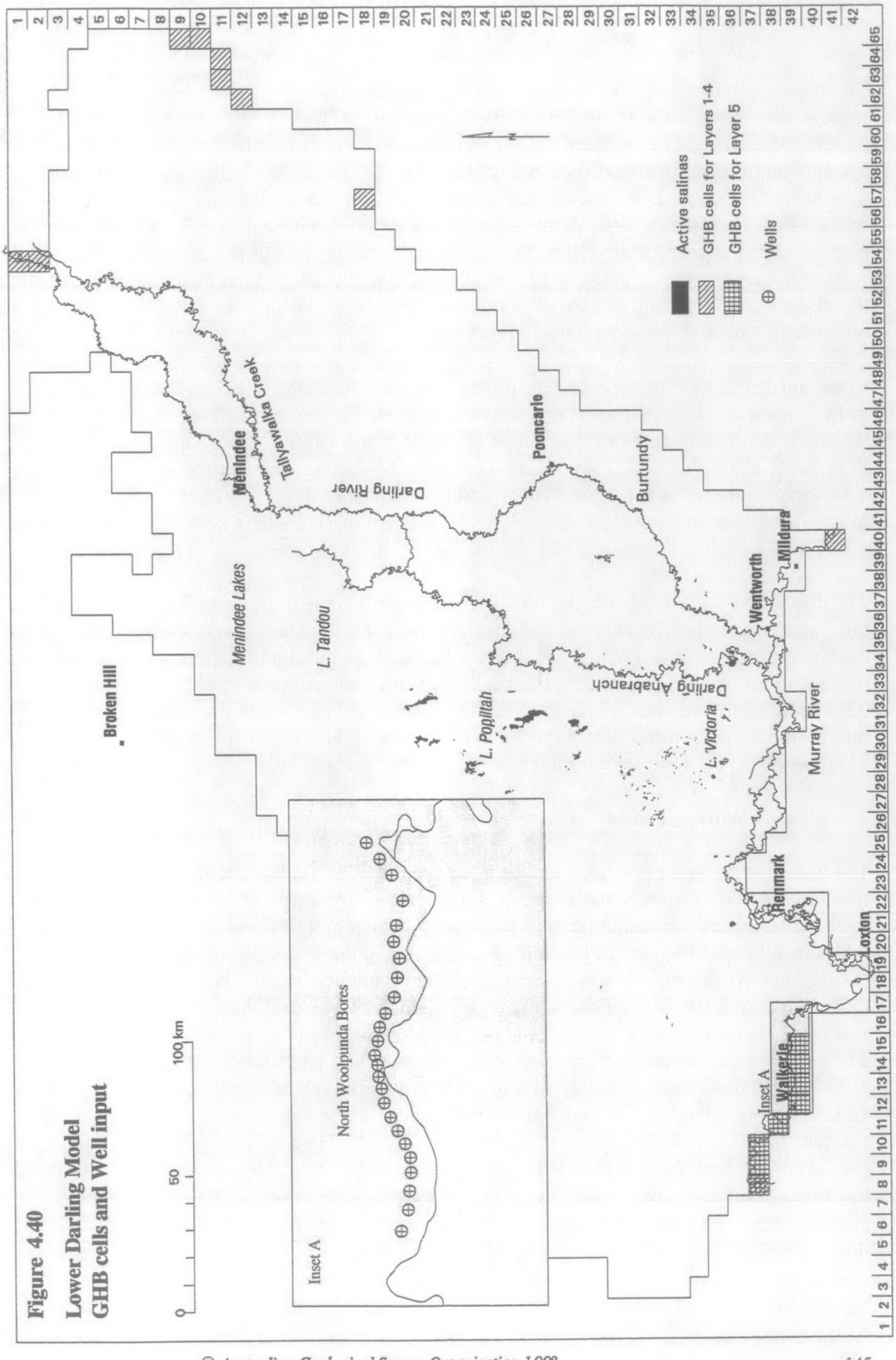

Figure 4.40
Lower Darling Model
GHB cells and Well input

4.9.2 Lower Cretaceous Aquifer

The interaction between the Tertiary sequence and the underlying Lower Cretaceous (Kl) is incorporated into the model as GHB cells. Since a vertical flux is being modelled, the conductance term relates to the aquifer prism defined by the lower half of the lowermost Tertiary aquifer and the uppermost half of the Kl unit. Due to the shallowing of the basin, the relevant model layer changes up-gradient from the lower Renmark Group (layer 5) to the middle Renmark Group (layer 4) and to the upper Renmark Group (layer 3). Conductance is calculated as the product of vertical hydraulic conductance and model cell area (7.5km x 7.5km) divided by the length of the flowpath (half the thickness of the model layer plus half the thickness of Kl). The array was subsequently modified during the calibration process, with the final model input depicted in Figure 4.41.

In the northern half of the model, the conductance is interpreted to increase from 5 to 20 m^2/d. This may be a function of the progression from the finer grained upper and middle Renmark Group sequences to the coarser lower Renmark Group. Since, the argillaceous Permian Urana Formation is sandwiched between the Tertiary and Cretaceous sequences in the deeper Renmark and Tarrara Troughs, the conductance in these areas are set low at 1 m^2/d. Conductance is set at 30 m^2/d along the western margin where both the lower Renmark Group and Lower Cretaceous thin over the Hamley Fault.

The direction of flux is defined by the difference between the head in the Kl aquifer and the head in the overlying Tertiary aquifer. Limited water level measurements suggest that heads in the Kl aquifer are about 1-2m lower than the heads in the overlying Renmark Group aquifers in the northern half of the model. Hence, a head difference trending southwards from -2 to -0.5m was used in this area. Like the Tertiary system, the leakage in the southern half is interpreted to be upwards, from the Kl aquifer. A positive head difference trending from +1m to +6m in the southwest corner was used in the calculations.

4.9.3 Storage Lakes

The use of large floodplain lakes as water storage facilities has had a serious impact on the local and regional groundwater systems. For example, the groundwater mound underlying the Menindee Lakes has significantly perturbed regional groundwater flow. Hydraulic loading by Lake Victoria, has caused lateral flow of shallow saline groundwater into the nearby floodplain environment. These external inputs are modelled as the GHB cells for the shallow model layer over the Menindee Lakes, Lake Victoria and Lake Bonney.

The polygons representing these lakes were subdivided on the basis of the model cells. This allowed the automatic calculation of the lake area within each relevant model cell. The clays and silts comprising the lake bed basically define the degree of interaction between the lake and the shallow aquifer. This is analogous to the river bed deposits characterised in the River package. The conductance term is largely defined by the vertical hydraulic conductivity and thickness of the lake bed sediments. These parameters were set at .00005 m/d and 5m respectively. The head parameter is based on a long term average of the operating levels for these storages (Table 4.3).

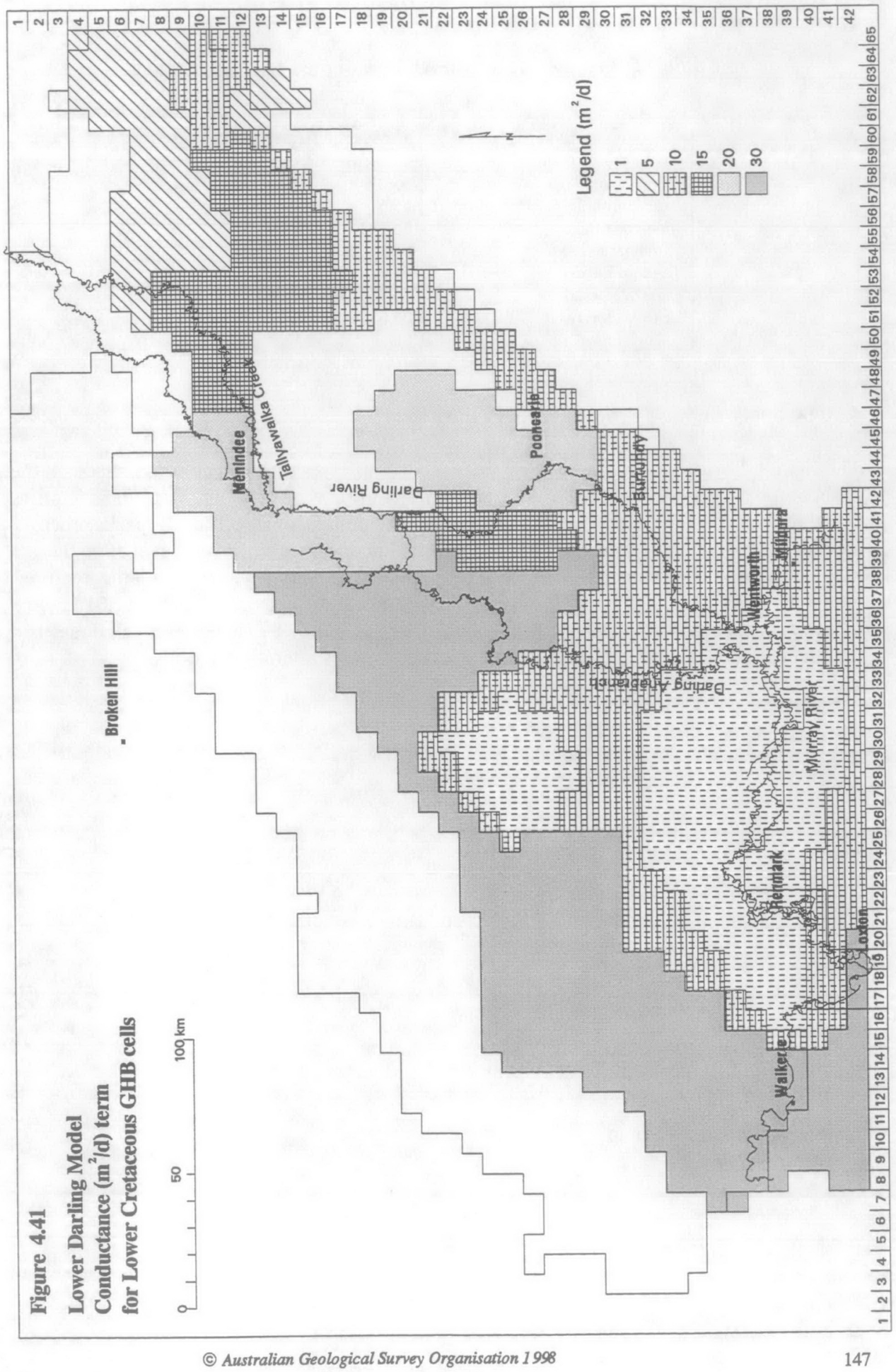

Figure 4.41
Lower Darling Model
Conductance (m^2/d) term
for Lower Cretaceous GHB cells

Table 4.5 Average Heads (m AHD) assigned to storage lakes

Lake	Average Head (m AHD)
Lake Cawndilla	55.0
Lake Eurobilli	55.6
Menindee Lake	56.3
Pamamaroo Lake	60.5
Tandure Lake	61.7
Lake Wetherall	61.7
Lake Victoria	25.0
Lake Bonney	9.8

4.10 Strongly Implicit Procedure (SIP) Package

The finite difference equation for each model cell, expresses the head at the cell node on the basis of the head at each of the six adjacent nodes at the end of each time step. This requires that the equations for the entire grid must be solved simultaneously. The SIP package was used to achieve this by iteration. The maximum number of iterations was set at 500, the number of iteration parameters used at 5, the acceleration parameter at 1, with the iteration parameter seed calculated by MODFLOW. The head change criterion was set as .01m, so that the iteration stops when the maximum absolute value of head change from all nodes is less than or equal to 1cm. The calibrated model converges after 44 iterations.

5. MODEL PERFORMANCE

5.1 The Calibration Process

Calibration of a groundwater model is achieved when predicted heads and flows match field measurements within reasonable error limits. For the Lower Darling model the error criteria was defined as ±2m of the aquifer potentiometry interpreted for 1988. Calibration involved trial and error manipulation of the aquifer parameter arrays, stresses and boundary conditions to reduce the difference between modelled and observed heads. This included;

1. Modifications to the horizontal hydraulic conductivity arrays to increase or reduce the horizontal flow through a model cell. Changes to horizontal hydraulic conductivity values were used to solve a particular calibration problem when cells were drying up where the layer thinned over the Woolpunda Ridge. These cells became inactive, damming the groundwater flow and causing extremely high heads in up gradient cells. By reducing the horizontal hydraulic conductivity in the problem cells, sufficient head could be maintained so that they remained saturated and active throughout the simulation.

Similarly, vertical groundwater movement could be enhanced or constrained by modifying the vertical hydraulic conductivity array to change leakance between layers. For example, under discharge conditions where flow is upwards, high heads in a layer may be alleviated by increasing leakance to the overlying model layer. Likewise, high heads in a model layer under recharge conditions where downwards flow prevails, may be reduced by increasing the leakance to the underlying layer.

2. Changing the stresses to the groundwater system. Rainfall and river losses are the principle forms of recharge into the groundwater system for the Lower Darling area. The raster based process used to define areal recharge (refer Figure 4.38) allowed input from different sources to be expressed as additions to the recharge array. In this way, the groundwater mounds developed under the irrigation districts could be simulated by adding a recharge increment in these areas. Along the basin margins, the Murray Basin sequence may receive additional influx of water via drainage off the surrounding basement ranges onto the sand plain. This is reflected in lower salinities in the shallow aquifers, with the dilution effect by Sandy Creek being a good example of this mechanism. This addition by run off was also modelled as a recharge increment to these areas.

For the RIVER package, the interaction between the aquifer and the river system was controlled by changing the vertical hydraulic conductivity of the river bed sediments. This determined the conductance term (Criv). Hence, the flux between the river and aquifer could be reduced by decreasing the vertical hydraulic conductivity of the river bed. In general, this defined how much the Darling River lost to the groundwater system. Conversely, varying the vertical hydraulic conductivity (hence conductance) of the river bed sediments determined the extent to which the Murray River acted as a groundwater drain. The other mechanism for groundwater loss is via the active salinas. These were modelled by the WELL package by calculating a discharge rate from the evaporation rate and the lake bed area. The pan evaporation rate was multiplied by a factor to calculate the actual evaporation rate. This multiplication factor was modified to vary extraction rates during calibration.

3. Alterations to the boundary conditions for the model. Groundwater flow across vertical and horizontal model boundaries are largely depicted as GHB cells. For instance, the three uppermost model layers receive westwards groundwater flow in the Baden Park Depression, depicted as GHB cells along part of the northeast model boundary. The seepage from the Menindee Lakes and Lake Victoria are also modelled as GHB cells.

However, the most important external source/sink modelled by the GHB package is the underlying Lower Cretaceous (Kl) aquifer. The model could not be successfully modelled without the GHB cells depicting the interaction between the lowermost model layer and the Kl aquifer. In the absence of these cells, the heads in all layers would be consistently overestimated in the northeast half of the model area. In the southwest, the modelled heads in layers 4 and 5 would invariably be too low. This indicates the importance of the Kl aquifer to act as a drain under recharge conditions in the northeast and as a groundwater source to the lower aquifers under an upward flow regime typical of the southwest of the model. Similar to the RIVER package, the flux was largely controlled by changing the conductance parameter during calibration. The head difference between the Kl aquifer and the lowermost model layer dictates the direction of vertical groundwater flow.

4. Improving the definition of the aquifer geometry, as defined by the top and base of layer arrays stored in the BCF package. Inconsistencies in the layer base arrays originally caused local anomalies in modelled heads. Artificial pits in the aquifer base surface tended to divert and accumulate groundwater flow and had to be corrected during the calibration process. Particular attention to the layer base arrays also had to be made at the model margins so that the resulting layer thickness calculations were not negative.

A scale problem was also evident when elevation data defined for the river was compared with the layer geometry. The base of the layer in each cell is averaged over a large area (7.5km x 7.5km) while the base of the river bed is defined for a specific linear feature. Inconsistencies arose where the base of the layer hosting the river was higher than the base of the river itself. This was particularly apparent for some of the Murray River cells and was largely resolved by excluding elevation data south of the river. The development of better averaging algorithms to sample the TINs depicting the surfaces to gridded output also reduced these inconsistencies.

5.2 Evaluating the Calibration

The comparison between observed heads as interpreted for 1988 and the heads simulated by MODFLOW is summarised in Table 5.1. The three common ways of expressing error, termed the calibration criteria, are the mean error (ME), the mean absolute error (MAE) and the root mean squared (RMS) error (Anderson & Woessner, 1992). The mean error (ME) is simply the mean difference between measured heads (h_m) and simulated heads (h_s);

$$ME = 1/n \sum_{i=1}^{n} (h_m - h_s)i$$

As this is calculated from both negative and positive differences, there is a tendency for these differences to cancel each other. For instance, a simulation which grossly under and overestimates measured heads may have a low mean error. Hence, the ME may not be a satisfactory measure of goodness of fit for the model. The mean absolute error (MAE) is a better measure of calibration as the absolute value of the differences is used;

$$MAE = 1/n \sum_{i=1}^{n} |(h_m - h_s)i|$$

The mean absolute error over the model domain is 2.43 m, varying from 1.34m for the basal lower Renmark Group sequence to 2.84m for the layer 2 Pliocene Sands.

The RMS error or standard deviation is the average of the squared differences in measured and simulated heads and is used where errors are normally distributed:

$$RMS = [1/n \sum_{i=1}^{n} (h_m - h_s)i^2]^{0.5}$$

The RMS error over the model is 2.25m.

Table 5.1 Statistics for Observed Heads minus Modelled Heads

Layer	Minimum	Maximum	Mean Error (ME)	Std Dev (RMS)	Mean Abs Error (MAE)
1	-13.0	9.8	-1.77	2.39	2.39
2	-10.7	18.0	-2.10	2.76	2.84
3	-6.6	10.7	-1.83	2.27	2.46
4	-9.9	11.9	-2.36	2.28	2.81
5	-5.4	1.9	-1.02	1.46	1.34

The effectiveness of the model calibration is measured by the cumulative percentage plot based on the absolute difference between measured and simulated heads (Figure 5.1). This shows that 93% of model cells have simulated heads within 5m of observed heads, and that about half of the model cells are within 2m. The actual percentage of cells within the 2m threshold varies between 35% and 78%, depending on the model layer. Layer 5 is the most successfully calibrated layer with over 90% of cells within 3m of observed heads.

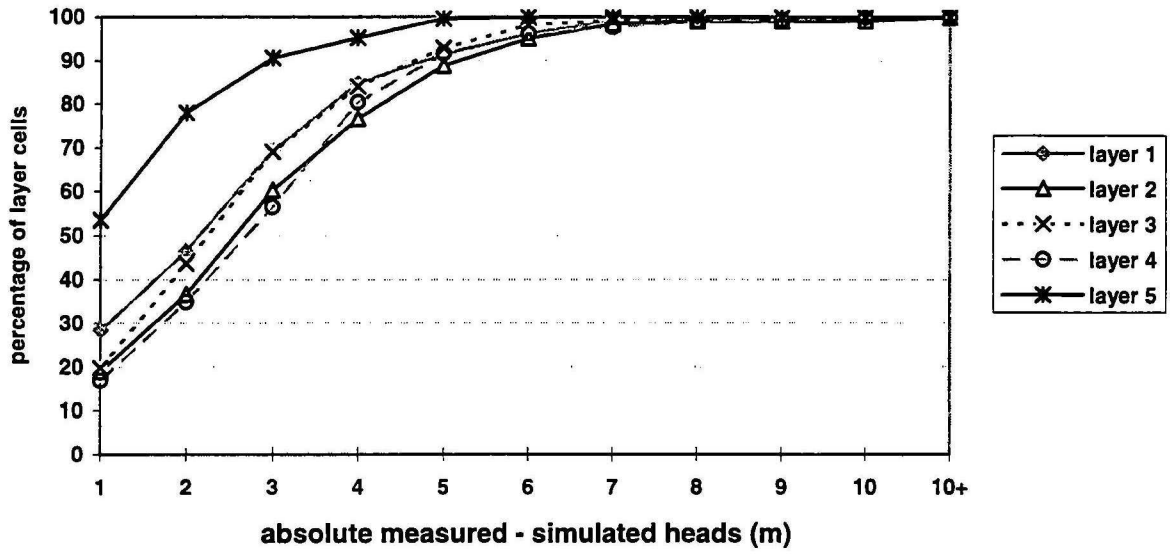

Figure 5.1 Cumulative percentage plot of absolute difference between measured and simulated heads

Figure 5.2 plots the residual between observed and simulated heads across the model domain for layer 1, the Quaternary sediments. This indicates a tendency for the model to underestimate heads in the alluvial aquifer of the Darling River. This is particularly true for two reaches - upstream of the Menindee Lakes and from the Ana Branch junction downstream towards Pooncarie. In contrast, the model overestimates the groundwater levels operating in the shallow alluvial aquifer of the lower reach of the Darling by around 2-3 m. Away from the Darling River, the modelled heads are consistently too high, with two problem areas, one on either side of the river. In these areas, the modelled head can exceed inferred observed heads by 5-7 m. The thin (5-20m) Blanchetown Clay component of Layer 1 found in the southern half has proven difficult to model. In the regional discharge zone north of Lake Victoria, many of the layer 1 cells have become unsaturated and inactive. The simulation of heads in the Coonambidgal Formation alluvial aquifer of the Murray River has been more successful, with the head in many cells being within 1m of observed levels.

Underestimation of heads also occur in the same two problem areas on the Darling River for Layer 2, the Pliocene Sands aquifer (Figure 5.3). The model has not adequately simulated the groundwater mound found in the Parilla Sands aquifer at and upstream of the Menindee Lakes, with residuals of 2-5m. Likewise the mound interpreted over the Lake Wintlow High is not well represented, with simulated heads 5-12 m too low. Like the shallow layer, modelled heads are consistently overestimated away from the Darling River, maximising at the same two locations in the model domain. Modelling along the layer margins is inconsistent in part, particularly in the northeast corner where heads are underestimated by 10-15 m and the southwest corner where heads are overestimated by 5-10 m. Along some parts of the western margin, the aquifer is modelled as dry where it has been mapped as saturated. The majority of cells along the southern margin of the layer near the Murray River are within 1 m of observed heads.

Figure 5.2

Observed heads minus modelled heads (m) array for model layer 1

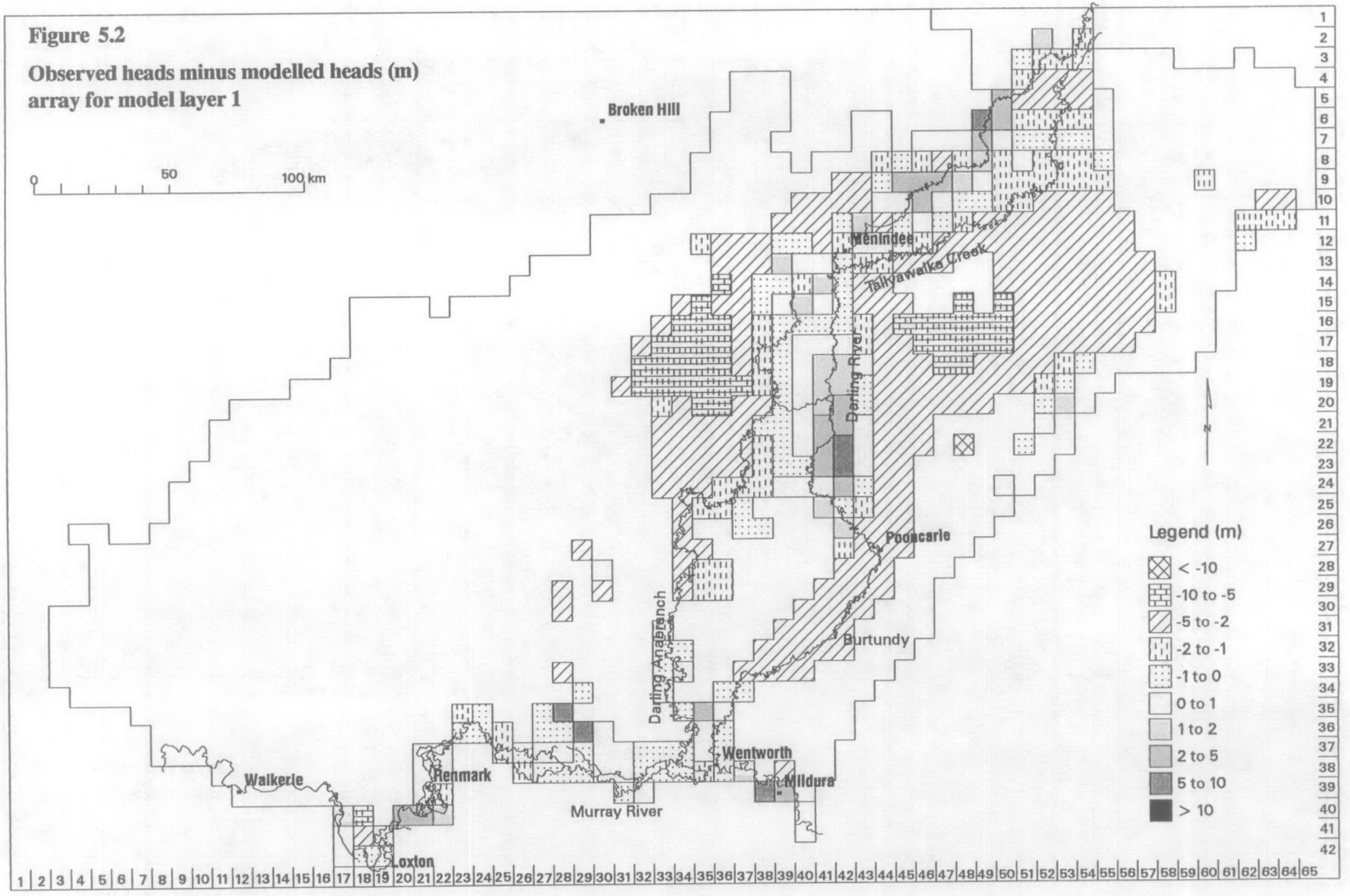

Figure 5.3

Observed heads minus modelled heads (m) array for model layer 2

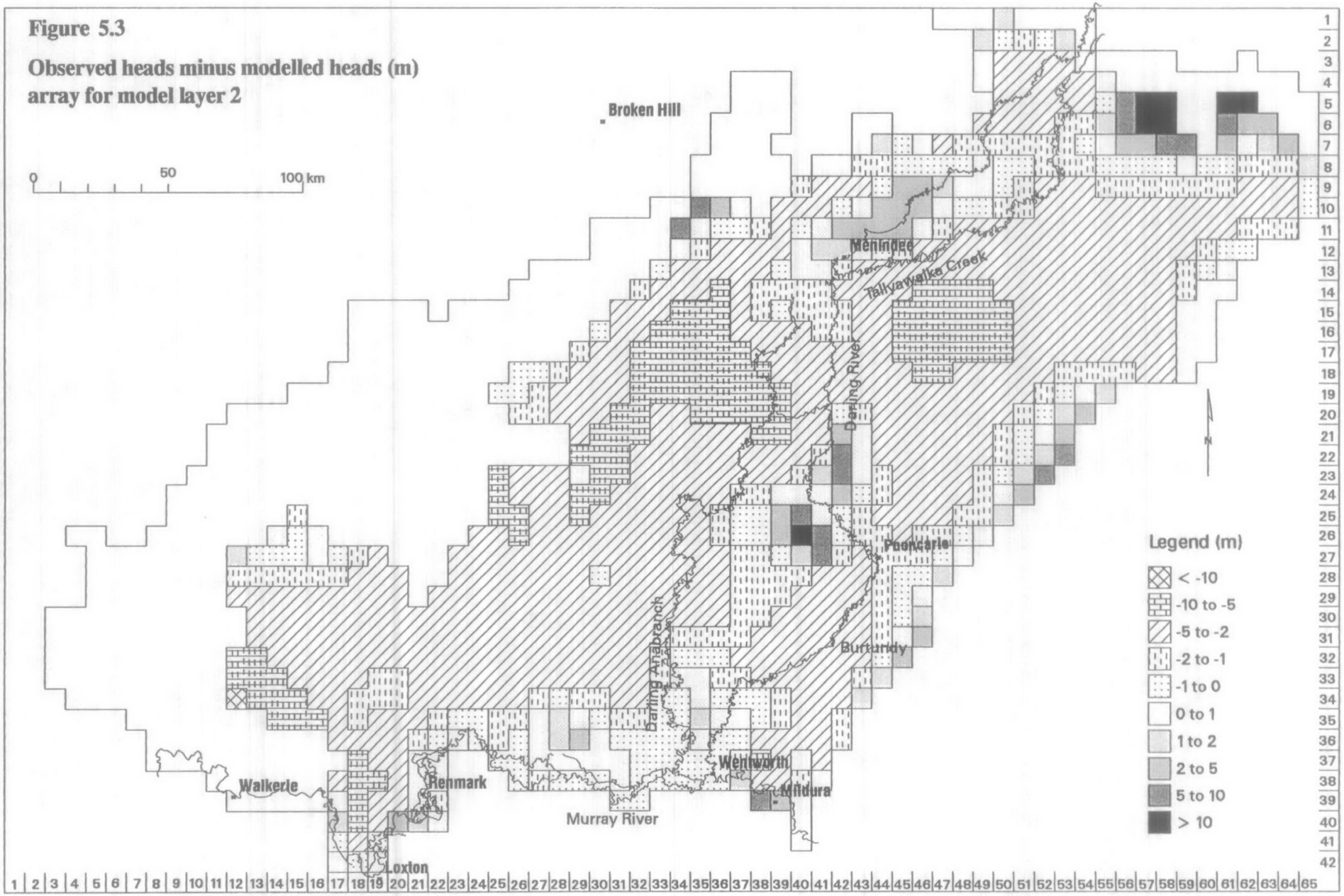

Figure 5.4

Observed heads minus modelled heads (m) array for model layer 3

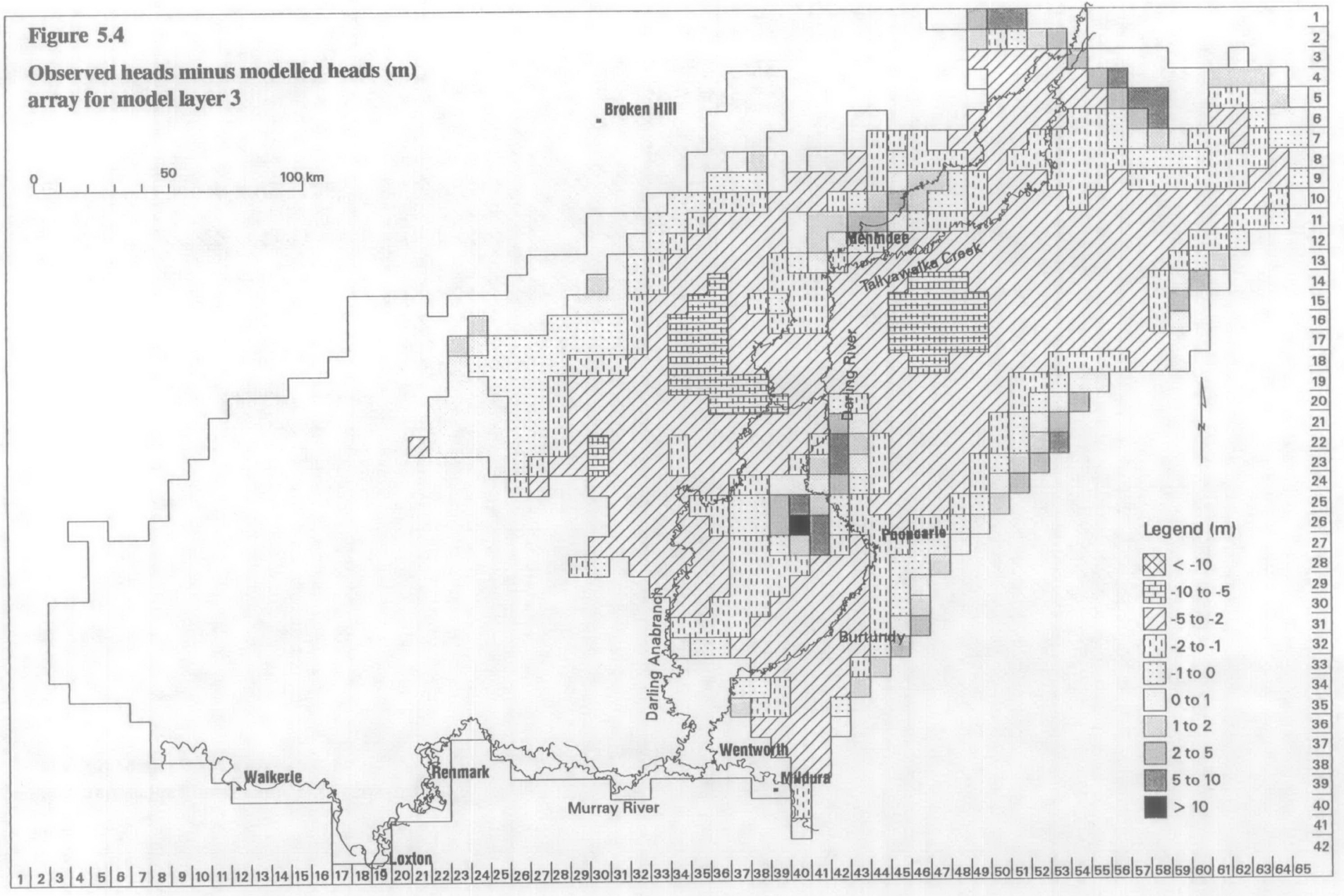

Figure 5.5

Observed heads minus modelled heads (m) array for model layer 4

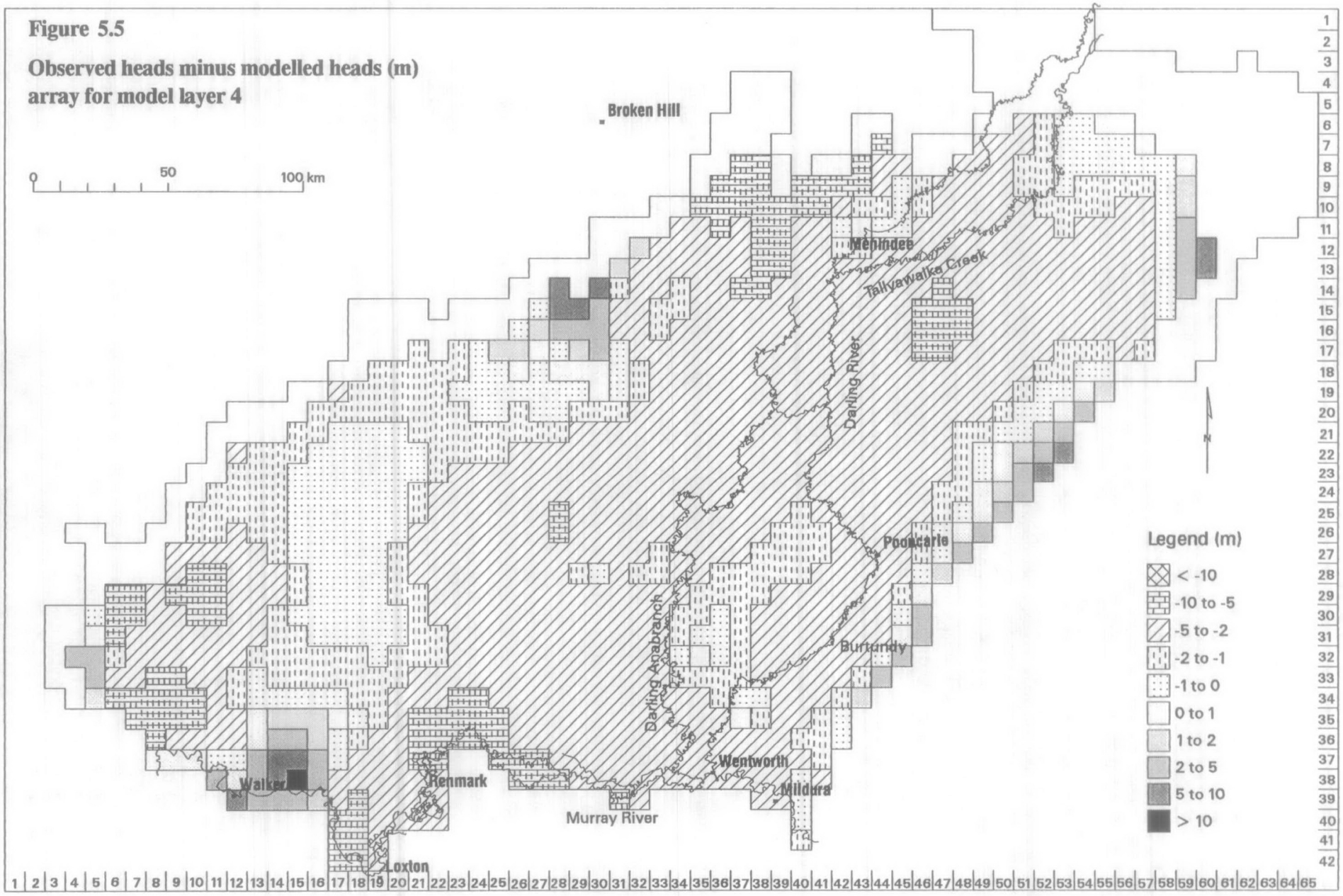

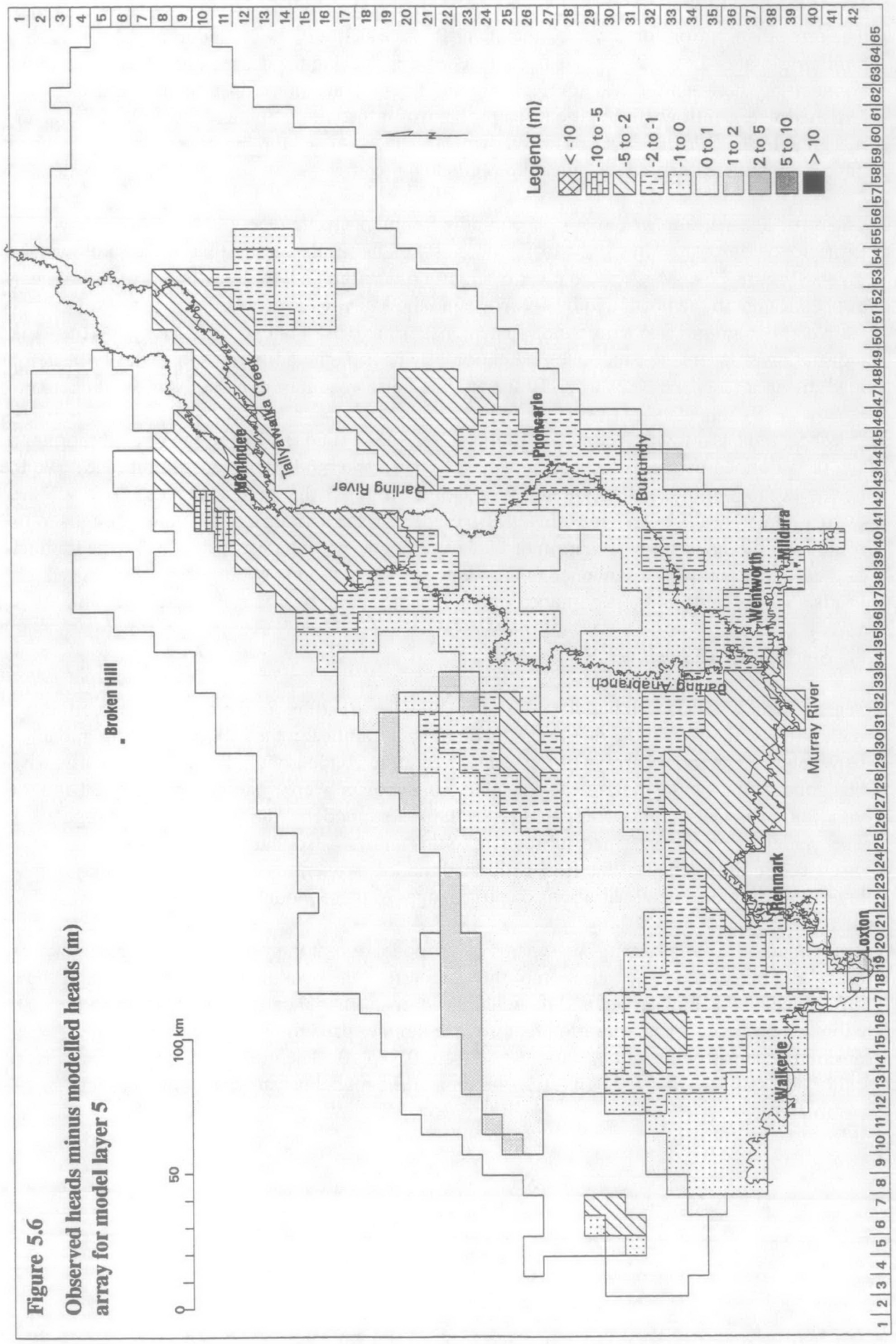

Figure 5.6
Observed heads minus modelled heads (m) array for model layer 5

The error distribution for Layer 3, the upper Renmark Group, as plotted in Figure 5.4 is very similar to that of Layer 2. This is not surprising considering the degree of hydraulic connectivity between the two aquifers. Again, the mounds inferred for the Menindee Lakes and the Lake Wintlow High has caused problems for the simulation and the bulk of the layer marginal to the Darling River has been overestimated. Along the margins of the layer, heads have been underestimated causing some cells to dry.

The error distribution for Layer 4, the middle Renmark Group/Geera Clay/Murray Group Limestone composite, has some differences as well as similarities to that of the shallower layers (Figure 5.5). Most of the layer is slightly overestimated, with extremes of 5-9 m near Scopes Range to the north and of 4-9 m around the Murray River near Berri to the south. Conversely, around the Woolpunda Reach, heads have been underestimated by 3-12m. Like the shallower layers, the modelled potentiometry near the layer margins have partly been too low, most notably the Neckarboo Ridge and the northwest margin along New Well Creek.

Layer 5, the basal lower Renmark Group aquifer, has a unique distribution of calibration errors as defined by the difference between observed and modelled heads (Figure 5.6). To the north, in the Menindee/Blantyre and Wentworth Troughs, the model has mostly overestimated heads by 2-5 m. This is also evident in the Tarrara and Renmark troughs to the south. Along the northwest margin of the layer, heads are underestimated by 1-2m. In much of the thinner part of the sequence to the west, the simulation is within ±1 m of observed heads. To the south in the Renmark Trough, heads tend to be overestimated by 2-3m.

5.3 Sensitivity Analysis

A sensitivity analysis was undertaken to gain an understanding of the degree of uncertainty within the calibrated model due to the inherent uncertainties in the estimation of the model parameters. The model arrays of horizontal hydraulic conductivity, leakance, recharge, river bed conductance and general head boundary conductance were systematically altered and the variation in model output, compared to the calibrated model at the time, was investigated. The model arrays were refined subsequent to this analysis, so that the results are not discussed in the context of the final calibrated model. Appendix 1 gives a detailed layer-by-layer description of head variations due to changes to these model parameters.

Three methods of expressing the sensitivity of model output to systematic input changes were used. Figure 5.7 plots the variation of the RMS error, the overall standard deviation of the difference between observed and modelled head in all model cells, with changes to the calibration factor. The calibration factor is the number used to multiply the relevant array during the sensitivity analysis, and varied from 0.1 to 10. The greater the departure from the calibrated standard deviation of 2.25, the greater the model is sensitive to that particular parameter.

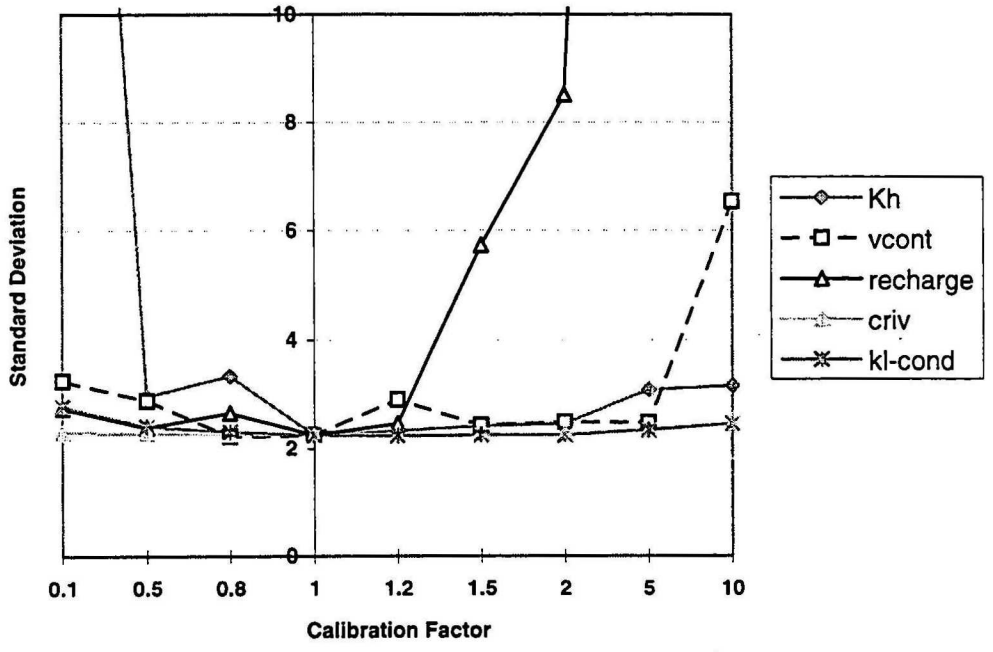

Figure 5.7 Variation in Standard Deviation with changes in calibration factor

Figure 5.8 uses the overall mean of the observed to modelled head difference (ME), rather than the standard deviation, as an evaluation statistic. This gives added information in terms of the direction of change in heads with changes in the model parameter. Any decrease from the calibrated ME of -1.74 implies that the modelled heads have generally increased relative to the observed heads. This is because the simulated heads is subtracted from the observed heads in the calculation of error.
Likewise, an increase in the mean error reflects an overall decrease in modelled heads.

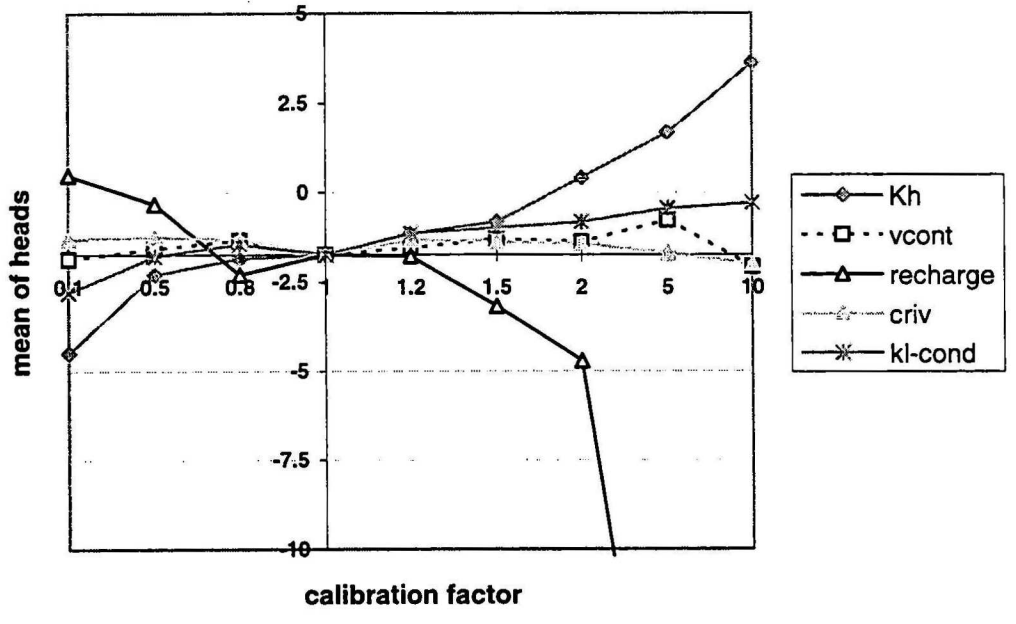

Figure 5.8 Variation in mean error (ME) with changes in calibration factor

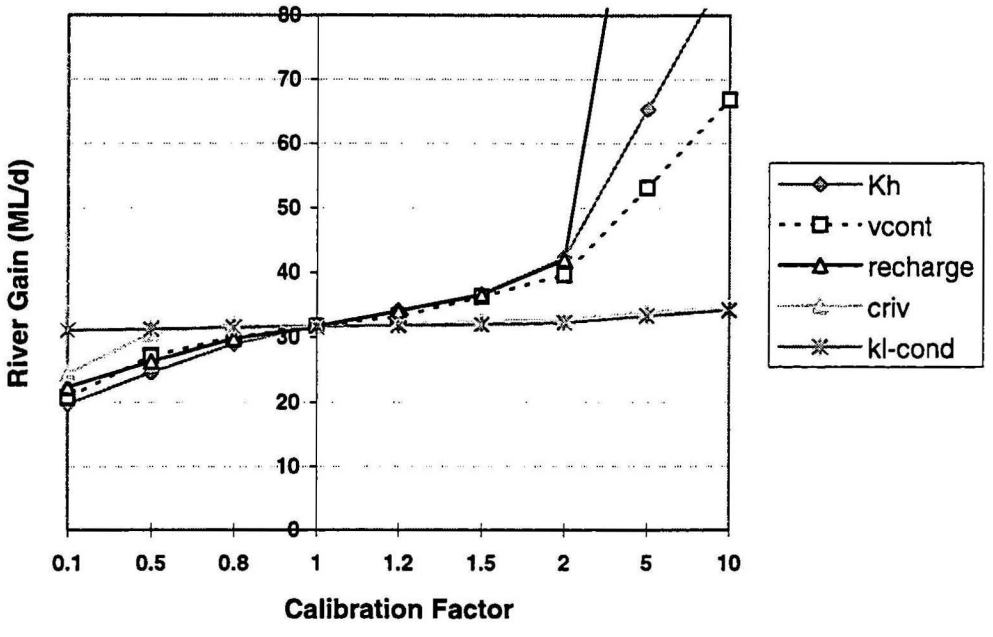

Figure 5.9 Variation in river gain (ML/d) with changes in calibration factor

Instead of modelled heads, variation in modelled flow can be used as an evaluating criteria. Figure 5.9 maps the changes to the rate of groundwater flow (m^3/d) into the river due to changes in the calibration factor. This is a particularly important model output as it represents the discharge of salt into the Murray River.

It is apparent from these figures, that changes to recharge, followed by horizontal hydraulic conductivity and leakance (vcont) caused the greatest response in model output. Increases in recharge caused relatively large increases in the RMS error for heads, indicated by the steep curve in Figure 5.7. Inflow rates into the rivers also increased dramatically (Figure 5.9). For example, a 10-fold increase in recharge caused river gains to increase from 32 ML/d to 119 ML/d. The progressive decrease in ME with recharge increments (Figure 5.8), relates to the increases in modelled heads (relative to observed heads). This effect was most apparent in the shallower layers, particularly in the southwest corner and the northern margin of the model. The recharge effects on the model are not symmetrical, as reductions in recharge caused much smaller changes to simulated heads and flows.

The model was also sensitive to variations in the horizontal hydraulic conductivity of the model layers. Figure 5.8 charts the decrease in modelled heads, relative to observed heads, resulting from increases in hydraulic conductivity. This reflects the concomitant decrease in the hydraulic resistance within the aquifer system. The increased transmission rates through the aquifers is also indicated by increases in the groundwater flow rate to the river (Figure 5.9). In general, the water budget expanded by 83% with a ten-fold increase in horizontal hydraulic conductivity. Evaporative loss at the active salinas as well as groundwater inflow to the rivers increased in magnitude, but export via the deeper GHB cells actually decreased. This is because the horizontal hydraulic conductivity increase would have encouraged horizontal flow at the expense of vertical flow, directing groundwater towards the shallower sinks. In terms of reduction of input arrays, the model was most sensitive to decreases in

horizontal hydraulic conductivity (Figure 5.7). The higher hydraulic resistance caused modelled heads to increase (Figure 5.8) and groundwater inflows to the river to decrease (Figure 5.9).

In general, the response of the model to changes in leakance was not as great as that displayed for horizontal hydraulic conductivity variations. The head variations were more complex, being both negative and positive within the layers. This is because the vertical flow regime differs across the model domain, being mostly downward in the northeast and upwards in the southwest. This is reflected in the erratic nature of the plotting of head statistics for changes in leakance. However, the variation in river gain with changes in leakance is much more consistent (Figure 5.9). Increasing leakance expanded the size of the water budget, due to the increase in groundwater transmission between vertically separated sources and sinks. This amounted to a 50% increase with a ten-fold leakance increase, with seepage to rivers rising from 32 ML/d to 67 ML/d.

The conductance of the GHB cells representing the underlying Lower Cretaceous was also systematically changed. However, the response by the model in terms of head and flow output was relatively small. Heads either increased or decreased, depending on the relative head difference between the deepest model layer and the Kl aquifer. For example, the potential groundwater flow in the northeast is downward, so conductance increases enhanced deep drainage, causing heads to drop in the modelled layers. On the whole, increases in conductance caused modelled heads to decrease (Figure 5.8).

The model was not sensitive to changes in the conductance of the river bed (criv) as defined in the RIVER package. This is indicated by the flat response defined by all three of the indicators used. With greater leakage through the channel bed, river gain should increase with increases in conductance. However, this only amounted to a rise from 31.5 ML/d to 34.5 ML/d with a ten-fold conductance increase.

5.4 Limitations of the Model

The Lower Darling groundwater model is a steady state regional model representing the current set of hydrologic inputs and outputs. Hence, the length of time for the groundwater system to reach equilibrium after being perturbed cannot be inferred. In addition, the 7.5km x 7.5km model cell limits the analysis to the effects of regional scale land and water management strategies.

The plots of the difference between modelled and observed heads for each layer (Figures 5.2-6) are a good indicator of the problem areas in the model. These include the groundwater mound in the shallow aquifers around the Menindee Lakes, the relatively high heads over the Lake Wintlow High in the centre of the model , and underestimates along the model margin. There may be other reasons, apart from unrealistic model input, which could be driving these inconsistencies:

1. The observed heads for 1988 may not be adequately represented, so that the head residuals map errors in the observed heads rather than the modelled heads. The observed head arrays are inferred from water level measurements from scattered boreholes in the model area. Some

of these boreholes are part of a monitoring network which are properly surveyed so that the potentiometry is reliable. However, the majority of the bores are used for stock and domestic supplies, and have not been levelled. Hence, the calculation of aquifer heads can easily have an error margin of ±5m. Also, the spatial distribution of boreholes varies, so that there are parts of the model with little or no groundwater data, requiring significant and error-prone extrapolation. Due to the lack of data, some non-1988 head measurements have been incorporated into the dataset. This situation is particularly prevalent along the basin margins and may explain the tendency for the model to appear to be underestimating heads there.

2. The 1988 observed heads used as calibration are not in equilibrium with the stresses defined in the model. This implies that the groundwater system has not fully equilibrated with hydrological changes in recent history. Apart from changes induced by mallee clearing, which has historically been restricted in the model area, and by irrigation, which tends to produce radical but local effects, the recharge component of rainfall is relatively stable. The largest change has occurred in the interaction between the groundwater system and the rivers, caused by river regulation and the maintenance of large surface water storages. This has encouraged greater leakage from the Darling River, as expressed by the low-salinity aureole in the floodplain and the groundwater mound under the Menindee Lakes. The head residuals indicate a tendency for the model to underestimate heads in the Darling floodplain and overestimate heads marginal to the floodplain, for the shallow aquifers. This is typified by the cluster of high heads on either side of the Darling, consistent in the first three layers. This lends evidence to the proposition that the process of lateral flow of fresher groundwater outwards from the Darling River is currently incomplete.

The Woolpunda Reach is another example of an area where the observed heads used in the model do not reflect the stresses defined in the model. The operation of the Woolpunda North bores is included as a stress condition in the model. Pumping commenced in 1990, but the model uses the head distribution observed in 1988. This explains why the modelled heads are significantly lower (3-12m) to that observed in layer 4 in 1988.

3. The need for the correction of heads to account for the density effects of groundwater salinity. The head in an aquifer varies with salinity and temperature, so that density corrections are needed to accurately determine flow dynamics. For horizontal flow, this requires the calculation of the freshwater head, which is the level of a column of fresh water which would match the existing column of more saline groundwater. For example, the column of groundwater found inside the casing of a borehole is balancing the pressure at the screen. The freshwater head is the higher column of freshwater that would equally balance that pressure. Due to the high salinities found in the Lower Darling area, this correction can become significant. For example, the freshwater heads for piezometers near the Scotia groundwater discharge complex were 0.2-1.0 m higher than the measured water levels (Ferguson et al, 1995). There is also a need to investigate variations in temperature. During drilling of the Pomona observation bores (36784) north of Wentworth, flowing groundwater at 41°C was intercepted in the lower Renmark Group aquifer (Evans, pers comm). Since the model essentially outputs freshwater heads, density corrections would lower these values. This would partly account for the consistent overestimates of head for large parts of the model domain.

5.5 Modelled Flow Regimes

The flow dynamics defined by the groundwater model is depicted in Figures 5.10-13. In these plots the arrows define the direction of groundwater flow with the arrow length a measure of the flux in that cell. The scaling factor used is identical for all of the layers, allowing direct comparison of flow between layers. On this basis, the flow in layer 1 was insufficient to be adequately depicted on a plot. Flow in the Shepparton Formation is invariably vertical, with lateral flow occurring in the coarser Coonambidgal Formation alluvials. This is radially outwards near the Menindee Lakes groundwater mound but follows the southwest gradient for most of the northern half of the layer. Groundwater flow is essentially downstream in the alluvial sediments of the Murray River.

In the vicinity of Menindee Lakes, flow in layer 2 is mostly downward leakage (Figure 5.10). Groundwater flows radially outwards from the margins of the water storage and the nearby Darling River, before being diverted to the southwest by the regional gradient. This occurs to a greater extent in two zones, one on either side of the rivers, as depicted by the larger arrows. These zones correspond to parts of the Pliocene Sands with higher transmissivities (150-200 m^2/d), which are separated by a less transmissive zone (10-50 m^2/d) found under the south-trending Darling River, between Menindee and the Ana Branch junction. Higher transmissivities (300+ m^2/d) in the Parilla Sands also causes the increased flow evident in the southern third of the layer. In this area, the dominant southwest flow system meets a smaller southeast directed flow emanating from the South Australian part of the model. These systems combine and are ultimately directed to the Murray River, mainly the reach from Lake Victoria to Berri.

Similar flow dynamics occur in the upper Renmark Group (Figure 5.11). Again, flow is downwards under Menindee Lakes, with lateral flow occurring outwards from the groundwater mound. This flow is directed to the southwest in two preferred pathways. One is immediately west of the Darling River and corresponds to higher transmissivities (80-120 m^2/d) associated with the channel sequence developed over the Menindee-Tarrara Troughs. The second pathway is via the channel sequence of similar transmissivities developed over the Wentworth Trough, east of the river. Here, the groundwater sourced from the river combines with the general flow from the northern margins of the model. The zone is bordered by less transmissive sediments (<10 m^2/d) where horizontal flow is limited.

Figure 5.10

Predicted steady state flow vectors for model layer 2

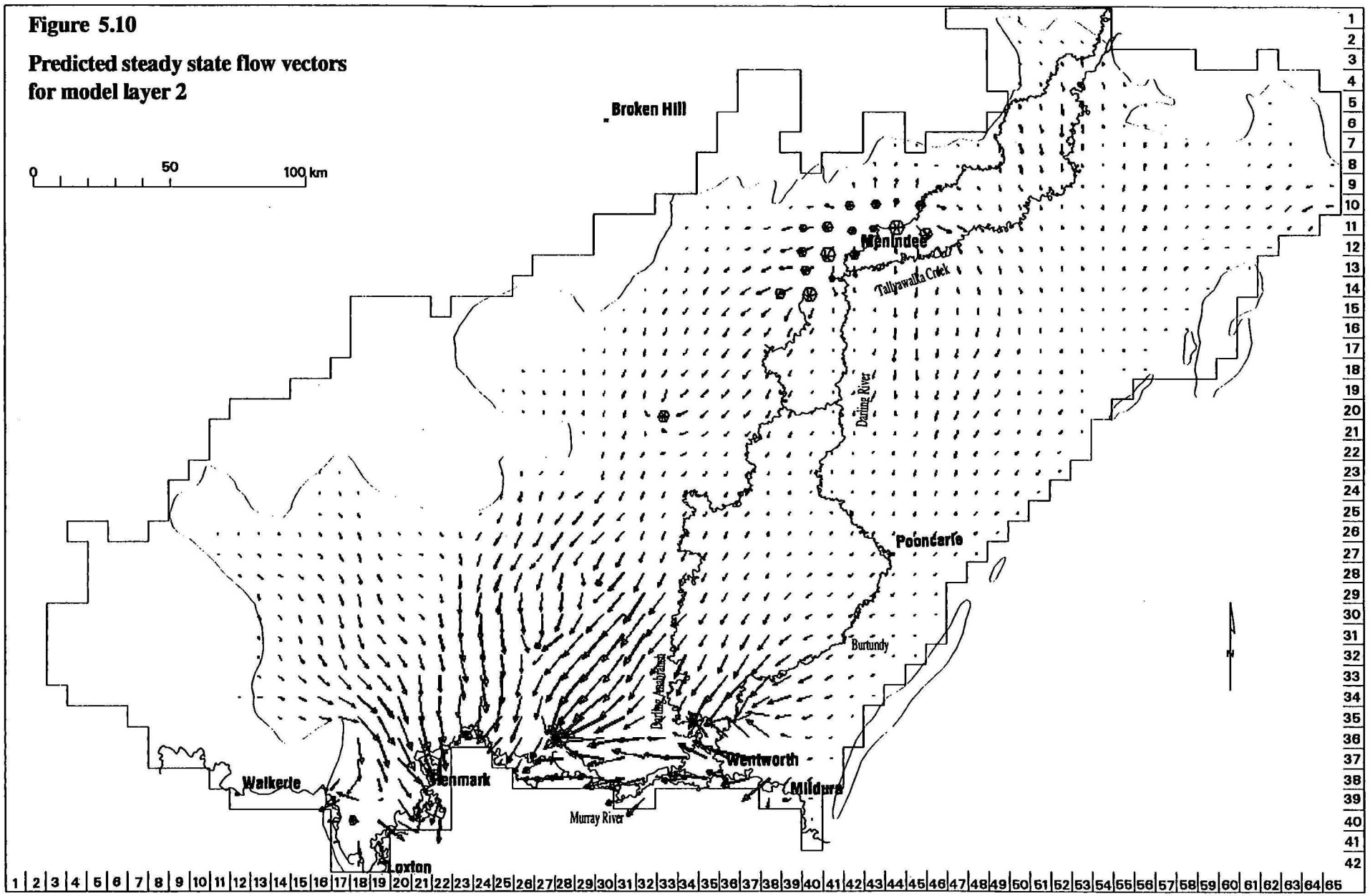

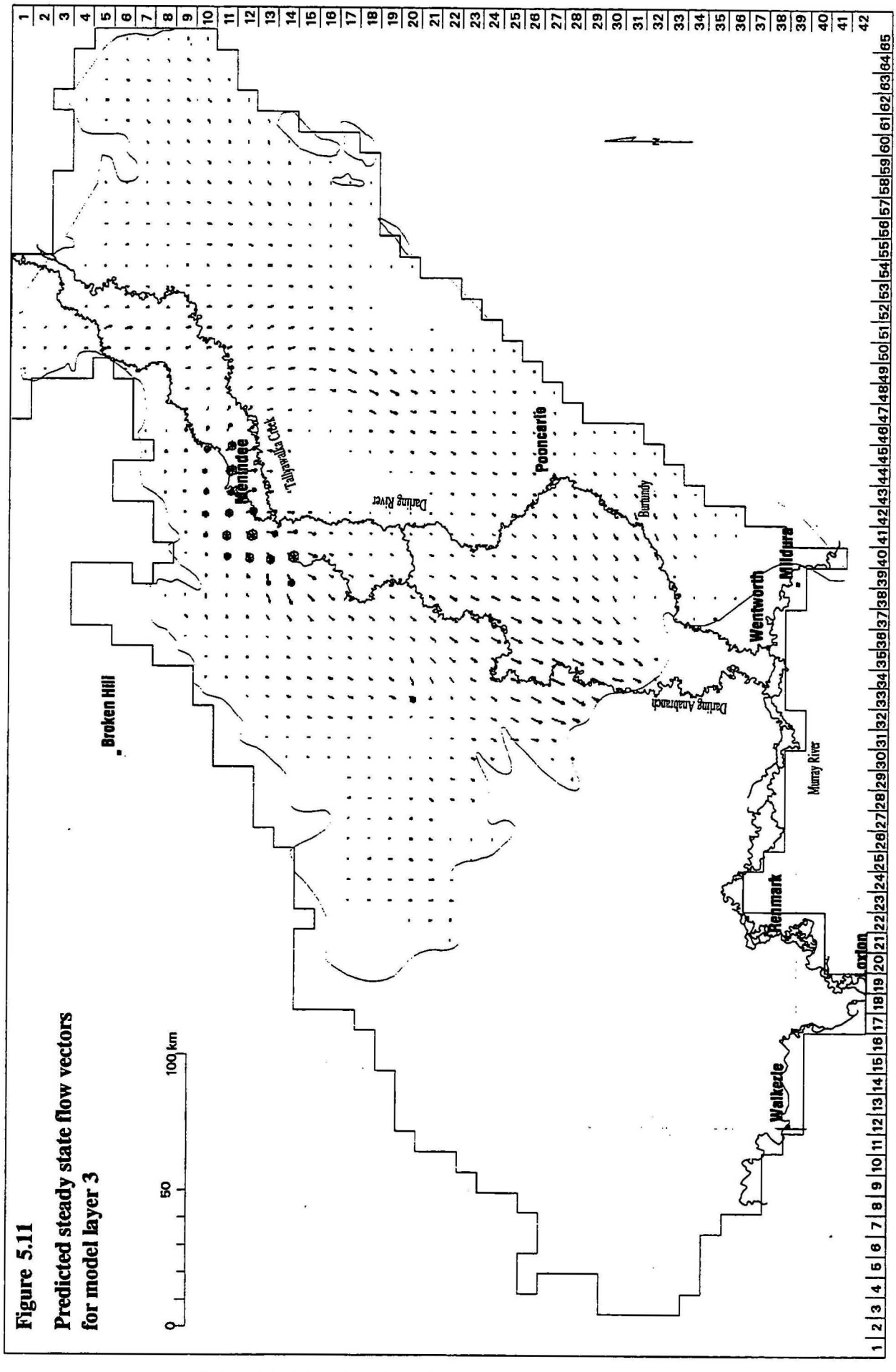

Figure 5.11

Predicted steady state flow vectors for model layer 3

Figure 5.12

Predicted steady state flow vectors for model layer 4

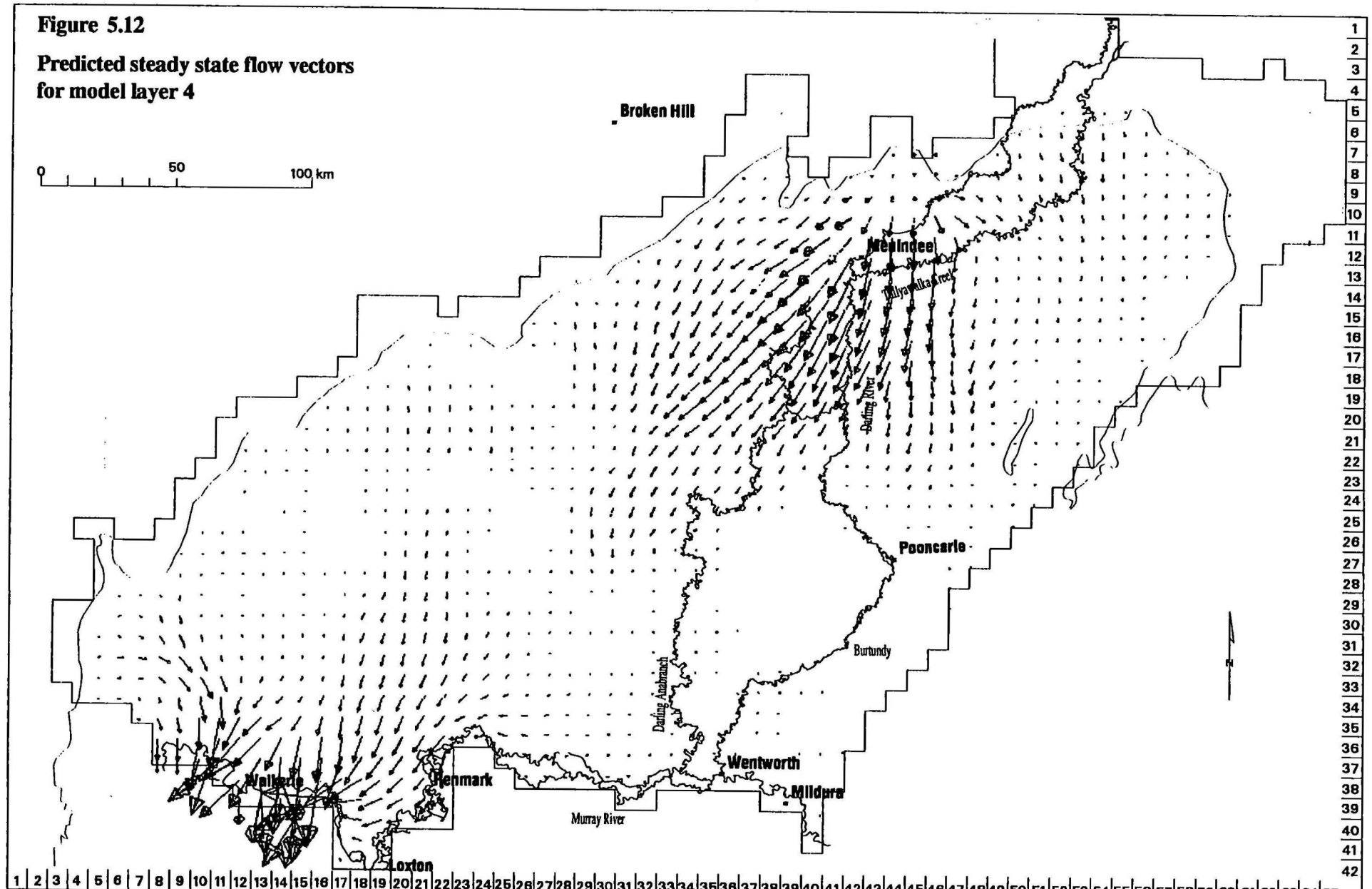

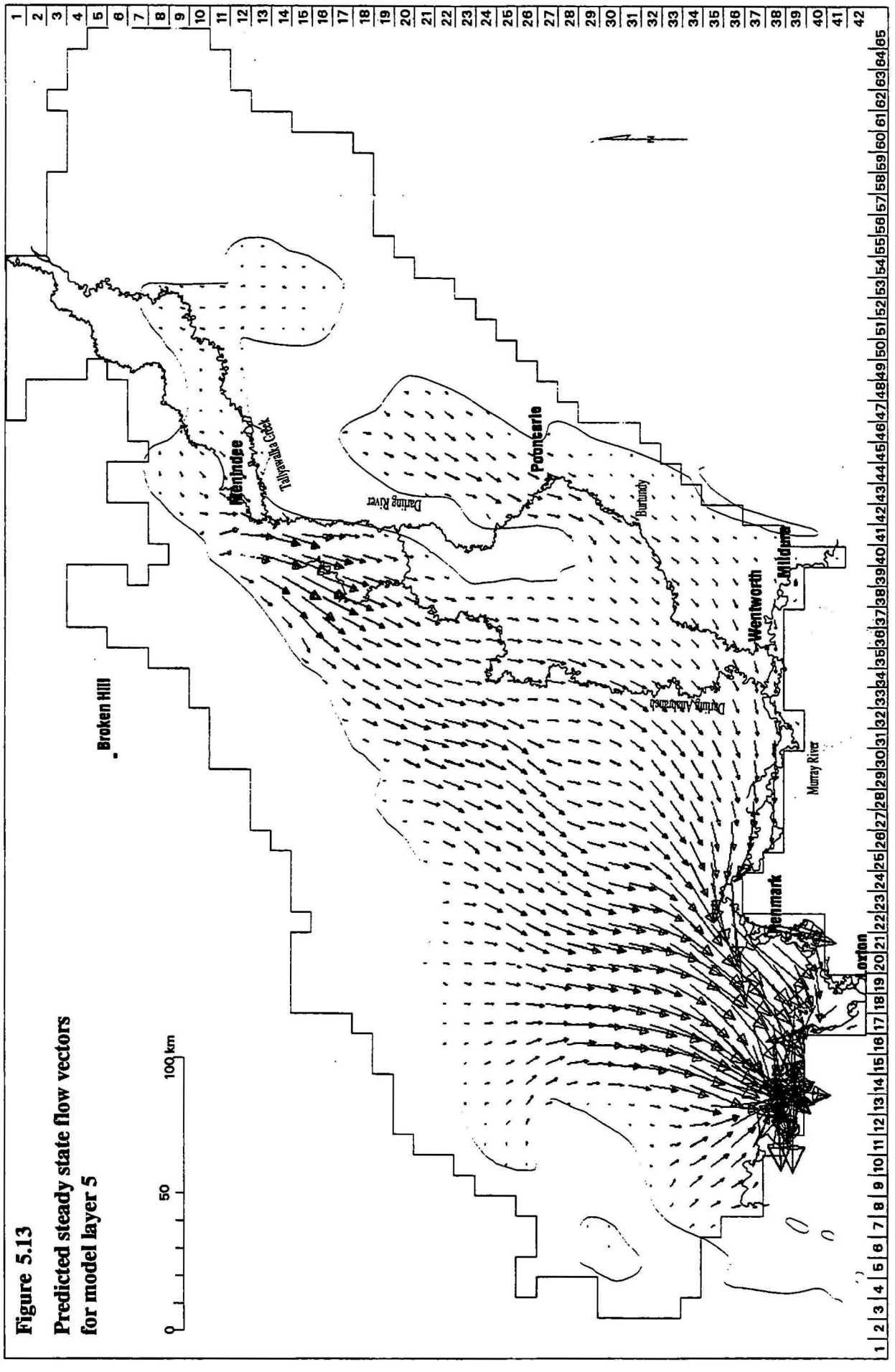

Figure 5.13
Predicted steady state flow vectors for model layer 5

The flow regime in layer 4 mirrors the variation in transmissivity found in the layer (Figure 5.12). To the north, the thick sequence of middle Renmark Group is relatively coarse grained in the palaeochannel sequence found overlying the Menindee and Tarrara troughs. This results in higher transmissivities (> 500 m^2/d) and enhanced horizontal flow evident south of Menindee Lakes. Lower transmissivities (<100 m^2/d) found along the northern margins of the layer is reflected in the smaller flow arrows. The fine grained nature of the marginal marine sequence of Geera Clay and Winnambool Formation (< 20 m^2/d) severely limits groundwater flow in the central part of the layer. It is only with lateral progression to the Murray Group Limestone aquifer (100-200 m^2/d) to the southwest that reasonable groundwater flow is restored. Flow is ultimately directed to the Woolpunda Reach of the Murray River.

The large flow arrows in Figure 5.13 indicates the highly transmissive nature of the lower Renmark Group sediments (>1000 m^2/d). Groundwater follows the southwesterly structural grain, towards the Woolpunda Reach of the Murray River. Here, groundwater either flows upwards into the overlying Murray Group Limestone or continues to flow southwards and out of the model domain.

5.6 Water and Salt Balance

The water and salt balance for the calibrated model is summarised in Table 5.2. In terms of water flux, this results in a surplus of 0.25 ML/d, or 0.35% of the total water input. Although the recharge component of rainfall is very small (0.05%), this amounts to the largest contribution of water (26.2 ML/d) into the groundwater system because of the large model area. Conversely, the irrigation areas cover a small proportion of the model area (<0.5%), but still provide accessions of 12.5 ML/d. According to the model, leakage from the Menindee Lakes storage occurs at a rate of nearly 11 ML/d. This is indicated by the underlying groundwater mound and the impacts on the regional flow system, as displayed in Figures 5.10-13. Leakage from the Lake Victoria storage occurs at a quarter of that rate, or about 2.6 ML/d.

Upwards leakage from the Lower Cretaceous accounts for 9.7 ML/d or 14% of inputs into the Tertiary aquifers. Most of this leakage occurs in the zone of high conductance (30 m^2/d) found in the southwest margin (refer Figure 4.15). This is where both the Lower Cretaceous and lower Renmark Group are relatively thin sequences. Here, gains to the lower Renmark Group cells progressively increase southwards from 0.01-0.02 ML/d to 0.11-0.12 ML/d near Woolpunda. In contrast, the groundwater inflows into the shallow layers from other external sources are relatively small.

Interestingly, the Murray River appears to be losing about the same volume of water to the groundwater system (4.1 ML/d) as the Darling (4.5 ML/d) system. This leakage occurs in only 9 out of 51 of the Murray cells, compared to the majority (102 out of 113) of Darling cells which lose water (Figure 5.14). The difference is largely due to the higher vertical hydraulic conductivity attributed to the river bed sediments. These river losses from the Murray tend to occur at or immediately upstream of the locks where the river stage is relatively high. The river leakage of 0.4 ML/d predicted upstream of Lock 6 at Chowilla is a good example. This loss corresponds to a local flushed zone of low groundwater salinity along the floodplain (Barnett, 1994). Elevated water levels in Frenchmans Creek due to Lock

9 has also resulted in downward leakage of about 0.8 ML/d. However, some of these river losses may be potentially spurious and relate more to the relationship between stresses defined in the model. For example, the losing cell along the Woolpunda Reach is probably due to the proximity of the interception wells. If this river loss is valid, than it implies that the long term implications of the pumping regime operating at Woolpunda is partial capture of flow from the river, at the expense of optimal interception of the regional saline groundwater .

Table 5.2 Water and Salt Balance for Steady State Model

Package	Source	Flow Rate m^3/d	Salt Flux t/d	Package	Sink	Flow Rate m^3/d	Salt Flux t/d
Wells		0	0	Wells	salinas	-12196	0
					Woolpunda N	-9979	-190.0
Recharge	rainfall	26239	0.2	Recharge		0	0
	irrigation	12497	3.3				
River	Darling	3984	1.2	River	Darling	-38	-0.6
	Tallyawalka	267	0.1		Tallyawalka	0	0
	Ana Branch	303	0.1		Ana Branch	-1	-0.0
	Murray	4109	1.0		Murray	-27766	-631.6
GHB	Cretaceous	9747	139.8	GHB	Cretaceous	-20143	-278.1
	Menindee Lakes	10742	4.5		Menindee Lakes	0	0
	Lake Victoria	2634	1.1		Lake Victoria	0	0
	Layer Inflow (1-4)	298	3.2		Layer Outflow (1-4)	-161	-3.0
	Layer 5 inflow	64	1.1		Layer 5 outflow	-700	-10.6
	Murray base flow	362	12.6		Murray base flow	0	0
	Darling base flow	0	0		Darling base flow	-12	-0.0
Total Source		**71246**	**168**	**Total Sink**		**-70996**	**1114**

Although the Darling is a losing stream for most of its length, much of the leakage (94% or 3.7 ML/d) occurs along the reach upstream of Menindee (Figure 5.14). This is understandable as the main weir raises the stage to about 12m above the river bed, backing the river up for many kilometres. Relatively high losses of nearly 0.2 ML/d also occurs along Tallyawalka Creek upstream of its confluence with the Darling. Both of these reaches have corresponding freshening of the groundwater in the alluvial aquifer with salinities around 600-700 mg/L. In comparison, the rest of the Darling cells, in particular along the Anabranch, have low losses to the shallow aquifer (<0 .01 ML/d). This is expressed by higher groundwater salinities found in the floodplain aquifer, ranging from 1500 to 4000 mg/L.

As expected, the Murray River is the major sink for groundwater in the region, with seepages totalling 28 ML/d. The highest rates of inflow of about 1-2 ML/d occur in cells peripheral to the irrigation areas, particularly Berri, Renmark and Mildura (Figure 5.14). In the steady state model, groundwater seepage from the north is limited to about 1.2 ML/d along the Woolpunda Reach. This is due to the impact of the Woolpunda North interception bores which are pumping out 10ML/d under current operating conditions. The groundwater inflows into the Darling system are insignificant, totalling about 0.04 ML/d along the lowermost reach near Burtundy.

Figure 5.14

Predicted steady state flow (m^3/d) between river system and shallow aquifer

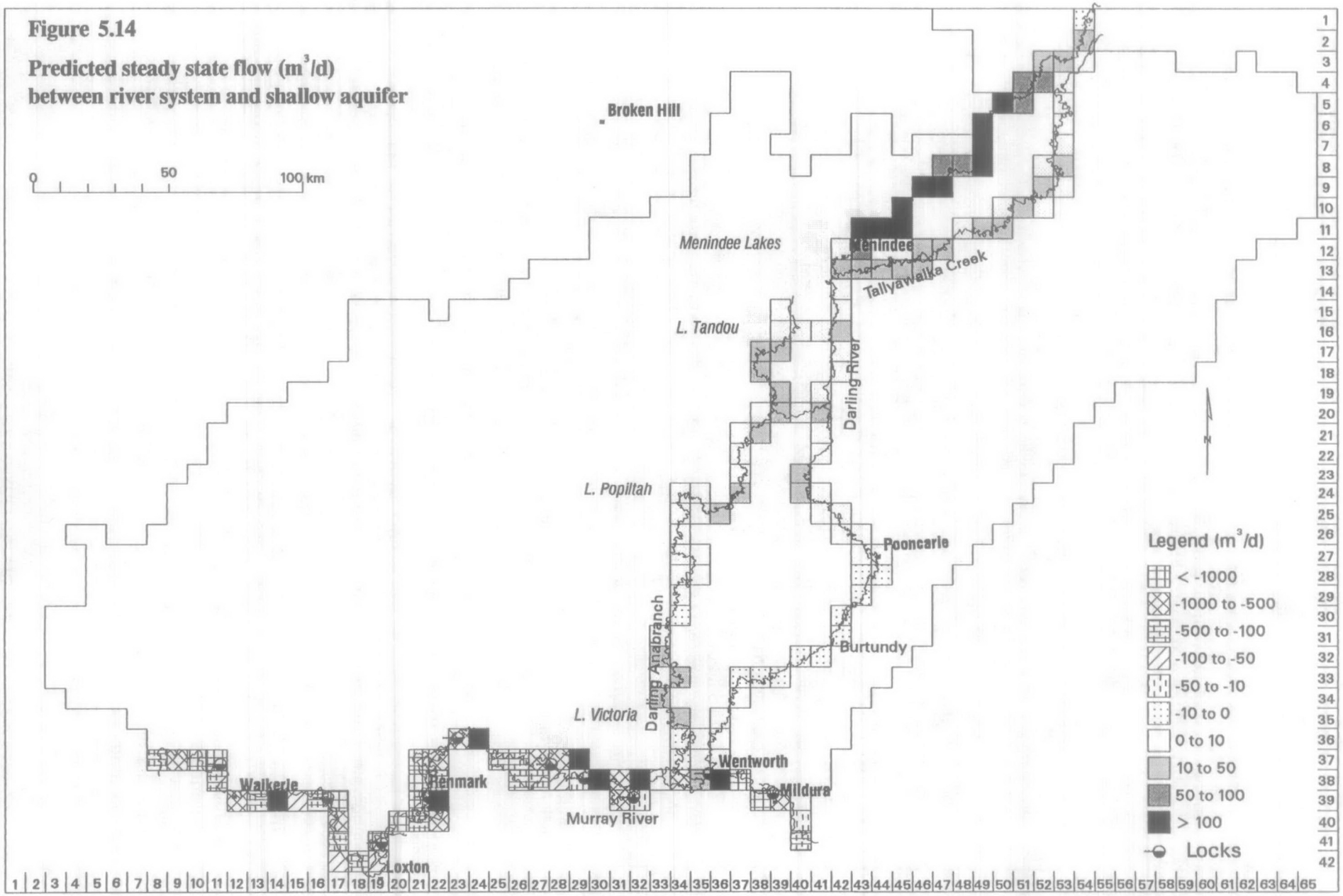

Figure 5.15

Predicted steady state salt flux (t/d) between river system and shallow aquifer

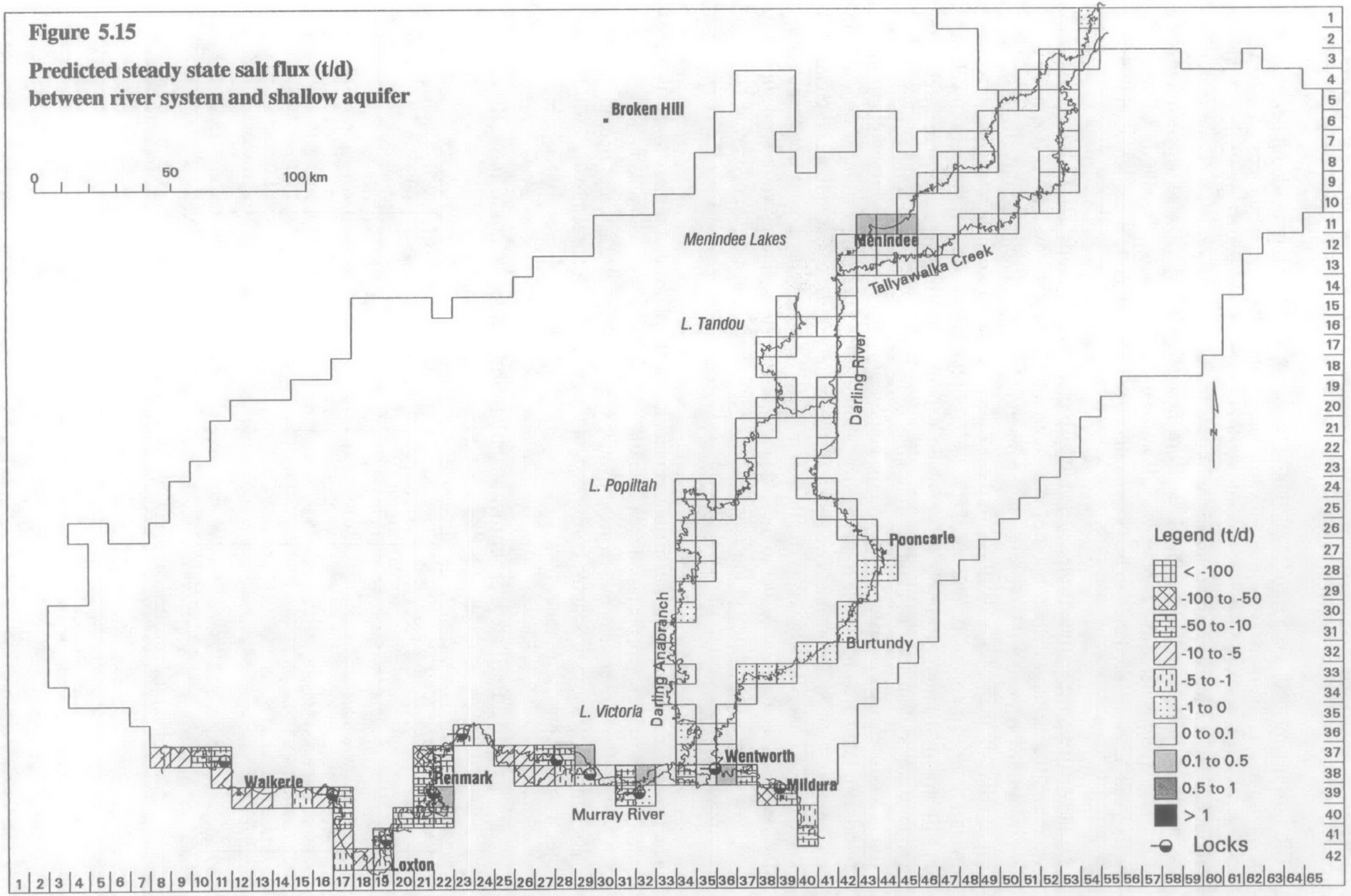

The Lower Cretaceous is a significant sink for groundwater from the Tertiary aquifers in the northern half of the model where downward leakage prevails. Over a quarter of the 20 ML/d lost to the Cretaceous occurs in close vicinity of the Menindee Lakes (Figure 5.15). Likewise, about 80% of the leakage is accounted for by loss from the lower Renmark Group in the Menindee and Wentworth Troughs. Loss from the model (0.7 ML/d) also occurs in the lower Renmark Group where flow continues southwards under Woolpunda Reach. In addition, the active salt lakes are predicted to be evaporating over 12 ML/d out of the shallow aquifer.

A salt balance for the groundwater system is also presented in Table 5.2. Although recharge via rainfall is the largest contributor of water into the groundwater system, it is a minor contributor of salt at 0.2 t/d. This is due the inherent low salt content of rainfall, set at 6.2 mg/L (Blackburn & McLeod, 1983) for these calculations. The enhanced recharge in the irrigation areas involves increments of river water of typical salinities ranging from 230 mg/L at Mildura to 310 mg/L at Berri. This explains why irrigation recharge contributes salt to the groundwater system at a rate about 16 times that of rainfall. Downward leakage from the rivers produces a salt transfer to the shallow aquifer of about 2.4 t/d. Salt transfers from the floodplain lakes are higher due to the higher salinities found in shallow storages operating in high evaporation environments. For instance, the salinity in Lake Cawndilla is typically 600 mg/L and in Lake Victoria it is typically 400 mg/L. The underlying Lower Cretaceous is by far the largest contributor of salt to the Tertiary aquifer system. The upwards seepage of 140 t/d assumes that the salinity of the Lower Cretaceous matches that of the overlying Tertiary aquifer.

The Lower Cretaceous gains salt at about twice the rate (278 t/d) that it loses to the Tertiary aquifers. However, this is less than half of the 632 tonnes of salt which is predicted to reach the Murray River every day due to groundwater seepage. This rate assumes operation of the Woolpunda Interception Scheme bores north of the river, which are removing 190t/d out of the Murray Group Limestone.

Table 5.3 Predicted groundwater inflow and salt loads into Murray River

Reach of Murray River	Predicted Flux *(ML/d)*	Predicted Salt Loads *t/d*	Published Salt Loads* *t/d*	River Modelling Salt Loads# *t/d*
Merbein-Red Cliffs	-4.0	-84	-44	-145
Mildura - Wentworth	-0.8	-19		-69
Wentworth - Lock 9	+0.8	-19		-10
Lock 9 - Lindsay Mouth	-3.3	-92		-180
Lock 6 - Lock 5	-4.6	-98	-200	-150
Lock 5 - Lock 4	-4.3	-140	-213	-160
Lock 4 - Lock 3	-2.2	-67	-193	-210
Lock 3 - Lock 2	-3.2	-65	-381	-270
Lock 2 - Lock 1	-2.1	-35	-25	0

* Refer Table 3.2

\# Salt inflows used to calibrate Murray River Salinity Model (Close, pers comm)

Table 5.3 compares the groundwater inflow and salt flows predicted by the model for various reaches of the Murray River with data from other sources. These sources include various publications and reports such as Smith & Watkins (1993) and Dudding *et al* (1989) as well as the model input for river salinity modelling (Close, pers comm). The salt loads inferred by other work tend to be higher than the model predictions as groundwater inflow from both sides of the river is considered in the former, while the latter only considers the groundwater regime north of the river. This explains why salt loads predicted by the groundwater model for many of the reaches are 30-70% of values used in salinity modelling of the river. The predicted salt loads (140 t/d) for the reach between Lock 5 and Lock 4 is comparable to the river salinity model input (160 t/d) as the dominant accessions due to the Renmark and Berri Irrigation Areas are included in the Lower Darling model. In contrast, the predicted salt loads for between Lock 3 and Lock 2 (65 t/d) are only about a quarter of the values used in the river salinity model (270 t/d). This is because the model is predicting the steady state outcome of pumping from the Woolpunda North bores, which significantly lowers the salt load along the Woolpunda Reach. When these bores are removed from the simulation, the predicted salt loads are comparable to the previous estimates.

6. MODEL APPLICATIONS

The Lower Darling model has been used to predict the likely changes to the groundwater system due to specific land and water management strategies in the region. This involved changing the stresses defined within the calibrated steady state model to those representing the particular management scenario.

6.1 Decommissioning of Woolpunda Interception Scheme.

Under current operating conditions, the bores of the Woolpunda Interception Scheme along the northern bank of the Murray remove 10 ML/d of saline groundwater from the Murray Group Limestone. To investigate how this pumping effects the groundwater system, the model was run without these bores being represented by the WELL package.

The removal of these bores had limited effect on the simulated heads of the shallow aquifers (layers 1 to 3) with only scattered increases of 0.1m evident over the central third of the model. This is because these layers are unsaturated in the general vicinity of Woolpunda. The largest change occurred in layer 4 as the bores are drawing from this aquifer. The head increase was 6-12 m in the cells close to the Woolpunda Reach, decreasing to 1-5m in an annulus extending from Waikerie to Renmark (Figure 6.1). Over the southern third of the layer, the head increase was in the order of 0.1-1m. The rise in heads in the underlying layer 5 was more subdued, ranging from 0.3-0.6m near Woolpunda, down to 0.2-0.1m in the surrounding southern half of the layer. The response in heads would be exaggerated as the model is steady state and does not account for aquifer storage.

Table 6.1 Water and Salt Balance for 'No Woolpunda North' scenario

Package	Source	Flow Rate m^3/d	Salt Flux t/d	Package	Sink	Flow Rate m^3/d	Salt Flux t/d
Wells		0	0	Wells	salinas	-12196	0
					Woolpunda N	0	0
Recharge	rainfall	26239	0.2	Recharge		0	0
	irrigation	12497	3.3				
River	Darling	3983	0.6	River	Darling	-38	-0.6
	Tallyawalka	267	0.1		Tallyawalka	0	0
	Ana Branch	302	0.1		Ana Branch	0	0
	Murray	3966	0.9		Murray	-35354	-765.0
GHB	Cretaceous	8202	117.7	GHB	Cretaceous	-20249	-281.0
	Menindee Lakes	10855	4.5		Menindee Lakes	0	0
	Lake Victoria	2633	1.1		Lake Victoria	0	0
	Layer Inflow (1-4)	298	3.2		Layer Outflow (1-4)	-161	-3.0
	Layer 5 inflow	0	0		Layer 5 outflow	-1342	-21.1
	Murray baseflow	362	12.6		Murray baseflow	0	0
	Darling baseflow	0	0		Darling baseflow	-12	-0.0
Total Source		**69604**	**144**	**Total Sink**		**-69353**	**1071**

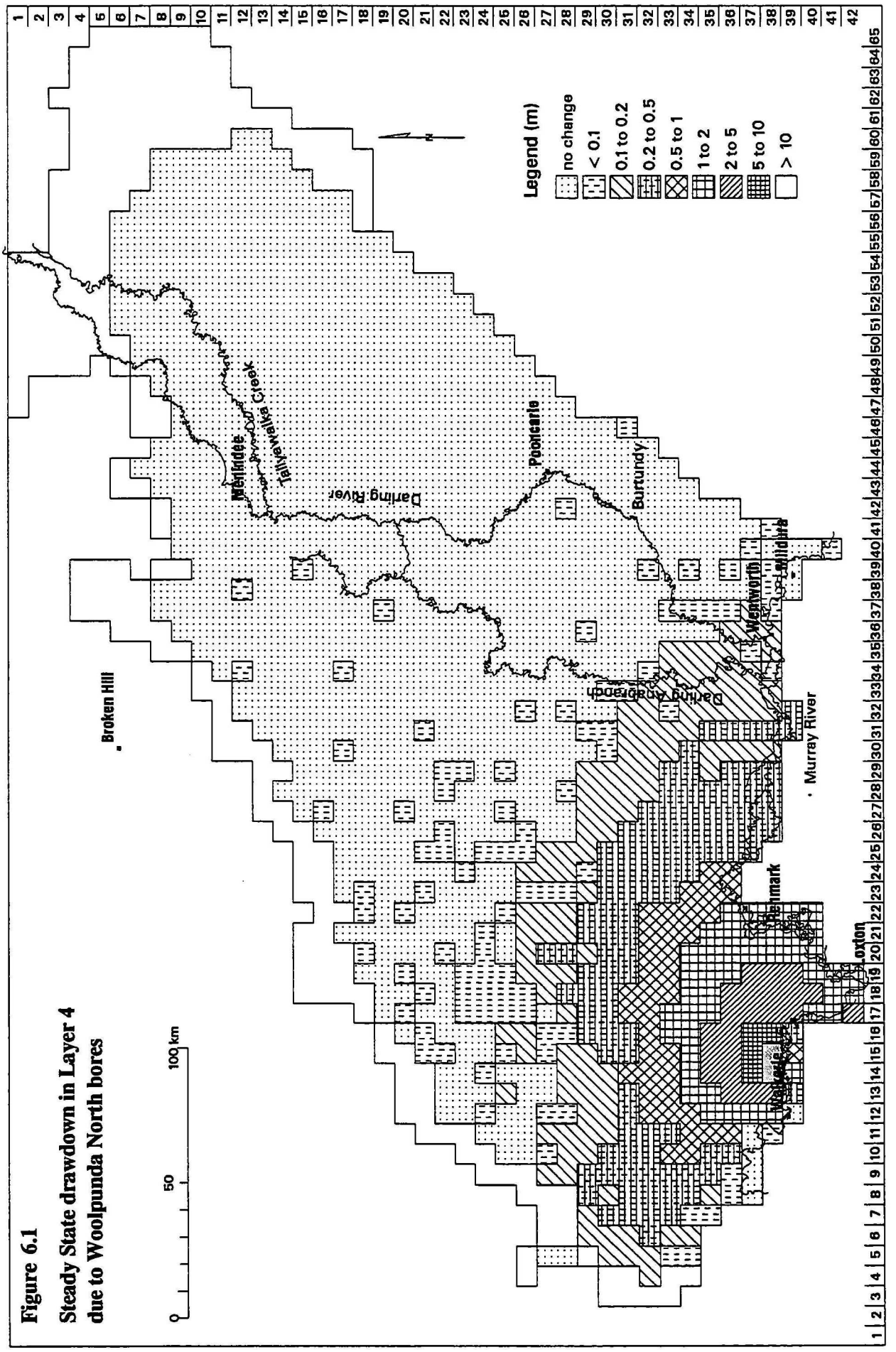

Figure 6.1
Steady State drawdown in Layer 4 due to Woolpunda North bores

The water budget for this simulation is presented in Table 6.1. The major consequence of cessation of pumping is a significant increase in salt loads to the Murray River from 632 t/d to 765 t/d, equating to a 32 EC increase in salinity of the Murray River at Morgan (Sharma, pers comm). This is due to increased groundwater inflows along the Woolpunda Reach, altering salt loads from 22 t/d to 145 t/d. This latter figure is comparable to previous estimates of salt loads along this reach (270-380 t/d, refer Table 5.3) considering that only inflows from north of the river are being simulated by the Lower Darling model. The rest of the Murray River experienced negligible changes to salt input via groundwater seepage (Table 6.2).

The southward through flow of groundwater out of the model area in the lower Renmark Group aquifer of layer 5 has also increased substantially from 0.7 ML/d to 1.3 ML/d. This has caused the salt export via lateral flow in layer 5 to be effectively doubled from 10.6 t/d to 21.1 t/d. This change is a consequence of the upward leakage from the basal aquifer being reduced with the cessation of pumping from the overlying Murray Group Limestone.

Table 6.2 Predicted salt loads into Murray River for model scenarios

Reach of Murray River	Calibrated Salt Loads *t/d*	Without Woolpunda *t/d*	All Mallee Cleared *t/d*	All Mallee Cleared (1%) *t/d*	Without L. Victoria *(t/d)*	Without Menindee L. *(t/d)*
Merbein-Red Cliffs	-84	-84	-92	-98	-84	-84
Mildura - Wentworth	-19	-19	-26	-31	-19	-19
Wentworth - Lock 9	-19	-19	-47	-62	-19	-19
Lock 9 - Lindsay Mouth	-92	-92	-135	-150	-86	-91
Lock 6 - Lock 5	-97	-98	-151	-264	-99	-97
Lock 5 - Lock 4	-140	-140	-151	-94	-140	-140
Lock 4 - Lock 3	-67	-67	-81	-25	-67	-67
Lock 3 - Lock 2	-65	-196	-84	-247	-64	-64
Lock 2 - Lock 1	-35	-36	-37	-51	-35	-35

6.2 Clearing of all Mallee Vegetation for Grazing

The effects on the groundwater system due to clearing of native vegetation for pastoral purposes in the Lower Darling region was investigated as a model scenario. This involved clearing all of the land system units containing dense stands of mallee, belah-rosewood, black box or cypress pine. These units are concentrated in two areas, namely the mallee with peripheral belah-rosewood assemblages north of the Murray in South Australia and the extreme west of New South Wales as well as between the Darling River and Willandra Lakes (Figure 1.11). There is also a smaller area of remnant mallee east of the Tallyawalka near Wilcannia. By adding a clearing component to the recharge algorithm (refer Figure 4.38), recharge in the designated areas of clearing was calculated on the basis of the nominal sand content of the land system rather than a percentage of rainfall established for undisturbed mallee (0.05%). Upon clearing of the remnant mallee vegetation, recharge increased from about 0.1mm/yr to 0.5-1.3 mm/yr, or 0.25-0.5% of rainfall, in the relevant model cells. This effectively increased the rate of rainfall accessions from 26 ML/d to 66 ML/d over the model area (Table 6.3). These increases in recharge rates may well be a conservative estimate, as

recharge through sandy soils has been measured at 5 to 15% of rainfall in cleared mallee south of the model (Cook *et al*, 1996).

All model layers experienced general increases in heads. The most significant rises in layer 1 were along the lower reaches of the Darling (5-8m) and in the regional discharge zone north of Lake Victoria (7-11m). Head increases of 2-4m were typical in the northern half of the layer, the exceptions being near Menindee and the northeast margin where the head increase was less than 1m. The heads in cells along the Murray River remained unchanged from the calibrated model.

A similar pattern was apparent for layer 2 where the southeast margin towards the lower reaches of the Darling (5-10m) and the southwest margin (7-20+m) experienced the greatest increase in water levels (Figure 6.2). These areas correspond to the areas of enhanced recharge as a consequence of clearing. Desaturation of cells also occurred in the southwest corner due to model instability over the Woolpunda Ridge. Away from these areas, there is a general trend in head increase from 1-2m in the north to 2-5m in the south. Around the Menindee Lakes and the northeast corner, the water level rise was less than 1m.

Layer 3 and 4 also had very similar head responses to mallee clearing. In layer 4, head rises were of 5-9m along the southeast margin and 8-20+m in the southwest corner. The majority of the layer experienced head increases of around 1-5m. The largest head increases (6-12m) in layer 5 occurred in the outlier found in the southwest corner of the model. Heads in the bulk of the basal layer only increased by 1-2m.

The grids of simulated heads were subtracted from the grid representing the topographic surface to derive depth to water levels. Areas with a high risk of land salinisation were highlighted where the watertable in the shallow aquifer was within 5m of the land surface (Figure 6.3). Salinas are likely to be reactivated or expand in these areas. These problem areas include;

- the floodplain of the lower reach of the Darling River,
- the central reach of the Ana Branch around Lake Popiltah,
- the regional discharge zone north of Lake Victoria, particularly along the northern margin such as the Scotia and Huntingfield complexes and
- the Chowilla floodplain (Figure 6.3).

Figure 6.3 also shows a wedge of artesian conditions in the southwest margin. This occurs in the Parilla Sands and relates to model instability caused by cells drying up over the Woolpunda Ridge and should be discounted.

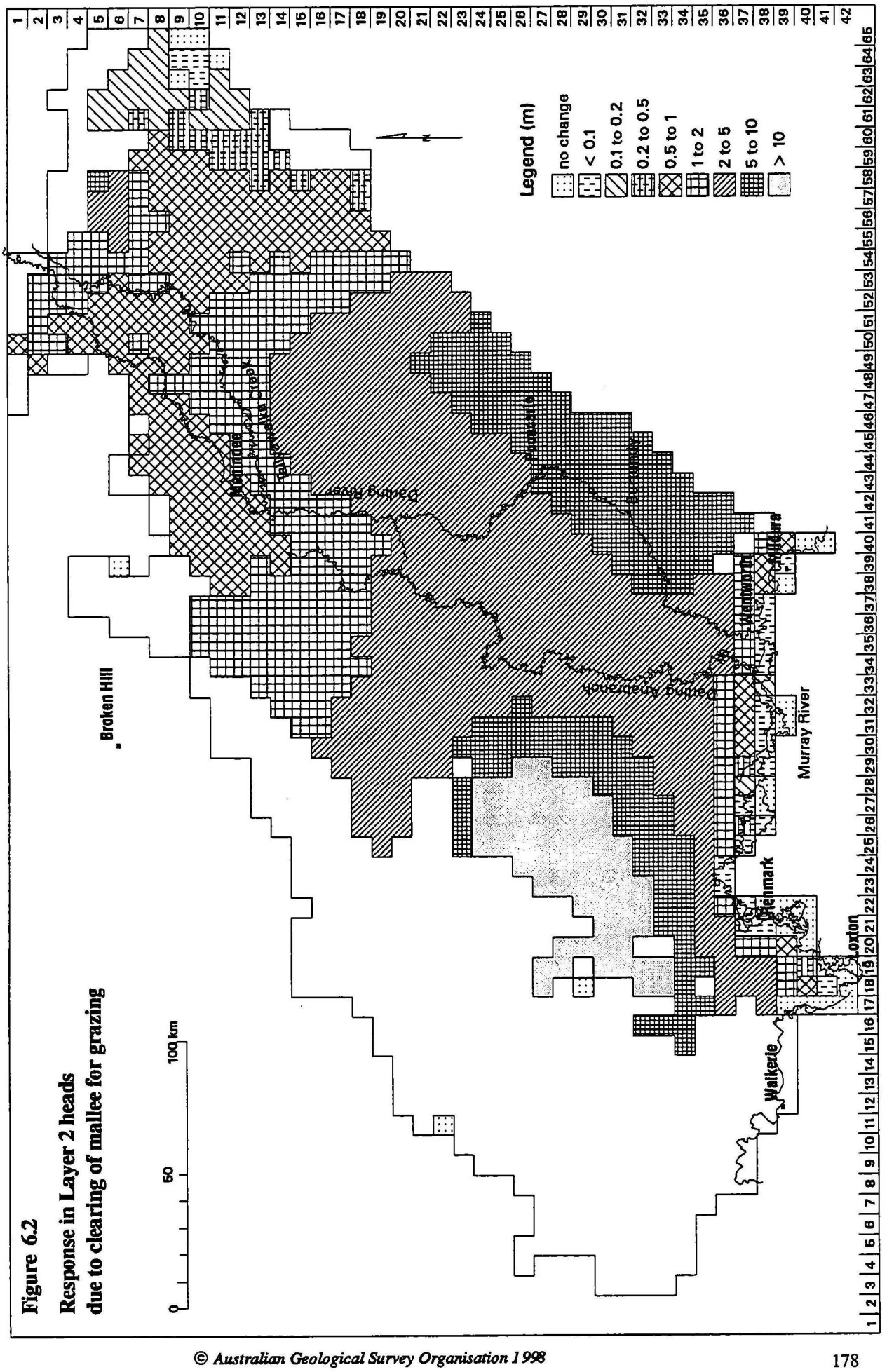

Figure 6.2
Response in Layer 2 heads due to clearing of mallee for grazing

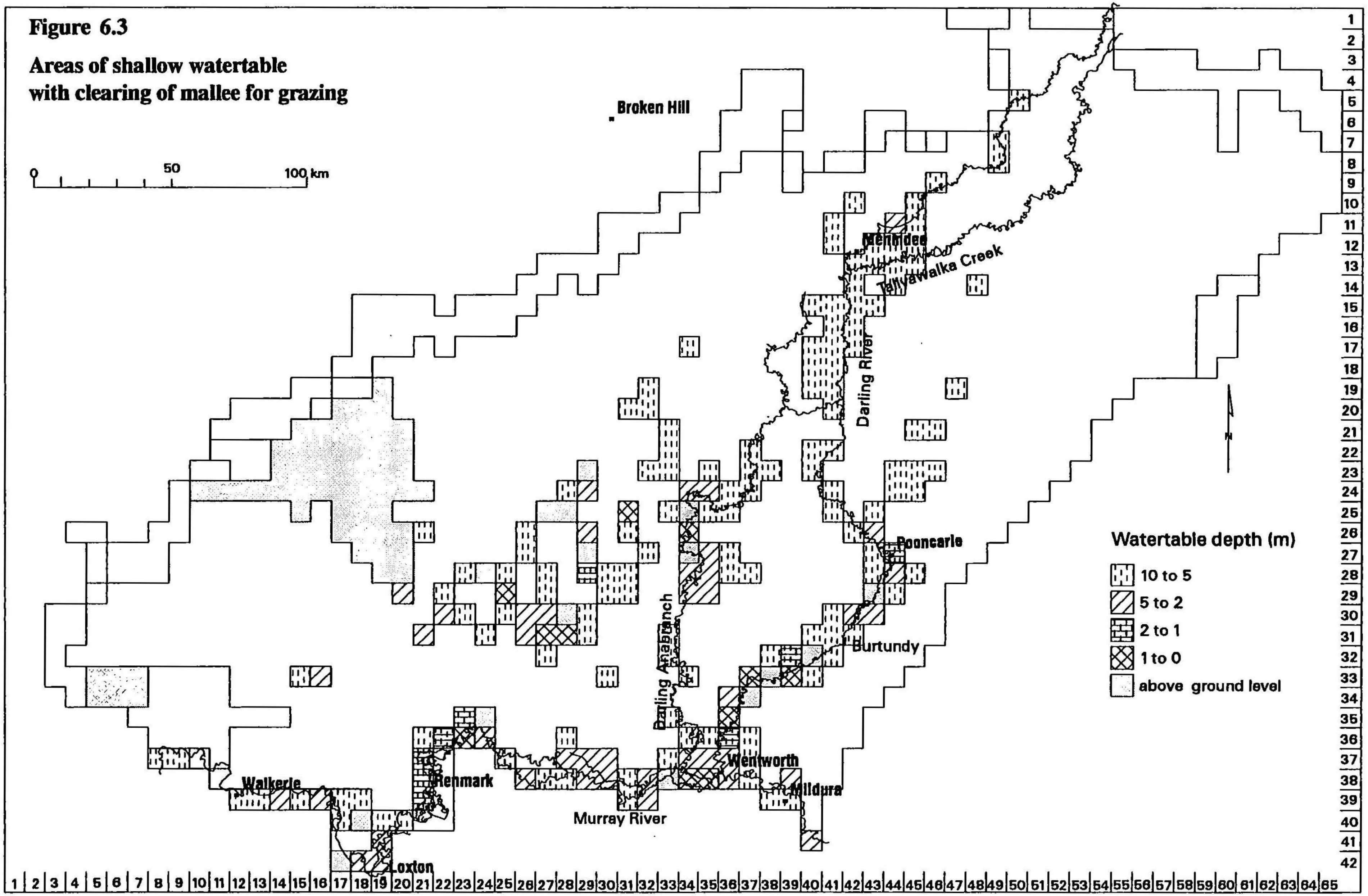

Figure 6.3

Areas of shallow watertable with clearing of mallee for grazing

The water and salt balance representing equilibrium conditions after clearing of all mallee vegetation for pasture is presented in Table 6.3. The most significant consequence of mallee clearing is the increased salt loads into the Murray, from a baseline of 632 t/d to 821 t/d. This increase of groundwater inflows is distributed along the length of the Murray River from Mildura to Morgan, with the central reach between Lock 9 and Lock 5 experiencing the greatest change (Table 6.2). It should be noted that these figures are derived from a simulation where the anticipated increase in recharge has been conservatively estimated and that the Woolpunda Scheme is assumed to be fully operational. The salinity of the Murray River at Morgan is expected to increase by 35 EC (Sharma, pers comm)

Table 6.3 Water and Salt Balance for 'Clearing all Mallee' scenario

Package	Source	Flow Rate m^3/d	Salt Flux t/d	Package	Sink	Flow Rate m^3/d	Salt Flux t/d
Wells		0	0	Wells	salinas	-10449	0
					Woolpunda N	-9979	-190
Recharge	rainfall	65760	0.4	Recharge		0	0
	irrigation	12497	3.3				
River	Darling	3603	1.0	River	Darling	-206	-2.7
	Tallyawalka	254	0.1		Tallyawalka	0	0
	Ana Branch	143	0.1		Ana Branch	-77	-0.9
	Murray	2407	0.5		Murray	-36940	-821.4
GHB	Cretaceous	4569	70.7	GHB	Cretaceous	-39449	-540.2
	Menindee Lakes	9624	4.0		Menindee Lakes	0	0
	Lake Victoria	1888	0.8		Lake Victoria	-22	-0.7
	Layer Inflow (1-4)	251	2.5		Layer Outflow (1-4)	-199	-3.7
	Layer 5 inflow	0	0		Layer 5 outflow	-1420	-22.1
	Murray baseflow	362	12.6		Murray baseflow	0	0
	Darling baseflow	0	0		Darling baseflow	-17	-0.0
Total Source		**101358**	**96**	**Total Sink**		**-98758**	**-1582**

Enhanced discharge of saline groundwater also occurs in the other streams in the model area. The increase in salt loads from 0.6 t/d to 2.7 t/d, coupled with the expansion of shallow watertables in the floodplain, makes the lower reach of the Darling River downstream of Burtundy at particular risk of degradation. Upon clearing of the mallee, part of the Darling Ana Branch switched from a losing stream to gaining groundwater with a salt load of 0.9 t/d. This would have dire consequences for the quality of the water stored in the series of small dams within the channel, which rely on a single annual replenishment from Lake Cawndilla. The water balance also suggests that groundwater seepage may develop along the margins of Lake Victoria, amounting to a salt influx of 0.7 t/d into the water storage.

The increased input of water into the groundwater system is also accommodated by downward leakage into the Lower Cretaceous almost doubling from 20 ML/d to 39 ML/d. The lateral flow in layer 5 out of the model also doubled from 0.7 ML/d to 1.4 ML/d.

An additional scenario was run where recharge after clearing was set at 1% of rainfall (2.2 - 2.6 mm/yr). This is the rate used in the neighbouring Lachlan Fan Model to simulate clearing

for grazing of similar mallee terrane (Kellett, 1997). This increased the total recharge rate by nearly 100 ML/d (Table 6.4) when compared with the previous clearing scenario. This significantly increased the rise in heads and the salt flux into the river. In the shallow aquifers (layers 1 to 3), the maximum head increases of 10-20+m occurred in a broad central band across the model. More subdued rises of 2-5m occurred in the northern third with heads remaining relatively unchanged along the Murray River. In layer 4, the resulting head rise was small in the north (2-5m), medium in the model centre (5-10m) and high in the south (10-30+m). More subdued increases in head occurred in layer 5, with 2-4m typical of the northern margin and near Woolpunda and 4-8m typical of the remainder. Land degradation is likely to be expanded in the areas defined by the previous scenario. In addition, the depressions in the sand plain north of the river at Waikerie are also at risk of salinisation.

Table 6.4 Water and Salt Balance for 'Clearing all Mallee with 1% of rainfall' scenario

Package	Source	Flow Rate m^3/d	Salt Flux t/d	Package	Sink	Flow Rate m^3/d	Salt Flux t/d
Wells		0	0	Wells	salinas	-12129	0
					Woolpunda N	-9979	-190
Recharge	rainfall	164233	1.0	Recharge		0	0
	irrigation	12497	3.3				
River	Darling	3034	0.9	River	Darling	-508	-5.7
	Tallyawalka	217	0.1		Tallyawalka	0	0
	Ana Branch	57	0.0		Ana Branch	-405	-5.2
	Murray	1711	0.4		Murray	-49284	-1046.8
GHB	Cretaceous	851	12.6	GHB	Cretaceous	-105656	-1383.0
	Menindee Lakes	7560	3.1		Menindee Lakes	0	0
	Lake Victoria	1276	0.5		Lake Victoria	-250	-8.4
	Layer Inflow (1-4)	162	1.2		Layer Outflow (1-4)	-379	-6.5
	Layer 5 inflow	0	0		Layer 5 outflow	-5545	-88.7
	Murray baseflow	361	12.6		Murray baseflow	0	0
	Darling baseflow	0	0		Darling baseflow	-30	-0.1
Total Source		**191959**	**36**	**Total Sink**		**-185875**	**-2734**

By assuming that recharge after clearing amounts to 1% of rainfall, the salt loads into the Murray increased by 416 t/d from base line steady state conditions (Table 6.4). This would result in an 80 EC increase in the salinity of the Murray River at Morgan. Under current conditions the Darling River is a losing stream for most of its length. However, with enhanced recharge, the river gains groundwater downstream of the Ana Branch off take, amounting to a salt load of 5.7 t/d. Likewise, the salt load due to groundwater inflow into the Ana Branch increased to 5.2 t/d, and into Lake Victoria increased to 8.4 t/d. This has serious repercussions in terms of environmental degradation and the effectiveness of maintaining long term storages of surface water.

6.3 Decommissioning of Lake Victoria storage

Artificially high levels in Lake Victoria and Frenchmans Creek has produced a groundwater mound which is causing salinisation problems in the surrounding landscape. By removing the GHB cells which represent the interaction between Lake Victoria and the shallow aquifer, the effect of decommissioning the water storage could be investigated.

The result of the simulation was a drop in head in the shallow layer 1 aquifer by 1-2m underneath the lake. The response by the Pliocene Sands aquifer was more difficult to reconcile, being a general 0.2-0.5 m rise in heads in the southwest corner of the model. The heads in the deeper layers experienced negligible change with the removal of Lake Victoria cells. The overall salt load into the Murray only decreased marginally, with the principal change occurring downstream of Lock 9 from 92 t/d to 86 t/d (Table 6.2).

This scenario highlights the issue of scale, with the model having insufficient resolution to simulate the effects of Lake Victoria. The storage is located close to the Murray River where a localised groundwater system involving lateral flow with a short path from lake to river occurs. In this case, it would be more appropriate to use the Lower Darling Model to help define the boundary conditions for a finer scale model.

Table 6.5 Water and Salt Balance for 'Without Lake Victoria' scenario

Package	Source	Flow Rate m^3/d	Salt Flux t/d	Package	Sink	Flow Rate m^3/d	Salt Flux t/d
Wells		0	0	Wells	salinas	-10005	0
					Woolpunda N	-9979	-190
Recharge	rainfall	26239	0.1	Recharge		0	0
	irrigation	12497	3.3				
River	Darling	3983	1.2	River	Darling	-38	-0.6
	Tallyawalka	267	0.1		Tallyawalka	0	0
	Ana Branch	302	0.1		Ana Branch	-1	-0.0
	Murray	4039	0.9		Murray	-27592	-628.0
GHB	Cretaceous	9951	143.4	GHB	Cretaceous	-20126	-279.5
	Menindee Lakes	10859	4.5		Menindee Lakes	0	0
	Lake Victoria	0	0		Lake Victoria	0	0
	Layer Inflow (1-4)	298	3.2		Layer Outflow (1-4)	-161	-3.0
	Layer 5 inflow	68	1.1		Layer 5 outflow	-691	-10.4
	Murray baseflow	362	12.6		Murray baseflow	0	0
	Darling baseflow	0	0		Darling baseflow	-12	-0.0
Total Source		**68865**	**171**	**Total Sink**		**-68605**	**-1112**

6.4 Decommissioning of Menindee Lakes storage

Downward leakage from the Menindee Lakes is a significant contributor to the underlying aquifers, as indicated by the watertable mound and the dilution of the groundwater. A scenario investigating the discontinuation of using the lakes as surface water storages was compiled by removing the GHB cells representing the lake-groundwater interaction. The increase in stage in river cells upstream of the main weir was also removed from the RIVER package input.

The overall result was a general decrease in heads in the model layers. This head decrease was most significant (7-11m) in the shallow layer 1 aquifer within 20 km of the storage lakes (Figure 6.4). This head reduction decreases radially outwards from the lake, being more like 1m about 90-100 km away. A further 100km to the south, the head decrease was only 0.1m.

The same radial pattern centred on the Menindee Lakes is apparent for the deeper layers. The maximum decrease in layer 2 heads is 6-7m near Menindee, trending to 1m about 60-70km distant. The maximum head decrease in layer 4 is 5-6m, compared to 3-5m for layer 5. The changes in head become insignificant about 200km away from the lakes.

Table 6.6 Water and Salt Balance for 'Without Menindee Lakes' scenario

Package	Source	Flow Rate m^3/d	Salt Flux t/d	Package	Sink	Flow Rate m^3/d	Salt Flux t/d
Wells		0	0	Wells	salinas	-12196	0
					Woolpunda N	-9979	-190
Recharge	rainfall	26222	0.1	Recharge		0	0
	irrigation	12497	3.3				
River	Darling	3321	1.0	River	Darling	-31	-0.5
	Tallyawalka	270	0.1		Tallyawalka	0	0
	Ana Branch	322	0.1		Ana Branch	-0.0	-0.0
	Murray	4195	0.9		Murray	-27649	-629.2
GHB	Cretaceous	10523	149.9	GHB	Cretaceous	-9624	-150.9
	Menindee Lakes	0	0		Menindee Lakes	0	0
	Lake Victoria	2654	1.1		Lake Victoria	0	0
	Layer Inflow (1-4)	400	3.8		Layer Outflow (1-4)	-131	-2.4
	Layer 5 inflow	69	1.1		Layer 5 outflow	-689	-10.4
	Murray baseflow	362	12.6		Murray baseflow	0	0
	Darling baseflow	0	0		Darling baseflow	-13	-0.0
Total Source		**60835**	**175**	**Total Sink**		**-60562**	**-992**

Table 6.6 describes the water and salt budget for the model scenario. The decomissioning of the lake storages has resulted in overall inputs into the groundwater system being reduced by about 10 ML/d. This includes a decrease in leakage from the Darling River by 0.6 ML/d with the removal of the main weir. The smaller water budget is basically accommodated in terms of groundwater output by a lowering in the rate of downward leakage to the Cretaceous from 20 ML/d to 10 ML/d. Of interest is the inference that the removal of the water storages should not significantly change the salt loads into the rivers. This is illustrated by the

relatively small decrease in salt loads into the Murray from 632 t/d to 629 t/d (refer Table 6.2). This probably relates to the vast distance between the Menindee Lakes and the locus of flow at the Murray River. Although the removal of the storage decreased heads in the local vicinity by over 10 m, the regional hydraulic gradient is not greatly effected.

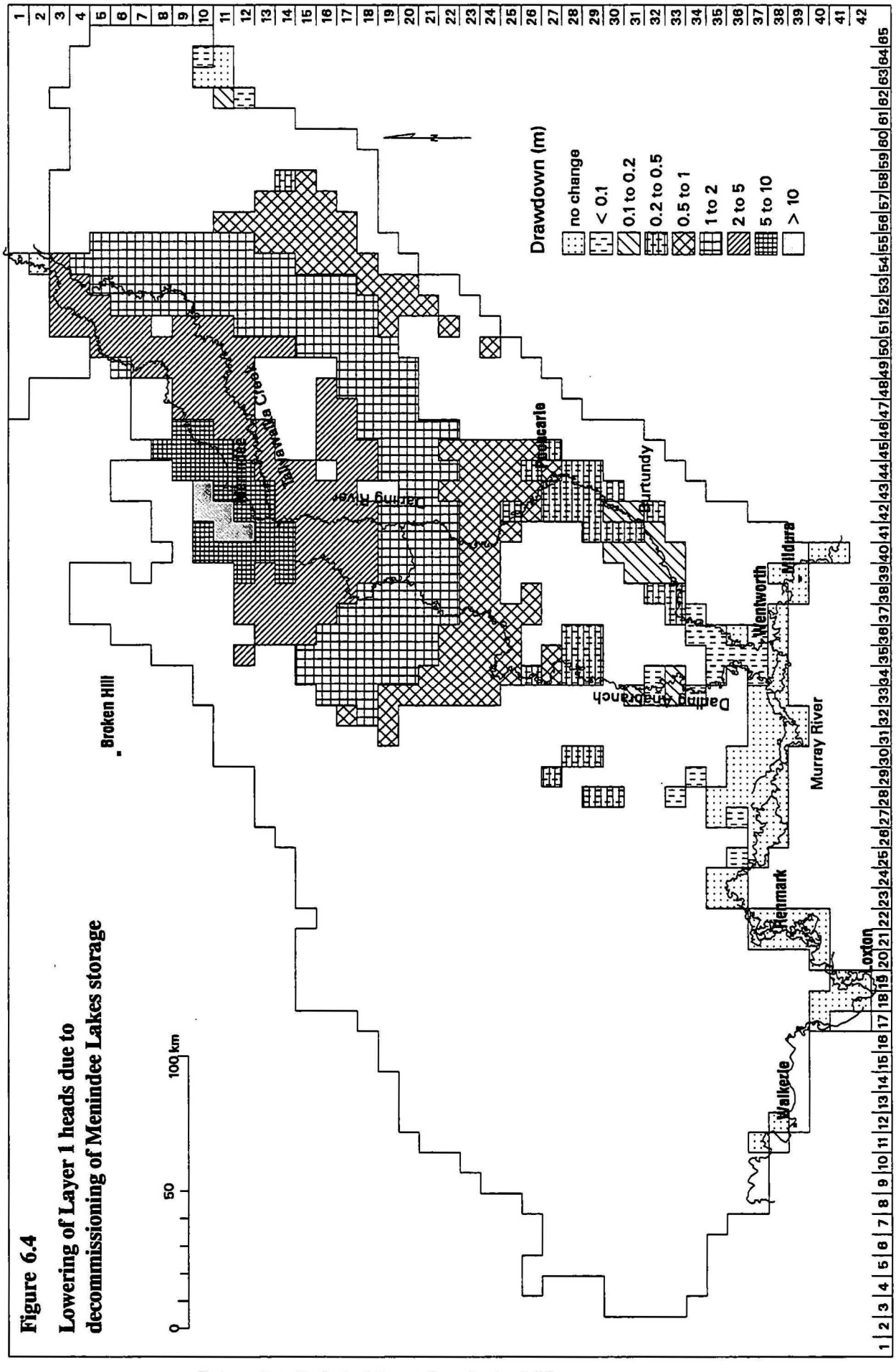

Figure 6.4

Lowering of Layer 1 heads due to decommissioning of Menindee Lakes storage

7. RECOMMENDATIONS

In a hydrogeological sense, the Lower Darling region is the least known of the groundwater provinces making up the Murray Basin. Excessive salinities, particularly in the southern half of the model area, has discouraged the active exploration and exploitation of the groundwater resource, limiting the historical borehole record. A regional monitoring network has only been established in the last decade. However, the experience gleaned from constructing the steady state model can be used to prioritise the data deficiencies that exist. These include:

Observed Heads - Due to the scattered distribution of boreholes and the lack of survey control, much of the observed head arrays used in the model have an error margin of ±5m. Hence, the residual between observed and modelled heads may be mapping errors in the former rather than the latter. A more reliable representation of the current potentiometry would reduce this problem, which is particularly evident around the model margins. Certainly, a concerted effort in levelling many of the livestock bores operating in the region would be of great use. This survey would also provide better control in the definition of the geometry of the aquifers ie. top and base elevations.

Recharge - The areal accession from rainfall is the largest contributor to the groundwater system and the model is particularly sensitive to changes in this parameter. This recognises that mallee clearing can increase recharge rates by several orders of magnitude and that, based on the sensitivity analysis, a 5-fold recharge increase can increase salt loads to the river by 4-fold. Further field measurements in the model area would be a useful adjunct. The work should focus on the effect on recharge of increasing aridity northwards, as the majority of recharge measurements previously taken in the mallee region have been in higher rainfall areas.

Hydraulic Conductivities - The sensitivity analysis also highlighted the importance of a reliable estimation of both horizontal and vertical hydraulic conductivities. For example, increases in Kh represents a decrease in hydraulic resistance, causing greater transmission rates of saline groundwater towards the Murray River. These parameters, particularly Kv, are difficult to quantify and reliable field estimates tend to be scarce or non-existent. Pump tests on strategic bores would provide useful field information to calibrate any representations of these conductivity arrays, particularly Kh.

As well as data deficiencies, there are strategies that can be implemented to improve model calibration. These include:

Variable density flow - Groundwater becomes more saline and stratified along the flow line, reaching brine concentrations (> 100,000 mg/L) in the Parilla Sands underlying the active salinas. Hence, there is a need to account for the density effects due to salinity, as MODFLOW assumes freshwater conditions. Density corrections may change simulated heads by over 1 m, and may partly offset the tendency for the model to overestimate heads over much of the domain. The MODFLOW program has been modified by AGSO to incorporate a variable density flow module (Tucker, 1991).

Optimisation techniques - There is scope to optimise input arrays such as conductance and leakance using available automated calibration packages. For example, the current understanding on these parameters can be used as prior information for input into a non-linear parameter estimate package like PEST. The package basically runs the model repeatedly, checking the simulated heads after each solution and systematically adjusting parameters, until the calibration target is reached. This target or objective function is typically the required difference between simulated and observed heads.

Surface Water - Groundwater Coupling - The salt load to the Murray River due to groundwater accessions is a critical output of the model. Hence, the interaction between the shallow aquifer and the river system has to be adequately represented. Due to a combination of data deficiencies and scale problems, this representation can be improved. There is scope for greater coupling between the Lower Darling model and the flow and salinity models constructed for the Murray River, such as BIGMOD (Close, 1996). The output of one model can be used in the calibration of the other, and vice-versa.

Lower Cretaceous (Kl) as Layer 6 - Model calibration required the inclusion of the Lower Cretaceous aquifer which underlies the Tertiary aquifers. Without the GHB cells representing the Lower Cretaceous (Kl), the model invariably overestimated heads in the northeast and underestimated heads in the southwest. However, groundwater flow can become unrealistically high across general head boundaries as there are no bounding limits (Anderson & Woessner, 1992). Hence, it would be preferable to model the Lower Cretaceous as the active basal layer in the model. The poor knowledge base for the aquifer, limited to a few petroleum exploration wells and groundwater exploration along the northeast margin, makes this difficult.

Analysis of Hydrographs - The heads in two areas in the centre of the model, one on either side of the Darling River, have consistently been overestimated by the model (eg Figure 5.3). One explanation for this is that the system is not in equilibrium with the process of lateral flow outwards from the regulated Darling River. A closer investigation of the available hydrographic record in these areas is required to detect any rising trend in heads.

Finer Discretisation - Some inputs into the regional groundwater system would be better modeled by using a finer resolution grid (eg. 2.5 x 2.5km cell). This is particularly true when attempting to define the magnitude of recharge under the irrigation areas along the Murray River. Only then would it be possible to model smaller infrastructure such as the Buronga and Rufus River interception schemes and disposal basins such as at Mourquong, Fletchers and Hollands Lakes.

8. ACKNOWLEDGMENTS

The construction of a regional scale groundwater model requires input from many people. The initial stage of the project involved contributions of data and reports from various state and federal agencies which provided a framework for the modelling. In the South Australian part of the model, this included borehole data, mapping and publications via Steve Barnett and Nick Watkins from Mines & Energy South Australia (MESA) and Andrew Telfer (ex SA Engineering and Water Supply Department). Phil Pfeiffer from SA Water provided survey data of the Murray River for input into the RIVER Package.

Borehole data for the New South Wales part of the model was provided by Michael Williams of the NSW Department of Land & Water Conservation (DLWC). The departmental reports dealing with hydrological investigations in the area were also made available, including those provided by Hugh Milner, David Salotti and Sarah Bish from the Parramatta office. David Harriss and Mike Erny at Dareton as well as Peter Clarke and Phil Craven at Buronga also provided the local perspective. Alan Hassett at Dareton compiled the available hydrographic record for the Darling River. John Hill (DLWC) organised the digital version of the land systems mapping of western New South Wales, while Karen Lawson (Geological Survey of NSW) did the same for the geological mapping along the northern margin of the Murray Basin.

Information was also derived from federal agencies. Phil Tickle provided a preliminary version of woodland mapping from the National Forest Inventory (NFI). Simon Veitch from the National Resource Information Centre (NRIC) provided rasterised climatic datasets such as average rainfall and evaporation. The Murray Darling Basin Commission (MDBC) was also an important data source with Andy Close and Ben Dyer providing the salinity, water level and profiling data for the Murray River used in the RIVER package. Paul Nanninga provided spatial data along the Murray floodplain.

A massive effort was required to organise the disparate datasets into the relational database and GIS supporting the model. Evert Bleys provided technical support for the duration of the project. Stephen Hostetler, Rob Kingham, Estoban Lopez, Vicki Manson, and Heather Rennie all contributed to the data entry, digitising, editing and processing that was required. Heather Rennie and Martyn Moffat were responsible for the bulk of the figures in this report.

The guidance and technical advice given by Ray Evans and Jim Kellett (AGSO) and Jay Punthakey (DLWC) were crucial during the calibration phase of the modelling. Ray Evans and Jim Kellett also reviewed the original manuscript of this report.

The Lower Darling groundwater model is part of NRMS Project D5039 - *Murray Darling Basin Groundwater Modelling*.

9. REFERENCES

Anderson, M.P & Woessner, W.W., 1992 - Applied groundwater modelling - simulation of flow and advective transport. Academic Press, 381pp.

Barnett, S.R., 1981 - Murray Basin hydrogeological investigation, data assessment - North western margin. Dept Mines & Energy South Australia Report 81/85

Barnett, S.R., 1989 - The effect of land clearance in the Mallee region on River Murray salinity and land salinisation. BMR Journal of Australian Geology & Geophysics, 11, 205-208.

Barnett, S.R. (SADME), 1991 - RENMARK hydrogeological map (1:250 000 scale) Bureau Mineral Resources, Canberra

Barnett, S.R (SADME), 1994 - BURRA-CHOWILLA-OLARY hydrogeological map (1:250 000 scale) Bureau Mineral Resources, Canberra

Barnett, S.R., 1995 - The rise and rise of confined aquifer pressures - Why? Extended Abstracts Murray Darling 1995 Workshop, Wagga Wagga Australian Geological Survey Organisation Record 1995/61, p24-25

Bellert, M.R., 1991 - Agriculture and fisheries - Great Anabranch of the Darling River. *in* Great Anabranch of the Darling River Proceedings, July 2-4 1991. NSW Dept of Water Resources.

Bewsher. D., Milner, H & Harriss, D., 1994 - Water resources investigations of Menindee Lakes, NSW. Water Down Under '94 IAH p 89-94

Blackburn, G. & McLeod, S., 1983 - Salinity of atmospheric precipitation in the Murray-Darling Drainage Division, Australia. Australian Journal of Soil Research, 21, 411-434.

Birchall, C., 1991 - Cropping of the anabranch lakebeds. *in* Great Anabranch of the Darling River Proceedings, July 2-4 1991. NSW Dept of Water Resources.

Bish, S. & Salotti, D., 1996 - Review of groundwater flow around Menindee Lakes Storages - Lake Menindee to Lake Cawndilla. Report TS 96.007, NSW Dept Land and Water Conservation.

Bowler, J.M., Stockton E. & Walker M.J. 1978 - Quaternary stratigraphy of the Darling River near Tilpa, New South Wales. Royal Society of Victoria, Proceedings 90, 79-88

Brigham Young University, 1996 - The Department of Defense Groundwater Modelling System GMS v2.0 Reference Manual. Brigham Young University Engineering Computer Graphics Laboratory, Utah.

Brodie, R.S., 1992 - ANA BRANCH hydrogeological Map (1:250 000 scale). Australian Geological Survey Organisation, Canberra

Brodie, R.S., 1993 - Documentation for MURBO: The Murray Basin Borehole Database. AGSO Record 1993/77. Australian Geological Survey Organisation, Canberra

Brodie, R.S., 1994 - MENINDEE hydrogeological Map (1:250 000 scale). Australian Geological Survey Organisation, Canberra

Brodie, R.S., Lane, J. & Overton, W. - 1995 - GIS Database of Murray Basin Hydrogeology. *in* AGSO Record 1995/46 - Second National Forum on GIS in the Geosciences. Australian Geological Survey Organisation, Canberra

Brown C.M., Tucker, D.H. & Anfiloff, V., 1988 - An interpretation of the tectonostratigraphic framework of the Murray Basin region of southeastern Australia, based on an examination of airborne magnetic patterns. Tectonophysic, 154, 309-333.

Brown, C.M., 1989 - Structural and stratigraphic framework of groundwater occurrence and surface discharge in the Murray Basin, southeastern Australia. BMR Journal Vol 11 No 243 p127-146.

Brown, C.M. & Radke, B.M., 1989 - Stratigraphy and sedimentology of mid-Tertiary permeability barriers in the subsurface of the Murray Basin, southeastern Australia. BMR Journal Vol 11 No 243 p367-385.

Brown, C.M. & Stephenson, A.E., 1991a - Geology of the Murray Basin, southeastern Australia. Bulletin 235, Bureau of Mineral Resources, Australia

Brown, C.M. & Stephenson, A.E., 1991b - Geology of the Murray Basin, 1:1 000 000 scale map, Bureau of Mineral Resources, Australia

Cameron, R.G., 1996 - Geology of the POONCARIE 1:250 000 map - Explanatory Notes. Geological Survey of NSW.

Close, A.F., 1996 - A new daily model 0f flow and solute transport in the River Murray. Hydrology and Water Resources Symposium, 1996.

Cook, P.G., Kennett-Smith A.K., Walker G.R., Budd G.R., Williams R.M. & Anderson R. 1996 - Impact of dryland agriculture on land and river salinisation in the western lands, New South Wales. CSIRO Technical Memorandum 96.16

Dixon, S., 1891 - On a subterranean Water-supply for the Broken Hill Mines. Trans R. Soc. SA Vol 14 p 200-209.

Dudding, M., Oakes A. & Thorne, R., 1989 - Lindsay River salinity assessment progress report. Technical Report 1989/23, Rural Water Commission of Victoria

Edwards, K., 1979 - Rainfall in New South Wales with special reference to soil conservation. Technical Handbook No. 3, Soil Conservation Service of NSW.

Evans, W.R., 1992 - The Murray Basin Hydrogeological Map Series. AWWA Water Journal Vol 19, No 6, 20-23.

Evans, W.R. & Kellett, J.R., 1989 - The hydrogeology of the Murray Basin, southeastern Australia. BMR Journal , Vol 11, No 243, 147-166

Ferguson, J. & Radke, B.M., 1992 - Hydrodynamics of the Scotia, Nulla and Murquong Groundwater Discharge Complexes. AGSO Report to MDBC (unpubl).

Ferguson, J., Radke, B.M., Jacobson, G., Evans, W.R., Chambers, L.A., White, I., Wooding, R.A., Whitford, D. and Allan, G.L., 1995 - The Scotia groundwater discharge complex, Murray Basin, SE Australia. AGSO Record 1995/43. Australian Geological Survey Organisation, Canberra.

Fox, M.D, 1991 - The natural vegetation of the Ana Branch - Mildura 1:250 000 map sheet (New South Wales). Cunninghamia Vol 2(3) 443-493.

Freeze, A.R. & Cherry, J.A. 1979 - Groundwater. Prentice-Hall Inc, New Jersey, USA, 604 p.

Gutteridge, Haskins and Davey Pty Ltd, (1992) The Riverine Plain groundwater model Stage 2 report - further calibration (*unpubl.*).

Harriss, D., Milner, H. & Everson, D., 1994 - Menindee Lakes and the Lower Darling River - Issues for Management. NSW Department of Water Resources.

Hostetler, S. & Radke, B., 1995 - An inventory of saline water disposal basins, Murray Basin (2 Vol) Australian Geological Survey Organisation Record 1995/4.

Howles, S.R., 1987 - Berri East Groundwater Interception Scheme Hydrogeological Investigation. Report RB 86/59, SA Dept Mines & Energy

Irish, J., 1993 - Nearie Lake Nature Reserve: Historical frequency of inflows. Report 92.017 NSW Dept Water Resources.

Jacobson, G., Ferguson, J & Evans, W.R., 1994 - Groundwater-discharge playas of the Mallee region, Murray Basin, southeast Australia, *in* Rosen, M.R., ed., Palaeoclimate and Basin Evolution of Playa Systems: Boulder, Colorado, Geological Society of America Special Paper 289.

Jayatilaka, C.J., Lakey, R.C. & Elder, G.M., 1994 - Estimating groundwater recharge rates following clearing of native vegetation: the CARE model. Water Down Under 94 XXV IAH Congress, Adelaide Australia pp479-484.

Jewell, C.M., 1993 - Lower Darling River, groundwater-river level relationships and qualitative indications of environmental flows in rivers and wetlands. NSW Dept Water Resources TS 93.040

Jolly, I.D., Cook, P.G., Allison, G.B. & Hughes, M.W., 1989 - Simultaneous water and solute movement through an unsaturated soil following an increase in recharge. J. Hydrol., 111:391-396.

Kellett, J.R., 1989 - The Ivanhoe Block - its structure, hydrogeology and effect on groundwaters of the Riverine Plain of New South Wales. BMR Journal, Vol 11, No 243, 333-353.

Kellett, J.R., 1991 - POONCARIE hydrogeological Map (1:250 000 scale). Australian Geological Survey Organisation, Canberra

Kellett, J.R., 1994a - MANARA hydrogeological Map (1:250 000 scale). Australian Geological Survey Organisation, Canberra

Kellett, J.R., 1994b - IVANHOE hydrogeological Map (1:250 000 scale). Australian Geological Survey Organisation, Canberra

Kellett, J.R., 1997 - Lachlan Fan/Ivanhoe Block steady state groundwater model - model development, calibration, sensitivity analysis and predictions. AGSO Record 97/029. Australian Geological Survey Organisation, Australia., 119 pp.

Kennett-Smith, A., Cook, P.G., and Walker, G.R., (1994) Factors affecting groundwater recharge following clearing in the south western Murray Basin. Journal of Hydrology, 154, p 85-105.

Kenny, E.J., 1934 - West Darling District - A geological reconnaissance with special reference to the resources of subsurface water. Mineral Resources No 36. NSW Department of Mines.

Laut, P., Heyligers, P.C., Keig, G., Loffler, E., Margules, C., Scott, R.M. & Sullivan, M.E., 1977 - Environments of South Australia, Province 2 Murray Mallee, Province 5 Eastern Pastoral, Province 6 Flinders Ranges. Division of Land Use Research, CSIRO.

Lindsay, J.M. & Barnett, S.R., 1989 - Aspects of stratigraphy and structure in relation to the Woolpunda Groundwater Interception Scheme, Murray Basin, South Australia. BMR Journal of Australian Geology & Geophysics, 11, 219-225.

Mackay, N. & Eastburn, D., 1990 - The Murray. Murray Darling Basin Commission. 363 pp.

Macphail, M.K., Kellett, J.R., Rexilius, J.P. & O'Rorke, M.E., 1993 - The "Geera Clay equivalent": a regressive marine unit in the Renmark Group that sheds new light on the age of the Mologa weathering surface in the Murray Basin. AGSO Journal Vol 14, 47-63.

McDonald, M.G. and Harbaugh, A., 1988 - A modular three-dimensional finite-difference ground-water flow model. Techniques of water resources investigations of the United States Geological Survey. Book 6 Chapter A1. US Department of the Interior, 589 pp.

Mullholand, C. St J., 1940 - Geology and underground water resources of the East Darling District. Mineral Resources No. 39, NSW Department of Mines.

Murray Darling Basin Commission, 1990 - The River Murray System - the regulation and distribution of River Murray waters. MDBC Canberra

Narayan, K. A. & Armstrong , D., 1995 - Simulation of groundwater interception at Lake Ranfurly, Victoria, incorporating variable density flow and solute transport. Journal of Hydrology 165, 161-184.

NSW Department of Land and Water Conservation, 1996a - A discussion paper of regional issues for clearing and cultivation. NSW Department of Land and Water Conservation, Far West Region.

NSW Department of Land and Water Conservation, 1996b - A reference paper of Department of Land and Water Conservation land resource management policy, standard conditions and regional statistics. NSW Department of Land and Water Conservation, Far West Region.

NSW Department Mineral Resources, 1996 - Murray Basin Mapping Progress. Minfo 52, p 56-59. NSW Department Mineral Resources.

NSW Department of Water Resources, 1994a - Menindee Lakes and the Lower Darling River - Summary of operations 1990 to 1994. NSW Department of Water Resources.

NSW Department of Water Resources, 1994b - Modelling of floods with lakebed cropping. Discussion Paper 6, Great Anabranch of the Darling River Water Management Plan

Prathapar, S.A., Williams, R.M. & Punthakey, J.F. 1994 - Optimising the short- to medium- term salinisation consequences of land clearing in the NSW mallee, Australia. CSIRO, Div. Water Resources., Div. Rpt. 94/2.

Punthakey, J.F., Somaratne, N.M., Prathapar, S.A., Merrick, N.P., Lawson., S. & Williams, R.M. , 1994 - Regional groundwater modelling of the Lower Murrumbidgee River Basin - model development and calibration. Report TS 94.069. NSW Dept Water Resources, 284 pp.

Reed, J.A., 1980 - Murray Basin hydrogeological investigation data assessment Upper Murray and Northern Region (2 Vol). Dept Mines & Energy South Australia Report 80/42

Rural Water Commission, 1991 - MILDURA hydrogeological map (1:250 000 scale). Bureau of Mineral Resources. Canberra

Scriven, R.N., 1988 - A review of information relevant to the Mallee Rangelands of Western New South Wales. Technical Report No 1, Soil Conservation Service of NSW.

Sinclair Knight Merz Pty Ltd, 1995 - South Australian/Victorian Mallee (SAVIC) groundwater model progress report. (*unpubl.*), 69 pp.

Smith, K. & Watkins, N., 1993 - Border to the Barrages - Natural resource criteria for sustainable irrigation on the River Murray. River Murray Water Resources Committee.

Stannard, M.E., 1981 - Irrigation development between Wentworth and Menindee. unpubl. NSW Department of Water Resources.

Stephenson, A.E., 1986 - Lake Bungunnia - a Plio-Pleistocene megalake in southern Australia. Palaeogeography, Palaeoclimatology, Palaeoecology, v.57, p.137-156.

Telfer, A., 1987 - Executive summary on hydrogeology of the Woolpunda Groundwater Interception Scheme, Preconstruction investigation and Design. Report 18/42. SA Engineering & Water Supply.

Tucker, A.G., 1991 - Documentation for variable density flow modifications to the USGS MODFLOW program (AGSO Release 1.3). unpubl report. Australian Geological Survey Organisation, Canberra.

Walker, P.J., 1991 - Land systems of Western New South Wales. Technical Report No 25, Soil Conservation Service of NSW

Waterhouse, J., 1989 - The hydrogeology of the Chowilla Floodplain. Salinity mitigation investigations in South Australia Report to MDBC. Australian Groundwater Consultants

Watkins, N., 1993 - Woolpunda Salt Interception Scheme Monitoring Strategy - groundwater modelling of flow and aquifer response to pumping. Report 93/7, SA Engineering & Water Supply.

Watkins, N., Teoh, K. & Way, D., 1995 - Sunlands/Qualco District - Data Report 2 , Hydrogeology and assessment of irrigation drainage impacts. Technical Report 238, MDBC Salinity & Drainage Strategy.

Williams, R.M., 1991a - Hydrogeology of the interaction between Pliocene Sand Aquifer and the Darling River Anabranch system. Technical report 91.035 NSW Department of Water Resources.

Williams, R.M., 1991b - Groundwater inflows to the Darling River Mungindi to Wentworth: Run of river study 1990/91. Technical Report 91.041 NSW Dept of Water Resources

Williams, R.M., Harriss, D. & Erny, M., 1993 - Land salinisation on the floodplain east of Lake Victoria - Progress to June 1993. Report TS 93.037, NSW Dept Water Resources.

Williams, R.M. & Beckham, J., 1995 - Stream/aquifer interactions along the lower Darling River, NSW. NSW Dept Water Resources TS 95.022.

Withers, M., 1994 - Flooding and water conservation in the Great Anabranch of the Darling River. unpubl. NSW Dept Water Resources.

APPENDIX 1

Results of Sensitivity Analysis

A sensitivity analysis was undertaken to gain an understanding of the degree of uncertainty within the calibrated model due to the inherent uncertainties in the estimation of the model parameters. The model input of horizontal hydraulic conductivity (Kh), leakance, recharge, river bed conductance and general head boundary (GHB) conductance were systematically altered and the variation in model output, as compared to the calibrated model, were investigated.

Increases in horizontal hydraulic conductivity (Kh)

Increasing the horizontal hydraulic conductivity (Kh) arrays of the model layers tended to have the effect of decreasing simulated heads. This reflects the concomitant decrease in hydraulic resistance within the aquifer system. In layer 1, this was most apparent for the Darling floodplain, particularly at and north of the Menindee Lakes. Here, heads dropped by 1-2 m with a 200% increase in Kh, 5-6m with 500% and 7-9m with 1000%. This caused some of the river cells near the northern model margin to dry up and deactivate. In comparison, heads in the lower reaches of the Darling only decreased by 3-5 m with a 10-fold change in Kh. The head in model cells along the Murray River remained static throughout the Kh increases.

The southwest corner of the model experienced the greatest change in heads for layer 2. Here, modelled heads dropped by 2-3m with an increase of 20% in layer Kh, 5-6m with 100% and 10-20m at 1000%. The Kh increases also caused occasional model instability with clusters of cells developing extreme modelled heads. This was partly due to cells over the Woolpunda Ridge drying up and becoming inactive, causing impoundment of groundwater in upgradient cells. At the maximum Kh increase, modelled heads decreased by 5-10m in the western half of the layer, and by 2-4m in the eastern half. Like Layer 1, the Menindee Lakes area also experienced relatively greater decreases in head (5-8m). Little change in heads occurred for layer 2 cells along the Murray River.

For layer 3, the Menindee Lakes area, the northwest basin margin and the southwest boundary with the marginal marine equivalents, were the locus of decreases in modelled heads with increases in Kh. For example, with a 500% increase in Kh, these areas displayed head decreases of 5-10m, while the remaining layer cells had only head decreases of 1-4m.

Like layer 2, the southwest corner of the model had the greatest head perturbations for layer 4 due to increasing Kh. Heads decreased by 3-5m at a 20% increase, 6-11m at 50%, 7-18m at 100%, 10-35m at 500% and 30-40m at 1000%. In contrast, a zone stretching along the eastern layer boundary and towards the model centre was more resistant to the Kh changes. Here, heads only decreased by 2-4m with a 1000% Kh increase. Cells around the Woolpunda Reach were unique for the layer, in that heads increased marginally (1-2m). This is due to the fact that this is the main collection point for groundwater flow in the layer which is receiving more water due the greater transmission rates afforded by the increases in Kh.

For layer 5, the outlier found in the southwest corner of the model experienced the greatest head variation with Kh increases. The head varied from 2-3m with a 20% Kh increase to 20-25m with a 1000% increase. In comparison, at the maximum Kh increase, heads in the Menindee-Blantyre Troughs decreased by 6-7m and by 2-3m in the remainder of the layer. Like the overlying layer 4, the Woolpunda area was an exception as heads actually increased by 2-4m.

Increasing Kh also produces significant changes to the water budget. In general, the magnitude of the water budget increased due to the higher transmission rates allowing greater movement of groundwater between source and sink. This expansion could be charted at 2% of calibrated budget with a 20% increase in Kh, 6% with 50%, 11% with 100%, 40% with 500% and 83% with 1000%. At the maximum Kh increase, the evaporative loss at active salinas increased by 108%, the water loss from the Darling River increased by 235% and the Murray River received 178% more groundwater. The input via GHB cells increased from 35 ML/d to 80 ML/d, but export via GHB cells actually decreased from 20 ML/d to 0.7 ML/d. The increase in Kh would have encouraged horizontal flow at the expense of vertical flow, so that water would be directed more to shallow sinks such as the river and salt lakes rather than deeper sinks such as the Lower Cretaceous and exit flow in the basal lower Renmark Group aquifer, which are represented as GHB cells.

Decreases in horizontal hydraulic conductivity (Kh)

Decreasing the Kh array, tended to result in increases in head due to greater hydraulic resistance. With a 20% decrease in layer 1 Kh, this was expressed as increases of 1-2m in two regions - at and north of the Menindee Lakes and in the lower reaches of the Darling and Anabranch. A cluster of cells with extreme heads was also generated in the southwest corner, but heads in the Murray River cells remained static. With a 50% reduction, heads in layer 1 increased by 2-4 m around where the Darling River meets the northern model margin. Significant perturbations occurred with an 80% reduction of Kh. The lower reaches of the Darling system actually dried up and deactivated, causing higher heads (by 6-7m) along the southern extent of the remaining Darling River cells. The northern margin also hosted head increases of 6-9m.

A similar pattern held for layer 2, with two zones of head increase due to Kh reduction. These were at and north of Menindee Lakes and a 100km wide arcuate zone from the Murray northwards to Pooncarie. With a 20% reduction, model instability caused a cluster of cells with extreme heads in the southwest corner. With a 50% decrease, these two regions experienced head increases of 2-5m. Cells west of the Woolpunda Ridge dried, causing minor lowering of heads (1m) east of the ridge. Similar head decreases occurred for cells around the Woolpunda Reach. Desaturation extended to a broad arcuate zone in the southern half of the layer with an 80% reduction in Kh. Head increases of up to 20-25m occurred in the remaining cells bordering this inactive zone. Increases were also generated along the northern model margin (6-14m) and near Berri (10-20m).

The western and southern margins of layer 3, were the main areas of head increase for layer 3. With a 20% reduction of Kh, this head increase was generally minor at 1-2m., However,

at the maximum Kh reduction of 80%, localised head increases of 10-20m occurred. The central core and eastern margin experienced a minor (1m) head decrease.

The southern half of layer 4 experienced a subtle 1m head increase with a 20% Kh decrease. Maxima of 6-7m occurred in the southeast corner of the model, near Mildura. Conversely, there was a 5-7m head decrease in the southwest corner. With an 80% Kh decrease, this regional head increase expanded from 1 m to 2-5m, with local maxima of 30-45m. Cells around the Woolpunda Reach actually decreased by 2-3m.

The maximum head increase for layer 5 was found in the southwest outlier. Here heads increased by 10-16m with a 50% Kh reduction and by 30-45m with an 80% Kh reduction. In contrast, the southern half of the model experienced minor head increases of 2-3m. The Woolpunda area had heads decrease by 5-7m with the maximum Kh decrease.

In a reverse situation to that found for increasing Kh, reductions in hydraulic conductivity decreased the overall water budget. This decrease amounted to 5% at a 20% Kh reduction, 12% at 50% and 23% at 80%. At the maximum Kh reduction, the shrinking of the water budget is accommodated by decreases in river loss (71%) and GHB inflow (34%) on the input side, and by evaporative loss (55%) and river gain (40%) on the output side. Export of groundwater through GHB cells actually increased by 40%. The decrease in Kh would tend to encourage flow in a vertical rather than a horizontal direction, allowing greater availability of water to the deeper aquifers and increase leakage to the underlying Lower Cretaceous.

Increases in leakance (vcont)

The systematic variation of the leakance arrays did not exhibit the same general magnitude of head changes as that displayed by changes to horizontal hydraulic conductivity. However, head variations were more complex, being both negative and positive within the layers. This relates to the differences in the vertical flow regime across the model domain. In the northwest, downward recharge conditions prevail and increases in leakance should enhance aquifer drainage and reduce heads. Under the discharge conditions operating in the southwest, increasing leakance would enhance leakage from the underlying aquifer causing heads to rise.

Only minor decreases (1m) in head occurred in layer 1 near Menindee Lakes and the northern model margin when leakance arrays were doubled. Multiplying leakance by 10 only caused heads to decrease by 1-3m in the centre of the layer. Some river cells dried and much of the layer north of Lake Victoria also became unsaturated. The heads along the Murray River remained relatively stable throughout the analysis.

Increasing leakance by 20% partially desaturated the Woolpunda Ridge, causing head perturbations in the southwest corner of layer 2. This included high heads to the west of the ridge and head decreases of 2-6m to the east. The remainder of the layer received minor decreases in head. This southwest corner is the main focus of change for layer 2. With a 10-fold increase in leakance, the partial desaturation over the Woolpunda Ridge caused extensive drying of cells and high heads in others (by up to 80m). However, the majority of the layer only experience marginal head decreases of 1-2m.

Heads in layer 3 were only really perturbed after leakance was increased 5-fold. Only then did heads decrease by 1-4m in the southern third of the layer and near the northern margin. Heads actually increased by 1-2m near the Menindee Lakes.

A 5-fold increase in leakance caused heads to increase by 1-2m near Menindee and by 2-4 m near Woolpunda. These areas were separated by a central zone where heads decreased by 1-5m. With a 10-fold increase in leakance, the head increase at Menindee was about 2-3m and about 3-6m at Woolpunda.

Increasing leakance by 500% had different effects for different parts of layer 5. In the southern half, heads decreased by 1-3m maximising to 5-6m at Woolpunda. In the northern half, the head increase was highest (2-3m) in the Menindee Trough. This dichotomy is due to the variations in vertical flow across the model. These perturbations changed marginally with a 10-fold increase in leakance.

Increasing leakance expanded the size of the water budget, similar in effect of that of increases in Kh. This is due to the increased transmission rates between vertically separated groundwater sources and sinks. This expansion can be charted at 1% with a 20% leakance increase, 8% with 50%, 13% with 100%, 39% with 500% and 50% with 1000%. In terms of groundwater input, most of the expansion is realised by GHB inflows more than doubling from 35 ML/d to 72 ML/d. River gain likewise expanded from 32 ML/d to 67 ML/d, accounting for most of the increases in groundwater output.

Decreases in leakance (vcont)

A 20% decrease in leakance caused minor changes in the modelled heads. In layer 1, the changes only amounted to a 1-2m increase around the lower reaches of the Darling system. With a 90% decrease in leakance, all of the Darling system had increased heads, by 2-4m in the floodplain and by 1-2m in the margins. The heads in the Murray River cells remained stable.

Head changes in layer 2 due to a 20% leakance reduction were also modest. Scattered increases in heads by 1-2m occurred in the southern half of the layer, reaching 2-4m near the Murray-Darling confluence. With halving of leakance, heads in the southern half increased by 1-2m, maximising in the southwest corner at 5-6m. Heads decreased by 1-2m around the Menindee Lakes. This southern zone of head increase expanded when leakance was reduced to 10% of calibrated values. The head increase was typically 2-4m, trending to 7-8m in the southwest margin.

Any significant response in layer 3 only occurred after a 50% reduction in leakance. Even then, this was limited to a general 1m increase in the southern half and a minor 1m head decrease near Menindee Lakes and Scopes Range. With a 90% reduction in leakance, the head variation was only 2-3m.

Layer 4 showed slightly more head variation with a halving of leakance. A head increase of 1-2m occurred in the centre of the layer, separating zones of head decrease of 1-4m to the

south (trending to 6-13m in the southwest corner) and of 1-2m near Menindee in the north. The head increase in this central zone were typically 2-3m when leakance was reduced by 90%. The southern third of the layer responded with head decreases of 4-8m, maximising at Woolpunda (10-12m).

The response of layer 5 to the halving of the leakance arrays differed across the domain. Modest increases in head occurred in the southern half, particularly near Woolpunda (2m). Head decreases occurred in the Menindee Trough to the north (1-2m) and the outlier to the southwest (4-5m). With a 90% decrease in leakance, the head variations were 3-4m for Woolpunda, 1-4m for Menindee Trough and 6-7m for the outlier.

Decreasing the leakance resulted in decreases in the size of the groundwater budget, due to the decrease in hydraulic connection between aquifers. This decrease in the water budget amounted to 5% when leakance was reduced by 20%, 14% at 50% and 32% at 90%. The majority of this reduction is accommodated by the GHB cells in terms of input. Specifically, GHB input declined from 35 ML/d in the calibrated model to 12 ML/d, when leakance is reduced by 90%. This represents the restriction of flow from the underlying Lower Cretaceous. The reduction in groundwater export was mostly via the shallow sinks of evaporative loss dropping from 23 ML/d to 13 ML/d and river gain decreasing from 32 ML/d to 21 ML/d.

Increases in Recharge (rech)

The head response due to increases in recharge were significant. Naturally, progressive increases in recharge generally resulted in increases in modelled heads, particularly in the shallower layers. With a 20% increase in recharge, this amounted to scattered increases by 1m in the Darling system for layer 1. With a doubling of recharge, the heads in the Darling system increased by 2-4m, except for around the Menindee Lakes which remained static. The head increases were more variable in layer 1 with a five-fold recharge increase. A range of 2-4m was typical of west of the Darling, 6-10m in the east and maximising to 15-30m in the northern margin. The head in cells around the Murray River remained close to those of the calibrated model.

Two specific areas of head increase developed in layer 2 with a 20% increase in recharge. These were the southwest corner (2-3m) and the northern margin (2-6m). With a 50% recharge increment, the head in most of the layer increased by at least 1 m, with a zone north of the Murray and the extreme northern margin experiencing rises of 2-4m. Partial drying of the Woolpunda Ridge caused anomalously high head increases of 20-30m in the southwest corner. With a five-fold increase, all of the layer experienced head increases, except in the vicinity of the Murray River. These were in the order of 2-4m in the northwest quadrant, 6-10m (locally 20m) in the eastern margin and anomalous 50+m in the southwest corner.

Similarly, layer 3 heads increased by at least 1m with a 50% increase in recharge. The general rise was 2-3m with a doubling of recharge. With a five-fold recharge increase, heads had increased by 7-10m (locally 20+m) particularly along the eastern margin.

Most of the northern half of layer 4 had heads increase by at least 1m with a 50% increase in recharge. The centre of the model experienced head increases of 2-3m while interestingly, heads actually decreased by 2-3m (locally 20-30m) in the southwest corner. With a 500% recharge increase, the head increase was typically 7-10m.

Up to a doubling of recharge, the head increases in layer 5 were only in the order of 1-2m. The outlier of lower Renmark Group aquifer is the only exception, where heads increased 6-9m. This general trend rises to 2-5m with a five-fold increase in recharge.

The extra input by recharge obviously increases the magnitude of the groundwater budget. With each increasing increment of recharge, there was a corresponding decrement of river leakage and GHB inflow on the input component of the budget. In terms of output, the excess recharge was offset by increases to river gains (32 ML/d to 119 ML/d) and GHB export (20 ML/d to 61 ML/d). The error for the water budget also increased from 0.56% to 5.15%.

Decreases in Recharge (rech)

Reduction in recharge did not match the same magnitude of effects on modelled heads caused by increases in recharge. However, as expected, the general trend was downwards. For layer 1, this was a general decrease by 1m for the Darling system with a halving of recharge. With input of 10% of calibrated recharge, the head decrease was still only mostly 1-3m. The Murray River cells had static heads during the decrements in recharge.

Similar decreases occurred for layer 2 with a 20% reduction in recharge. In the southwest corner, the head decrease was around 2-3m. In contrast, there was a slight increase (2-3m) in heads near the confluence of the Murray and Darling. The southwest corner experienced head decreases of 5-10m with halving of recharge, and a 5-15m decrease with a 90% recharge decrease.

For layer 3, the head variation was confined to scattered 1m decreases with a 20% recharge reduction, a general 1-2m decrease with 50%, and a 1-3m decrease increasing to 4-5m along the margins with 90%.

Like layer 2, the southwest corner of layer 4 experienced the greatest change due to recharge reduction. Here, heads decreased by 5-15m with a 20% reduction and 10-20m with a 90% reduction. In contrast, heads in the northern half typically dropped by 1-4m. The outlier of layer 5 also had relatively larger head decreases (5-6m) compared to the rest of the layer (1-2m).

The overall water budget decreased in magnitude with the decreases in recharge input. Inversely, the other model inputs of river loss and GHB inflow correspondingly increased. The overall inputs reduction was matched by decreases in river gain and GHB export in terms of groundwater outputs. The evaporative loss via salt lakes remained relatively constant.

Increases in River Bed Conductance (criv)

The modelled heads seemed to be not particularly sensitive to increases in the conductance of the river bed, as defined in the RIVER package. For layer 1, this was limited to scattered 1m increases in head in the northern part of the Darling floodplain with a 20% conductance increase. With a doubling of riverbed conductance, the head increase around the floodplain north of Menindee Lakes was 1-3m, and with a 5-fold increase it was 2-6m.

Similar conditions applied for layer 2 in the northern Darling floodplain. In addition, heads increased to 3-4m in the southeast corner of the layer with a 20% increase in conductance, rising to 5-16m with a 50% increase. With a doubling of conductance, the southwest corner showed a general 1-3m head decrease with some drying of cells. A similar pattern held for layer 3, with the northern margin near the Darling River having a 1-2m head increase with a 100% increase, and a 2-5m increase with a 500% increase.

Heads in layer 4 only changed after a doubling of river bed conductance. In the northern Darling floodplain this was a 1-2m head increase with scattered minor 1m increases in the rest of the layer. With a five-fold increase, this was translated into a 2-5m increase in the northern floodplain, similar to layer 2. With a ten-fold increase, the head increase in this area was 2-7m, with a general 1m increase in the rest of the northern-central part of the layer, except for the margins. Heads actually dropped in the southwest corner by 1-3m, with some desaturation of cells.

Head variations in layer 5 were limited, even up to a five-fold increase in conductance. There was a maximum of 2m increase in heads in the Menindee-Blantyre Troughs, and rare 1m decreases near Woolpunda due to a ten-fold conductance increase.

With the greater leakage through the river bed, the water budget is likely to expand with the increases in conductance. This occurred but not by an inordinate amount, only by 11% with a ten-fold increase. Naturally, the increasing inputs was represented by greater leakage from the river system, from 7 ML/d to 17 ML/d. The corresponding increase in output was not solely accommodated by changes to groundwater seepage to rivers from 31.5 ML/d to 34.5 ML/d but also increases in through flow in deeper aquifers, from 20 ML/d to 26 ML/d.

Decreases in River Bed Conductance (criv)

The head response from decreases in riverbed conductance were also relatively limited. Again, the northern floodplain of the Darling was a focus area. In layer 1, heads decreased by 1m with some river cells drying up with a 20% decrease in conductance. With a 90% decrease, the heads were generally lowered by 1-2m, ranging up to 4-5m in the northern margin. In the lower reaches of the Darling, heads in some cells actually rose by 1-3m.

With a 90% reduction, layer 2 experienced a general 1-3m decrease in the northern floodplain of the Darling as well as in the southwest corner. In the southwest quadrant, heads increased by 1-2m, trending to 3-6m near Mildura. Layer 3 had a similar pattern with a 1-3m decrease to the north and a 1-3m increase in the southeast corner of the layer.

Layer 4 displayed a similar pattern of head response as in layer 2, but less extensive. A ten-fold decrease caused scattered to general 1-2m head decreases in the north and a similar pattern of increases in the south, maximising to 3-6m near Woolpunda and 2-3m near Mildura. Layer 5 was even less responsive to conductance decreases. With a 90% reduction, scattered 1m head decreases in the Menindee-Blantyre Troughs and scattered 1m increases in the south occurred.

The water budget shrank with the restriction of leakage through the river bed. This was mapped as 2% at 20% decrease, 5% at 50% and 13% at 90%.

Increases in Lower Cretaceous conductance (cond)

Like variations in the riverbed conductance, changing the conductance of the GHB cells representing the underlying Lower Cretaceous (Kl) did not produce significant variations in head. The direction of head response was also variable, dependant in the relative head difference between the deepest model aquifer and the Kl aquifer. In the north, where potential groundwater flow is downward, increases in conductance encourages deep drainage into the Lower Cretaceous causing heads to drop in the modelled layers.

With a 20% increase, head variation amounted to scattered 1m decreases throughout the northern half of the layer, with no change occurring in the Lower Darling and Murray floodplains. The head decrease in the northern floodplain was still only 1-3m with a ten-fold increase in conductance.

Heads only decreased by 1m in layer 2, specifically in the northern half, with a 20% conductance increase. A 1000% increase only caused a general 1-3m decrease in the north and scattered 1m decreases in the south. A similar pattern occurred for layer 3 at the maximum increase in conductance. Heads in the layer generally decreased by 1-3m, except in the southern margin which remained static. The heads in the southwest corner of the layer partially rose by 1m.

The response by layer 4 to a ten-fold increase in conductance varied across the model domain. There was a transition from 1-3m head decreases in the north to 1-3m increases in the south. A similar pattern was maintained for layer 5.

As increases in conductance increases the flux between the model and the external Lower Cretaceous source/sink, the water budget correspondingly increased. This amounted to a 19% increase with a 1000% conductance increase, with leakage from GHB cells increasing from 35 ML/d to 48 ML/d and leakage to GHB cells increasing from 20 ML/d to 31 ML/d.

Decreases in Lower Cretaceous conductance (cond)

Decreasing the conductance term for GHB cells representing the Lower Cretaceous produced a reverse head response to that of the previous increases. For example, there was a subtle increase in heads in the northern half of the model due to the reduction in downward leakage to the Lower Cretaceous. For layer 1, this amounted to a 2-4m increase in heads for the

northern half, except for Menindee Lakes (0-1m), for a 90% reduction in conductance. Little change occurred in the lower reaches of the Darling and in the Murray.

The head variation in layer 2 for a 90% reduction was transitional across the model. Heads increased from 2-4m in the northern third, increased by 1-2m in the central third and increased by 0-1m in the southern third. Likewise for layer 3, heads increased by 2-4m for most of the layer except for the southern margin which only had minor head increases of 0-1m.

Layer 4 heads also varied across the layer. Like the shallower layers, heads increased by 2-4m in the north, trending to 0-1m towards the centre of the layer. In the southwest quadrant, heads actually decreased by 1-2m. An almost identical pattern emerged for layer 5.

The restriction of flow between the model and external GHB cells is reflected by the decrease in the water budget, amounting to a 9% reduction with conductance reduced to 10% of original calibrated values. Inflow via GHB cells reduced from 35 ML/d to 29 ML/d and GHB outflow from 20 ML/d to 13.5 ML/d.